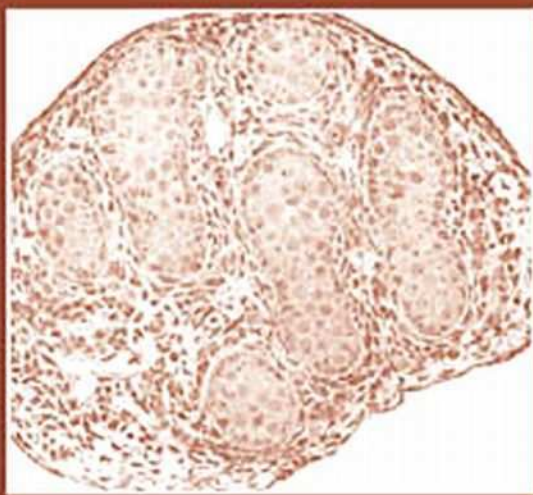# International REVIEW OF CYTOLOGY

A SURVEY OF CELL BIOLOGY

Edited by

Kwang W. Jeon

International Review of Cytology

A Survey of Cell Biology

VOLUME 260

International Review of Cytology
A Survey of Cell Biology

Edited by

Kwang W. Jeon
Department of Biochemistry
University of Tennessee
Knoxville, Tennessee

VOLUME 260

CONTENTS

Cell Proliferation in Pathogenesis of Esophagogastric Lesions in Pigs

Milijana Knežević, Sanja Aleksić-Kovačević, and Zoran Aleksić

Molecular Mechanism of Phase I and Phase II Drug-Metabolizing Enzymes: Implications for Detoxification

Takashi Iyanagi

Effects of Growth Factors on Testicular Morphogenesis

Sarah Mackay and Robert A. Smith

Flagellar Length Control in *Chlamydomonas*—A Paradigm for Organelle Size Regulation

Kimberly A. Wemmer and Wallace F. Marshall

Molecular Mechanism and Evolutional Significance of Epithelial–Mesenchymal Interactions in the Body- and Tail-Dependent Metamorphic Transformation of Anuran Larval Skin

Katsutoshi Yoshizato

CONTRIBUTORS

Numbers in parentheses indicate the pages on which the authors' contributions begin.

Zoran Aleksić (1), *Department of Pathology, Faculty of Veterinary Medicine, University of Belgrade, 11000 Belgrade, Serbia*

Sanja Aleksić-Kovačević (1), *Department of Pathology, Faculty of Veterinary Medicine, University of Belgrade, 11000 Belgrade, Serbia*

Takashi Iyanagi (35), *Biometal Science Laboratory, RIKEN SPring-8 Center, Harima Institute, Hyogo 679-5148, Japan*

Milijana Knežević (1), *Department of Pathology, Faculty of Veterinary Medicine, University of Belgrade, 11000 Belgrade, Serbia*

Sarah Mackay (113), *Division of Neuroscience and Biomedical Systems, Institute of Biomedical and Life Sciences, University of Glasgow, Glasgow, UK G12 8QQ*

Wallace F. Marshall (175), *Department of Biochemistry, University of California, San Francisco, San Francisco, California 94158*

Robert A. Smith (113), *Division of Neuroscience and Biomedical Systems, Institute of Biomedical and Life Sciences, University of Glasgow, Glasgow, UK G12 8QQ*

Kimberly A. Wemmer (175), *Department of Biochemistry, University of California, San Francisco, San Francisco, California 94158*

Katsutoshi Yoshizato (213), *Department of Biological Science, Graduate School of Science, Hiroshima University, Higashihiroshima, 739-8526, Japan*

Cell Proliferation in Pathogenesis of Esophagogastric Lesions in Pigs

Milijana Knežević, Sanja Aleksić-Kovačević, and Zoran Aleksić
Department of Pathology, Faculty of Veterinary Medicine,
University of Belgrade, 11000 Belgrade, Serbia

Esophagogastric ulcer is an independent disease in swine that is characterized by ulcerous autodigestion of the cutaneous mucosa, which does not exhibit a tendency to recover, but, on the contrary, a tendency toward severe hemorrhaging, with a predominantly lethal outcome. Since it develops in the part of the stomach that is morphologically and functionally different from other glandular mucosa, it was questioned earlier whether it could be a peptic ulcer based on its nature. Spontaneous ulcers, usually of the stomach, commonly occur in many domestic animals. Some of these lesions are chronic and they may occur in either the glandular or squamous-lined regions of the stomach. As with the human disease, the pathogenesis in domestic animals is multifactorial, poorly understood, and variable between and within species. Environmental stress and dietary factors are very important in the ulcer disease in swine. It has been shown that the *Helicobacter* spp. is strongly associated with naturally occurring ulcer and preulcer lesions of the pars esophagea in swine, which raises the possibility that *Helicobacter* spp. is an important factor in the pathogenesis of these lesions. The dynamics of the development of esophagogastric ulcers imply hyperplastic lesions (parakeratosis and hyperkeratosis), keratolysis, erosions, peptic necrosis, and the development of ulcers with all the characteristics of peptic ulcerations in other localities. In addition, K6 is expressed in association with the mucosal changes. The pattern of the intermediate filaments of keratin suggests that epithelial proliferation, which leads to visible hyperkeratosis, constitutes the essence of gastric ulcers in swine.
KEY WORDS: Swine, Esophagogastric ulcer, Parakeratosis, Hyperkeratosis, Keratin.   © 2007 Elsevier Inc.

I. Introduction

Esophagogastric ulcer is an independent disease in swine that is characterized by ulcerous autodigestion of the cutaneous mucosa, which does not exhibit a tendency to recover, but does exhibit a tendency toward severe hemorrhaging, with a predominantly lethal outcome. Since it develops in the part of the stomach that is morphologically and functionally different from other glandular mucosa, it was questioned earlier whether it could be a peptic ulcer based on its nature. These dilemmas stemmed from the belief that peptic ulcerations can develop only in the duodenum and the glandular part of the stomach. However, peptic ulcerations today imply ''holes in the mucosa'' in any part of the gastrointestinal tract that is exposed to acidopeptic secretion.

The morphological similarity between peptic ulcers in humans and in swine does not also imply an identical etiopathogenesis, although it can be assumed that there are certain common mechanisms of this multifactorial disease. With the exception of the epithelium, which has been affected (squamous stratified glandless epithelium of the esophageal region), all morphological manifestations are identical to peptic ulcerations in other animal species and in humans. It is known that peptic ulcerations in humans and other animals are usually localized in the duodenum, the first portion of the stomach, usually the antrum, at the gastroesophageal junction, in the setting of the gastroesophageal reflux or Barrett's esophagus, within the margins of a gastrojejunostomy, in the duodenum, stomach, and/or jejunum of patients with Zollinger–Ellison syndrome, and within or adjacent to an ileal Meckel diverticulum that contains ectopic gastric mucosa (Kumar *et al*., 2005), as opposed to swine, in which under natural and experimental conditions, ulcers predominantly develop in the pars esophagica. The most logical explanation for this localization is the fact that the squamous stratified epithelium of the esophageal part of the stomach of swine does not secrete mucoproteins, which weaken the natural mechanisms of defense from acidopeptic digestion.

An ulcer of the esophageal part of the swine stomach was described for the first time in the United States in 1951, which was followed by more intensive investigations of its incidence in countries all over the world. Data during that period indicate that ulcers were present in Belgium in 4.7% of all examined swine, in Ireland in 53% (Muggenburg *et al.*, 1964), and in the United States in 13.25–22% (Griffing, 1963). In Slovenia the incidence of this disease was followed in swine in intensive breeding conditions from 1963 until 1965, and a frequency of 0.9–12.68% was established (Šenk and Šabec, 1965).

Numerous papers report that the incidence of this ulcer is most frequent in swine with a body mass of 40–90 kg (Bisson, 1967; Kowalczyk, 1970; Šenk, 1978). However, there are also data on frequent findings of esophagogastric

ulcers in far younger swine, aged only 14 days (Curtin *et al.*, 1963), or on the occurrence of ulcers on the pars pylorica of newborn piglets (Rothenbacher *et al.*, 1963). According to certain references, ulcers are most frequent in swine with a body mass of up to 60 kg; this incidence declines in swine of 70–100 kg and again increases in swine with body mass over 100 kg.

It has been observed that ulcers appear more frequently in male than in female animals, and the ratio is 1:25. The percent representation of these changes is, according to certain investigations, 23.5% in males and 17.6% in females (Curtin *et al.*, 1963). It has also been claimed that the incidence of ulcers is not related to the sex of the animal (Aleksić, 1987; Guise *et al.*, 1997; Milić *et al.*, 1968; Muggenburg *et al.*, 1964; Olivier and Houix, 1969).

There is frequent disagreement regarding the influence of the breed of swine on the incidence and frequency of esophagogastric lesions in swine. Gastric ulcers have been established in swine of different breeds. More primitive breeds are more resistant (Lecompte, 1966), and it has been claimed (Aleksić, 1987; Curtin *et al.*, 1963) that breed has no influence on the appearance or frequency of esophagogastric ulcers.

Opinions of researchers are divided regarding the influence of the seasons of the year on the appearance or frequency of ulcers. According to some (Curtin *et al.*, 1963; Hoextra, 1967), they occur most frequently in the winter months, especially in December and January, although there are views that the season has no effect on the appearance of this disease (Aleksić, 1987; Šenk, 1978).

II. Morphofunctional Features of Swine Stomach

The shape of the swine stomach is sack-like and it is positioned sideways in the abdominal cavity. It has two different ends (the left or cardiac and the right or pyloric), two surfaces (cranial and caudal), and two edges (dorsal and ventral), and the **central** part—the corpus ventriculi. There are two openings on the stomach—the opening that links it to the esophagus, the ostium cardiacum, and the opening that leads to the small intestine, the ostium pyloricum. The cardia has a circular muscle (m. sphincter cardiae) and the pylorus has the m. sphincter pylori. The left side of the stomach is larger and more rounded, while the right side is smaller and narrower. The cranial surface is slightly extended and leans on the diaphragm and liver—the facies diaphragmatica. The caudal surface of the stomach is curved and leans on the intestines—the facies intestinales. The dorsal edge is concave and is marked as a small curve—the curvatura ventriculi minor, and it spreads between the esophagus and the duodenum. The ventral edge of the stomach, or the ventral curve, is extended, almost semicircular in shape, and larger, so that it is marked as

the big curve—the curvatura ventriculi major. The stomach is connected to neighboring organs through the esophagus to the diaphragm, to the dorsal abdominal wall, actually to the aorta, through blood vessels, and to the spleen, liver, and duodenum through the duplication of the peritoneum (Sison, 1962). Cutaneous and glandular mucosa of swine, as in most domestic animals, follows one another within this organ, which is why it is called a complex stomach—the ventriculus compositus. The part of the stomach that has cutaneous mucosa and that is located around the entry of the esophagus into the stomach is called the esophageal or prestomach part—the pars esophagica or proventricularis. The other part of the stomach, which is lined with glandular mucosa, is called the glandular or real stomach—the pars glandularis. The border between the two mucosa consists of a fold, and there is also a very visible difference in its color.

The gaster mucosa of swine has four regions. The initial esophageal part along the line of the big curve covers 3.13 cm, actually, depending on the size of the stomach, from 2.4–5.25 cm. There are no glandular elements in this region, while there is squamous stratified epithelium on the surface. The transition from this part into the cardiac area is marked by the appearance of glands that are spread across 8.5 cm (6.7–11.6). From the beginning of this zone, at a distance of 5.2–9.6 cm, there are bordering, and somewhat further also main cells, which mark the beginning of the fundus area that covers an average of 19.58 cm (14.2–23.8) of the big curve. Further on there is the pylorus, which imperceptibly turns into the duodenum (Petrosjan, 1975). Beginning from the cardia, up until the end of the stomach, the internal surface of this organ is covered with one row of cylindrical or prismatic cells that also coats the gastric foveolas. Numerous granules containing specific mucus have been discovered in the cytoplasm of these cells using cytochemical investigations (Panasjuk *et al.*, 1979). Surface cells of the stomach mucosa make up a very unstable cell population. It has been proven that the entire surface layer is replaced every 3–9 days. This regeneration is secured from immature cells located in the lower part of the crypt and in the neck of the fundic glands. A further characteristic of the superficial epithelium is its uniformity, which is why it is impossible to observe in certain morphological types of cells, on the grounds of which the chain of functional activity could be reconstructed (Panasjuk *et al.*, 1979).

The lamina propria of the stomach mucosa, in addition to cardiac and pyloric glands of predominantly mucous character, also contains the main glands in the fundus. The border, chief, mucous, and endocrine cells are located in them. Regarding the numerical ratio of these elements in the fundic glands of the swine stomach, data available so far are very scant, and sometimes even contradictory. While some (Keneth, 1975; Otto and Hugo, 1960) believe that they are equally represented along the entire length of the glandular tubule, others report that individual parietal cells are interspaced

between the primary ones, and that there is a slightly larger number of them in the upper and central third of the glands. According to Petrosjan (1975) parietal cells are not located individually, but in groups, closely adjacent to each other, so that they sometimes fill out the entire lumen of the tubule. The role of parietal cells also includes the secretion of HCl. Since these cells do not have the ability to multiply, their regeneration is secured from immature cells of the glandular necks.

The main cells are mostly located in the basal part of the gland. Their function is the synthesis and secretion of pepsinogen (Keneth, 1975). The origin of these cells has not been defined with certainty yet. Mucous cells of the stomach glands secrete mucoproteins that form a net in their physiological concentration. The net presents a viscous elastic gel that continuously lines the entire mucosa of the stomach, functioning like a barrier against numerous harmful agents (Allen *et al.*, 1984; Rokkjaer *et al.*, 1979; Turner *et al.*, 1985). Stanley and associates (1983) have demonstrated that mucins of the swine stomach are a very heterogeneous group according to both size and composition, and that they can be divided into two groups: one with a high content of sulfur and another with a lower content. Mucus glucoproteins have been isolated from the cardiac, fundic, and pyloric parts of the swine stomach. There was more mucin in the cardial and pylorus regions than in the fundus. The protein part of glucoproteins is characterized by a smaller content of threonine and serine in the following declining sequence: cardia, fundus, pylorus.

Based on hydrocarbon composition, five populations of mucins have been isolated from the region of the cardia, corpus, and antrum of the gastric mucosa in swine. Using gas chromatography and mass spectrometry, 30 different oligosaccharides have been described, composed of up to six monosaccharide units. One group of oligosaccharides in the central part contains Galβ1–3/GalNAcα1 and another with a Galβ1–3/GalNAcβ1–6/GalNAcα1 structure is widely represented, while oligosaccharides with a structure containing Ga1NAcβ1–3/GalNAcα1 are present in mucins of the cardia and corpus. An oligosaccharide unit composed of GalNAcβ1–3/GalNAcβ1–6/GalNAcα1 was found in cardia mucin. Gastric mucin of the swine contains large quantities of free fatty acids and cholesterol, as well as some sphingomyelin and phospholipids. As lipids have the ability to collect free radicals from oxygen, they maintain the stability of the mucoprotein viscosity within physiological limits. The main characteristics of the mucus from which their primary protective function is derived are adhesivity, viscosity, and the ability to absorb and neutralize acid. Most of these characteristics are conditioned by the presence of mucoproteins, which are an important component of mucus. The mucin population of the swine stomach is structurally diverse and it is determined as neutral (fucomucin) and more (sulfomucin) or less (sialomucin) acidic using histochemical methods.

Histochemical investigations of stomach mucins of mammals show that there are differences among them, both regarding topography, and also regarding animal species. In dogs, for instance, fuco-, sialo-, and sulfomucins have been established in the surface epithelium of the pylorus, while sulfomucins were established in the foveolas of these regions. In humans, fucomucins have been found in the superficial epithelium of the fundus and antrum, and sialomucins in gastric pits of these regions (Keneth, 1975).

Histochemical analysis of quantitative–qualitative relations between acid and neutral mucins in the stomach of healthy swine revealed differences in the regional distribution. At the cardiac level in the surface and foveolar epithelium there are only acid mucins, while glandular tubules contain exclusively neutral mucins. In the fundus, at the level of the surface and foveolar epithelium, there is a mixture of acid and neutral mucoproteins, and gastric glands contain only neutral ones. In the pylorus, mixtures of acid and neutral mucosubstances are evident at all three levels (Aleksić, 1987; Aleksić and Knežević, 1989a–c).

The swine stomach and intestinal mucosa also contain disseminated individual endocrine cells that lie directly on the basal membrane of the epithelium (Cetin, 1992; Kvetnoy *et al.*, 1997; Solcia *et al.*, 1995b; Zufarov *et al.*, 1978). According to general cytochemical and functional characteristics, they belong to a specific group of different cell types, which together form the so-called APUD system. A unique hypothesis on the existence of individual cells responsible for production and the secretion of polypeptide hormones was established by Pearse (1960). Investigations of the APUD system and its significance in the pathogenesis of ulcer and other diseases have been continued (Grube, 1976; Grube and Forssmann, 1978; Pearse, 1960; Pearse *et al.*, 1974, 1977).

Enteroendocrine cells stained using empirical methods are observed with light microscopy as different morphological forms localized along the basal membrane of the epithelium of the entire gastrointestinal tract . They are most numerous in the pars pylorica and the duodenum. Electron microscopic observations reveal their relatively light cytoplasm, small and wide mitochondria, and very developed microvilli. The most important characteristic of enteroendocrine cells is the morphology of their secretory granules. In addition to cells with polymorphic granules, of large electronic density, there are also cells with oval and round granules. The different appearance of the granules was earlier considered hypothetically as an equivalent to the different functions of endocrine cells, on the basis of which they were classified (Grube and Forssmann, 1978; Kretutzfeldt, 1970). Today, APUD cells are identified on the basis of the type of hormone that they produce (Kvetnoy *et al.*, 1997).

So far, G, ECL, EC, D, and A enteroendocrine cells have been established in different regions of the stomach. Each of them has the ability to synthesize a certain polypeptide hormone or biogenic amine.

Using classical hematoxylin and eosin staining, G cells have been described as "light" and triangular, with a large ovoid nuclei (Solcia *et al.*, 1969), whose topographic distribution depends on the biological species, so that they are most numerous in the mammals examined in the antropyloric mucosa (Bussolati and Canese, 1972; Bussolati and Monga, 1973; Bussolati and Pearse, 1970; Larsson, 1975; Vassallo *et al.*, 1969, 1971). They are also present in substantial numbers in the duodenum of the cat, the dog, and in humans (Solcia *et al.*, 1975). In the mouse, rat, and rabbit, G cells are localized in the basal half of the antropyloric mucosa, while in the cat, dog, and humans, they are located in the central part of the glandular zone of this region (Solcia *et al.*, 1975). Using immunocytochemical analysis (peroxidase–antiperoxidase) in sections of stomachs of healthy swine, it was established that G cells are located mostly along the central zone of the antral mucosa. They are located in the surface epithelium and pyloric glands, individually or in groups, interspersed between other glandular cells. The average number of G cells in the pylorus of healthy swine amounts to 9.27 (Knežević *et al.*, 1994).

The number of G cells/mm^2 was similar in swine with or without esophagogastric ulcer. Investigations of the level of serum gastrin did not reveal significant differences between swine with and those without this ulcer (Silva *et al.*, 2002). Today, it is certain that this type of cell secretes gastrin, whose experimental effect depends on the size of the applied dose. Small doses stimulate secretion of water and electrolytes at the level of the stomach, pancreas, and Brunner glands and the contraction of the cardiac sphincter and the stomach muscle. At the same time, gastrin inhibits the tonus of the sphincter of Oddi and the absorption of water and electrolytes in the ileum. Furthermore, it increases the blood flow through the stomach mucosa, releases histamine, and induces the activity of histidine decarboxylases in the stomach mucosa. Large doses of gastrin have a trophic effect on cells of the stomach mucosa, as well as a stimulative effect on the smooth muscles of the intestines, the gallbladder, and the uterus. In humans with a stomach peptic ulcer, the number of G cells is extremely reduced, which points to their role in the complex etiopathogenesis of these diseases (Katić, 1979). In swine with experimentally induced lesions in the esophagogastric region, it has been proven that the number of G cells is reduced in comparison with their number in healthy animals (Knežević *et al.*, 1994).

Ultrastructural investigations have resulted in the identification of two (Bordi *et al.*, 1995) and three (Solcia *et al.*, 1995a; Valverde *et al.*, 1993) types of endocrine cells, which have been marked, depending on their presence in certain parts of the gastrointestinal tract, as stomach, intestinal, and duodenal. The stomach type of endocrine cells is elongated in shape with small rodlike and pear-shaped granules, which are set parallel to the basal membrane and are of an open type (Katić, 1979). In humans, they are localized in the pyloric glands and immediately adjacent to the lamina muscularis of the mucosa. They

are uniformly wedge-shaped with a narrow cytoplasmatic edge. Their number is most often reduced in humans with a stomach ulcer (Katić, 1979). Intestinal endocrine cells are large, pyramidal, or bottle-shaped, with a greater quantity of granules that are somewhat larger localized in all parts of the intestine (Sasagawa *et al.*, 1974). In the stomach antrum mucosa of humans with a stomach ulcer, their number is significantly increased with the almost complete disappearance of G cells (Katić, 1979). The third duodenal type of endocrine cells contains large irregular (ovoid or angular) granules, pyramidal or bottle-shaped. Using cytochemical methods, 5-hydroxytryptamine (5-HT) was discovered in very small quantities in granules of endocrine cells. It is believed that this biogenic amine has a role in the control of stomach secretion by inhibiting the secretion of acidogen (Wise, 1974). Its stimulative effect on mucin secretion and its effect on the smooth muscles and tonus of blood vessels are also known.

Sections of fundic mucosa of stomachs of healthy swine reveal enteroendocrine cells of different morphology, along the entire length of the gastric glands. The most numerous shapes of these cells are dark brown to black stained granules that completely mask the nucleus, the largest in size, round-shaped, with marginally distributed dark stained granules, with a centrally placed nucleus. Spindle-shaped, slightly less stained than the previous cells, which are dominant according to their presence are elliptical with extremely dark brown stained granules. All endocrine cells are located between other glandular elements and are mostly placed along the basal membrane. Most of them are concentrated at the basal portion and in the body of the gastric glandules.

Histochemical analysis of sections of the pyloric region of stomachs of healthy swine shows endocrine cellular elements deeply dispersed in the lower and central third of the pyloric glands. Cells of round and roundish shape are predominant, with clearly expressed granules in the cytoplasm, filling out the contours of the cell membrane, sometimes completely giving them the appearance of homogeneous black cells. Most often, the number of granules is smaller and they are lightly stained, making the cell appear transparent. In some cases, the granules are concentrated at the poles, similar in appearance to polar caps.

Stereometric processing showed an average of 25.85 cells/mm^2 of fundus, and 38.28 endocrine cells in the pylorus (Grimelius positive). A significantly greater number of endocrine cells was discovered in the pylorus than in the fundus ($p < 0.001$) (Aleksić, 1987; Aleksić *et al.*, 1993; Knežević *et al.*, 1994).

Stereometric analysis of a series of sections of the stomach mucosa of swine with spontaneous ulcers showed an average of 18.69 Grimelius-positive cells/mm^2 of fundus, and 25.85 on the pylorus. A significantly smaller number of endocrine cells was also established in the fundus ($p < 0.005$) and

in the pylorus ($p < 0.001$) in the stomachs of these swine in comparison with controls (Aleksić, 1987; Aleksić *et al.*, 1993; Knežević *et al.*, 1994).

Stereometric analysis of a series of sections of the stomach mucosa of swine with experimentally induced ulcers showed 30.47 endocrine cells/mm^2 of fundus, and 27.04 cells in the pylorus. No statistically significant differences were established in the number of these cell elements in the fundus of this group ($p < 0.05$) versus the control. Significance was established in the pylorus ($p < 0.001$) (Aleksić, 1987; Aleksić *et al.*, 1993).

The precise role of hormones in the regulation of glandular mobility has not been completely elucidated yet. It seems that gastrin, which is secreted by pylorus cells, increases the motility of the stomach. Cholecystokinin, secretin, and gastric inhibitory peptide suppress gastric motility.

Gastric secretions are produced by gastric glands and epithelial cells of the stomach mucosa. It is composed of water, K^+, Na^+, Mg^{2+}, H^+, Cl^-, HPO_4^{2-}, SO_4^{2-}, pepsinogen, labferment, lipase, protective mucins, and the internal factor. When gastric glands are maximally stimulated they secrete a solution of HCl of pH 1 into the lumen. Hydrogen and chloride ions are secreted by parietal cells through different cellular mechanisms. Hydrogen is secreted through primary active transport with the help of the H^+/K^+-ATPase pump, which is located on the luminal side of parietal cells. This enzyme replaces a hydrogen ion with one K^+ ion by ejecting one hydrogen for every potassium, which returns from the stomach lumen to the cytoplasm of parietal cells. As K^+ ions are accumulated in the cell by a passive mechanism they return to the stomach lumen, which is known as potassium recirculation. Chloride ions originating from blood also passively enter the stomach lumen. For each hydrogen ion that is secreted into the stomach lumen, one bicarbonate ion leaves the cell and returns into the circulation. Chloride ions at the same time return to parietal cells through an antiport mechanism. Carbon acid originates from enzyme activities of carbonic anhydrase, which is present in a high concentration in the gastric mucosa. As in other cells, the Na/K-ATPase pump is active in the basal part of parietal cells (Cuningham, 1992).

Pepsin is usually marked as one enzyme, even though it is in fact a group of proteases that is secreted by gastric glands. They are formed in the main cells in the form of the proenzyme pepsinogen. Pepsinogens are deposited in granules of the main cells until secreted into the stomach lumen, where they are activated under the activity of hydrogen ions. The presence of inactive proenzymes is necessary because active enzymes could destroy the cell that synthesized them. Gastric gland secretion is stimulated by the intake of food, as well as the presence of undigested content in the stomach. When the animal begins to eat, parasympathetic vagus impulses stimulate cells of the intramural gastrointestinal nervous system, and acetylcholine is released near parietal and G cells. These cells have, on their surface, acetylcholine

receptors and respond by secreting gastrin and HCl. Through blood, gastrin (the endocrine effect) reaches parietal cells, which also have gastrin receptors. A combined effect of gastrin and acetylcholine on parietal cells leads to the secretion of large quantities of HCl. Monitoring of the level of plasmatic gastrin and pepsinogen in swine with hyperplasia of the epithelium and ulcerations of the pars esophagica did not reveal any differences in comparison with healthy swine (Bunn *et al.*, 1981). However, in cases with parakeratosis, erosions and ulcerations in the esophageal region show increased concentrations of pepsinogen in serum (Nappert *et al.*, 1990).

The role of histamine in HCl secretion is still not sufficiently clear. It is released by mast cells of the stomach mucosa under the effects of gastrin and acetylcholine. Parietal cells also contain Hl and H2 receptors, which means that their secretion is stimulated by three mediators—acetylcholine, gastrin, and histamine. The secretion of pepsinogen seems to be under the same regulatory effects as the secretion of HCl.

III. Esophagogastric Ulcer in Swine

A. Etiology and Pathogenesis

The most numerous investigations pertain to the role of food and its individual components in the development of esophagogastric ulcers. It was mostly attempted under experimental conditions to provoke an ulcer using certain ingredients of a fodder mix, or to determine which feed component prevents or eases the appearance of ulcerous processes. Some of the first papers published in this area concluded that food can have an effect on the appearance of an ulcer (Fugate *et al.*, 1965; Mahan *et al.*, 1966a; Nuner *et al.*, 1966; Perry *et al.*, 1962; Resse *et al.*, 1966). Data presented later also concur with these findings, and the causes should not be sought in the composition of the food itself, but rather in the form in which it is administered, especially regarding the size of its granules (Baustad and Nafstad, 1969; Dirrsen, 1964; Ehrensperger *et al.*, 1976; Fugate *et al.*, 1965; Lengnick, 1972; Mahan *et al.*, 1966b; Mastronardi, 1964; Perry *et al.*, 1962; Pococov *et al.*, 1968; Reimann *et al.*, 1967). A diet of finely ground and floury feed with large numbers of tiny granules, as well as with feed in pellet form, favors the appearance of keratinization of the esophageal mucosa and the creation of erosions. According to the latest research in swine with frequent keratinization of the mucosa and ulcers in the esophagogastric part, 90% of the feed, regardless of how the ration is composed, has a floury structure with a radius of the granules of less than 1.5 mm (Larenaudie *et al.*, 1966; Lengnick, 1972; Wondra *et al.*, 1995). On farms where medium-sized granules of 1.5 mm and

larger account for at least 3% of the feed, and finely ground granules for 96%, changes in the cutaneous mucosa of the stomach are the most frequent and of the gravest form. However, if the feed contains a larger part of rougher granules, changes in the esophageal part of the stomach have been observed less frequently. The size of the granule determines its disintegration in the stomach. If the food fails to contain a sufficient number of rough and coarse fragments there is no natural wasting and renewal of the epithelium of the cutaneous mucosa of the proventricular part of the stomach. Furthermore, food of very fine structure passes the gaster more quickly so that there are no mechanical factors responsible for the shedding and renewing of the epithelium. Perhaps this could explain the excessive keratinization of the stomach mucosa, and primarily of its esophageal part (Elbers *et al.*, 1995; Lengnick, 1972). The disorders in the keratinization could be a consequence of long-term acidosis connected to the chemical processes of digestion under the influence of stomach juices and microbiotic activities. Disrupted keratinization, as it is known, does not necessarily lead to the appearance of an ulcer, even though most researchers consider it as its initial stage.

Microbiological investigations of material from the ulcer have shown that there are often fungi of the *Candida* species present, which has led to the conclusion that they could be the possible cause of the appearance of an ulcer (Curtin *et al.*, 1963; Ehrensperger *et al.*, 1976; Griffing, 1963; Hunziker and Nicolet, 1968b). Experimental works have proven that *Candida albicans* presents as a normal member of the stomach flora of swine (Griffing, 1963; Kadel *et al.*, 1969; Smith, 1976), as well as that the injection of its pure culture in the course of 49 days did not reveal the appearance of any lesions in the esophagogastric region (Stenham *et al.*, 1967). Even though one study discovered the presence of fungi of the genus *Candida* in the parakeratotic layer in ulcerous lesions and detritus in peptic necrosis, they have not been given any importance in the morphogenesis of the ulcer (Šenk, 1978). Colonization by the spiral bacteria *Helicobacter* type 1 or *Gastrospirilum suis* was established in swine with spontaneous peptic ulcerations in the pars esophagica (Mall *et al.*, 2004; Szeredi *et al.*, 2005). Even though these microorganisms do not invade pars esophagica cells and do not perform toxic destruction of the cellular elements, a role in the pathogenesis of lesions has been attributed to them. These microorganisms have been established in 100% of examined swine that had a developed ulcer and in 90% of swine with preulcerous lesions (hyperkeratosis) (Barbosa *et al.*, 1995; Krakowka *et al.*, 1995, 2005a,b; Querioz *et al.*, 1996; Suarez *et al.*, 1997). One possibility for the ulcerogenic effect of bacteria could be their ability to create lower fatty acids. Nondissociated lower fatty acids quickly pass through the outer barrier of the stomach mucosa and increase the acidity of the stomach mucosa. Cellular acidification inhibits the Na pump and osmoregulation, which leads to cellular edema and necrosis (Argenzio and Eisemann, 1996).

The effect of certain vitamins on the etiopathogenesis of lesions in the esophageal region has been examined. Thus, it has been reported for vitamins A and D that they have a protective role (Larenaudie *et al.*, 1966), and for vitamins E and K that, when added to food or applied intramuscularly, they prevent the development of erosions in the stomach mucosa (Coates *et al.*, 1998; Hannan and Nyhan, 1962). The latest investigations have shown that the administration of melatonin in feed (5 mg/kg feed) significantly reduces the frequency of the incidence of esophagogastric ulcer in swine (Bubenik *et al.*, 1998).

An especially interesting group of investigations, which deal with the etiopathogenesis of this disease, involve the effects of different technological procedures in the industrial maintenance of swine. This deals particularly with the type of maintenance conditions, the accommodation facilities for the animals, their treatment, and the like. It has been emphasized that a stomach ulcer develops in swine, as the ulcer in humans, under the effect of stress. In contemporary breeding conditions, swine are exposed to numerous nonspecific irritants, which causes them to feel anxiety, tension, fear, pain, and so on (Benčević, 1972; Hunziker and Nicolet, 1968a; Kowalczyk and Muggenburg, 1963; Milić *et al.*, 1968; Šabec *et al.*, 1971; Tournut and Lebie, 1970). This acts as a stress factor of a psychosomatic and physical nature, demanding the occasional or permanent adapting of the animal to the given conditions of the environment and its frequent changes. Esophagogastric ulcers should therefore be classified in the group of diseases whose causes are a consequence of a general syndrome of adapting. More recent literature warns against an entire series of possible nonspecific factors for which it has been proven, or it is believed, that they considerably increase the incidence of ulcers. The observations deal with stress situations caused by limited living conditions (Curtin *et al.*, 1963; Handlin *et al.*, 1972; Kowalczyk and Muggenburg, 1963; Larenaudie *et al.*, 1966; Muggenburg *et al.*, 1971; Resse *et al.*, 1966). Changes in temperature and atmospheric conditions of the environment (Curtin *et al.*, 1963), transportation, the stay in the depot prior to slaughter, the mixing of animals that are not familiar with each other, and a new unknown environment are also dealt with (Hoextra and Grummer, 1967; Kowalczyk, 1970; Resse *et al.*, 1966; Tournut *et al.*, 1966). Especially prominent are the experimental works by researchers from France, who have observed significant changes in the digestive tract of piglets forcibly immobilized with the help of a special device (Labie *et al.*, 1966; Le Bars and Tournut, 1962; Tournut *et al.*, 1966). Changes of the ulcer type have been established in the mucosa of their stomachs.

In swine with esophagogastric ulcers, neuroendocrine regulation has been disrupted in the sense that there is a reduced secretion of the thyreotropic hormone of the adenohypophysis, triiodothyronine and thyroxine of the thyroid gland, and increased secretion of cortisone. Since there is an

increased secretion of corticotropin at the expense of thyreotropin under conditions of stress, and they are both under the control of the hypothalamus, the described changes in endocrine correlation could be interpreted as a contribution to evidence that neurostress is very important in the etiopathogenesis of ulcer disease (Simov, 1977).

To understand the etiology of the stomach ulcer in swine, the significance of excess acidity of stomach juice was investigated (Huber and Wallin, 1967; Muggenburg et al., 1966b). Imitating histamine secretion in stress conditions, it was applied in a dose of 2.5 mg/kg body mass of swine, inducing great ulcers in the esophageal part of the stomach (Kokue et al., 1981; Muggenburg et al., 1966b). The same effect was obtained with the intramuscular application of reserpine in quantities of at least 0.055 mg/kg body mass, during 15, or 14 and 21 days (Aleksić, 1987; Aleksić and Knežević, 1989a; Muggenburg et al., 1966a), or with the parallel administration of histamine and reserpine (Muggenburg et al., 1967). It was shown that histamine and reserpine considerably increase the secretion of HCl, thus lowering the pH of the stomach content. Throughout this, pepsin activity is not altered, or it is increased as well. It is believed that the ulcerogenic effect of reserpine is mostly based on the lesions that it causes in the diencephalon (Mastronardi, 1964), which in yet another way confirms the assumption about the role of neurovegetative disorders in the etiopathogenesis of the ulcer (Hunziker and Nicolet, 1968b; Simov, 1977). In addition to histamine and reserpine, sodium salicylate also causes lesions in the pars esophagica (Petrosjan et al., 1976). Prednisolone, as well as the binding of the pylorus in experimental conditions, also leads to the appearance of an ulcer (Nelson, 1966).

There is irrefutable evidence that the decreased secretion of stomach mucus and changes in its composition have a role in the occurrence of esophagogastric ulcers in swine. A histochemical analysis of the distribution and qualitative–quantitative relations of mucin in the normal gastric mucus of humans has proven the increased presence of neutral mucins in the surface epithelium of the fundic (corpus) mucosa and the antrum, in the upper half of the foveolar epithelium of the same region, as well as in the pyloric glands, while a smaller presence was observed in the lower half of the foveolas, and somewhat higher quantities in the neck part of the corpus glands. Gaster mucosa in humans with a stomach ulcer was found to contain a smaller reduction of fucomucin in 60% of patients, while mucins in traces were present in 7% of the studied patients (Katić, 1979).

The question of the pathways for the occurrence of increased viscosity of mucin in the swine stomach has not been fully explained yet because of the numerous contradictory data that have been obtained. There is no doubt that the mucin viscosity is altered with the reduction of the pH value of the stomach juices. It increases up to 100 times, which indicates the physiological importance of the changes in the rheological characteristics of mucus.

This is one of the ways in which mucins protect the stomach mucosa when pH values are low. It remains an outstanding issue whether the formation of extremely large aggregates of mucus glycoproteins at pH values that go down to 2 or 1 is a result of the merging of polypeptide components of proteoglucan, of a molecular mass of 2.54×10^6 and 1.5×10^6 Da (Bennett and McLean, 1985; Bhaskar *et al.*, 1991), or whether it is a matter of carbohydrate reactions that cause aggregation (Sellers and Allen, 1989). A binding peptide is also probably involved in this process, which is a glycopeptide. This protein has been found in mucins of the gastrointestinal tract, including the salivary glands, the stomach, intestine, and colon. Its molecular mass is 118 kDa, and it enables mucin polymerization by forming disulfide bridges between mucin glycoprotein subunits (Roberton *et al.*, 1989). Polymerized gastric mucins cover the stomach mucosa, protecting it from the harmful effects of acid, proteases, and in particular, pepsin and bile salts. An important common characteristic of mucins is the ability to bind lipids. Bound lipids collect free radicals of oxygen. Gastric mucins of swine contain large quantities of free fatty acids and cholesterol, as well as some sphingomyelin and phospholipids. The iron/ascorbate system creates free radicals of oxygen, which reduce the specific viscosity of mucins by more than 50% (Grisham *et al.*, 1987). Excessive production of oxygen radicals can be inhibited by catalases, deferoxamine, and mannitol, while superoxide dismutase has no effect. In the event the mucins are purified, actually freed of the fatty acids, the oxygen metabolites have no effect, which shows that bound lipids protect the surface of the stomach mucosa from depolymerization of native mucins (Fouad *et al.*, 1993; Gong *et al.*, 1990). In swine with experimentally induced esophagogastric ulcerations, there was a higher protein content in the mucus in comparison with healthy swine, and a reduced amount of *N*-acetylgalactosamine and fucosis (Mall *et al.*, 1997).

In the appearance of peptic ulcerations, it is possible that changes in the regenerative ability of mucosa cells in the stomach and intestines can play a certain role. Here, the primary reference is to the disorders in the control of proliferation, differentiation, and migration of gastric epithelial cells. These disorders can be a result of genetic factors or factors of the environment. Among the local factors that can be considered are the diet, microcirculation, and growth factors (Kawai and Rokutan, 1995; Šabec *et al.*, 1967).

The present understanding of the etiopathogenesis of ulcers is based on the fact that the essential reason for the appearance of lesions is actually the disturbed relations between so-called aggressive and defensive factors of the stomach mucosa. The aggressive factors include stomach acid and proteolytic ferments, while mucins and the great regenerative power of the surface epithelium present defensive factors (Curtin, 1966; Palavicin *et al.*, 1971).

Histochemical analyses of stomachs of swine with spontaneous esophagogastric ulcers show a considerably reduced total amount of mucins,

even though no differences have been established in the qualitative distribution of acid and neutral mucoproteins (Aleksić, 1987; Aleksić and Knežević, 1989c).

In stomachs of swine with experimentally induced lesions in the esophageal region (reserpine), the amount of total mucins is greater than in the stomachs of healthy animals. The quantity of established mucins is also greater in comparison with the stomachs of swine with spontaneously developed ulcers. Even though the total amount of mucins is increased, neutral mucins were not established at the level of the foveolar epithelium of the fundus (Aleksić, 1987; Aleksić and Knežević, 1989b).

B. Pathomorphological Findings

1. Macroscopic Findings

Since the pathomorphological picture of possible changes in the pars proventricularis in the presence of an ulcer is not unique, it follows that the reviewed literature dealing with this matter provides very diverse data. Nevertheless, most studies divide all alterations into three groups: acute erosions, subacute ulcers, and chronic ulcers (Kretutzfeldt, 1970; Šenk and Šabec, 1965).

Due to the desquamation of the epithelium, the areals of papilla propria remain bare, and their conflation results in the occurrence of acute erosions. Their size varies, and ranges from those hardly noticeable, 0.2 cm in diameter, to the largest ones, 2 cm in diameter. They are irregular in shape and often elongated or egg-shaped. Their base is covered with pseudomembranes, dark brown in color from ingredients from the blood, or reddish due to local hyperemia. They are most often surrounded by a yellow-gray rough hyperkeratotic surface (Thoonen and Hoorens, 1963a) (Fig. 1).

Subacute ulcers are flat, larger, and have deeper defects in the esophagogastric region from erosions, from 0.5–4 cm in diameter. They are mostly inflamed and oval or crescent shaped in appearance. Their bottom is covered with necrotic sediments under which is a layer of edematous granulation tissue, light pink in color (Thoonen and Hoorens, 1963b).

Chronic ulcers are deep defects in the mucosa, clearly defined from the surrounding unchanged tissue with a sharp edge that rises above the ulcer crater. They are most often round or irregularly ovoid in shape and of different dimensions (Fedorov *et al.*, 1977; Petrosjan, 1975). Their size depends on the age of the animal. In younger animals, it reaches the dimensions of a child's palm (4–5 × 4–6 cm); in older animals they can be up to 8 × 9 cm (Šenk and Šabec, 1965). They often cover the entire esophageal area. Their base is dark gray in color and in folds.
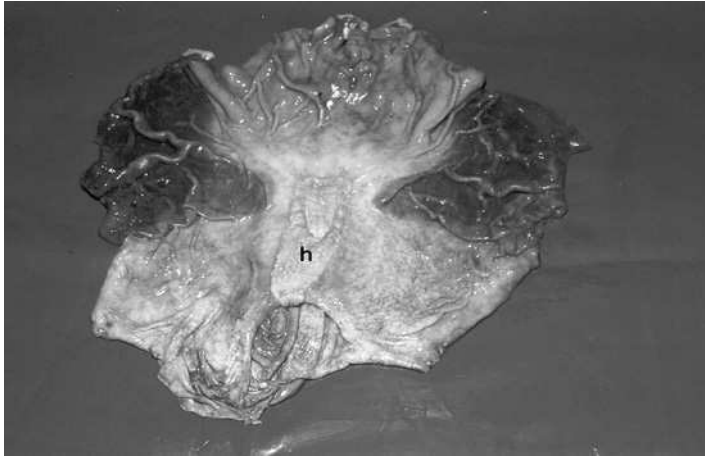
FIG. 1   Gaster of pig, hyperkeratosis (h).

Based on examinations of large numbers of pigs with esophagogastric ulcers who died spontaneously, it can be said that they basically have the same macroscopic and microscopic appearance. There are usually round or oval defects in the mucosa that penetrate at least into the submucosa, usually to the muscularis, and sometimes even deeper. They are clearly separated from the other, unchanged, parts of the mucosa, and have sharp or slightly rounded edges that are higher than the ulcer crater. The base of the ulcer is uneven, and it is covered with pseudomembranes or coagulum residue of dark brown color. They are from 4×6 cm–8×10 cm in diameter, sometimes covering the entire area of the cutaneous mucus. The depth of the ulcer differs from case to case, and ranges within the limits of 3–6 mm. Sometimes, the ulcer crater penetrates the stomach wall, leading to localized or generalized peritonitis, or perforation of the neighboring tissue structure, such as the omentum, liver, or pancreas (Aleksić, 1987) (Fig. 2).

Under experimental conditions, intramuscular application of reserpine in quantities of 0.055 mg/kg body mass for 14 days caused lesions in the esophagogastric mucus in swine. In a number of cases, a surface defect was observed, localized in the central part of the cutaneous region. One was of irregular roundish shape, with dimensions of 4×5 mm, about 2 mm deep, with a bright pink base and almost invisible borders that limit it from the unchanged mucosa. In another case, a somewhat larger defect was discovered, about 8 mm long and 2 mm deep, with a rough surface on the base that was light pink in color. Swine to which administration of reserpine was continued until day 21 showed dark yellow warty deposits in the esophageal region—hyperkeratosis, diffusely distributed along the entire surface of
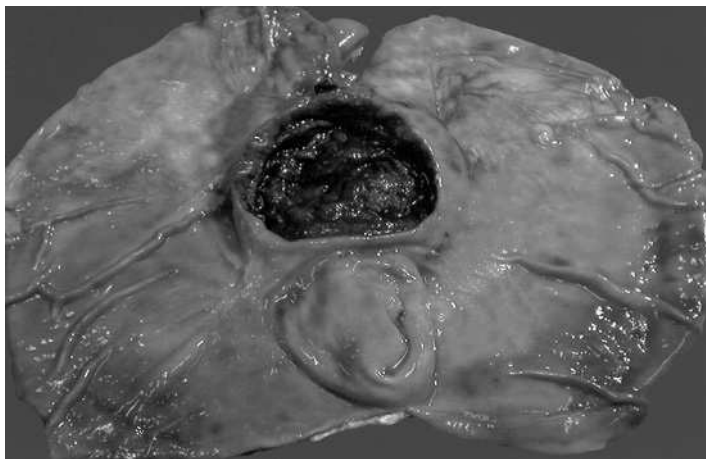
FIG. 2   Gaster of pig, esophagogastric ulcer.

the cutaneous mucosa, making it similar in appearance to the bark of an oak tree. Between the hyperkeratotic deposits there was discrete damage to the mucosa, bright red in color and 3–6 mm in length (Aleksić, 1987).

2. Microscopic Findings

Investigations of histological changes in the pars esophagica have been the subject of numerous studies, starting from the very first descriptions of esophagogastric ulcer to the present day. The large number of data from the literature in this area are at the same time very heterogenic regarding the systematization of the observed changes. Nevertheless, most studies indicate that three basic groups of changes can be described, depending on the nature of the alteration in the esophageal region: (1) preulcerous-parakeratotic keratinization of the mucosa, (2) erosive-ulcerous lesions, and (3) postulcerous and residual alterations (Aleksić, 1987; Ehrensperger, 1974; Hänichen, 1975; Penny *et al.*, 1972; Petrosjan *et al.*, 1976; Ristoski, 1999; Rothenbacher, 1965; Ryaszkowaki and Gambara, 1976; Šenk, 1969; Šenk and Šabec, 1967; Thoonen and Hoorens, 1963).

    In more recent times, certain researchers have given more detailed descriptions of these changes in their papers, depending on quantitative–qualitative alterations in the mucosa of the proventricular part. Within preulcerous-prekeratotic changes, two types are evident, depending on the degree of damage. The first type includes cases in which the stratified squamous epithelium is of normal thickness and without signs of proliferation, but with the simultaneous appearance of a thin layer on the surface—keratinization with

parakeratosis. The other type covers changes that are reflected in a thickening of the stratified epithelium at the expense of multiplication of cells of the stratum spinosum (acanthosis) with hyperkeratosis and parakeratosis on the surface. Within this type, and based on the degree of keratinization of the stratified squamous epithelium, the following is prominent: (1) keratinization of a smaller degree—moderate hyperplasia of the epithelium (the tips of the papillary shoots reach the chromophobic layer of epithelial cells); (2) keratinization of a higher degree—intensive hyperplasia of the epithelium with stronger keratinization on the surface (the stratified squamous epithelium is thickened and partly shedding; the papillary layer of the propria reaches deep into the epithelium); there is a thick dense layer of squamous keratinized cells with a nucleus on the surface—parakeratosis; (3) extreme hyperplasia of the epithelium with intensive keratinization and the appearance of microerosions (Fig. 3).

This degree presents a transition between preulcerous and erosive-ulcerous changes. Alterations in the epithelium are similar as in the previous two degrees, and they differ from these in that the surface of the hyperkeratotic layer shows keratotic processes, uncovering the papillary bodies and causing the appearance of microlesions (Šenk, 1978).

Pathological alterations of the stratified squamous epithelium of the pars proventricularis have been described as atypical hyperkeratosis (Kowalczyk, 1969), parakeratosis, pseudokeratosis (Benčević, 1972), or dyskeratosis (Lengnick, 1972). Furthermore, ballooning degeneration of cells of the stratum spinosum has also been described, which, together with dyskeratosis,
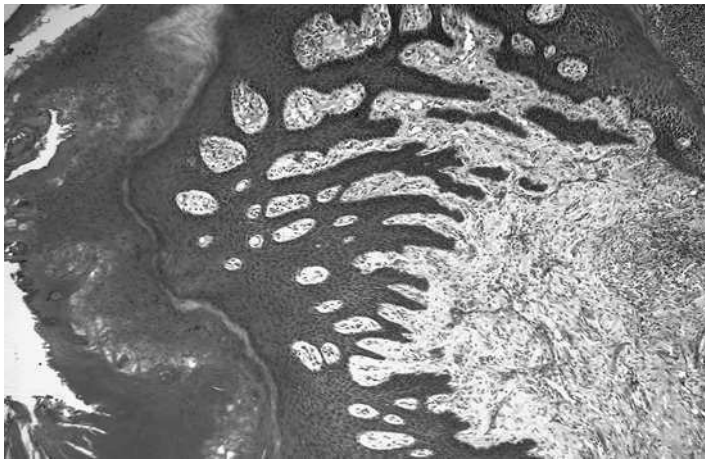
FIG. 3   Gaster of pig, pars esophagica, huge hyperkeratosis deposits. H&E, ×200.

leads to a thickening of the cutaneous mucosa, making it very hard and yellow-brown in color.

Histological examinations of the region of the stomach with spontaneously developed ulcers showed identical changes in all cases. The preserved cutaneous mucosa shows thick nonstructural homogeneous hyperkeratotic sediments. Although rarely, groups of vacuolized cells of the stratum spinosum can be seen in this mass, giving it the appearance of cartilaginous tissue. Thorny shoots of the papillary bodies are placed deep inside the propria, sometimes even reaching the submucosa. In places where there are breaks in the continuity of the hyperkeratotic layer, shallower or deeper defects can be seen, which always cross the lamina muscularis of the mucosa, shaped like a volcanic crater whose edges go down to the base. In certain cases, the base and edges of such defects are covered by a layer of necrotized tissue under which a reactive inflammation is observed. In closer or further proximity of the ulcus, mature connective tissue is regularly observed, permeated with a tiny-cellular infiltrate and clearly differentiated fatty tissue. The walls of the blood vessels in the zone of the ulcerous defect, as in the other parts of the stomach wall, are thickened and frayed. It is especially difficult to observe them in the area of the scar connective tissue when their contours merge with the environment without any clear borders. The lumen of such altered blood vessels is reduced as a result of obliteration. In addition, blood vessels with thrombs in organization can also be seen (Aleksić, 1987) (Fig. 4).

Under experimental conditions, following intramuscular application of reserpine in quantities of 0.055 mg/kg body mass over a period of 14 days,
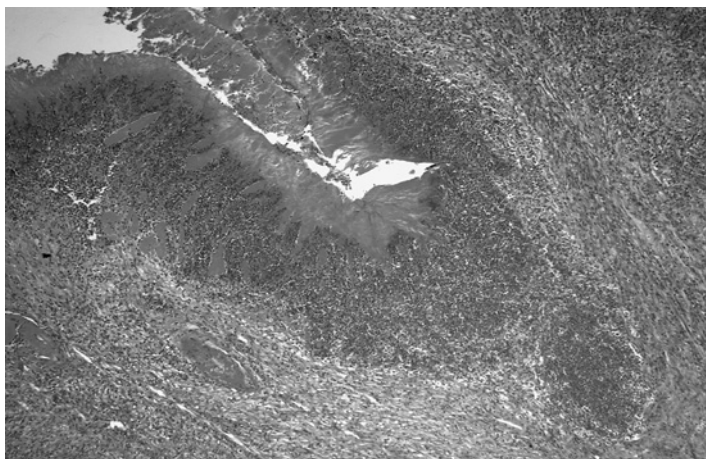
FIG. 4   Gaster of pig, erosion with secondary inflammatory reaction (microabscess). H&E, ×200.

intensive proliferation of papillary bodies of the propria is observed, with spreading to the lamina muscularis of the mucosa. The surface of the epithelium shows a hyperkeratotic layer of different thickness, which is so reduced due to keratolytic processes that the papillary shoots of the propria are completely bare—microulcerations. Sites of deeper effects are characterized by the absence of tissue of the papillary body. The base of such shallower or deeper defects formed in this way consists of a partially narrow necrotic zone under which there is connective tissue rich in tiny roundish cells with very little connective tissue, which can be seen especially clearly in sections stained with selective methods. The propria of the mucosa around the defect, as well as the submucosa, show inflammable cellular infiltrates of diffuse or focal character. Thus formed cellular infiltrates are also often observed in the starting part of the cardiac zone of the stomach, especially along the very edge of the defect. Blood vessels, as a rule, have thickened walls and are hyperemic (Aleksić, 1987).

In one study, immunohistochemical staining with Ki67 (clone MIBI) and AgNOR protein silver staining were used to evaluate, by means of image analysis, cell proliferation in normal and parakeratotic (parakeratotic hyperkeratosis) epithelia of the pars esophagea. Apoptotic activity was also assessed with the TUNEL assay and compared with cell proliferative parameters. Early lesions of the pars esophagea were characterized by a significant increase in epithelial proliferative activity, while there was no difference in apoptotic activity between normal and parakeratotic epithelia (Preziosi *et al.*, 2000).

Histopathological examinations of erosions and ulcerations accompanied by hyperkeratotic changes have led to the conclusion that erosions occur directly from the hyperkeratotic changes in the cutaneous mucosa. The latest investigations indicate that the epithelium of the pars esophagica of the swine stomach is more sensitive to irritating effects of acid stomach content because of the changes in keratin expression. The keratin pairs K4/K13 are present both in normal and in damaged epithelium and their expression in both states is the same. K4 and K13 are expressed in all suprabasal cells, and K5 and K14 only in basal and epibasal cells. K6 is a significant marker of epithelial proliferation and its expression is increased due to hyperkeratosis. Intermediary keratin filaments indicate that epithelial proliferation, which leads to visible hyperkeratosis, is the fundamental element in gastric ulcers in swine (Ristoski *et al.*, 2001; Roels *et al.*, 1997) (Fig. 5).

Even though hyperkeratosis is definitely considered a preulcerous lesion, the factors that cause it are still unknown. Activities by aggressive factors of the stomach juice (pepsinogen, HCl) lead to the destruction of the keratinized layer of the epithelium of the pars esophagica, uncovering the tips of the papilla and the upper layers of the epithelium. These tips are unprotected from mechanical and chemical effects of the stomach content, which causes
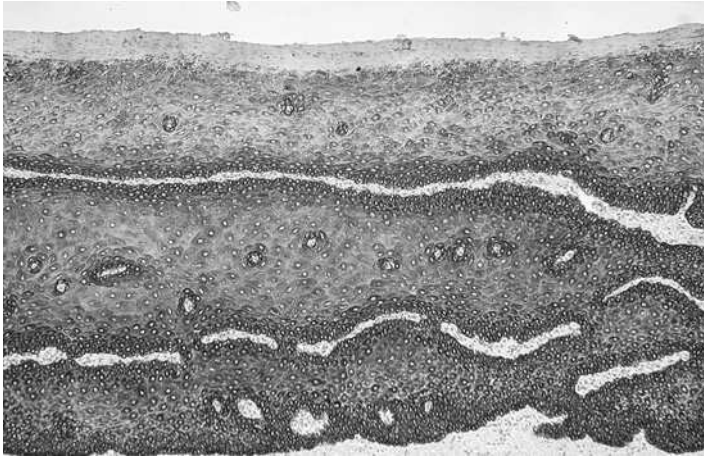
FIG. 5 Gaster of pig, pars esophagica, keratin's pattern in hyperkeratosis, DP-anticytokeratin, ×100.

tissue reactions among which hyperemia and papillary corpus edema dominate. Consequently, papillae swell even more, becoming more exposed to the effects of the aggressive factors that cause surface necrosis. This is, at the beginning, limited only to the tips of the papilla, but later penetrate deeper into the tissue. In that way, microscopically visible erosions, microerosions, are formed in the spaces between two papillary tips. Peptic necrosis spreads further, covering the denuded propria, the remnants of the denuded papillary bodies, which increases the erosion and makes it macroscopically visible. These initial changes most often begin on the ventral edge of the pars proventricularis, as well as in the vicinity of the orificium esophagus. At the surface of this defect is a narrow zone of necrosis under which the tissue of the propria is hyperemic, edematous, and richly infiltrated with leukocytes. On the blood vessels of the propria and the submucosa, there are no changes other than dilatation (Bisson, 1967; Šenk and Šabec, 1965).

The ulcer develops with the penetration of the erosive processes into the muscularis of the mucosa and the submucosis. The process begins with the disintegration of the muscle fibers of the muscularis mucosa as a logical consequence of edemic dissociation or direct necrosis, which moves from the surface into the depth (Šenk, 1978). Due to the intensive hyperemia and the edema of the submucosis, the tissue swells and the ulcers cannot be observed macroscopically as defects in this phase of their genesis, because they lie at the level of the mucosa of the esophageal part. In edematous tissue, in addition to serous fluid, there are also many fibrin fibers, polymorphonuclears, and local histiocytes. Numerous capillaries are dilated and

thrombosed (Aleksić, 1987; Fedorov *et al.*, 1977; Kowalczyk, 1969; Šenk, 1978). In the arteries of the submucosa and muscularis, edema intimae and tunicae of the elasticae internae were observed, as well as vacuolization of endothelial cells (Embaye *et al.*, 1990; Hunziker and Nicolet, 1968a).

In the next phase of the genesis of the ulcer there is the swelling of the granulation tissue in the propria and parts of the submucosa, which makes a morphological transition from acute to chronic ulcers. Granulation tissue spreads to the intermusculary connective tissue of the tunicae muscularis, making the intermuscular septa thicker. At the beginning, the ulcer is irregular and crescent shaped, and it later takes on the shape of the letter U, or circularly covers the entire esophageal area. Sometimes, the ulcerous changes are limited not only to the pars proventricularis, but also penetrate into the neighboring glandular mucosa. Not rarely, in such cases necrosis covers even the larger blood vessels, which causes extensive bleeding, resulting even in a lethal outcome. On the surface of the chronic ulcers, there is often a wide layer of fibrinoid peptic necrosis, under which a leukocyte demarcation line is formed. In some cases, there is no necrosis, and there is only granulation tissue on the surface, lying on a solid connective-scar basis.

The outcome of residual and postulcerous conditions depends on the character and the dimensions of the previously existing defects. Surface erosions are completely reepithelized, without signs of cicatrization. Focal ulcers heal with a small scar, which somewhat alters the appearance of the esophageal region due to retraction. Ulcers that are spread over the entire surface of the esophagogastric region, or cover its greater part, heal but leave a completely changed normal relief of that part of the stomach. The deeper the ulcer has penetrated, the more scar tissue prevents the closing of the edges of the former crater. In such cases, the retracted remainder of the ulcer stays, lying immediately along the cardia, causing stenosis of its opening with resulting hypertrophy of the muscles in the esophageal wall (Dvornik and Teleonov, 1976; Šenk, 1978).

C. Clinical Picture and Differential Diagnosis

The clinical picture that accompanies esophagogastric ulcer correlates with the stage of development and the intensity of the pathomorphological changes in the pars esophagica.

In peracute cases, due to the extremely rapid development of ulcerous changes, there are no visible disorders in the general health of the diseased animal. Due to the massive gastrorrhagias, the swine die suddenly, or are in a state of collapse for a brief period of time. The extreme paleness of the mucosa and the skin of the carcasses indicates that esophagogastric ulcers are the most probable cause of death.

In acute cases of the disease, the skin and mucosa are extremely pale over a certain period prior to death because of the permanent or occasional bleeding into the stomach lumen. The body temperature is within physiological limits. Certain animals gnash their teeth, and because of the pain in their stomach, they take less food, or occasionally refuse to take it. They withdraw to the corners of the facility, move listlessly, and usually lie down. In some cases vomitus can be observed. The vomited stomach contents are dark due to the presence of blood, and similar to ground coffee deposits. Also due to the presence of blood, their feces is also dark, almost the color of tar (melena) (Mackin *et al.*, 1997; Trobo *et al.*, 1994).

The clinical picture of the disease in subacute and chronic cases is similar to the course of the acute cases, but the symptoms are somewhat less intense because of the longer course of the disease. The animals are anemic, they take less food, and gradually lose weight. Melena is occasionally observed. Often, the only indication of the presence of an ulcer is the occasional appearance of a hard stool as a result of the obstipation and melena. The course of the disease can be quite long. In many cases, the symptoms of the disease can be covered up by the more strongly expressed symptoms of some other disease (colibacillosis, dysentery, parasitic invasion, and others). Hematological changes depend on the duration of the course of the disease and the intensity of the bleeding. In almost all cases there is oligocythemic and hypochromic anemia.

Clinical symptoms similar to those that accompany esophagogastric ulcer are also encountered in cases of the appearance of dysentery, salmonellosis, transmissive—gastroenteritis, intestinal adenomatosis, coccidiosis, ileus, and others. Bacterial and viral infections are most often manifested with a high body temperature and the outbreak of the illness in large numbers of animals simultaneously, contrary to esophagogastric ulcer, where the body temperature is within physiological limits and that occurs sporadically.

Unless esophagogastric ulcer is timely diagnosed and unless the necessary therapy is administered, the disease has a lethal outcome following a shorter or a longer time period.

D. Therapy and Prophylaxis

Treatment of the initial stage of the ulcerous disease is often lacking because it is practically impossible to set a diagnosis at this stage of the disease. The administration of medicines that (step up the process) stimulate blood coagulation (hemostatics) has not produced any satisfactory results so far. In certain cases, antacid preparations are applied successfully (aluminium hydroxide or magnesium silicate), which are added to food in quantities of 2–3%. Since treatment is in all cases symptomatic, the administration of

infusion solutions (5% glucose solution—ionlactate and others) or preparations based on iron, vitamin B complexes, and tranquilizers is recommended. The peroral administration of astringents (acidum tannicum, bismuthum subnitricum), as well as preparations that protect the mucosa (mucosin), is indicated. During treatment, the animals should be isolated into separate boxes and protected from stressful effects.

Since physical and chemical characteristics of food present one of the most important factors that cause morphological changes in the stomach mucosa, special attention during prophylaxis must be paid to the size of the feed particles, which should not be smaller than 3 mm. Furthermore, the food must be kept in conditions that will not permit the growth of fungi, thus preventing the formation of unsaturated fatty acids. The enrichment of fodder mixes with vitamin E (18 mg/kg feed with or without added selenium) yields modest results in the prevention of this disease. The application of vitamin U (20 g/100 kg feed—0.001%) has an anti-inflammatory and analgetic effect, it protects the mucosa, and it secures the speedier regeneration of the damaged epithelium. When copper is used as a feed additive to stimulate growth, the application of zinc carbonate, in quantities of 100 ppm, prevents the ulcerogenic effect of copper. Prophylaxis also implies any other procedure that prevents keeping food in the stomach longer, and that reduces the possibility of increasing the acidity of its contents. The addition of antacid compounds that have a certain buffer effect can be an additional measure toward reducing the risk of this disease. It is necessary to enable the animals' optimal ambient conditions of accommodation and to carry out the corresponding procedures in all stages of breeding. Possible stress situations (loading, transportation, unloading, introduction into a new herd, and similar) should also be prevented with the application of tranquilizers.

E. Forensic Evaluation

Literature that deals with esophagogastric ulcers in swine from different aspects is quite numerous, but there are nevertheless very few data on the elements that determine the duration of this disease. It is known that the course of the disease can be peracute, acute, subacute, and chronic (Curtin *et al.*, 1963; Muggenburg *et al.*, 1964). The peracute course is very brief and the animals die suddenly, in good condition, due to intensive gastrorrhagia. The rapid development of the disease and its brief course are indicated by the fact that piglets aged 6 weeks have died of it (Muggenburg *et al.*, 1967), as well as the observation of clinical signs of the disease and the finding of ulcers in piglets aged only 14 days (Curtin *et al.*, 1963). Exitus sometimes occurs during the acute course of the disease because of progradient ulcer disease, when the process leads to the perforation of the stomach wall and

the consequently resulting peritonitis (Bussolati and Canese, 1972). The subacute and chronic course can last up to 50 days and end with the death of the swine due to extreme cachexia (Kowalczyk and Muggenburg, 1963).

Necrosis can develop very rapidly, in a few minutes only, or much more slowly, in several days. The type of cell as well as the degree of the aggressiveness of the etiological factor are of primary importance in this.

Literature data and our own results on the pathomorphological characteristics of esophagogastric ulcers in swine indicate that they can be manifested as acute erosions, subacute ulcers, or chronic ulcers.

The time limits of the duration of such changes are not given (Curtin *et al.*, 1963; Fedorov *et al.*, 1977; Muggenburg *et al.*, 1964; Šenk and Šabec, 1965; Thoonen and Hoorens, 1963). Pathohistological examinations of esophagogastric ulcers undoubtedly indicate the possible evolution of changes from the preulcerous keratinization of the mucosa to the erosive ulcerous processes. The appearance of granulation tissue in the propria and submucosa is taken as a sign of the micromorphological transition of acute to chronic ulcers. In the course of the further duration of the process, the granulation tissue also covers the intermuscular connective tissue of the tunica muscularis, which leads to marked thickenings of the intermuscle septae. Ulcer processes sometimes end with a connective tissue scar, whose formation had certainly been preceded by development over several weeks.

Preulcerous erosive changes in the form of smaller surface defects of the mucosa are characterized histologically by dystrophic and necrobiotic changes in surface epithelial cells, with the appearance of neutrophil leukocytes in the propria (Curtin *et al.*, 1963; Thoonen and Hoorens, 1963), which, according to the duration of the process, belongs to the acute course lasting from several hours to several days. In the further course of this still acute condition, larger and deeper erosions develop, when propria edema is developed in addition to the dystrophic-necrobiotic changes in the epithelium, and macrophages appear along with the infiltration of leukocyte cells (Fedorov *et al.*, 1977).

A formed chronic ulcer is characterized, in addition to the progressive penetration of peptic necrosis of the epithelium and propria into the muscularis of the mucosa and submucosa, by changes in the cellular infiltrate, which is located immediately adjacent to the necrotized tissue of the ulcer. Along with the rare neutrophil leukocytes and macrophages, cell elements appear that are otherwise found in young granulation tissue—lymphocytes, plasma cells, and fibroblasts. In the further progress of the chronic course of the disease and the maturing of the granulation tissue, a connective capsule is formed on the ulcer periphery, with dominant fibrocytes and collagen fibers (Fedorov *et al.*, 1977).

The forensic evaluation of the changes in the duration of the organization processes is based on the timed inclusion of proliferation and migration of

parenchymatous cells and fibroblasts, protein synthesis in the extracellular matrix, the creating of new blood vessels (angiogenesis), and the maturing and retraction of the scars. The reparation process begins 24 h after the damage. Fibroblasts and vascular endothelial cells proliferate and create granulation tissue in 3–5 days. The migration of fibroblasts to the site of the damage and their later proliferation are controlled by growth factors (FRPT, EFR, FFR, and TFRβ) originating from the macrophages. Some of these growth factors at the same time stimulate the synthesis of collagen and other molecules of the connective tissue. New blood vessels are created through the filling up of the endothelium from the existing blood vessels (angiogenesis) in 3–7 days. The new capillaries have permeable intraendothelial connections, permitting the passage of proteins and erythrocytes into the extravascular space, which is why the granulation tissue is often edematous. Angiogenesis is induced most probably by the basic FFR growth factor, and, according to some authors, by the vascular-endothelial growth factor (VEFR). Macrophages are always present in the stroma of the granulation tissue, provided there is a corresponding chemoattractant stimulation and there are neutrophils, eosinophils, and leukocytes, within a period of 3–7 days. As of this period, the number of blood vessels is reduced, and the number of fibroblasts, the collagen density, and the amount of extracellular matrix are increased.

The appearance of leukocytes can be established after several minutes; they are most numerous at up to 7 days as well as during chronic processes, which last for months. Macrophages and fibroblasts appear after the third day, and during the process at up to 7 days at least, and longer, and elastic fibers are formed only after the fourth week. The finding of lymphocytes indicates that the process has lasted at least 7 days, and of plasmocytes, 10 days. The extremely long duration of the organization process of 3 or more months is established with the finding of collagen fibers that refract light twice.

Swine deaths due to esophagogastric ulcers contribute to economic damage on a farm or some other swine breeding facility, and they also have forensic significance in certain cases of sales. Due to the absolutely disguised course of the disease and the possibility of a sudden lethal outcome, this disease meets two of the three basic criteria for evaluation as a material fault in the animal, in keeping with national legal regulations (Aleksić *et al.*, 1984). Thus, in addition to the covertness and significance of the disease, this third element of the evaluation of its duration—the existence of stomach ulcers in swine before sales, or the development of pathological changes only after an animal has changed owners—can be determined only on the grounds of the changes found during autopsy. Pathomorphological characteristics of spontaneously developed ulcers in swine provide the possibility that its duration can be determined in chronic courses of the disease within limits of at least

6 weeks and up to 2 or at most 3 months. These are the size and depth of the defects on the mucosa of the esophagogastric region, rounded and raised edges of the ulcer and a base with a granulated appearance, a pathohistological finding of a reactive inflammatory process in the neighborhood of the ulcer, changes in blood vessels, and the proliferation of groups of fatty cells in granulation or already mature connective tissue. With the development of erosive changes in a hyperkeratotically altered mucosa, the evaluation of the duration can range between 14 and 21 days.

IV. Concluding Remarks

Spontaneous ulcers, usually of the stomach, commonly occur in many domestic animals. Some of these lesions are chronic and they may occur in either the glandular or squamous-lined regions of the stomach. As with human disease, the pathogenesis in domestic animals is multifactorial, poorly understood, and variable between and within species. Environmental stress and dietary factors are extremely important in ulcer disease in swine. It has been shown that the *Helicobacter* spp. is strongly associated with naturally occurring ulcer and preulcer lesions of the pars esophagea in swine, which raises the possibility that *Helicobacter* spp. is an important factor in the pathogenesis of these lesions.

   The dynamics of the development of esophagogastric ulcers imply hyperplastic lesions (parakeratosis and hyperkeratosis), keratolysis, erosions, peptic necrosis, and the development of ulcers with all the characteristics of peptic ulcerations in other localities. In addition, K6 is expressed in association with the mucosal changes. The pattern of intermediate filaments of keratin suggests that epithelial proliferation, which leads to visible hyperkeratosis, is at the essence of gastric ulcers in swine.

References

Aleksić, Z. (1987). Morfološka i histohemijska ispitivanja žlezdane sluznice želuce svinja sa preulceroznim i ulceroznim lezijama ezofagealnog područja Dissertation, Beograd.

Aleksić, Z., and Dukić, B. (1984). Odgovornost za naknadu šteta prouzrokovanih opasnim stvarima i opasnom delatnošću po Zakonu o obligacionim odnosima u oblasti veterinarske delatnosti. *Vet. gl.* **38**(2), 121–127.

Aleksić, Z., and Knežević, M. (1989a). Histohemijska analiza želudačnih mucina kod ezofagogastričnog ulkusa u svinja. *Zb. XII Jugoslovenskog savetovanja vet.* 91.

Aleksić, Z., and Knežević, M. (1989b). Ispitivanje odnosa kiselih i neutralnih mucina u sluznici želuca svinja sa eksperimentalno izazvanim ezofagogastričnim ulkusom. *Zbornik radova VI savetovanja veterinara Srbije*, Zlatibor, 130–134.

Aleksić, Z., and Knežević, M. (1989c). Kvalitativno-kvantitativni odnosi kiselih i neutralnih mucina u sluznici želuca svinja. *Vet. gl.* **10,** 833–841.

Aleksić, Z., Knežević, M., Jovanović, M., and Todorović, D. (1993). Lokalizacija i distribucija endokrinih ćelija u želucu svinja sa ezofagogastričnim ulkusom. *Acta Vet.* **4,** 199–204.

Allen, A., Cunliffe, W. J., Pearson, J. P., Sellers, L. A., and Ward, R. (1984). Studies on gastrointestinal mucus. *Scand. J. Gastroenterol. Suppl.* **93,** 101–113.

Argenzio, R. A., and Eisemann, J. (1996). Mechanisms of acid injury in porcine gastro-esophageal mucosa. *Am. Vet. Res.* **4,** 564–573.

Barbosa, A. J. A., Silva, J. C. P., Nogueira, A. M. M. F., Paulino, E., and Miranda, C. R. (1995). Higher incidence of Gastrospirillium sp. in swine with gastric ulcer of the pars oesophagea. *Vet. Pathol.* **32,** 134–139.

Baustad, B., and Nafstad, I. (1969). Gastric ulcers in swine. Effect of dietary particle size and crude fiber kontens ulceration. *Pathol. Vet.* **6,** 546–552.

Benčević, K. (1972). Želučane upale i ulkusi u svinja. *Vet. gl.* **26,** 449–455.

Bennett, R., and McLean, V. (1985). Structural studies on dissociated porcine gastric mucus gel. *Comp. Biochem. Physiol.* **4,** 711–714.

Bhaskar, R., Gong, H., Bansil, R., Pajevic, S., Hamilton, A., Turner, S., and LaMont, T. (1991). Profund increase in viscosity and aggregation of pig gastric mucin at low pH. *Am. J. Physiol.* **5**(1), 827–832.

Bisson, P. (1967). Sur l'hyperceratose et l'ulcer gastrooesophagien du porcine. *Rev. Med. Vet.* **118,** 197–215.

Bordi, C., D'Adda, T., Azzoni, C., Pilato, F. P., and Caruana, P. (1995). Hypergastrinemia and gastric enterochromafin-like cells. *Am. J. Surg. Pathol.* **1,** 8–19.

Bubenik, G. A., Ayles, H. L., Friendship, R. M., Brown, G. M., and Ball, R. O. (1998). Relationship between melatonin levels in plasma and gastrointestinal tissues and the incidence and severity of gastric ulcers in pigs. *J. Pineal Res.* **1,** 62–66.

Bunn, C. M., Hansky, J., Kelly, A., and Titchen, D. A. (1981). Observations on plasma gastrin and pepsinogen in relation to weaning and gastric (pars oesophagea) ulceration in pigs. *Res. Vet. Sci.* **3,** 376–378.

Bussolati, G., and Canese, M. G. (1972). Electron microscopical identification of the immuno-fluorescent gastrin cells in the cat pyloric mucosa. *Histochemie* **29,** 198–206.

Bussolati, G., and Monga, G. (1973). Histochemical and ultrastructural investigation on the endocrine cells of the stomach in hypersecreting (pyloris ligated) rats. *Virchows Arch. B.* **13,** 55–67.

Bussolati, G., and Pearse, A. E. (1970). Immunofluorescent localisation of the gastrin-secreting G cells in the pyloric antrum of the pig. *Histochemie* **21,** 1–4.

Cetin, Y. (1992). Chromogranin A immunoreactivity and Grimelius' argyrophilia. A correlative study in mammalian endocrine cells. *Anat. Embyol. (Berl.)* **3,** 207–215.

Coates, J. W., Holbek, N. E., Beames, R. M., Puls, R., and O'Brien, W. P. (1998). Gastric ulceration and suspected vitamin A toxicosis in grower pigs fed fish silage. *Can. Vet. J.* **3,** 167–170.

Cuningham, J. (1992). "Veterinary Physiology" (L. Mills, Ed.). W. B. Sanders Pub. Co., Philadelphia, PA.

Curtin, T. M. (1966). Some altered gastric mucins asociated with esophagogastric ulcers in swine. *J. Am. Vet. Res.* **27,** 1013–1036.

Curtin, T. M., Goetach, G. D., and Hollandbeck, R. (1963). Clinical and pathologic characterization of esophagogastric ulcers in swine. *J. Am. Vet. Med. Assoc.* **143,** 854–860.

Dirrsen, G. (1964). Die Motorik der Vormagen das Weiderkauers zachr Tierphysiol. *Tiererähk. Futer mitelk* **19,** 1–4.

Dvornik, L. B., and Teleonov, V. A. (1976). Patomorfologija jazvenoj bolezni želudka u svinei. *Veterinaria* **8,** 96–99.

Ehrensperger, F. (1974). Das Ulcus oesophagostricum beim Schwein Einbeitrarag zur aetiologie, pathogenese und Bedeutung. Dissertation, Zürich.

Ehrensperger, F., Jucker, F. H., Pfirter, H. P., Pohlenz, J., and Schleter, Ch. (1976). Einfluss der Futerbeschaffenheit auf das Auftreten oseophagogastricher Gaschwüre und die Msteleisttung beim Schwein. *Zbl. Vet. Med.* **23,** 265–276.

Elbers, A. R., Vos, J. H., Hemke, G., and Hunneman, W. A. (1995). Efect of hammer mill screen size and addition of fibre or S-methylmethionine-sulphonium chloride to the diet on the occurrence of oesophagogastric lesions in fattening pigs. *Vet. Rec.* **12,** 290–293.

Embaye, H., Thomilson, R., and Lawrence, I. (1990). Histopathology of oesophagogastric lesions in pigs. *J. Comp. Pathol.* **103,** 253–264.

Fedorov, A. I., Dvorkin, L. B., and Telepnev, V. A. (1977). Patomorfologičeskie izmenenia u svinei pri jazvenoj bolezni želudka. *Materiali VI vsesojuznoj konferenciii po patpogičeskoj anatomii životnih* 115–118.

Fouad, F. M., Marshall, W. D., Farrell, P. G., and Prehem, P. (1993). Immunoelectrophoretic pattern of native mucosal intracellular glycoproteins of hog healthy and drug-intoxicated stomach and of hog body fluids. *J. Toxicol. Environ. Health* **30,** 355–374.

Fugate, W. H., Pickett, R. A., Pery, T. W., and Cutin, T. M. (1965). Influence of feed preparation on performance and occurrence of ulcers in swine. *J. Anim. Sci.* **24,** 837–841.

Gong, D. H., Turner, B., Bhaskar, R., and Lamont, J. T. (1990). Lipid binding to gastric mucin: Protective effect against oxygen radicals. *Am. J. Physiol.* **4**(1), 681–686.

Griffing, W. J. (1963). Fungi-gastric ulcers correlation in pigs told at Kansas extension. *Vet. Med. Lett. Iowa State Univ.* **34,** 286–288.

Grisham, B., Von Ritter, C., Smith, F., Lamont, T., and Granger, N. (1987). Interaction between oxygen radicals and gastric mucin. *Am. J. Physiol.* **1**(1), 93–96.

Grube, D. (1976). Die endocrinen Zellen das Magendarmepithels und der Stoffwechsel der biogenen Amine in Magendarmtrakt. *Prog. Histochem. Cytochem.* **8/3,** 1–128.

Grube, D., and Forssmann, W. G. (1978). Morphology and function of the entero-endocrine cells. *Horm. Metab. Res.* **11,** 589–606.

Guise, H. J., Carlyle, W. W., Penny, R. H., Abbott, T. A., Riches, H. L., and Hunter, E. J. (1997). Gastric ulcers in finishing pigs: Their prevalence and failure to influence growth rate. *Vet. Rec.* **22,** 563–566.

Handlin, D. L., Ballington, D. A., Skelley, G. C., Crook, L., and Johnston, W. E. (1972). Effect of space restriction and ration on the incidence of stomach ulcers in swine. *J. Anim. Sci.* **35,** 767–771.

Hänichen, T. (1975). Magenulzera beim Schwein. *Tierärztl. Prahis* **3,** 191–197.

Hannan, J., and Nyhan, J. F. (1962). The use of some vitamins in the control of ulcerative gastric haemorrhage in pigs. *Irish Vet. J.* **16,** 196–197.

Hoextra, W. G., and Grummer, R. H. (1967). Effect of certain management variables on the incidence and severity of gastric lesions in swine. *Vet. Med. (Small Anim. Clin.)* **62,** 1090–1096.

Huber, W. G., and Wallin, R. F. (1967). Pathogenesis of porcine gastric ulcers. *Am. J. Vet. Res.* **28,** 1455–1459.

Hunziker, O., and Nicolet, J. (1968a). Geschwüsbildungen des Magens. *In* "Handbuch der speziellen pathologischen Anatomie der Haustiere" (J. von Joest and P. Parey, Eds.), 3rd ed., pp. 440–452. Springer-Verlag, Berlin.

Hunziker, O., and Nicolet, J. (1968b). Oesophsgogastrasche Läsionen beim Schwein. *Arh. Tierheilk* **110,** 302–308.

Kadel, W. L., Kelley, D. C., and Coles, E. H. (1969). Survey of yeastlike fungi and tissue changes in esophagogastric region of stomach of swine. *Am. J. Vet. Res.* **30,** 401–408.

Katić, V. (1979). Histohemijska studija endokrinih ćelija (G, EC i ECL) i mucina u sluznici želuca bolesnika sa peptičkim ulkusom. Dissertation, Niš.

Kawai, K., and Rokutan, K. (1995). Kinetics of gastric epithelial cells in duodenal ulcer local environmental factors controlling the proliferation and differentiation of gastric epithelial cells. *J. Gastroenterol.* **3,** 428–436.

Keneth, J. H. (1975). *Djuksova fiziologija domaćih životinja (prevod),* 379–387, Sarajevo.

Knežević, M., Aleksić, Z., and Božić, T. (1994). Citomorfološke karakteristike žlezdane sluznice želuca svinja sa ezofagogastričnim ulkusom. *Zbornik radova VI Kongresa patologa Jugoslavije, Zlatibor* 166–169.

Kokue, E., Kurebayashi, Y., Shimoda, M., and Hayama, T. (1981). Serial endoscopic observation of swine gastroesophageal ulceration induced by injection of a histamine-oil-beeswax mixture. *Am. J. Vet. Res.* **10,** 1807–1810.

Kowalczyk, T. (1969). Etiologic factors of gastric ulcers in swine. *Am. J. Vet. Res.* **30,** 393–400.

Kowalczyk, T. (1970)."Gastric Ulcers in Disease of Swine" (H. W. Dunne, Ed.). 3rd ed. Iowa State University Press, Ames, IA.

Kowalczyk, T., and Muggenburg, B. A. (1963). Recent developments in gastric ulcers in swine. *XVII Welt-Tierärzt. Kongresa, Hannover, Kongres aberichte* **2,** 1311–1314.

Krakowka, S., Eaton, K. A., and Rings, D. M. (1995). Occurrence of gastric ulcers in gnotobiotic piglets colonized by Helicobacter pylori. *Infect. Immun.* **6,** 2352–2355.

Krakowka, S., Ringer, S. S., Flores, J., Kearns, R. J., Eaton, K. A., and Ellis, J. A. (2005a). Isolation and preliminary characterization of a novel Helicobacter species from swine. *Am. J. Vet. Res.* **66**(6), 938–944.

Krakowka, S., Rings, D. M., and Ellis, J. A. (2005b). Experimental induction of bacterial gastritis and gastric ulcer disease in gnotobiotic swine inoculated with porcine Helicobacter-like species. *Am. J. Vet. Res.* **66**(6), 945–952.

Kretutzfeldt, W. (Ed.) (1970). "Origin, Chemistry, Physiology and Pathophysiology of the Gastrointestinal Hormones." Schattauer, Stuttgart, Germany.

Kumar, V., Fausto, N., and Abbas, A. (2005). "Robbins and Cotran Pathologic Basis of Disease," 7th ed. W. B. Saunders Pub. Co., Phildelphia, PA.

Kvetnoy, I. M., Yuzhakov, V. V., and Raikhlin, N. T. (1997). APUD cells: Modern strategy of morpho-functional analysis. *Eur. Microsc. Anal.,* May, 13–15.

Labie, C., Le Bars, H., and Tournut, J. (1966). Lesions de l'appareil digestiv determineea par l' immobilisation forcee chez le porc. *Soc. Biol.* **160**(3), 675–677.

Larenaudie, B., Poulan, R., and Lecompte, A. (1966). Etude du syndrome de l' ulcera gastro-oesophagien du porc et essai de traitment. *Encycl. Vet. Period.* **21,** 110–112.

Larsson, L. I. (1975). Histochemical studies on gastrin-producing cells. Dissertation, Lund, Sweden.

Le Bars, H., and Tournut, J. (1962). Calvet de l'ultertion gastriqes chez la porc. *Acad. Sci.* **225,** 3501–3504.

Lecompte, A. (1966). Contribution a l'etiologie de la pathogrnie et du traitment de l'ulcere gastro-oesophagein chez le porc. Dissertation, Alfort.

Lengnick, H. D. (1972). Eiu Beitrag zur Pethogenese und Atilopgie der Ulcera in der Pars proventricularis das magens beim Schwein. Dissertation, München.

Mackin, A. J., Friendship, R. M., Wilcock, B. P., Ball, R. O., and Ayles, H. L. (1997). Development and evaluation of an endoscopic technique permitting rapid visualization of the cardiac region of the porcine stomach. *Can. J. Vet. Res.* **61**(2), 121–127.

Mahan, D. C., Pickett, R. A., Perry, T. W., Curtin, T. M., Fethertone, W. R., and Besson, W. M. (1966a). Genetic analysis of gastric ulceration in swine. *J. Anim. Sci.* **26,** 884.

Mahan, D. C., Pickett, R. A., Perry, T. W., Curtin, T. M., Fethertone, W. R., and Besson, W. M. (1966b). Influence of various nutritional factors and physical form of feed on esophagogastric ulcers in swine. *J. Anim. Sci.* **25,** 1019–1023.

Mall, A. S., Merrifield, E., Fourie, J., McLeod, H., and Hickman, R. (1997). Alterations in porcine gastric mucin during the development of experimental ulceration. *Digestion* **2,** 138–146.

Mall, A. S., Suleman, N., Taylor, K., Kidd, M., Tyler, M., Lotz, Z., Hickman, R., and Kahn, D. (2004). The relationship of a Helicobacter heilmannii infection to the mucosal changes in abattoir and laboratory pig stomach. *Surg. Today* **34**(11), 943–949.

Mastronardi, M. A. (1964). Propisitio delazione ulcerogena della reserpina sul tubo gastro-enteritico. *Acta Med. Vet. Napoli* **10,** 441–449.

Milić, D., Stokić, Z., Levajić, D., Milinović, M., Grus, I., Lončarević, A., Stanković, Č., and Pavlović, A. (1968). Problem ezofagogastričnog ulkusa kod svinja na farmama otovorenog tipa. *Acta Galen.* **8,** 7–9.

Muggenburg, B. A., Reese, N., Kowalczyk, T., Grummer, R. H., and Hoextra, W. G. (1964). Survey of the prevalence of gastric ulcers in swine. *J. Am. Vet. Res.* **25,** 1673–1678.

Muggenburg, B. A., Kowalczyk, T., Hoextra, W. G., and Grummer, R. H. (1966a). Experimental production of gastric ulcers in swine by reserpine. *Am. J. Vet. Res.* **27,** 1663–1669.

Muggenburg, B. A., Kowalczyk, T., Reese, N., Hoextra, W. G., and Grummer, R. H. (1966b). Experimental production of gastric ulcers in swine by histamine in mineral oil-beeswax. *Am. J. Vet. Res.* **27,** 292–299.

Muggenburg, B. A., Reimann, E. M., Kowalczyk, T., and Hoextra, W. G. (1967). Effect of reserpine and histamine in mineral oil beeswax vehicle on gastric secretion in swine. *Am. J. Vet. Res.* **28,** 1427–1435.

Muggenburg, B. A., Kowalczyk, T., and Olson, W. (1971). Effect of ambient temperature on gastric lesions and gastric secretion in swine. *Am. J. Vet. Res.* **32,** 603–608.

Nappert, G., Vrins, A., Beauregard, M., Vermette, L., and Lariviere, N. (1990). Radioimmu-noassay of serum pepsinogen in relation to gastric (pars oesophagea) ulceration in swine herds. *Can. J. Vet. Res.* **3,** 390–393.

Nelson, W. (1966). Nitrite toxicosis and the gastric ulcer complex in swine. Part I. Nitrite toxicosis. Part II. Gastric ulcers complex. *Dis Abstr. Int.* **26,** 40–41.

Nuner, A. J., Perry, T. W., Pickett, R. A., and Cuetin, T. M. (1966). Expanded or heat-processed fractions of corn and their relative ability to elicit esophagogastric ulcers in swine. *J. Anim. Sci.* **26,** 518–525.

Olivier, L., and Houix, Y. (1969). Incidence de l'ulcere gastrooesophagien dans un tropeau experimental porcin et ses repercussions sur la croiasance et la qualite des caracasses. *Ann. Zootech.* **18,** 209–219.

Otto, K., and Hugo, S. (1960). *In* "Lehrbuch der histologie und vergeleichenden Anatomie der Haustiere" (A. Trautmann and J. Fiebiger, Eds.), pp. 234–244. Springer-Verlag, Berlin.

Palavicin, G., Aureli, G., and Castellani, A. (1971). Chemical changes in the gastric mucin of the pig with spontaneous or experimental gastric ulcer. *Atti. Soc. ital. aci. vet.* **24,** 209–212.

Panasjuk, B. B., Skiljarov, J. P., and Karpenko, L. N. (1979). Ultrastrukturnie i mikrohemičeskie procesi v želudočnih železa, 94–101.

Pearse, A. G. E. (1960). Comon cytochemical properties of cells producing polypeptide hormones, with particular reference to calcitonin and the thyroid cells. *Vet. Res.* **79,** 587–590.

Pearse, A. G. E., Julia, M., Polak, J. M., Bloom, S. R., Adams, C., Dryburgh, J. R., and Brown, J. C. (1974). Enterochromaffin cells of the mammalian small intestine as the source of motilin. *Virchows Arch. B Cell Pathol.* **16,** 111–120.

Pearse, A. G. E., Polak, J. M., and Bloom, S. (1977). The newer gut hormones: Cellular sources, physiology, pathology, and clinical aspects. *Gastroenterology* **72,** 746–761.

Penny, R. H. C., Edwards, M. J., and Mulley, R. (1972). Gastric ulcer in the pig, a new South Wales abattoir survey of the incidence of lesions of the pars oesophagea. *Br. Vet. J.* **128,** 43–49.

Perry, T. W., Jimenez, A. A., Shivrly, J. E., Piccett, R. A., Curtin, T. M., and Beeson, W. B. (1962). Effect of type of ration on the incidence of swine gastric ulcers. *J. Anim. Sci.* **21,** 1008–1014.

Petrosjan, F. R. (1975). Materiali VI Vsesojuznoj konferencii po patologičeskoj anatomii životnih (zb. radova), 223–225, Talin.

Petrosjan, F. R., Torpakov, F. G., Šigorec, N. E., and Marjušina, Z. K. (1976). Kliničko anatomičeskoe pojavlenie jazvenoj bolezni želudka svinei. *Veterinaria* **8,** 94–95.

Pococov, E. F., Bayley, H. S., and Roe, C. K. (1968). Relationship of pelleted autoclaved heat-expanded corn or starvation to gastric ulcers in swine. *J. Anim. Sci.* **27,** 1296–1302.

Preziosi, R., Sarli, G., and Marcato, P. S. (2000). Cell proliferation and apoptosis in the pathogenesis of oesophagogastric lesions in pigs. *Res. Vet. Sci.* **68,** 189–196.

Querioz, D. M., Rocha, G. A., Mendes, E. N., De Moura, S. B., De Oliveira, A. M., and Miranda, D. (1996). Association between Helicobacter and gastric ulcer disease of the pars esophagea in swine. *Gastroenterology* **1,** 19–27.

Reimann, E. M., Maxwell, C. V., Grunner, R. H., Kowalszyk, T., Benevenga, N. J., and Hoextra, W. G. (1967). Different effects of various regions of swine stomach. *J. Anim. Sci.* **26,** 1498–1504.

Resse, N. A., Muggenburgh, B. A., Kowalczyk, T., Grunner, R., and Hoextra, W. G. (1966). Nutritional and environmental factors influencing gastric ulcers in swine. *J. Anim. Sci.* **25,** 14–20.

Ristoski, T. (1999). Histohemijska i imunocitohemijska ispitivanja sluznice želuca svinja sa lezijama na ezofagealnom delu Magistarska teza, Beograd.

Ristoski, T., Knežević, M., and Kovačević, S. (2001). Distribution of cytokeratin on the oesophagogastrical region in swine gasters with different degrees of lesions. 12th Ljudevit Jurak International Symposium on Comparative Pathology, 38–39.

Roberton, M., Mantle, K., Fahim, E., Specian, D., Bennik, A., Kawagishi, S., Sherman, P., and Forstner, F. (1989). The putative "link" glycopeptide associated with mucus glycoproteins. Composition and properties of preparations from the gastrointestinal tracts of several mammals. *Biochem. J.* **2,** 637–647.

Roels, S., Ducatelle, R., and Broekaert, D. (1997). Keratin pattern in hyperceratotic and ulcerated gastric pars oseophagea in pigs. *Res. Vet. Sci.* **2,** 165–169.

Rokkjaer, M., Sogaard, H., Kruse, A., and Amdrup, E. (1979). Bile-induced chronic gastric ulcer in swine with excised oxintic gland area. *Scand. J. Gastroenterol.* **5,** 521–528.

Rothenbacher, H. (1965). Esophagogastric ulcer syndrome in young pigs. *Am. J. Vet. Res.* **26,** 12–24.

Rothenbacher, H., Nelson, L. W., and Ellis, D. J. (1963). The stomach ulcer gastrorrhagia syndrome in Michigan pigs. *Vet. Med.* **56,** 806–816.

Ryaszkowaki, J., and Gambara, K. (1976). Wrzody zoladka u tucznikow. *Med. Vet. Lublin* **32,** 474–476.

Šabec, D., Šenk, L., Kranjc, A., and Bajt, G. (1967). Pojavljivanje ezofagogastričnog ulkusa kod svinja u vezi sa promenama ishrane i okoline. *Zb. III Kongres vet. i vet. tehničara Jugoslavije,* str. 707–710.

Šabec, D., Šenk, L., Štabe, A., and Kranjc, A. (1971). Der Einfluss einger Unweltfaktoren auf das Vorkommen von Magengeschwüren bei Schweinen in einem Grosabetrieb. Proceedings of the 19th World Veterinary Congress, **2,** 433–434.

Sasagawa, T., Cobayashi, S., and Fujita, T. (1974). Electron microscope studies on endocrine cells of human gut and pancreas. *In* "Gastro-Entero-Pancreatic Endocrine System" (T. Fujita, Ed.), pp. 17–38. Georg Thieme Publishers, Stuttgart.

Sellers, A., and Allen, A. (1989). Gastrointestinal mucus gel rheology. *Symp. Soc. Exp. Biol.* **43,** 65–71.

Šenk, L. (1969). Morfologia ezofagogastričnega čira prašičev. *Zbor. biotechn. fak. Vet.* **6,** 69–72.

Šenk, L. (1978). Želodčni čir prašičev. *Zbor. biotechn. fak. Vet.* **15,** 47–63.

Šenk, L., and Šabec, D. (1965). Ezofagogastrični ulkus kod svinja u intenzivnom uzgoju. *Vet. gl.* **19,** 595–611.

Šenk, L., and Šabec, D. (1967). Ezofagogastrični ulkus kod svinja u Sloveniji sa naročitim osvrtom na frekvenciju pojavqivanja, patomorfologiju i ishod bolesti. *Zbor. III Kongr. vet. i vet. tehn. Jugoslavije,* 711–713.

Silva, J. C., Santos, J. L., and Barbosa, A. J. (2002). Gastrinaemia, tissue gastrin concentration, and G cell density in the antral mucosa of swine with and without gastric ulcer of the pars oesophagea. *J. Comp. Pathol.* **126,** 235–237.

Simov, A. (1977). Ispitivanje funkcije adenohipofize, kore nadbubrežne žljezde i štitnjače kod svinja nekih njihovih hormona u krvi, s posebnim osvrtom na učestalost ezofagogastričnog ulkusa. Dissertation, Zagreb.

Sison, S. (1962). Anatomija domaćih životinja Poljoprivredni nakladni zavod, Zagreb.

Smith, J. M. B. (1976). Candidiasis in animals in New Zealand. *Saboraudis* **5,** 220–224.

Solcia, E., Vasallo, G., and Capella, C. (1969). Studies of the G cells of the pyloric mucosa, the probable site of gastrin secretion. *Gut* **10,** 379–388.

Solcia, E., Capella, C., Vasallo, G., and Buffa, R. (1975). Endocrine cells of the gastric mucosa. *Int. Rev. Cytol.* **42,** 223–286.

Solcia, E., Fiocca, R., Rindi, G., Villani, L., Lunetti, O., Burrell, M., Bosi, F., and Silini, E. (1995a). Endocrine tumors of the small and large intestine. *Pathol. Res. Pract.* **4,** 366–372.

Solcia, E., Fiocca, R., Villani, L., Lunetti, O., and Cepella, C. (1995b). Hyperplastic, dysplastic, and neoplastic enterochromaffin-like cell proliferations of the gastric mucosa. Classification and histogenesis. *Am. J. Surg. Pathol.* **1,** S1–S7.

Stanley, A., Lee, P., and Roberton, M. (1983). Heterogeneity in gastrointestinal mucins. *Biochim. Biophys. Acta* **760**(2), 262–296.

Stenham, M. A., Kalley, D. C., and Stanley Coles, E. H. (1967). Influence of dietary sugar on growth of Candida albicans in the porcine digestive tract and lesions in the esophageal area of the stomach. *Am. J. Vet. Res.* **28,** 153–159.

Suarez, D. L., Wesely, I. V., and Larson, D. J. (1997). Detection of Aerobacter species in gastric samples from swine. *Vet. Microbiol.* **57,** 325–336.

Szeredi, L., Palkovics, G., Solymosi, N., Tekes, L., and Mehesfalvi, J. (2005). Study of the role of gastric Helicobacter infection in gross pathological and histological lesions of the stomach in finishing pigs. *Acta Vet. Hung.* **53**(3), 371–383.

Thoonen, J., and Hoorens, J. (1963a). Magengeschwürde der Pars oesophagea mit varblutungstod bei Schweinen. *Dtsch. Tierärztl. Wochenschr.* **70,** 394–395.

Tournut, J., and Lebie, C. (1970). L'ulcere gastroesophagien du porc. Hypothese pathogeni ue. *Rev. Med. Vet.* **121,** 1105–1113.

Tournut, J., Le Bars, H., and Labie, C. (1966). Les lesions gastriques du porc: Role de la contrainte dans leur etiologie. *Rev. Med. Vet.* **117,** 365–370.

Trobo, J. I., Lorente, L., Aller, M. A., Duran, M. C., Betriu, C., and Arias, J. (1994). Hemorrhagic gastroesophageal ulceration by pulmonary infection in extrahepatic cholestatic pigs. *J. Med.* **25**(3–4), 251–254.

Turner, N. C., Martin, G. P., and Marriott, C. (1985). The influence of native porcine gastric mucus gel on hydrogen ion diffusion: The effect of potentially ulcerogenic agents. *J. Pharm. Pharmacol.* **11,** 776–780.

Valverde, E., Eiaz, D., de Rada, O., Burell, M. A., Rovira, J., and Sesma, P. (1993). Immunocytochemical and ultrastructural characterization of endocrine cells and nerves in the intestine of Rana temporaria. *Tissue Cell* **4,** 505–516.

Vassallo, G., Solcia, E., and Capella, C. (1969). Light and electron microscopic identification of several types of endocrine cells in the gastrointestinal mucosa of the gut. *Z. Zellforsch.* **98,** 333–356.

Vassallo, G., Capella, C., and Solcia, E. (1971). Endocrine cells of the human gastric mucosa. *Z. Zellforsch.* **118,** 49–67.

Wise, L. (1974). The significance of serotonin in the gastrointestinal tract. *Clin. Notes* **74,** 315–326.

Wondra, K. J., Hancock, J. D., Behnke, K. C., and Starak, C. R. (1995). Effects of mill type and particle size uniformity on growth performance, nutrient digestibility, and stomach morphology in finishing pigs. *J. Anim. Sci.* **9,** 2564–2573.

Zufarov, K. A., Rasulov, K. I., and Zhuraev, Sh. R. (1978). Endocrine apparatus of human gastric mucosa. *Fiziol. Zh. SSSR Im. I. M. Sechenova* **64**(9), 1229–1233.

Molecular Mechanism of Phase I and Phase II Drug-Metabolizing Enzymes: Implications for Detoxification

Takashi Iyanagi

Biometal Science Laboratory, RIKEN SPring-8 Center,
Harima Institute, Hyogo 679-5148, Japan

Enzymes that catalyze the biotransformation of drugs and xenobiotics are generally referred to as *d*rug-*m*etabolizing *e*nzymes (DMEs). DMEs can be classified into two main groups: oxidative or conjugative. The NADPH-cytochrome P450 reductase (P450R)/cytochrome P450 (P450) electron transfer systems are oxidative enzymes that mediate phase I reactions, whereas the *U*DP-*g*lucuronosyl*t*ransferases (UGTs) are conjugative enzymes that mediate phase II enzymes. Both enzyme systems are localized to the endoplasmic reticulum (ER) where a number of drugs are sequentially metabolized. DMEs, including P450s and UGTs, generally have a highly plastic active site that can accommodate a wide variety of substrates. The P450 and UGT genes constitute a supergene family, in which UGT proteins are encoded by distinct genes and a complex gene. Both the P450 and UGT genes have evolved to diversify their functions. This chapter reviews advances in understanding the structure and function of the P450R/P450 and UGT enzyme systems. In particular, the coordinate biotransformation of xenobiotics by phase I and II enzymes in the ER membrane is examined.

KEY WORDS: Drug-metabolizing enzymes, Cytochrome P450 reductase, Cytochrome P450, Microsomal electron transfer system, Endoplasmic reticulum, UDP-glucuronosyltransferases, Supergene family, UGT1 gene complex, Antley-Bixler syndrome, Crigler-Najjar syndrome.   © 2007 Elsevier Inc.

I. Introduction

Almost all drugs that undergo metabolic transformation are converted to metabolite, which are more polar than the parent compound. Biotransformation not only promotes drug elimination but also often results in inactivation

of pharmacological activity, thereby changing the overall biological properties of the drug (Wilkinson, 2001). However, a number of relatively inert xenobiotics, which are foreign to living organisms (Greek; *xenos* and *biot,* for "stranger to life"), has been found to be converted by enzymes in the body to extremely toxic products. DMEs, which can be involved in complex metabolic networks of the body, are classed as phase I or phase II enzymes. Phase I enzymes often catalyze oxidation, reduction, and hydrolysis reactions. Most phase II enzymes catalyze conjugation reactions: UDP-glucuronosyltransferases (UGTs), sulfotransferases (SULTs), or glutathione S-transferases (GSTs). Drugs are often metabolized by sequential reactions involving phase I and II enzymes. The time taken for a drug to be cleared from the body is a function of both the rate of biotransformation and excretion. The major role of P450s is to introduce polar functional groups into nonpolar molecules. Conjugating enzymes catalyze the addition of more polar functional groups to the drug, such as glucuronate, sulfate, glutathione, or amino acids. NAD(P)H: quinone:oxidoreductase (also called DT-diaphorase), methyltransferase, and acetyltransferase are also classed as phase II enzymes. Sequential biotransformations by both the P450R/P450 system and UGTs constitute one of the major routes for drug metabolism. These sequential reactions might be facilitated by the close spatial association of the enzymes on the endoplasmic reticulum (ER). The metabolites generated by phase I and II reactions are excreted from the body with the aid of membrane efflux pumps that include the multidrug resistance-associated proteins (phase III reactions).

The P450R/P450 system and UGTs play a vital role in the metabolism and detoxification of xenobiotic (exogenous) and endobiotic (endogenous) compounds. The P450 and UGT superfamily of genes encode proteins that metabolize a diverse set of substrates. P450 proteins are encoded by distinct genes, whereas the P450R protein is encoded by a single gene. Thus, P450R can donate electrons to all microsomal P450s. In contrast, UGT proteins are encoded by both distinct genes and a complex gene. Both the P450 and UGT genes have evolved to diversify their functions (Gibbs *et al*., 2004). The combinatory pharmacogenetics of these enzymes is an increasingly important research field in clinical medicine (Wilke *et al*., 2005).

II. Phase I: NADPH-Cytochrome P450 Reductase (P450R)/Cytochrome P450 (P450) System

Phase I enzymes (functionalization reactions), which mediate oxidation, reduction, or hydrolysis reactions, introduce a functional group (-OH, -SH, -NH$_2$, or -COOH) into the drug molecule. The P450R/P450 is a major oxidative enzyme system (Gibson and Skett, 2001). The P450-containing microsomal electron

transfer system catalyzes the oxidation of drugs and xenobiotics. Although there are numerous functional P450 genes in mammals (e.g., 84 in rat, 87 in mouse, 57 in human) (Gibbs *et al.*, 2004), there is only one P450R gene in each species. P450 genes are distributed on several chromosomes, although they are often found in clusters. The human genome project has identified 57 functional P450 genes: seven encode mitochondrial enzymes, all of which play key roles in sterol biosynthesis, and 50 encode microsomal enzymes (Guengerich, 2005; Nelson *et al.*, 2004). Of the 50 microsomal enzymes, 20 participate in the biosynthesis of endobiotic substrates, such as steroids and eicosanoids; 15 principally metabolize xenobiotic compounds; and 15 are orphan enzymes (named because their substrates have not been identified). P450R can donate electrons to 50 microsomal P450s, which are located in the ER. In this section, the structure/function of the microsomal electron transfer system is described. In addition, the differences between P450R and nitric oxide synthase (NOS) reductase domains are discussed.

A. Historical Perspectives

In the early 1950s, little was known about the oxidative enzymes involved in metabolizing drugs and xenobiotics. Mason *et al.* (1955), Hayaishi *et al.* (1955), and Hayano *et al.* (1955) independently demonstrated direct substrate incorporation of molecular oxygen. These pioneering experiments opened a new field in the area of biological oxidation, including cytochrome P450s. Molecular oxygen is metabolized by three broad classes of enzymes: (1) dioxygen transferases, (2) mixed-function oxidases, and (3) electron-transfer oxidases (Mason, 1957). The microsomal deamination of amphet-amine (Axelrod, 1955) and dealkylation of aminopyrine (Gillete *et al.*, 1957; La Du *et al.*, 1955) requires the reduced form of nicotinamide adenine dinucleotide phosphate (NADPH) and molecular oxygen (O_2). Enzymes of the liver microsomes are of major importance in the detoxification of many drugs and foreign organic compounds. In the 1950s–1960s, these enzyme systems were shown to perform a variety of reactions such as the hydroxyl-ation of aromatic compounds, side chain oxidation of barbiturates, and deamination of amines. These reactions were characterized as a mixed-function oxidation, in which the enzyme system catalyzes the consumption of one molecule of oxygen/molecule of substrate (RH); one atom of this oxygen molecule inserts into the product (ROH), and the other undergoes two equivalents of reduction (Eq. 1).

$$NADPH + RH + O_2 + H^+ \rightarrow NADP^+ + ROH + H_2O \qquad (1)$$

Klingenberg (1958) and Garfinkel (1958) discovered a novel carbon monoxide-binding pigment with an optical absorption peak at 450 nm in

liver microsomes. Omura and Sato (1962, 1964a,b) purified this pigment as a P420 form from liver microsomes and showed that it was a cytochrome, which they named cytochrome P450 (Kresge *et al.*, 2006; Omura, 2005). Hashimoto *et al.* (1962) demonstrated the electron spin resonance detectable "microsomal Fe_x signal" at g = 2.25 in liver microsomes, derived from a low-spin ferric hemoprotein, which was preferentially reduced by NADPH. Mason *et al.* (1965) suggested that a more active enzyme toward P450 and microsomal Fe_x reduction is TPNH (NADPH)-cytochrome *c* reductase, which was first identi-fied by Horecker (1950) as an NADPH-specific cytochrome *c* reductase, and characterized by Williams and Kamin (1962) and Phillips and Langdon (1962). Using submicrosomal particles containing P450, Miyake *et al.* (1968) demonstrated that the microsomal Fe_x signal is derived from low-spin ferric P450. Estabrook *et al.* (1963) showed that this pigment from the photoactivation spectra of CO-inhibited mixed-function oxidations appears to be the func-tional site of several microsomal mixed-function oxidases. Lu and Coon (1968) demonstrated that microsomal fatty acid hydroxylase requires three fractions containing P450, cytochrome *c* reductase activity, and phospholipids for activity.

   Iyanagi and Mason (1973) found an air-stable g = 2 signal in liver micro-somes, which was increased by the addition of NADPH. This signal was derived from air-stable semiquinone of the NADPH-cytochrome *c* reductase. Furthermore, the enzyme was shown to contain one molecule of FAD and FMN per protein molecule, with each flavin performing an individual func-tion. The spin concentrations of air-stable semiquinone and their spectra were compared with those of flavodoxin (Iyanagi *et al.*, 1974). The data indicated that the enzyme contained a flavodoxin-type flavin, which is a FMN-containing small bacterial flavoprotein. Flavodoxin can substitute for the low-potential ferredoxin during growth under low-iron conditions (Knight and Hardy, 1966; Mayhew *et al.*, 1969). An iron sulfur protein with g = 1.94 signal could not be detected in liver microsomes (Miyake *et al.*, 1967). These observations strongly suggested that NADPH-cytochrome *c* reductase participates as an electron carrier in microsomal electron trans-fer. Iyanagi *et al.* (1974) postulated that this enzyme could directly reduce cytochrome P450, which was named NADPH-cytochrome P450 reductase (P450R). These studies led to the discovery of a new microsomal electron transfer system, including P450R and P450 (Fig. 1).

B. P450R/P450 Electron Transfer System

1. Electron Transfer System

The mixed-function oxidase system of liver microsomes was resolved into three fractions, consisting of P450R, P450, and a lipid component (Lu and Coon, 1968; Lu *et al.*, 1969). P450R can directly reduce P450s in a
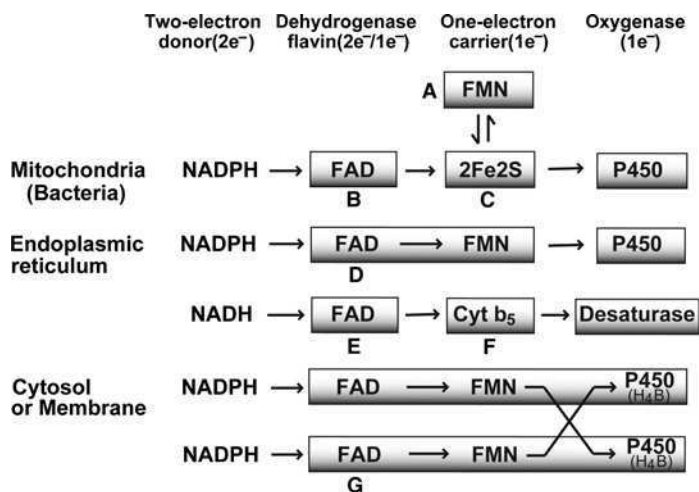
FIG. 1 The electron transfer systems in the mixed-function oxidases. (A) flavodoxin; (B) ferredoxin reductase; (C) ferredoxin; (D) NADPH-cytochrome P450 reductase (P450R); (E) NADH-cytochrome b_5 reductase (b_5R); (F) cytochrome b_5 (b_5); (G) nitric oxide synthase (NOS) (dimmer structure); H4B, tetrahydrobiopterin.

purified reconstituted system (Imai *et al.*, 1977; Iyanagi *et al.*, 1978; Strobel and Dignam, 1978; Vermilion and Coon, 1974; Yasukochi and Masters, 1976). Taniguchi *et al.* (1979) reported a reconstituted system in phosphatidylcholine vesicles. These studies confirmed that the microsomal electron transfer system consists of two components: P450R and P450. The low potential flavin, FAD, accepts two reducing equivalents from NADPH and the high potential flavin, FMN, acts as a one-electron carrier for the net two-electron transfer from NADPH to P450 (Iyanagi *et al.*, 1981; Vermilion *et al.*, 1981).

The cDNA cloning (Porter and Kasper, 1985; Yamano *et al.*, 1989), direct complete amino acid analysis (Haniu *et al.*, 1986, 1989) and crystallographic structure of P450R (Wang *et al.*, 1997) confirmed that the protein evolved by fusion of two ancestral genes encoding proteins related to ferredoxin-NADP$^+$ reductase (FNR) and flavodoxin. Bredt *et al.* (1991) isolated the cDNA of neuronal nitric oxide synthase (nNOS), which is localized to neurons throughout the peripheral and central nervous system (CNS). The C-terminal reductase domain of nNOS bears 58% sequence similarity with P450R. In the case of the microsomal desaturase system, the cytochrome b_5 (b_5) can function as a one-electron carrier. In contrast, the mitochondrial system comprises adrenodoxin reductase (a single subunit, mono–FAD-containing enzyme) and adrenodoxin (adrenal ferredoxin; an iron ferredoxin-type redox protein), which together function as an electron carrier from NADPH to P450 (Kimura

and Suzuki, 1967; Omura *et al.*, 1966). In general, the bacterial systems consist of three components, including a ferredoxin. This fact suggests that the mitochondrial P450 electron transfer system in eukaryotes is derived from bacteria. However, *Bacillus megaterium* cytochrome P450BM3 (P450BM3) is a single component fatty acid hydroxylase. It is composed of an N-terminal P450 mixed-function oxygenase domain fused to an FMN- and FAD-binding reductase domain, which is related to mammalian P450R (Narhi and Fulco, 1987). These electron transfer events indicate that a one-electron carrier is necessary for the sequential electron transfer from a two-electron donor (NAD[P]H) to a P450, which is a one-electron acceptor (Fig. 1).

In principle, the sequence of electron transfer for mixed-function oxidases is summarized as follows: two-electron donor → dehydrogenase flavin → one-electron carrier → oxygenase (P450) (Fig. 1). In these electron transfer systems, the FMN domains of P450R and NOS can also function as a one-electron carrier. These electron transfer systems require three functions: (1) dehydrogenase from NAD(P)H, (2) one-electron carrier, and (3) stepwise activation of molecular oxygen by an oxygenase. A ''step down'' reaction from a two-electron donor to a one-electron acceptor is an essential step in biological oxidations. The oxygenases accept electrons from a constant oxidation-reduction potential.

2. Structure of P450R and nNOS Reductase Domain

NADPH-cytochrome P450 reductase (P450R) is a 78 kDa (678 aa for rat enzyme) flavoprotein associated with the cytoplasmic surface of the ER and the outer membrane of the nuclear envelope in eukaryotic cells (Gonzalez and Kasper, 1981). The gene expression of functional domains (Smith *et al.*, 1994) and the crystal structure of rat P450R (Wang *et al.*, 1997) clearly indicate that the enzyme is composed of four domains: an FMN-binding domain (residues 70–225), the connecting domain (residues 325–450) and the FAD- and NADPH-binding domains (Fig. 2). The connecting domain is inserted in the NADPH/FAD domain. The enzyme also contains a membrane-binding domain at the N-terminus (Fig. 2). The structure of the FMN-binding domain is similar to that of flavodoxin, whereas the two C-terminal dinucleotide-binding domains are structurally homologous to those of ferredoxin-NADP$^+$ reductase (FNR), NADPH-flavodoxin reductase and NADH-cytochrome b_5 reductase (b_5R) (Porter and Kasper, 1985; Wang *et al.*, 1997). The distance between the isoalloxazine components of the flavins is 4 Å, indicating direct electron transfer between the dimethylbenzene edges of the two flavin molecules. A high degree disorder in the FMN domain, observed in the crystal structure of P450R, suggests that this domain retains a considerable degree of mobility. Mutant studies have been performed to investigate the nature of the intramolecular interactions during
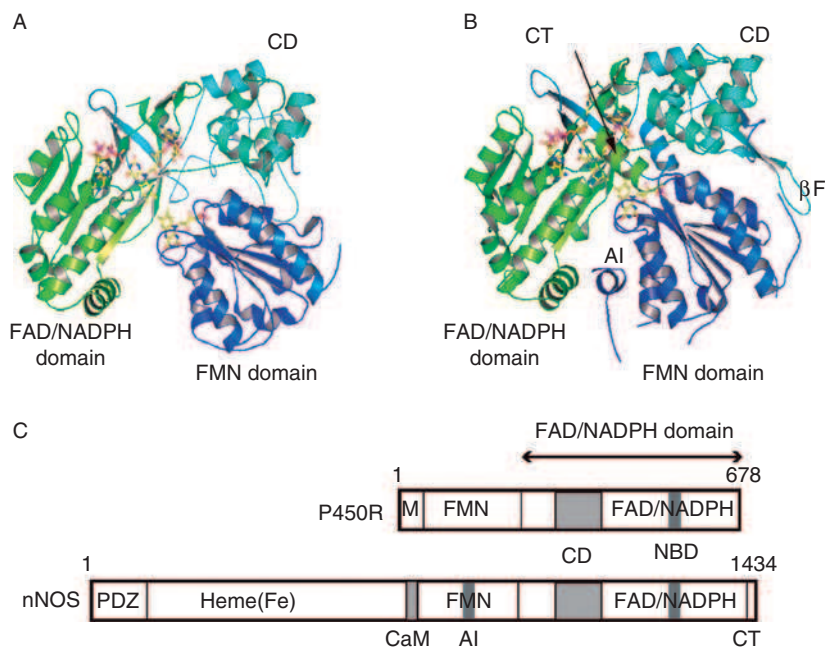
FIG. 2   The domain structure of NADPH-cytochrome P450 reductase (P450R) (A), neuronal nitric oxide synthase (nNOS) reductase domain (B), and functional domains of P450R and nNOS (C). M, Membrane-binding domain; PDZ, PDZ domain; CaM, CaM-binding region; AI, autoinhibitory domain; CD, connecting domain; CT, C-terminal motif; βF, β−finger; NBD, highly conserved nucleotide-binding domain in the P450R family (Wang *et al.*, 1997). A and B are cited from Protein Data Bank Codes 1AMO and 1TLL, respectively.

catalysis. Superimposition of the mutant and wild-type structures revealed the flavin–flavin distance varies from 3.9 Å to 5.8 Å (Hubbard *et al.*, 2001), strongly suggesting movement of the FMN domain during catalysis.

Nitric oxide (NO) has diverse biological functions and is generated in mammals by NOS enzymes. Three NOS isozymes participate in distinct physiological processes (Roman *et al.*, 2002). Inducible NOS (iNOS) is involved in the immune system when NO is produced as a cytosolic agent. Endothelial NOS (eNOS) is involved in the maintenance of blood pressure, whereas nNOS participates in neuronal transmission. All NOSs are homodimeric enzymes that catalyze an NADPH- and O_2-dependent oxidation of L-arginine (L-Arg) to L-citrulline (L-Cit) and NO (Fig. 1). Each NOS consists of a C-terminal reductase domain that contains binding sites for FAD, FMN, and NADPH, an intervening calmodulin-binding domain, and an N-terminal P450-like domain that contains binding sites for iron protoporphyrin IX (heme), 6R-tetrahydrobiopterin (H_4B),

and Arg. The structure of rat nNOS reductase domain, which lacks the calmodulin (CaM)-binding domain, has been reported by Garcin *et al.* (2004) and is very similar to that of rat P450R (Wang *et al.*, 1997). The crystal structure of rat P450R and rat nNOS reductase domains is considered representative of this family of proteins (Fig. 2). Although the overall structural organization of P450R and nNOS reductase domain is similar, significant differences are evident in nNOS. Interestingly, the autoinhibitory (AI) motif is inserted within the FMN domain of rat nNOS (residues 831–870) and bovine eNOS (residues 600–640) reductase domains (Salerno *et al.*, 1997), and is located between the FMN- and NADPH-binding sites (Garcin *et al.*, 2004). Furthermore, the β-finger (residues 1070–1080) and N-terminal β-loop-helix (residues 963–986) are found on the rat nNOS structure (Zhang *et al.*, 2001). The distance between the FAD and FMN moieties is less than 5 Å, and the position of the two flavin cofactors differ significantly from that of P450R (Fig. 3).

The air-stable (neutral) semiquinone form is characteristic of both the P450R and NOS reductase domains and contain the oxidized flavin (FAD) and semiquinone form of FMN (FMNH$^\bullet$) in equimolar amounts. In the flavodoxin, the FMN semiquinone form is stabilized by the interaction with apoprotein. In the P450R and NOSs, the value of the semiquinone formation constant Ks is larger than unity, indicating an increase in the separation between the oxidized/semiquinone couple ($E_{m.1}$) and semiquinone/fully reduced couple ($E_{m.2}$) in each flavin (Iyanagi, 2005a,b). This stabilization of neutral semiquinone is due to hydrogen bond formation between the polypeptide backbone of the protein and the N(5) of the reduced FMN, lowering its activity. Specifically, FMN hydrogen bonds to Gly[141] in rat P450R, and Gly[810] in rat nNOS, whereas FAD hydrogen bonds to Ser[457] in rat P450R and Ser[1176] in rat nNOS (Garcin *et al.*, 2004; Wang *et al.*, 1997). However, the fully reduced form is destabilized by constraints from the unfavorable planar conformation, and its activity is increased. Therefore, this state has more activity than that of the semiquinone.

By contrast, the semiquinone of the FMN domain of bacteria P450BM3, in which a hydrogen bond at the (N)5 is formed to the peptide nitrogen of Asn537, stabilizes the anionic red semiquinone (FMN$^{\bullet-}$) (Hanley *et al.*, 2004). Because of the stabilization of anionic semiquinone, this enzyme may have a high turnover rate. The anionic red semiquinone form is also observed in the b_5R (Iyanagi, 1977; Iyanagi *et al.*, 1984; Kobayashi *et al.*, 1988; Marohnic *et al.*, 2003), but its neutral blue semiquinone form is partially stabilized in the mutant of T66V (Kimura *et al.*, 2003), which is positioned near the (N)5 atom of the isoalloxazine ring of FAD. In this mutant, b_5R activity is decreased.

The reduction potentials of the individual one-electron redox couples ($E_{m.1}$ and $E_{m.2}$) of FAD and FMN of P450R have been reported (Iyanagi *et al.*, 1974; Munro *et al.*, 2001). In both FAD and FMN, the semiquinone formation
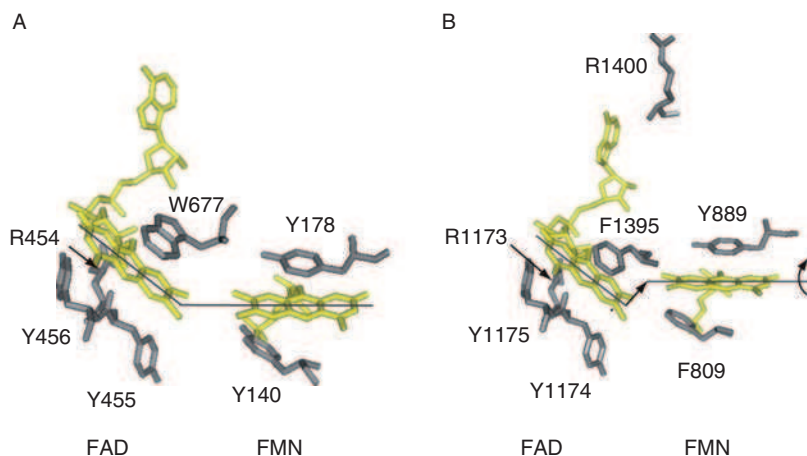
FIG. 3   The structures of the FAD- and FMN-binding sites of P450R (A) and nNOS reductase domain (B). In B, arrows indicate the shift and rotation of the plane of FMN molecule from that of P450R. A and B are cited from Protein Data Bank Codes 1AMO and 1TLL, respectively.

constant is larger than unity. In the case of NOSs (Gao *et al.*, 2004; Ghosh *et al.*, 2006; Noble *et al.*, 1999), the overall redox potentials are very similar, although the values for the FAD domains are greater than those of P450R. In both enzymes, the air-stable semiquinone form, FAD–FMNH$^\bullet$ has a relatively high reduction potential and low reactivity with electron acceptors. Therefore, the semiquinone/fully reduced couple (FMNH$^\bullet$/FMNH$_2$), could function as a one-electron carrier in the catalytic cycle for both the FAD–FMN pairs in P450R and NOSs. The couples (FMNH$^\bullet$/FMNH$_2$) of each enzyme are -270 mV for P450R (Iyanagi *et al.*, 1974), -180 mV for iNOS, -180 mV for nNOS, and -210 mV for eNOS (Ghosh *et al.*, 2006). The first and second electrons from the reductase to P450 or P450-like hemoprotein are sequentially transferred from these states, which can donate an electron at a constant oxidation-reduction potential.

However, in the bacterial P450BM3 the oxidized/semiquinone couple (FMN/FMN$^{\bullet-}$) functions as a one-electron carrier in the catalytic cycle (Murataliev *et al.*, 2004; Sevrioukova *et al.*, 1999), in which the anionic red semiquinone form can donate electrons to P450. The couples, FMN/FMN$^{\bullet-}$ and FMN$^{\bullet-}$/FMNH$_2$ are -240 mV and -160 mV, respectively (Hanley *et al.*, 2004). The redox potential is unique among flavodoxin-like domains, as compared with those of P450R and NOSs. The oxidation-reduction potentials of the flavin cofactor in flavoproteins are controlled by a variety of noncovalent flavin–protein interactions (Mayhew and Ludwig, 1975; Swenson and Krey, 1994).

3. Evolutionary Aspects

Mammalian P450-containing electron transfer systems are divided into two types: mitochondrial and microsomal (Fig. 1). The mitochondria of animal species arose via the incorporation of purple bacteria into eukaryotic cells, whereas the ER could have arisen from other eubacterial species, possibly of the Gram-positive type. The microsomal and mitochondrial P450s separated about 950 million years ago, which is close to the accepted time of divergence between the plant and animal kingdoms at about 1000 million years ago (Lewis, 2001; Lewis *et al.*, 1998). This is also coincident with the development of sexual reproduction. The mitochondrial P450s are crucial for the biosynthesis of steroid hormones, whereas microsomal P450s are crucial for the metabolism of xeno-biotics, such as plant toxins, prostanoids, and eicosanoids. Indeed, this is a natural consequence of more complex multicellular organisms such as plants, fungi, and primitive animals (Lewis, 2001). The mitochondrial and microsomal P450s have also evolved synergistically for the biosynthesis of endobiotics, such as steroid hormones and vitamin D.

The domain families have been extensively duplicated within a genome and combined with different domain partners giving rise to different multi-domain proteins (Orengo and Thornton, 2005).

It is possible to speculate about the evolutionary development of microsomal P450 redox systems and NOSs in terms of the structure and function of the one-electron carrier, ferredoxin, and flavodoxin (Fig. 4). The structure and function of the FAD- and FMN-binding domains of P450R and NOS isozymes show a striking evolutionary relationship with plant FNR and bacterial flavodoxins in terms of electron transfer and its regulation. It is thought that the ancestor of these enzymes might have evolved from at least four discrete genes, encoding ferredoxin or flavodoxin reductase (FAD), ferredoxin (2Fe2S), flavodoxin (FMN), and a heme (Fe) domain (Fig. 4). Bacterial flavodoxin (FMN) can substitute for the low-potential ferredoxin (2Fe2S) during growth under low-iron conditions. The flavodoxin reductase, a FAD containing bacterial flavoprotein, catalyzes the reversible transfer of electrons between NADPH and flavodoxins or ferredoxins (Ingelman *et al.*, 1997). Flavodoxin reductase and flavodoxin are involved in cobalamin-dependent methionine synthesis (Hall *et al.*, 2001). However, in the mammalian system, the methionine synthase reductase has a similar prosthetic group with that of P450R (Olteanu and Banerjee, 2001; Olteanu *et al.*, 2004; Wolthers *et al.*, 2003), but it is a soluble protein. The other proteins, including the α-subunit of sulfite reductase (Sulfite R) and P450BM3 carry domains homologous to flavodoxin and flavodoxin reductase or FNR on a single polypeptide chain. It has been hypothesized that these enzymes arose from a gene fusion of flavodoxin and flavodoxin reductase or FNR. The structure of flavodoxin, in which the dimethylbenzene ring of FMN molecule is exposed to solvent, is also superimposable on those of the
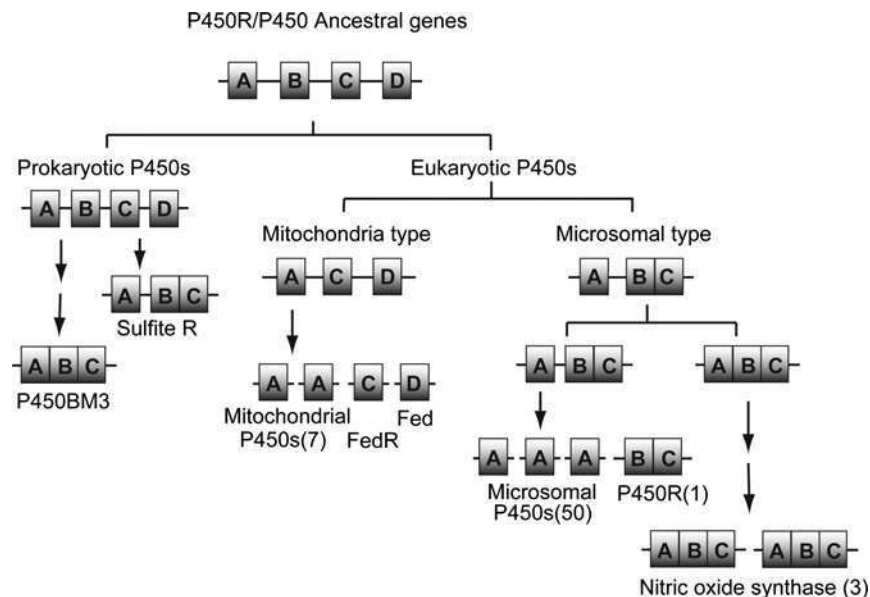
FIG. 4 A model for the evolution of functional domains in P450R, P450s, and nitric oxide synthase genes. A–D indicate ancestral domains of each gene: A, heme domain; B, FMN domain; C, FAD domain; D, Fe-sulfur cluster domain. Fed, ferredoxin; Fed R, ferredoxin reductase; Sulfite R, sulfite reductase; P450BM3, *Bacillus megaterium* P450BM3. The number of functional isozymes is shown in parentheses.

α-subunit of Sulfite R, P450R, and NOS FMN-binding domains (Garcin *et al.*, 2004; Sibille *et al.*, 2005; Wang *et al.*, 1997). The NADPH/FAD domain for both enzymes is also superimposable on that of FNR (Jachymova *et al.*, 2005; Mayoral *et al.*, 2005).

In the modeling of the FNR–flavodoxin complex, P450R is a good example of an efficient interflavin electron transfer between FAD and FMN (Figs. 2, 3), the shortest distance between the two flavin rings being ~4.1 Å (Mayoral *et al.*, 2005). No intervening residues are present between the two cofactors, thereby allowing direct electron transfer. In the complexes of FNR–ferredoxin, the distance between the [2Fe-2S] cluster of ferredoxin and the dimethylbenzene edge of FAD is 6.0 Å (Kurisu *et al.*, 2001). In the complexes of adrenodoxin reductase-adrenodoxin, in which an electron is transferred from the pyrimidine ring of FAD to the iron center, the distance between the [2Fe-2S] cluster of adrenodoxin and the isoalloxazine ring of FAD is 10 Å, in which two possible electron transfer tunneling pathways have been proposed on the basis of the crystal structure (Muller *et al.*, 2001). Taken together, the data suggest that the distance between FAD and FMN is less than that between the FAD and [2Fe-2S] cluster in these redox systems.

In addition, P450R acquired the membrane-binding domain for efficient electron transfer with P450 on the ER membrane. NOS comprises a single soluble enzyme, in which the reductase FAD–FMN domain and oxygenase heme-domain are fused, together with a regulatory motif (Figs. 2, 4).

The P450R and NOS reductase proteins are presumably derived from an ancestral FAD- and FMN-containing flavoprotein (Ghosh and Salerno, 2003). The FAD can function as a dehydrogenase, whereas FMN is a one-electron carrier (Fig. 1). Although the partner to the FAD domain is a flavodoxin, alternative combinations of one-electron carrier are also possible (e.g., ferredoxins and cytochromes). The functional significance of P450R and NOS having a flavodoxin domain is unclear, although it could be related to the degree of interaction between the various redox centers. Interaction between the edges of the dimethylbenzene rings of the two flavin molecules may be favored because it is less hindered than an equivalent interaction between a flavin and a [2Fe-2S] cluster, the latter being buried within the protein by amino acid residues acting as ligands. However, a novel flavohemoprotein, which contains a cytochrome b_5-like domain at the N-terminus and a b_5R-like domain at the C-terminus, has been identified in the ER membrane, although its function remains unknown (Zhu et al., 2004).

The rat P450R gene comprises 16 exons; exons 2 and 3 encode the membrane anchor region, exons 4–7 the FMN-binding domain, and exons 8–16 the FAD/NADPH-binding domain (Porter et al., 1990). Comparative analysis of the intron splice location between rat P450R and the human NOS genes indicates that the three human NOS genes are derived from a common ancestral gene by duplication. Moreover, the analysis also showed that the NADPH/FAD- and FMN-binding domains of the P450 and NOS systems display similarity (Hall et al., 1994). Consequently, evolutionary transformation of the cofactor binding sites can occur without major structural changes. nNOS have acquired additional regulatory sequences that control enzyme activity: CaM-binding, AI, β-finger, and C-terminal motifs (Roman et al., 2000). The iNOS isozyme does not contain the AI motif and has a shorter C-terminal tail than that of the nNOS and eNOS isozymes.

However, the oxygenase domains of NOSs do not reveal any sequence homology with known P450s, although they have a common cysteine residue as the proximal thiolate ligand (Masters, 2005; Omura, 2005). This suggests that the origin of the NOS oxygenase domain may be different from those of microsomal or mitochondrial P450s. Proteins homologous to the mammalian NOS oxygenase domain have been found in prokaryotes. One example from Bacillus subtilis has been demonstrated to produce nitric oxide when incubated with NADPH and a mammalian NOS reductase domain (Adak et al., 2002). This suggests that the bacterial electron transfer system may comprise the flavodoxin-type reductase (FAD) and flavodoxin (FMN). It is hypothesized that the mammalian NOSs are fusion proteins of

the bacterial oxygenase domain and reductase domain from sulfite reductase flavoprotein (Zemojtel *et al.*, 2003). Although the complex multidomain structure of different higher eukaryotic NOSs is the result of several gene fusions, the structure of both P450R and NOSs has evolved synergistically.

4. Mechanism

a. Catalytic Cycle of P450R   P450R catalyzes the transfer of electrons from NADPH to P450. In this system, the electron transfer is divided into three steps: (1) direct hydride transfer from NADPH to FAD, (2) interflavin electron transfer from FAD to FMN, and (3) electron transfer to electron acceptors, including P450s. In NOSs, these steps may be activated by CaM-binding. The reduction process begins with the formation of $NADP^+$-$FADH_2$-FMN via hydride transfer from enzyme-bound NADPH, followed by an interflavin one-electron transfer from $FADH_2$ to FMN yielding a disemiquinone species ($FADH^{\bullet}$-$FMNH^{\bullet}$). Oxidized FAD then accepts electrons from a second molecule of NADPH during the subsequent interflavin electron transfer, resulting in a four electron-reduced form ($NADP^+$-$FADH_2$-FMN_2). These half-reactions have been studied in detail (Gutierrez *et al.*, 2001, 2002; Iyanagi *et al.*, 1981). In this case, the steps are in equilibrium distribution, the redox state being determined by the relative redox potentials (Backes *et al.*, 1998; Iyanagi *et al.*, 1974; Munro *et al.*, 2001; Oprian and Coon, 1982). In contrast, the reduction of P450 is by electron transfer from the fully reduced FMN. During steady-state turnover the enzyme cycles predominantly between the one- and three-electron reduced states (Fig. 5). In this catalytic cycle, the low-level reactivity of a neutral (blue) FMN semiquinone with electron acceptors enables one-electron transfer, and the FMN shuttles between the neutral semiquinone and fully reduced states. The first and second electrons from the reductase to P450 are sequentially transferred from the fully reduced states (V and IX) of FMN, which can donate an electron at constant oxidation-reduction potential. This model could apply to that of the NOS reductase domain (Guan and Iyanagi, 2003; Guan *et al.*, 2003). It is likely that the state, VI (FAD-$FMNH^{\bullet}$) is a common predominant intermediate in the catalytic cycle, and the V and IX states can donate electrons to electron acceptors, including P450 (Garcin *et al.*, 2004; Yamamoto *et al.*, 2005).

b. Electron Transfer from P450R to P450   The three-dimensional (3-D) structures of P450R (Wang *et al.*, 1997) and nNOS reductase domain (Garcin *et al.*, 2004) indicate that the dimethylbenzene edge of the isoalloxazine ring of FMN, which is exposed in the FMN domain, is covered by FAD (Fig. 2). The pyrimidine ring of the FMN isoalloxazine is slightly buried by two loops, while the dimethylbenzene edge is exposed to solvent. There are several possible mechanisms for electron transfer from the FAD–FMN pair to the electron acceptor, including P450 and cytochrome *c*. Electron transfer from the FMN to

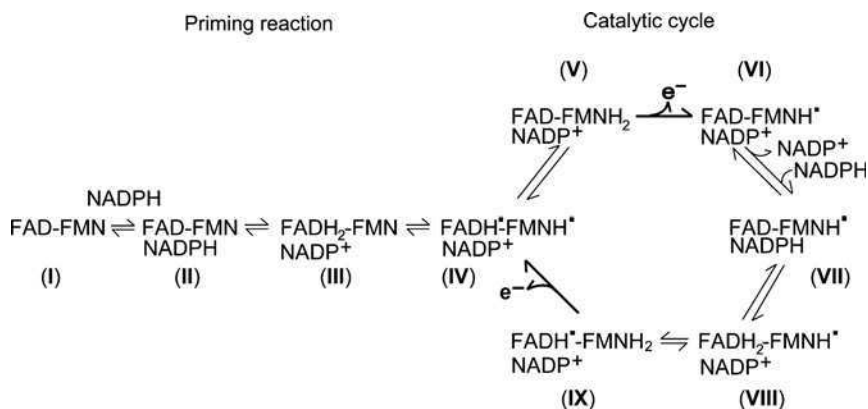Priming reaction   Catalytic cycle

FIG. 5   Reaction mechanism of P450R.

the electron acceptor could occur without an associated conformational change (Nikfarjam *et al.*, 2006; Shen and Strobel, 1994), or with a large scale movement of the FMN domain (Auchus *et al.*, 1998; Iyanagi, 2005a,b). The former model infers that electron transfer involves the pyrimidine ring. In this case, an electron tunneling pathway is presumably involved because the pyrimidine ring is buried in the protein. The aromatic amino acids, which sandwich the isoalloxazine ring of the FMN moiety, may participate in electron tunneling during transfer to the electron acceptor (Fig. 3). In this case, domain movement is not necessary for electron transfer.

Alternatively, the fully reduced FMN may transfer electrons to P450 by interaction between the P450 and the FMN-binding domain. This interaction may occur at the same structural region of the FAD-binding domain (Auchus *et al.*, 1998). Therefore domain movement may be needed to facilitate relative domain-domain reorientation during the electron transfer process. Intramolecular one-electron transfer from the reduced FAD to FMN occurs directly at the closest distance, as described previously. The dimethylbenzene ring of the FMN moiety must be positioned adjacent to the P450, which could be facilitated by a flexible linker between the FMN domain and the remainder of the molecule. Intriguingly, the isolated FAD domains of P450R and NOSs do not significantly reduce the isolated CaM-bound FMN domains (Iyanagi, unpublished data). This observation suggests that the electrostatic interaction between FAD and FMN domains is less specific, indicating flexibility in the relative orientation between electron donors and electron acceptors during the catalytic cycle. Furthermore, crystal structures of wild-type and various mutant P450Rs strongly suggest that the relative orientation and position of two flavin domains with respect to each other is quite flexible (Hubbard *et al.*, 2001).

The interaction surface of a P450 is not well understood, but mutagenesis experiments indicate that P450R interacts with the proximal surface of P4502B4 (Bridges *et al.*, 1998). The proximal surface, which contains the C-helix and adjacent to the heme prosthetic group, is highly conserved in the residues from various P450, and relatively electron positive when compared with the distal surface (Bridges *et al.*, 1998; Williams *et al.*, 2000; Zhang *et al.*, 2005; Zhao *et al.*, 2006). This electropositive region may interact with the negative-charged surfaces of FMN domain of P450R and/or b_5, facilitating association and electron transfer (Allorge *et al.*, 2005; Bridges *et al.*, 1998; Scott *et al.*, 2004; Zhao *et al.*, 2006). The electrons from P450R might be transferred from the FMN of the reductase by interacting at the opposite side of P450 with respect to the membrane (see Fig. 12).

The FMN-binding domain interacts with P450 to transfer electrons during catalysis. Therefore, mutations in the FMN-binding domain of P450R affect the interaction with P450. The electrostatic potential surface of the FMN domain of P450R shows distinct regions of positive and negative charge, which results in a significant electrical polarity. The negative charge is located in the area of the FMN-binding site. Zhao *et al.* (1999) carried out mutation analysis and demonstrated the importance of the electrostatic inter-actions involved in the binding of P450R to P450, including cytochrome *c*. The mutation D148N affected several acidic residues near the FMN molecule. The results suggest that P450 binds at the tip of P450R to cover the FMN cofactor. This hypothesis is also supported by the fact that the much larger P450 molecule cannot fit into the crystal structure of P450R (Wang *et al.*, 1997). The P4502D6*31 (CYP2D6) alleles are characterized by mutations encoding three amino acid substitutions: R296C, R440H, and S486T, although the R440H exchange alone is the inactivating mutation. The docking model between this mutant and P450R suggest that R440 constitutes part of a cluster of basic amino acid residues that play a role in P450R binding (Allorge *et al.*, 2005). Jenkins *et al.* (1997) have shown that substitution (E154Q) in the corresponding acidic cluster of *Anabaena* flavo-doxin affects its ability to transfer electrons to P450c17 (P45017A1). The flavoprotein component of the *Escherichia coli* sulfite reductase can act as a mammalian P45017A1 reductase. These data indicate that plant and bacteri-al flavodoxin, including flavodoxin-like domains, can donate electrons to mammalian P450. The mutation Q153R in human P450R (rat Q150), located at the FMN-binding site, reduces the activity of P45017A1 and cytochrome *c*. P45017A1 is located on the ER of steroidogenic tissues, and catalyzes the hydroxylation of the steroid 17α.

The *B. megaterium* P450BM3 fatty acid monooxygenase system is con-sidered the best model system for understanding P450R–P450 interactions (Sevrioukova *et al.*, 1999). However, this system operates as a dimer, and the P450 may accept electrons from the FMN of the reductase domain located on

the polypeptide partner (Neeli *et al.*, 2005). Therefore, intramolecular electron transfer from FMN to heme may not occur. NOS also functions as a dimer in which the P450-like domain accepts electrons from the FMN of the reductase domain located on the polypeptide partner (Garcin *et al.*, 2004) (Figs. 1, 2).

In the bacterial system, the flavodoxins can shuttle between the semiquinone and fully reduced states during the catalytic cycle (Nogues *et al.*, 2005). In P450R, the fully reduced FMN states (V and IX) may be the open form in which they can transfer electrons to an electron acceptor (Fig. 6). States I, II, III, IV, VI, VII, and VIII are closed forms in which intramolecular electron transfer between flavins occurs (Iyanagi, 2005a,b). However, it is difficult for the P450 and cytochrome *c* to gain access to the active site of these states. Therefore, the latter model assumes that intramolecular electron transfer between flavins is linked to a significant movement of the FAD domain. This model involves a redox-linked conformational change during electron transfer (Figs. 5, 6).

The electron acceptors accept an electron from $FMNH_2$, whereas $FMNH^{\bullet}$ is an inactive intermediate observed during the catalytic cycle. Therefore, the initial reaction in the catalytic cycle starts from the air-stable semiquinone species VI, and the V and IX states are active species for electron acceptors. With cytochrome *c* as the electron acceptor, a different molecule accepts electrons independently from these states. In contrast, a P450 requires two electrons delivered in two one-electron transfer steps. The same P450, which accepts the first electron from state V has to either move away from the reductase and accept an electron from a different reductase molecule or interact with a different site of the reductase (states VI, VII, VIII). This is followed by a redox-dependent conformational change, where a second electron is accepted from state IX. The second electron is also supplied from b_5, although the role of this transfer depends on the P450 isozyme, the substrate, and the precise experimental conditions (Zhang *et al.*, 2005). These findings indicate that the proximal surface involved in the
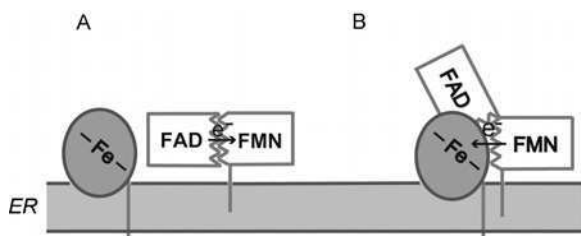

FIG. 6   The proposed model for closed (A) and open (B) forms of P450R. The P450R might be in redox-linked dynamic equilibrium between the closed and open forms (Iyanagi, 2005a,b).

interaction with P450R or b_5 are either identical or partially overlapping. Therefore, when the P450 interacts with b_5, the reductase must be displaced from the P450.

c. Activation of Molecular Oxygen by P450   The prokaryotic and eukaryotic P450s exhibit a conserved secondary structure and folding pattern (Mestres, 2005), and possess a common thiolate anion as the axial ligand of the heme (Omura, 2005). In the substrate-binding cavity, molecular oxygen (O_2) is activated by sequential one-electron reduction of heme iron (Fig. 7). The first step involves substrate binding, resulting in a substrate-bound form in equilibrium between high- and low-spin states. Substrate binding causes a change of redox potential, which facilitates the initial reduction of substrate-bound P450 by the reductase (Sligar *et al.*, 1979). The introduction of the first electron involves the reduction of ferric P450 (Fe^{3+}) and binding of O_2. The second electron addition enables the heterolytic O-O bond scission, in which the thiolate axial ligand of P450 promotes the cleavage of heme-bonded dioxygen by increasing the electron density of the iron atom (Denosov *et al.*, 2005; Hlavica, 2004). This reaction is coupled with proton donation. The 3-D structure of the oxygenated form of P450eryF (Nagano *et al.*, 2005) and P450CAM (Nagano and Poulos, 2005) supports the idea that the proton is supplied from a hydrogen-bonding network including water molecule(s), forming the water and the ferryl, $Fe^{4+} = O$ species.

This active motif, $O = Fe^{4+} -S-$ can act as an electrophilic oxidant (Groves, 2006). The oxygen of the ferryl species may be transferred to either a
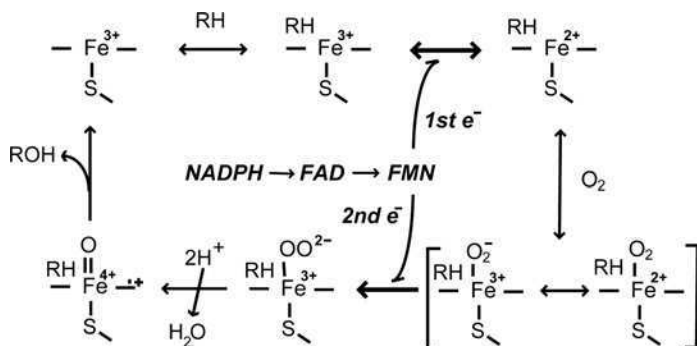
FIG. 7   The role of first and second electrons for molecular oxygen activation by P450. The first and second electrons are supplied from $FMNH_2$ of the P450R. In the NOS (Stuehr *et al.*, 2005), the hydroxylated Arg (ArgOH) formed in the first turnover is further oxidized by a second turnover cycle, resulting in the formation of L-citrulline (L-Cit) and nitric oxide (NO). RH indicates substrate, and the S indicates the axial ligand, thiolate anion from cysteine.

carbon-hydrogen bond (C-H) (hydroxylase), π bond (epoxidation), and heteroatom, such as a nitrogen or sulfur atom (hetero atom oxidation). Thus, the active oxygen-transferring species, assumed to hydroxylate the substrate, may be formed by a concerted cleavage in a "push and pull" effect mediated via the thiolate axial ligand and proton donation (Yoshioka *et al.*, 2002). The strong axial electron donation to the iron center allows hydrogen atoms to be abstracted from R-H bonds by ferryl radicals. It has been proposed that the hydroxylation reaction proceeds during the abstraction of a hydrogen atom from the substrate (RH), and one oxygen atom rebound as shown in Eqs. 2 and 3.

$$RH + O = Fe^{4+}{-}S{-} \rightarrow R^{\bullet} + (HO\text{-}Fe^{+4}{-}S{-}) \qquad (2)$$

$$R^{\bullet} + (HO\text{-}Fe^{+4}{-}S{-}) \rightarrow R:OH + Fe^{+3}{-}S{-} \qquad (3)$$
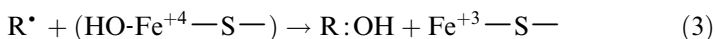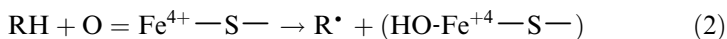
The hydroxylation mechanism, including the hydrogen transfer (Eq. 2) and oxygen rebound (Eq. 3), appears to be the predominant mechanism (Groves, 2006). Bach and Dmitrenko (2006) proposed a modified mechanism in which the isomeric metastable hydroperoxide intermediate, $OH^{\bullet}{\cdot}{\cdot}O\text{-}Fe^{3+}{-}S{-}$, which is formed from $HOO\text{-}Fe^{3+}{-}S{-}$, is the primary oxidant in the hydrocarbon reaction. Furthermore, electron transfer to generate a carbocation followed by capture of a hydroxyl anion has been proposed as an alternative oxygenating principle (Ullrich, 2003).

The NOS has been shown to catalyze a P450-like reaction (McMillan *et al.*, 1992), and converts L-Arg into L-Cit and NO in two consecutive reaction cycles with the intermediate formation of $N^{\omega}{-}$hydroxy-L-arginine (ArgOH) within the same substrate-binding site (Stuehr *et al.*, 2005). In the first reaction, H_4B serves as a transient one-electron donor to the ferrous oxyheme complex, because the radical form can accept one electron from the reductase, but the role of H_4B in the second reaction is unknown. These reactions occur inside a dimeric complex enzyme, in which the first and second electrons are supplied from $FMNH_2$ of the reductase located on the other subunit (Fig. 1). Likewise, because the P450R/P450 system is composed of distinct protein components, these reactions also occur by interaction between two different molecules. In both systems, thiol ligation to the heme iron enables the formation of the $Fe^{4+} = O$ species and oxygen transfer to substrates by sequential electron transfer from a reductase, containing FAD and FMN (Fig. 7).

d. Regulation of FAD-FMN Pair in P450R and NOS Reductase Domain   Electron transfer between most reactants in a biological system occurs between spatially fixed and oriented sites. A theory by Marcus and Sutin (1985) introduces a steric factor S for the intramolecular electron transfer, which takes into account the restricted orientation of donor (D) and acceptor (A)

at a distance appropriate for electron transfer in protein systems. The reaction between D and A proceeds as follows:

$$D + A \rightleftarrows D \cdot \cdot A \rightleftarrows D - A \rightleftarrows D^+ - A^- \\ \rightleftarrows D^+ \cdot \cdot A^- \rightleftarrows D^+ + A^- \tag{4}$$
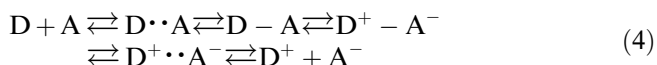
where $D \cdot \cdot A$ and $D-A$ represent the encounter complex and the active electron transfer complex, respectively. The $D-A$ complex is formed from the encounter complex $D \cdot \cdot A$ by suitable reorientation of D and/or A. The distance between D and A is regulated by the dynamics of the conformational changes in the complex. The electron transfer rate constant (k_{et}) is largely dependent on the separation distance between the electron donor and acceptor, and the redox potential difference, ΔG^0, between the donor and acceptor sites. These processes include at least three elemental steps: (1) formation of an active donor–acceptor complex; (2) electron transfer between the donor and acceptor; and (3) dissociation of the oxidized and reduced products. In the FAD–FMN pair of P450R and NOS isoforms, electron transfer occurs from FAD (donor) to FMN (acceptor). The active complex (FAD–FMN) is formed between the FAD and FMN molecules and electron transfer takes place directly between these flavins (Fig. 3).

Although the FAD–FMN pair of P450R is not strictly regulated, the reductase domains of nNOS and eNOS are regulated by CaM-binding. In contrast, the iNOS isozyme, which can bind CaM tightly at physiological concentrations of Ca^{2+}, is already in the activated form. Comparison of NOS reductase with P450R shows it to contain additional regulatory loops that control enzyme activity (Fig. 2). Regulation of nNOS and eNOS is achieved by the reversible binding of CaM to the inter-domain hinge region brought about by changes to the intracellular level of Ca^{2+}. Binding of CaM activates electron transfer from FMN to heme, resulting in the turnover of L-Arg and oxygen at the heme site. Interestingly, the isolated reductase domain of nNOS and eNOS is also activated by CaM. Cytochrome *c,* which can act as an artificial electron acceptor, is able to accept an electron from FMN of the nNOS reductase domain in the absence of CaM, but its rate of electron transfer is significantly accelerated ($\sim$20-fold) in the presence of CaM (Guan and Iyanagi, 2003; Guan *et al.*, 2003; Matsuda and Iyanagi, 1999). In contrast, the reduction of ferricyanide, which mainly accepts electrons from FAD, is activated only two- to fivefold by the binding of CaM. The data strongly suggest that either the reduction of FAD or interflavin electron transfer between FAD and FMN are activated by binding of CaM. As suggested from the position of the AI motif and C-terminal a-helix (Fig. 2), CaM binding might participate in increasing the efficiency of electron transfer by adjusting the distance and orientation between the FAD and FMN cofactors. Another model for the activation of the cytochrome *c* reductase activity suggests

that conversion from the CaM-free closed form to the CaM-bound open form is controlled by the binding of CaM (Craig *et al.*, 2002). In this model, cytochrome *c* can react with the CaM-bound open form. However, the conformational change induced by CaM-binding is not absolute, because the reduction of the flavins is increased by CaM-binding (Guan and Iyanagi, 2003; Guan *et al.*, 2003; Matsuda and Iyanagi, 1999). Both mechanisms may be involved in the activation of cytochrome *c* reductase activity.

The crystal structure of a CaM-free nNOS reductase domain revealed an ionic interaction between Arg 1400 in the C-terminal tail regulatory element and the 2′-phosphate group of bound NAD(P)H. Mutations of this residue (Arg1400Ser or Glu) increase cytochrome *c* reductase activity, indicating destabilization of a "shielded" conformation for the FMN module. However, no NO synthesis can be detected in the CaM-free state. These reports indicate that additional structural changes induced by the binding of CaM allow an interaction of the FMN module and the oxygenase heme domain to facilitate efficient electron transfer (Tiso *et al.*, 2005). Roman *et al.* (2000) reported about 30 amino acids from the C-terminal region of NOS repress enzyme activity in the absence of CaM. C-terminal deletion mutants possess increased cytochrome *c* activity in the absence of CaM, as well as displaying NO synthase activity. Roman *et al.* (2000) also suggested that this tail region, which is located between the flavins and/or between FAD and NADPH (Garcin *et al.*, 2004), might affect interflavin electron transfer in NOS (Jachymova *et al.*, 2005).

The turnover numbers for NO synthesis catalyzed by the isoforms of NOS have been determined as $\sim$200 min^{-1} for iNOS, 100 min^{-1} for nNOS, and 20 min^{-1} for eNOS (Roman *et al.*, 2002). The overall rate-limiting step in the NOS system is the reductase domain and heme center. An increase in flavin domain activity increases NO synthase activity (Nishida and de Montellano, 1998), indicating the different regulation by CaM of the reductase domain in the NOS isoenzymes. It is interesting to speculate whether interflavin electron transfer or dynamic equilibrium between the closed (shielded) and open (deshielded) forms might be differentially controlled. Both reductase domains have a different activity for ferricyanide and cytochrome *c*. Ferricyanide activity for both enzymes is greater than of cytochrome *c*. The cytochrome *c* activity for eNOS is lower than for nNOS, which correlates with the interflavin electron transfer in the two isoforms (Nishino *et al.*, 2003). Moreover, the extent of activation of eNOS by CaM is lower than of nNOS. Therefore, activation of the nNOS and eNOS isoforms by CaM might involve both (1) activation of the reductase domain, including electron transfer between flavins, accompanied by conformational change (Craig *et al.*, 2002; Iyanagi, 2005a,b; Matsuda and Iyanagi, 1999), and (2) interaction between the FMN module and heme domain accompanied by conformational change (Feng *et al.*, 2006; Garcin *et al.*, 2004; Roman and Masters, 2006). Thus, an electron transfer

may be directly linked to a change in conformation, which is differentially controlled in the nNOS and eNOS isoforms.

C. Antley-Bixler Syndrome/Missense Mutations of P450R

Although there are numerous functional cytochrome P450 genes in mammals, there is only one P450R gene in each species. Thus a single P450R is responsible for electron transfer to all the microsomal P450s. Knocking out the P450R gene in mice leads to embryonic lethality (Otto *et al.*, 2003; Shen *et al.*, 2002), and missense mutations of the human P450R gene cause multiple steroidogenic defects and a skeletal dysplasia called Antley-Bixler syndrome (Adachi *et al.*, 2004; Arlt *et al.*, 2004; Fluck *et al.*, 2004; Huang *et al.*, 2005a; Miller, 2005).

The P450R missense mutations could affect the reduction of microsomal P450 enzymes involved in the biosynthesis of steroids by several different mechanisms. For example, mutations in P450R may interfere with: (1) cofactor binding (NADP(H), FAD or FMN), (2) hydride transfer from NADPH to FAD, 3) interflavin electron transfer between FAD and FMN, or (4) interaction of P450R with P450 (Figs. 5, 6). This syndrome is also caused by disorders of steroidogenic P450s, which accept electrons from microsomal or mitochondrial P450-containing electron transfer systems (Fig. 1). Intriguingly, the mutations in P450R that give rise to Antley-Bixler syndrome might also have parallels with mutations affecting the NOS reductase domains. Such mutations are likely to cause disorders in neuronal transmission, the immune system, and control of vascular wall functions.

The Shen and Kasper group (1989, 1991, 1995, 1996, 1999, 2000) have used site-specific mutation analysis to probe important amino acid residues involved in catalysis. Huang *et al.* (2005a) have analyzed the mutations in P450R in patients with Antley-Bixler syndrome by using reconstituted system. Several missense mutants of human P450R (Y181D, R616X, R457H, Y459H, V492E) result in low activities of cytochrome *c,* 17α-hydroxylase, and 17,20 lyase. However, the mutations Q153R, L565P, C569Y, and V608F result in only a mild impairment of these electron acceptors. The isoalloxazine ring of FAD and FMN molecules are sandwiched between two aromatic groups (Fig. 3). The hydrogen bonding and van der Waals interactions between amino acid residues and the FAD and FMN cofactors serve to regulate both the binding and reactivity of the flavins. The Y140 residue, located on the *re*-side, lies at an angle of $\sim 40°$ to the isoalloxazine ring, whereas the Y178 residue is parallel to the *si*-side of the FMN ring. These two aromatic amino acid residues are involved in binding of FMN to the protein (Wang *et al.*, 1997). To test this hypothesis, Shen *et al.* (1989) prepared rats carrying the P450R mutant Y178D (equivalent to human Y181). A lowering of the FMN levels in the Asp mutant reduced the cytochrome *c* reductase

activity. These results are entirely consistent with the hypothesis that an aromatic residue at position 178 is required for binding of FMN (Fig. 3). The corresponding mutation in human P450R (Y181D) results in the anticipated enzyme defects. The FAD molecule is also sandwiched between two aromatic groups: W677 stacked against the *re*-face, and Y456 positioned at an angle of 60° to the *si*-face. This arrangement of aromatic residues is similar to that found in the FMN-binding site (Fig. 3). Mutation of Y456, which hydrogen bonds to the ribityl 4′-hydroxyl moiety of the flavin, results in a drastic loss in affinity for FAD (Shen and Kasper, 2000). The corresponding human Y459H (rat 456) mutation causes a decrease in the activity of enzymes associated with P450R. The negative charge of the pyrophosphate moiety of the FAD molecule is stabilized by the R454, V489, and T491 (Wang *et al.*, 1997). Mutation of T491 has a relatively modest effect on FAD-binding compared with mutation of R454 (Shen and Kasper, 2000). The corresponding human R457H mutant (rat 454) and V492E (rat 489) results in a marked reduction of the activities associated with P450R (Adachi *et al.*, 2004; Fluck *et al.*, 2004; Huang *et al.*, 2005a). Mutations of R457H and V492E cause a decrease in the FAD-binding affinity (Marohnic *et al.*, 2006). Alkylation, using iodoacetic acid, of the conserved cysteine (C566) residue in P450R (Haniu *et al.*, 1984; Shen *et al.*, 1991), causes a decrease in enzyme activity. The cysteine residue is protected from alkylation by the presence of NADPH, indicating a role for C566 (corresponding to human C569) in the binding of NADPH. A mutation of C569Y in humans causes a disorder in steroidogenesis, suggesting that the insertion of a bulky amino acid residue (i.e., tyrosine) reduces binding of NADPH.

However, mutations on the interflavin electron transfer between FAD and FMN, and interaction with P450 have not been identified.

III. Phase II: UDP-Glucuronosyltransferase (UGT)

Phase II conjugation reactions lead to the formation of a covalent linkage between a functional group either on the parent compound or on one introduced as a result of a phase I reaction. UDP-glucuronosyltransferases (UGTs) are the major class of enzymes that catalyze phase II reactions, such as the transfer of glucuronic acid (GlcUA) of UDP-glucuronic acid (UDP-GlcUA) to a functional group (-OH, -SH, -NH$_2$, C-C, or -COOH) of a xenobiotic and endobiotic. The xenobiotic may be a drug molecule or an endobiotic, such as bilirubin, bile acid, thyroxin, biogenic amine, fat-soluble vitamin, or steroid (Belanger, 2003; Bock, 2003; Clarke and Burchell, 1994; Guillemette *et al.*, 2003; King *et al.*, 2000; Mackenzie, 1990; Radominska-Pandya *et al.*,

1999; Siest *et al.*, 1987; Tukey and Strassburg, 2000). The enzymes comprise a large superfamily that can be classified, based on the degree of amino acid similarity between isoforms, into four gene families (Burchell *et al.*, 1991; Mackenzie *et al.*, 1997, 2005; Owens *et al.*, 2005). There are numerous functional UGT genes in mammals (i.e., 17 in rat, 18 in mouse, 19 in human). In this section, the structure/function of microsomal UGTs and their gene organizations are described.

A. Historical Perspective

In 1959, Williams (Williams, 1959) proposed that drugs and foreign molecules are metabolized in two distinct phases (phases I and II). In the early 1950s, however, little was known about the UGT enzymes involved in the metabolism of xenobiotics and endobiotics. Dutton and Storey (1951, 1953) discovered a thermostable cofactor in liver required for the formation of a phenol glucuronide in a cell-free preparation. They isolated and identified uridine diphosphate glucuronic acid (UDP-GlcUA) and its components, including uridine, two phosphates, and GlcUA, by paper chromatography (Dutton and Storey, 1954; Storey and Dutton, 1955). It was suggested that UDP-GlcUA may act as a GlcUA donor in the formation of glucuronides. Strominger and coworkers (1954, 1957) purified uridine diphosphate glucose dehydrogenase, which catalyzes the conversion of UDP-glucose (UDP-Glc) to UDP-GlcUA.

In 1954, Axelrod and Brodie (reflection by Axelrod, 2003) studied the formation of morphine glucuronide after incubating microsomes and the cytosolic fraction of rat liver with UDP-Glc and either TPN^+ ($NADP^+$) or DPN^+ (NAD^+). Morphine glucuronide was formed in the presence of DPN^+ (NAD^+). These pioneering experiments opened a new field into the enzymatic formation of glucuronide conjugates, including phase II reactions. Furthermore, these studies also led to the discovery of the role played by bilirubin glucuronide formation in jaundice. Analysis of the hereditary jaundiced Gunn rat (Axelrod *et al.*, 1957; Gunn, 1938; Schmid *et al.*, 1957) paved the way to understanding the human disease Crigler-Najjar syndrome (Crigler and Najjar, 1952).

In the 1950s–1960s, UDP-GlcUA was established as the glucuronyl donor during the biosynthesis of glucuronide derivatives of esters, aliphatic/aromatic compounds, steroids and bilirubin.

$$UDP\text{-}GlcUA + ROH \rightarrow UDP + RO\text{-}GlcUA \qquad (5)$$

In general, conjugation reactions result in the formation of water-soluble, pharmacologically inactive metabolites. However, some biologically active or

highly reactive conjugated metabolites can also be generated. For example, morphine-6-O-glucuronide is a more highly analgesic substance than the parent compound in suppressing pain symptoms in humans (Shimomura *et al.*, 1971; Yamada *et al.*, 2003; Yoshimura *et al.*, 1968). Furthermore, acyl-GlcUA derivatives can be quite reactive, resulting in the transfer of GlcUA to albumin (Smith *et al.*, 1989).

UGTs are membrane-bound enzymes with a markedly lower activity in native microsomes compared to disrupted microsomes. Two hypotheses, known as ''compartmentalization'' and ''conformation,'' were put forth to explain this observation. The former model proposed that the enzyme is located on the luminal side of the ER, with translocation of UDP-GlcUA from the cytosol being a rate-limiting step (Battaglia *et al*., 1996; Bossuyt and Blanckaert, 1997; Vanstapel and Blanckaert, 1988). In contrast, the latter model proposed that the enzyme is constrained by interactions between the protein and the membrane lipid bilayer (Vessey and Zakim, 1971; Zakim and Dannenberg, 1972). These models led to an understanding of the structural features of UGT as a membrane-binding enzyme and the localization to the ER membrane.

The purification and characterization of UGTs provided important information concerning the heterogeneity and properties of these enzymes. Isselbacher *et al.* (1962) partially purified the enzyme from rabbit liver microsomes after treatment with detergent. This pioneering work suggested the existence of more than one glucuronosyltransferase activity. Further purification of the enzyme was reported from many laboratories (Bock *et al.*, 1979; Burchell, 1977; Ishii *et al.*, 1993; Mackenzie *et al.*, 1985; Weatherill and Burchell, 1980; Yokota *et al.*, 1988). However, the isoforms of UGT were systematically separated from rat liver microsomes by chromatofocusing and affinity chromatography (Falany and Tephly, 1983). This systematic study has resulted in significant advances in our understanding of the biochemistry of UGTs.

In the mid 1980s, three groups (Iyanagi *et al.*, 1986; Jackson and Burchell, 1986; Jackson *et al.*, 1985; Mackenzie, 1986a,b; Mackenzie *et al.*, 1984) isolated cDNA of UGTs. These studies have allowed the analysis of the gene structure and the detection of specific UGT isoforms in tissue samples and cell lines.

Nagai *et al.* (1988) suggested that bilirubin and phenol UGT genes are closely linked on the same chromosome. In addition to bilirubin, the Gunn rat is also deficient in a 3-methylcholanthrene-inducible UGT isoform that has high activity toward phenolic substrates (Iyanagi *et al.*, 1989). Indeed, these two genes were subsequently located on the UGT1 gene complex (Emi *et al.*, 1995). The UGT genes are mainly encoded by the UGT1 gene complex locus, family 1 (Emi *et al.*, 1995; Ritter *et al.*, 1992; Zhang *et al.*, 2004) and family 2 (Mackenzie and Rodbourn, 1990) genes.

B. UGT

1. Structure and Function

UGTs are a family of membrane-bound enzymes that are concentrated in the ER and nuclear envelope of hepatocytes (Roy Chowdhury *et al.*, 1985). The major part of the enzyme is orientated on the luminal side of ER where the catalytic site is located. Each UGT enzyme includes an amino-terminal signal peptide that is cleaved during synthesis of the polypeptide chain and a stretch of 17 hydrophobic amino acids near the C-terminus that anchors the protein to the lipid bilayer (Iyanagi *et al.*, 1986) (Fig. 8). Indeed, the C-terminal 20–30 amino acid residues are responsible for the retention of UGTs in the ER (Jackson *et al.*, 1990; Teasdale and Jackson, 1996).

The mammalian UGT gene superfamily can be divided into four families: UGT1, UGT2, UGT3, and UGT8 (Burchell *et al.*, 1991; Mackenzie *et al.*, 1997, 2005). Members of the UGT1A family share an identical C-terminus (ca. 245 amino acids), which includes the binding site for the common
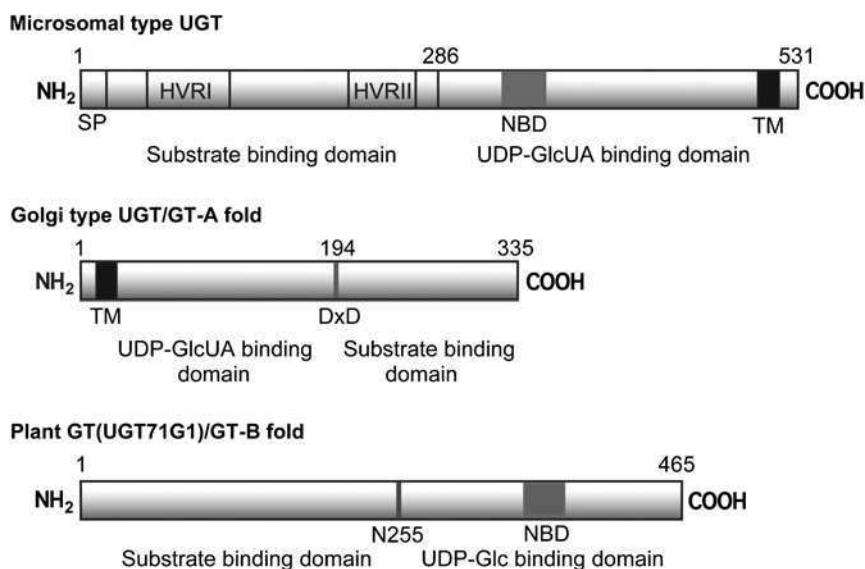

FIG. 8   Functional domains of microsomal- and Golgi-type UGTs and plant GT. Microsomal-type UGT indicates rat UGT (Iyanagi *et al.*, 1986). Golgi-type UGT indicates human β1, 3-glucuronosyltransferase 1(GlcAT-I) (Pedersen *et al.*, 2000). Plant GT indicates the UGT71G1 (Shao *et al.*, 2005). SP, signal peptide; NBD, highly conserved nucleotide-binding domain; TM, transmembrane domain; DxD, DxD motif. HVRI and HVRII indicate the hypervariable region I and II (Iyanagi, 1991), respectively. The N255 in the UGT71G1 is located in the loop linker between the N- and C-terminal domains.

cosubstrate UDP-GlcUA, whereas the N-terminal region (ca. 286 amino acids) shows a markedly lower level of identity (37–49%). The N-terminal portion of the enzyme contains the substrate-binding site and includes two hypervariable regions (Iyanagi, 1991) (Fig. 8). In contrast to the UGT1 family, the UGT2 family enzymes do not share a common C-terminal domain. However, the human genome project suggests that UGT2A1 and UGT2A2 genes can share a common C-terminal domain (Mackenzie et al., 2005). Comparison of members of the UGT2 gene family indicates that amino acid differences between different isoforms occur throughout the length of the protein, although the C-terminal halves are highly conserved.

The proteoglycan-associated β1,3-glucuronyltransferase 1 (GlcAT-I) and human natural killer-1 (HNK-1)–associated glucuronyltransferase (GlcAT-P) are localized on the luminal side of the Golgi membrane and have a transmembrane and stem region at the N-terminus (Kakuda et al., 2004; Negishi et al., 2003; Sugahara et al., 2003). The overall 3-D structures of both enzymes are similar and comprise two subdomains—an N-terminal subdomain containing the UDP-GlcUA-binding site and a C-terminal subdomain for substrate binding. Although GlcAT-I and GlcAT-P catalyze the transfer GlcUA from UDP-GlcUA to an acceptor sugar, they do not display any significant sequence homology with that of the microsomal UGTs. This indicates the existence of different UDP-glucuronosyltransferase families in the Golgi and ER membranes (Fig. 8).

The 3-D structure of GlcAT-I and GlcAT-P in the presence of both donor and/or acceptor substrate suggests that the inverting glycosyl transfer reaction proceeds through an S_N2-type in-line displacement mechanism, which generates a β−bond from the α-linked nucleotide sugar. In both enzymes, a glutamate residue acts as a catalytic base that deprotonates the 3-hydroxy of the terminal sugar in the acceptor substrate to form a strong nucleophile. The nucleophile then attacks the C-1 carbon of GlcUA in the UDP-GlcUA donor and forms an oxocarbenium ion-like transition state, similar to that proposed for glycosidase reactions (Cetinbas et al., 2006). This results in the formation of a β1-3 linkage and the subsequent dissociation of UGT (Kakuda et al., 2004; Negishi et al., 2003).

A similar mechanism may be operating in microsomal UGTs (Radminska-Pandya et al., 1999), although the 3-D structure of a microsomal enzyme has not been solved. Ouzzine et al. (2000) suggested that histidyl and aspartic/glutamic acid residues are likely candidates as base catalysts in microsomal UGTs. Interestingly, H38 and H485 in the sequences of rat and human UGTs are critical for activity because mutation results in an inactive enzyme. The structures of plant UDP-flavonoid/triterpene GT, UGT71G1 (Shao et al., 2005) and UDP-glucose:flavonoid 3-O-glycosyltransferase, VυGT1 (Offen et al., 2006) suggest that the H22-D121 (UGT71G1) and H20-D119 (VυGT1) pairs can function as catalytic bases (Fig. 9), respectively. In contrast,
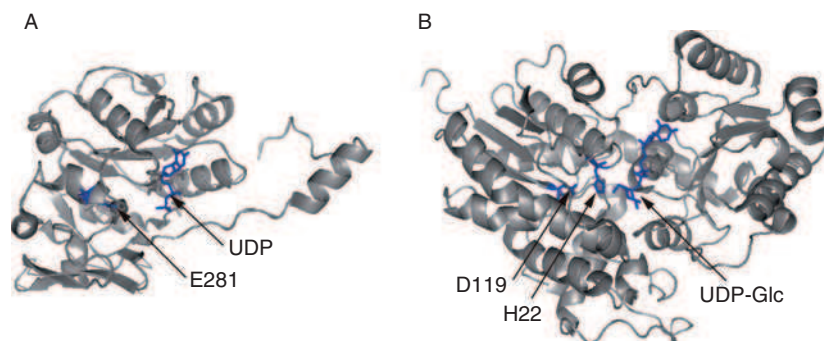
FIG. 9 The structures of GT-A fold (A) and GT-B fold (B). A, β1,3-glucuronosyltrans-
ferase I (GlcAT-I) (PDB code 1FGG). B, UDP-flavonoid/triterpene GT, UGT71G1 (PDB code
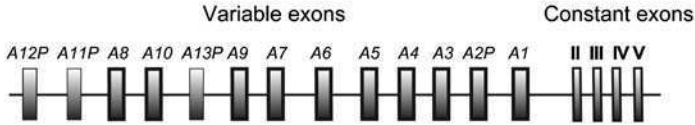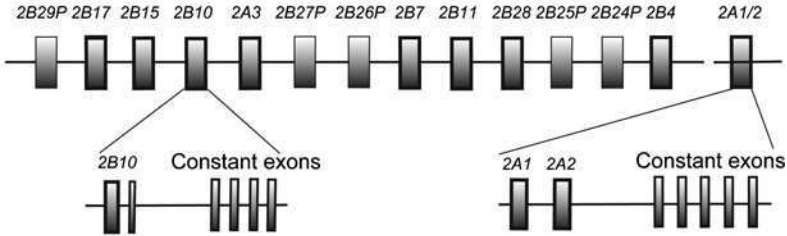2ACW).

the E281 in the GlcAT-I (Negishi *et al.*, 2003; Pedersen *et al.*, 2000) and E284 in
the GlcAT-P (Kakuda *et al.*, 2004) can function as catalytic bases.

2. Gene Organization

The organization of the UGT1 gene complex is unique among the genes
involved in the metabolism of druglike molecules. The UGT1 isoforms are
generated by alternative splicing of the transcript. The 5′-exon genes of the
UGT1 family each contain a unique first exon, plus four exons shared between
the genes (Fig. 10A). The first exons appear to have evolved by a process of
duplication, leading to the synthesis of proteins with identical C-terminal
(constant exon) and variable N-terminal domains (variable exons) in human
(Gong *et al.*, 2001; Owens *et al.*, 2005; Ritter *et al.*, 1992), rat (Emi *et al.*, 1995;
Iyanagi, 1991) and mouse (Zhang *et al.*, 2004). The human UGT1 gene complex
is located on chromosome 2(2q37). Thus the C-terminal domain of UGT1
family is responsible for the function of all UGT1 isoforms. Therefore, the
mutations of this domain may lead to defects of multiple UGT1 enzymes
(Iyanagi, 1991).

In contrast, the human UGT2 genes are clustered on chromosome 4q13–
4q21.1 (Turgeon *et al.*, 2000). Exon-sharing is also seen with the six-exon
UGT2A1 and UGT2A2 genes. However, UGT2A3 and those of the UGT2B
(six exons), UGT3 (seven exons), and UGT8 gene families (five or six exons)
do not share exons and are probably derived by a process of duplication of
all exons in the gene (Mackenzie *et al.*, 1997, 2005; Turgeon *et al.*, 2000).
Analysis of the C-terminal domain of the UGT1 and UGT2 families indicates
a high degree of sequence conservation to accommodate a common UDP-
GlcUA-binding site. Most UGT1 and UGT8 enzymes have been characterized

FIG. 10 The UGT1 gene complex and UGT2 family genes (A), and other complex genes (B). (A) The human UGT1 gene complex contains at least 13 variable exons, A1–A13 (Gong *et al.*, 2001; Mackenzie *et al.*, 2005), which can be spliced to constant exons, II–V. The variable exons are named A1, A2, A3..., and their gene products UGT1A1, UGT1A2, UGT1A3, etc. The human UGT1 and UGT2 loci extended over approximately 200 kb and 1.45 Mb, respectively. Pseudogene names end in the label *P*. The exons are not drawn to scale. (B) Complex gene locus for human immunoglobulin heavy chain (IGH), human protocadherins (PCDH) (Zhang *et al.*, 2004) and human β1,6-N-acetylglucosaminyltransferase (Inaba *et al.*, 2003; Yu *et al.*, 2003).

in detail, although the catalytic functions of the UGT3A enzymes and several UGT2 enzymes remain to be investigated (Mackenzie *et al.*, 2005).

The expression of specific UGT1 isoforms is achieved by selective activation of promoters preceding each variable exon (Emi *et al.*, 1995; Owens *et al.*, 2005; Sugatani *et al.*, 2005; Usui *et al.*, 2006). The UGT2 isoforms are also regulated by the promoter of each gene (Gardner-Stephen *et al.*, 2005; Mackenzie *et al.*, 2003). There is compelling evidence that the expression of the mouse, rat, and human UGT1 and UGT2 genes are regulated in a tissue-specific manner (Bock, 2003; Bock and Kohle, 2005; Chen *et al.*, 2005; Emi *et al.*, 1995, 1996, 2005; Gardner-Stephen *et al.*, 2005; Leung and Ho, 2002; Mackenzie *et al.*, 2003; Owen *et al.*, 2005; Shelby *et al.*, 2003; Tukey and Strassburg, 2000; Zhang *et al.*, 2004).

The UGT1 gene is found in several animal species, including mouse (Zhang *et al.*, 2004), rat (Emi *et al.*, 1995), rabbit (Lamb *et al.*, 1994), monkey (Albert *et al.*, 1999), and human (Gong *et al.*, 2001; Ritter *et al.*, 1992). The arrangement of genes akin to the UGT1 complex is not observed for other drug-metabolizing activities, including phase I, II, and III enzymes.

However, a similar gene organization is found for protocadherin, a diverse group of genes encoding cell surface proteins with an N-terminal cadherin-like extracellular domain (Wu and Maniatis, 1999). The protocadherin genes are organized into three sequentially linked clusters, designated α, β, and γ (Fig. 10B). The gene cluster consists of tandemly arrayed variable exons, which encode an extracellular domain consisting of six cadherin-like ectodomain repeats, a transmembrane domain, and a short cytoplasmic tail. At the 3′ end of both the α and γ subclusters are an additional three short exons that are alternatively *cis*-spliced to each α and γ variable exon, providing a constant cytoplasmic region. This gene cluster has been reported in zebrafish, mouse, rat, chimpanzee, and human (Hirayama and Yagi, 2006; Wu, 2005). As for the UGT1 gene cluster, the protocadherin genes are expressed in a tissue-specific manner with each variable gene preceded by a distinct promoter (Zhang *et al.*, 2004). Although the splicing of the protocadherin variable exon to the constant exons is not fully understood, the mechanism is likely be the same as for the UGT1A gene complex. The DNA rearrangement and somatic substitution do not occur in this gene complex (Hirayama and Yagi, 2006). This precise *cis*-alternative splicing may be achieved by the tight coupling of transcription to translation (Maniatis and Reed, 2002). Furthermore, the I-branching β-1,6-N-acetylglucosaminyltransferase (β1,6GlcNAcT) proteins are a family of type II transmembrane proteins, with the three isoforms encoded by genes similar to those of UGT1 and protocadherin (Inaba *et al.*, 2003; Yu *et al.*, 2003) (Fig. 10B).

3. Evolutionary Aspects

The bacterial and plant glycosyltransferases (GTs) are involved in cell wall and secondary metabolite biosynthesis. In plants, the glycosylation of small-molecular-weight lipophilic acceptors is thought to be involved in a key mechanism of metabolic homeostasis. UDP-Glc is the major activated sugar donor, although some isoforms use UDP-GlcUA instead (Bowles *et al.*, 2005; Li *et al.*, 2001; Sawada *et al.*, 2005). The P450s and GTs are involved in the biosynthesis of secondary metabolites. Although the P450R/P450 system has a similar cellular organization to the mammalian system, most plant GTs are soluble enzymes. The GTs can function to increase the stability and solubility of secondary metabolites as well as facilitating their detoxification (Bowles *et al.*, 2005, 2006). For example, the P450s and GTs are involved in the biosynthesis of glucosinolates, in which the toxic thiohydroximate is formed. The glycosylation of this compound can be considered as a detoxification reaction.

The structures of GTs have been studied in bacterial, plant, and mammalian species. Interestingly, the majority of GTs belong to only two structural superfamilies—GT-A and GT-B folds (Bourne and Henrissat, 2001; Hu and Walker, 2002; Unligil and Rini, 2000)—and utilize an activated UDP-sugar as a donor. The GT-A comprises two dissimilar domains (Fig. 9): an N-terminal subdomain with a Rossman fold, which includes the donor UDP-sugar-binding site, and a C-terminal subdomain composed mainly of mixed β sheets to which the acceptor sugar binds. The diversity of the acceptors is relatively low. The structure of human GlcAT-I and GlcAT-P shares this fold (Breton *et al.*, 2006; Kakuda *et al.*, 2004; Negishi *et al.*, 2003), whereas the GT-B superfamily is remarkably diverse although they possess a highly conserved two-domain architecture (Figs. 8, 9). The typical GT-B fold has been found in various glycosyltransferases (Breton *et al.*, 2006): phage T4 DNA-glucosyltransferase (BGT), which attaches glucose to hydroxymethyl cytosines on the DNA duplex; *E. coli* MurG, a glycosyltransferase that catalyzes the transfer of N-acetylglucosamine from UDP to the C-4 position of a lipid-linked N-acetylmuramyl peptide acceptor; bacterial vancomycin UDP-glycosyltransferases (Gtfs), which attach a glucose unit to a hydroxyl moiety; and plant UDP-flavonoid/triterpene GT, UGT71G1 and UDP-glucose:flavonoid 3-O-glycosyltransferase, VvGT1, which are involved in the biosynthesis of saponins and anthocyanins. These enzymes contain two α/β open sheet domains separated by a deep cleft. Structural analysis suggests that the C-terminal domain contains the UDP-GlcNAc-binding site, whereas the N-terminal domain contains the acceptor's (substrate's)-binding site.

The structures of these enzymes are characterized by two similar Rossman fold subdomain. Sequence alignments of GT-B superfamily members reveal a conserved motif that corresponds to the $\alpha/\beta/\alpha$ fold, composed of about 30

amino acid residues, in the C-terminal domain of BGT and MurG (Ha *et al.*, 2000; Hu and Walker, 2002; Kapitonov and Yu, 1999). The microsomal UGT isoforms (Clarke and Burchell, 1994; Mackenzie, 1990; Mackenzie *et al.*, 1997; Radominska-Pandya *et al.*, 1999) also possess this consensus sequence in the UDP-GlcUA-binding site (Fig. 8). This sequence is conserved in plant GTs (Gachon *et al.*, 2005). It is likely that the microsomal UGTs belong to the GT-B family. In contrast, Golgi-type UGTs contain the conserved DXD motif, which interacts with the ribose of the UDP moiety of UDP-GlcUA, as well as with the catalytically required divalent cation (Negishi *et al.*, 2003).

In addition to the bacterial enzymes, plant UDP flavonoid/triterpene GT (UGT71G1) also belongs to the GT-B fold (Shao *et al.*, 2005) (Fig. 9). Indeed, the structure of UGT71G1 is superimposable on bacterial GtfD despite the low level of sequence identity ($\sim$10%). The greatest difference between the two enzymes is observed in the N-terminal domain (residues, $\sim$155–210), which forms one side of the substrate's (acceptor molecule's) binding pocket. The C-terminal domains of UGT71G1 and GtfD share a greater level of sequence similarity because they bind similar nucleotide sugar donor molecules in contrast to the N-terminal domains, which recognize quite different acceptor molecules. Indeed, a conserved steroid-binding sequence has been identified in the N-terminal domain of plant GT isoforms (Kohara *et al.*, 2005; Moehs *et al.*, 1997). No microsomal UGT crystal structure is available, but structures of GT-B fold family proteins from different species suggest that mammalian microsomal UGTs might be composed of two subdomains.

Microsomal UDP-galactose:ceramide galactosyltransferase (CGT), which transfers galactose to lipophilic ceramide, belongs to family 8 (Ichikawa *et al.*, 1996; Mackenzie *et al.*, 2005) and is located in the ER membrane. The enzyme contains a nucleotide recognition domain which is located close to the C-terminal end of the C-terminal transmembrane domain. In contrast, plant diacylglycerol galactosyltransferase (DAGGalT), which catalyzes the synthesis of the major chloroplast membrane, is involved in the final step of peptidoglycan synthesis. This observation implies that the mechanism of chloroplast membrane biosynthesis is related to that of the bacteria cell wall. Although plant DAGGalT (Miege *et al.*, 1999) and bacterial MurG (Ha *et al.*, 2000) lack an identifiable terminal transmembrane domain, they are known to be membrane-associated proteins. However, the greatest difference between mammalian UGTs and bacterial/plant GT-B is in a C-terminal transmembrane hydrophobic domain. This motif has not been reported in bacterial and plant GTs (Gachon *et al.*, 2005).

Taken together, the data strongly suggest that microsomal UGTs are evolutionarily related to GTs from bacteria and plants (Bock, 2003; Mackenzie *et al.*, 1997). The structure of GT-A fold and the N- and C-terminal domains of GT-B fold are similar to each other (Shao *et al.*, 2005), although GT-A fold enzymes contain only a single extended domain that recognizes both domain

and acceptor. This suggests that GT-A and GT-B enzymes are evolutionarily related.

The GT-B enzymes, which are domain recognizing similar domains and another adapting divergent acceptors in the natural environment, might be produced as discussed in Fig. 11. One can speculate on the evolution of two domain enzymes, C-V for GT-A enzymes or V-C for GT-B enzyme, in which one domain recognizes similar nucleotide sugar donors (conserved domain, C) whereas the other has adapted to recognize different acceptors (variable domain, V). The vertebrate enzymes have also acquired a membrane-binding domain (Fig. 11). For example, the GT family of proteins from *Caenorhabditis (C.) elegans* contain a nucleotide sugar-binding motif and a C-terminal transmembrane domain and C-terminal motif similar to the ER retention signal (Kapitonov and Yu, 1999; Mackenzie *et al.*, 1997). These domains may have played an important role in the evolution of multicellular organisms. Fish, which are the most ancient vertebrates, contain multiple UGT isoforms with similar functional and structural properties to mammalian UGTs. This demonstrates a strong evolutionary conservation between phyla that diverged over 350 million year ago (Clarke *et al.*, 1992a). Moreover, the zebrafish EST project did not provide any evidence for an elaboration of family 1A genes by alternative splicing of multiple exons (George and Taylor, 2002).

Mammalian UGTs have developed the ability to accept different substrates by forming a gene complex as well as duplicating gene clusters.

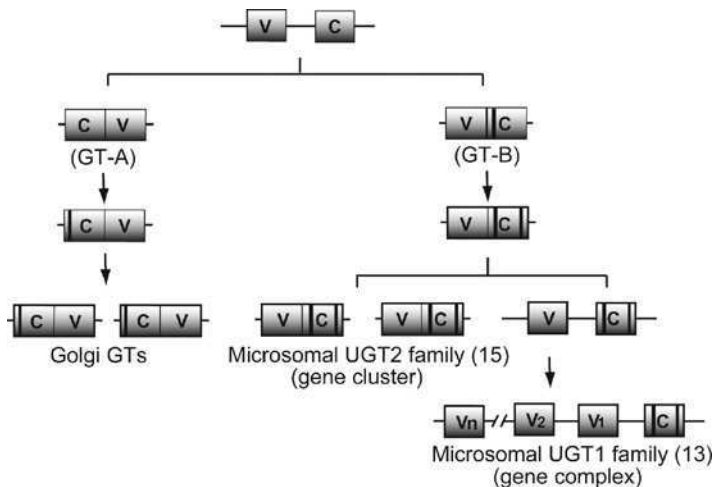FIG. 11   A model for the evolution of domains in the microsomal UGT family 1 and 2 genes and Golgi GTs (UGTs) genes. C indicates the nucleotide-sugar-binding domain. V indicates the substrate-binding domain. The number of human UGT1 and UGT2 isozymes, including pseudogenes is shown in parentheses. The putative transmembrane and the proposed nucleotide-binding domains are indicated by bars (Fig. 8).

The genomic ordering of variable exons of the UGT1 gene and their phylogenetic tree indicate that the UGT1A family can be broadly divided into two groups. The substrate specificity for UGT1A isoforms suggests that adaptive evolution has been involved in diversifying their functions. The variable exons are organized in a tandem array, so that a base substitution may result in gene conversion, as discussed for the protocadherin genes (Noonan *et al.*, 2004). Interestingly, the two hypervariable regions in the UGT1 family are located at the N-terminus (Iyanagi, 1991). Comparison of the UGT family members from several species shows that the C-terminal domain is the most highly conserved region. It is likely that the C-terminal domain was under evolutionary pressure to retain the binding site for the common UDP-GlcUA substrate. The ratio of nonsynonymous (Ka) to synonymous mutations (Ks) in the conserved nucleotide-binding segment of plant GTs is smaller than unity (Gachon *et al.*, 2005).

C. Hyperbilirubinemia

Bilirubin, the oxidative product of heme biotransformation in mammals, is a highly toxic compound that can cause severe brain damage in early childhood if allowed to accumulate in the body (Roy Chowdhury *et al.*, 2001). The nonpolar characteristics of bilirubin allow the molecule to pass through the blood brain barrier. Bilirubin is excreted in bile after esterification with GlcUA to form polar mono- and diconjugated derivatives (Fig. 12). Accumulation of unconjugated bilirubin in the body is caused by hereditary disorders known as Crigler-Najjar (CN) syndrome. The Gunn rat is a good model for unconjugated hyperbilirubinemia and valuable tool for the development of CN syndrome gene therapy. Severe hyperbilirubinemia may result from interaction with other mutated genes, such as glucose-6-phosphate dehydrogenase (Kaplan *et al.*, 1997, 2003) and beta-thalassemia (Sampietro *et al.*, 1977). In addition to severe hyperbilirubinemia, single nucleotide polymorphism (SNP) in UGT family 1 enzymes can also cause a mild hyperbilirubinemia (Burchell, 2003; Guillemette *et al.*, 2003; Koiwai *et al.*, 1995; Mackenzie *et al.*, 1997; Maitland *et al.*, 2006; Owens and Ritter, 1992, 2005; Saeki *et al.*, 2006).

1. Formation of Bilirubin

Bilirubin is derived from the heme of hemoglobin and hepatic hemoproteins such as P450 and catalase, which contain the heme as a prosthetic group. The biotransformation of heme by heme oxygenase isoform I (HO-1) proceeds in three successive oxygenation steps, via α-*meso*-hydroxyheme, verdoheme, and biliverdin. These reactions are catalyzed by microsomal HO-I, which has a hydrophobic C-terminus for binding to the microsomal membrane.

The N-terminal domain contains the heme-binding site. Both molecular oxygen (O_2) and NAD(P)H are required for the cleavage reaction, which proceeds via a multistep mechanism that depends on reducing equivalents provided by microsomal P450R (Colas and Ortiz de Montellano, 2003; Schacter *et al.*, 1972). The two proteins are held together by electrostatic interactions between the positively charged HO-I and negatively charged FMN-binding site of P450R. Intriguingly, the affinity of HO-I for P450R increases upon addition of NAD(P)H (Higashimoto *et al.*, 2005). It is likely that P450R combines with NAD(P)H to give the active conformation, which possesses a higher affinity for HO-I.

The first step in the biotransformation of the heme group to bilirubin is the cleavage of its α-methene bridge to form biliverdin IXα (Yoshida *et al.*, 1981). The HO reaction starts with the formation of the ferric heme–HO complex which is reduced to a ferrous state by the first electron donated from P450R. Molecular oxygen then binds to the complex to form the oxygenated species. Upon receiving a second electron from P450R and a proton from the distal water pocket, the iron-bound oxygen is converted to a hydroperoxide intermediate (Fe^{3+}-OOH). The terminal oxygen of Fe^{3+}-OOH attacks the α-*meso* carbon of the porphyrin ring to form ferric α-*meso*-hydroxyheme (Davydov *et al.*, 1999; Kikuchi *et al.*, 2005). The hydroxylated compound is converted by two further oxidation steps to biliverdin IXα. The ultimate products of these reactions are biliverdin, iron, and carbon monoxide. The overall rate-limiting step is in the release of biliverdin from the enzyme.

The central methene bridge of biliverdin at C-10 is then reduced by a cytosolic enzyme, NAD(P)H-biliverdin reductase, to bilirubin. It is interesting to speculate whether the biliverdin reductase accepts biliverdin from the cytosol or directly from HO-1. The release of biliverdin from HO-1 is promoted by biliverdin reductase (Schuller *et al.*, 1999), suggesting that HO-1 interacts directly with biliverdin reductase to deliver biliverdin. The structure of HO-1 indicates that half of the heme molecule is exposed to solvent. It has been proposed that biliverdin recognition by biliverdin reductase is achieved largely through an electrostatic interaction between the negatively charged propionate side chains of biliverdin and the positively charged residues of biliverdin reductase. Kikuchi *et al.* (2001) suggested that four basic residues of biliverdin reductase, located on the upper side of the putative NAD(P)H-binding pocket, are important components of the interaction site. This pocket, which can accommodate both biliverdin and NAD(P)H, may accept biliverdin directly from HO-1. Another possibility is that the liganding may mediate delivery of biliverdin from HO-1 to biliverdin reductase.

Bilirubin is an unsymmetrically substituted dicarboxylic acid. The introduction of CH_2 at C-10 induces a conformational change by rotation of the dipyrrinone groups about the central CH_2 group. The conformational change promotes

intramolecular hydrogen bonding of the propionic acid carbonyl to the amino groups of the dipyrrinone lactam and pyrrol ring. Indeed, these changes may explain some of the unusual properties of bilirubin, such as its high lipid/water partition coefficient and resistance to hepatobiliary excretion (McDonagh and Lightner, 1985). Furthermore, the proposed conformation of bilirubin is extremely hydrophobic resulting in a high affinity for tissues of the CNS.

2. Glucuronidation of Bilirubin and its Excretion in Bile

The conjugated compounds with glucuronate, sulfate, or glutathione are substrates for organic anion uptake transporters in the basolateral (sinusoidal) membrane as well as substrates for the ATP-driven conjugate efflux pump in the apical (canalicular) membrane, termed multidrug resistance protein 2 (MRP2; systematic name ABCC2) (Keppler, 2005).

Bilirubin is a highly toxic and hydrophobic endobiotic. The oxidative biotransformation pathway from heme to bilirubin could be considered a phase I reaction, and its subsequent glucuronidation a phase II reaction (Fig. 12). Bilirubin, which is an organic anion with limited water solubility, is essentially unexcretable in its native form. Organic anion transport proteins, OATP2 (Kamisako et al., 2000; Konig et al., 1999) are involved in uptake of bilirubin from the plasma membrane. The UGT1A isoform, UGT1A1, in rats (Clarke et al., 1992b; Iyanagi, 1991) and humans (Bosma et al., 1994) have been implicated in bilirubin glucuronidation. The mechanism of uptake, modification, and excretion of bilirubin is thought to constitute a typical model system for the biotransformation of xenobiotics in vivo.

The predicted topology of UGT on the ER membrane necessitates translocation of UDP-GlcUA, which is synthesized in the cytosol, to the lumen of the ER. This step is thought to be rate-limiting for UGT activity in the ER. Indeed, enzyme activity is increased upon disruption of vesicles with membrane-permeabilizing agents, such as detergent or alamethacin. UDP-N-acetylglucosamine (UDP-GlcNAc) stimulates the internalization of UDP-GlcUA into
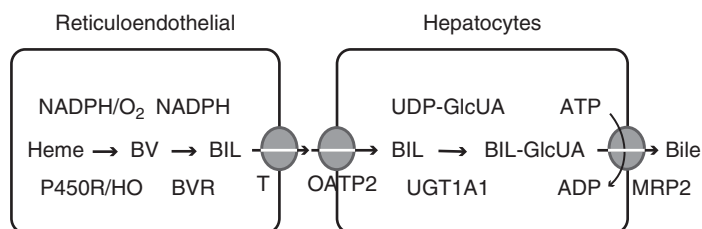

FIG. 12   Metabolic pathway from the heme group to bilirubin. P450R, NADPH-cytochrome P450 reductase; HO, heme oxygenase; BV, biliverdin; BIL, bilirubin; BVR, biliverdin reductase; UGT1A1, UDP-glucuronosyltransferase 1A1; OATP2, organic anion transporter 2; MRP2, multidrug resistance protein 2; T, proposed transporter.

intact microsomal vesicles (Ikushiro *et al.*, 1999). These observations strongly suggest the presence of transporters capable of delivering the UDP-GlcUA from the cytosolic surface to the active site of the enzyme.

Hauser *et al.* (1988) suggested that UDP-GlcUA is transferred from the cytoplasm to the luminal side of ER by a specific transporter. Muraoka *et al.* (2001) discovered a novel human nucleotide sugar transporter, which transfers both UDP-GlcUA and UDP-N-acetylgalactosamine (UDP-GalNAc). The same transporter can participate in glucuronidation at the ER membrane and/or proteoglycan biosynthesis in the Golgi membrane. Microsomal UDP-galactose:ceramide galactosyltransferase (UGT8A1), which is found exclusively in the ER, forms a complex with the transporter for UDP-Gal (Sprong *et al.*, 2003). Although the transporter is confined to the Golgi, it can also be retained in the ER, allowing the formation of Gal-ceramide. Furthermore, Csala *et al.* (2004) provide strong evidence for the presence of at least three different glucuronide transporters in the ER membrane with partly overlapping substrate specificity. The data also indicate that the size and/or shape of the substrate, rather than the GlcUA moiety per se, is/are the important determinant(s) of transporter specificity (Battaglia and Gollan, 2001; Csala *et al.*, 2004). In contrast, Ikushiro *et al.* (1997) suggested that the oligomer structures of UGTs might act as a common channel for the substrate and their conjugated products, although this does not require a specific transporter.

The resulting bilirubin mono- and diglucuronides are then transported to the cytosolic side across the ER membranes and excreted into the bile by conjugate export pump, MRP2.

3. Hyperbilirubinemic Gunn Rat

In 1938, Gunn (1938) described a mutant of Wistar rats (Gunn rats), which had hereditary hyperbilirubinemia. Homozygous Gunn rats are an excellent model of Crigler-Najjar syndrome type 1, and have provided valuable information on bilirubin metabolism, bilirubin toxicity, treatment of hyperbilirubinemia, and the molecular mechanism of inherited jaundice. Defects of the UGT1 family in Gunn rats result in the formation of a common truncated C-terminus. Therefore, all UGT1 isoforms are defective in the mutant rats, without affecting the other UGT family (Iyanagi, 1991). This defect is caused by a −1 frameshift mutation, which generates a premature termination codon, resulting in truncated UGT1 proteins that lack the C-terminal 116 amino acids (Emi *et al.*, 1995; Iyanagi, 1991; Iyanagi *et al.*, 1989). The truncated 43 kDa proteins, which have been detected in Gunn rat liver and kidney cells (ElAwady *et al.*, 1990), are subject to rapid degradation by the proteasome (Emi *et al.*, 2002).

Therefore, Gunn rat has been a valuable model for investigating the effect of multiple UGT1A enzymes in xenobiotic metabolism and toxicity (Kessler *et al.*, 2002; Krishnaswamy *et al.*, 2004; Narayanan *et al.*, 2004).

4. Crigler-Najjar Syndrome

In 1952, Crigler-Najjar described a syndrome characterized by a severe chronic nonhemolytic unconjugated hyperbilirubinemia (Crigler and Najjar, 1952). Two clinical forms of this syndrome have been described. The normal serum bilirubin levels are between 3–15 µM. Crigler-Najjar (CN) syndrome type 1 patients have unconjugated serum bilirubin levels > 340 µM, whereas type 2 patients have levels ranging between 60–340 µM. Gilbert syndrome has levels < 60 µM (Burchell, 2003). The molecular basis of these syndromes has been characterized by genetic analysis. As a result of the elucidation of the hyperbilirubinemic Gunn rat and of the rat and human UGT1 gene complex, several groups have discovered the genetic lesions that cause hyperbilirubinemia. The mutations that result in CN syndrome type 1 (http://som.flinders.edu.au/FUSO/ClinPharm/UGT/) have been found in the common exons and splicing sites as well as the first exon. Mutations in the first exon of UGT1A1, such as C280Stop(840C → A), and G276R(826G → C), indicate that human UGT1A1 is the major bilirubin isoform under physiological conditions (Bosma *et al.*, 1994). CN type 2 and Gilbert syndrome are caused by mutations of both the first and common exons. Gilbert syndrome is also caused by a TA insertion in the TATA element (A [TA]$_6$ TAA) in the promotor region of the first exon of UGT1A1 (Burchell, 2003). CN alleles are heterozygous in the coding region. The position of the mutation and its effect on the activity toward bilirubin may determine the type of hyperbilirubinemia (Ciotti *et al.*, 1999; Sugatani *et al.*, 2001).

5. Gene Therapy

Gene therapy is suitable for the most severe of the inherited defects of bilirubin conjugation, such as CN syndrome type 1. Treatment is based on the knowledge obtained for the rat and human UGT1 gene complex (Emi *et al.*, 1995; Gong *et al.*, 2001; Iyanagi, 1991; Ritter *et al.*, 1992). As mentioned previously, the Gun rat is a good animal model for the molecular analysis of human hyperbilirubinemia. A major advantage of the Gun rat is that the bilirubin glucuronides are not excreted into the bile. This allows direct and precise quantitation of the metabolic effect of the transfer of a therapeutic gene. The Gunn rat has been used extensively for evaluating UGT1A1 gene transfer using different vectors (Nguyen and Ferry, 2004) or oligonucleotide-based gene therapies (Kren *et al.*, 1999).

Recombinant retroviruses and adenoviruses have been used for somatic gene therapy. For example, Takahashi *et al.* (1996) have used adenovirus vectors. When the recombinant vectors expressing human UGT1A1 were injected into newborn Gunn rats, the protein was predominantly detected in rat liver. However, the immune response was mainly directed against adenoviral protein. By contrast, Toietta *et al.* (2005) used helper-dependent adeno-viral vectors devoid of all viral coding sequence. Induction of prolonged transgene expression gave a significantly reduced chronic toxicity compared to early-generation adenoviral vectors. The use of a tissue-specific promoter, such as the rat phospho*enol*-pyruvate carboxykinase promoter, is also possi-ble. Bellodi-Privato *et al.* (2005) have used murine retroviral vector to treat neonate Gunn rats. The data indicate the liver is the main site of expres-sion of the UGT1A1 protein, but there was also evidence of anti-UGT1A1 antibodies in the rat serum.

The third-generation vectors, known as lentiviral vectors, have been used for safe, efficient, and stable gene therapy in quiescent cells. This series of vectors, based on human immunodeficiency virus type 1 (HIV-1), have been developed for the transduction of hepatocytes. Various *in vivo* promoters, such as human cytomegalovirus (CMV), human phosphoglycerate kinase, and the mouse albumin promoter, can be introduced into the HIV-1–based vector. van der Wegen *et al.* (2006) used the lentiviral vector, which is under the control of the 1.9-kb distal enhancer of the mouse albumin gene fused to 0.3 kb of the mouse albumin promoter. The human UGT1A1 protein was mainly expressed in the liver parenchymal cells. Nguyen *et al.* (2005) used the lentiviral vector under the control of a liver-specific transthyretin promoter. Seppen *et al.* (2003, 2006) constructed a human UGT1A1 lentiviral expres-sion vector under the control of a liver-specific human phosphoglycerate kinase promoter, and found the recombinant protein expressed in several tissues. However, antibodies against UGT1A1 were detected in sera from rats injected during the fetal and neonatal period. These observations indi-cate that the xenogenic human UGT1A1 protein elicits a stronger immune response than endogenous rat UGT1A1.

An alternative approach to using a gene transfer vector is the direct introduc-tion of naked DNA into the target tissue (Danko *et al.*, 2004). Jia and Danko (2005a) reported nonviral gene transfer of UGT1A1 using naked plasmid DNA injected into liver and muscle tissue. Expression was under the control of a CMV promoter. However, although repeat injections reduced serum bilirubin levels, the effect did not exceed 2 weeks. Further studies to bring about more long-term corrections are currently underway (Jia and Danko, 2005b).

Kren *et al.* (1999, 2002) reported a novel method of gene therapy involving an *in vivo* site-directed gene repair system. The technique relies on cellular DNA repair mechanisms to correct point mutations by using a synthetic

RNA-DNA chimera. The nucleotide sequence in the chimera is designed to be complementary to the target genomic sequence, except for a single mismatch. The mismatch between the DNA limb of the chimeric molecule and the complementary strand of the genomic DNA triggers the cell's mismatch repair enzymes, resulting in correction of the mutation. For correction of the single guanosine base deletion in UGT1A1 exon 4 of the Gunn rat gene (Emi *et al.*, 1995; Iyanagi, 1991; Iyanagi *et al.*, 1989), the RNA-DNA chain was constructed to contain the wild-type sequence. The delivery system was targeted to the asialoglycoprotein receptor of hepatocytes. The presence of functional UGT1A1 protein was demonstrated by the appearance of bilirubin glucuronides in the bile and the concomitant reduction of serum bilirubin levels to 35–40% of pretreatment levels in Gunn rats. Furthermore, long-term correction was observed at least 2 years after treatment.

Experiments involving the gene therapy of Gunn rats have confirmed: (1) functional human UGT1A1 protein is expressed in the ER membrane of Gunn rat livers; (2) mono- and dibilirubin glucuronides are detected in bile; (3) a significant decrease of serum bilirubin levels can be elicited; (4) the UGT1A1 DNA is integrated in the chromosomal DNA; and (5) long-term correction for UGT1A1 activity is also observed.

IV. Coordinated Biotransformation by P450 and UGT

A. Subcellular Localization of the P450R/P450 System and UGT

The cellular membrane consists of a bilayer of amphipathic lipid molecules, made up of a polar head group and a nonpolar hydrocarbon tail. The hydrophobic tails are buried within the bilayer whereas the hydrophilic head groups are exposed at the surface. All eukaryotic cells have an ER, which comprise a system of membranes that enclose a space, or lumen (Palade, 1956). The space or lumen is physically separated from the cytosol by the ER membrane, which mediates selective transfer of molecules between the two compartments. The ER is involved in the biosynthesis of cellular molecules, including proteins, carbohydrates, and lipids. In addition, the ER membrane plays an important role in the metabolism of druglike molecules. The typical phase I, P450R/P450 system is localized on the cytosolic side of the ER membrane, whereas the phase II, UGTs are localized on the luminal side (Fig. 13).

Iyanagi *et al.* (1986), Mackenzie and Rodbourn (1990), Clarke and Burchell (1994), and Ishii *et al.* (2005) proposed a generally accepted model for the
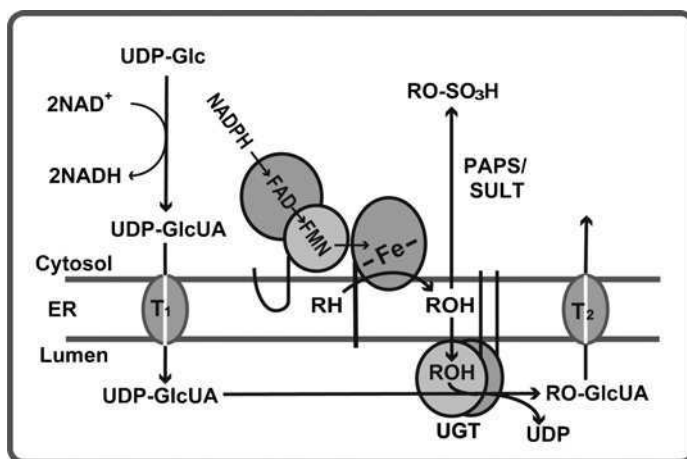
FIG. 13   The proposed model for topology of P450 reductase (FAD–FMN), P450 (Fe), UGT, and Transporters (T1 and T2) in the membrane of the ER. UGT is depicted as a dimer. T1 and T2 in the membrane of the ER represent the proposed transporters of UDP-GlcUA (Muraoka *et al.*, 2001) and glucuronides (Csala *et al.*, 2004), respectively. UDP-Glc, UDP-glucose; UDP-GlcUA, UDP-glucuronic acid; SULT, sulfotransferase; PAPS, 3′-phospho-adenosine 5′-phosphosulfate.

arrangement of the P450R/P450 system and UGTs in the ER membrane, although the biological significance of this orientation was unclear at the time. However, the given topology brings into question how the hydroxy-lated products of the P450s are delivered to the UGTs for further modifica-tion. Mammals possess numerous functional P450 genes (e.g., 84 in rat, 87 in mouse, 57 in human) (Gibbs *et al.*, 2004) and UGT genes (e.g., 17 in rat, 18 in mouse, 19 in human) (Mackenzie *et al.*, 2005). If the sequential reactions between P450s and UGTs occur on the ER membrane, approxi-mately 10^3 possible combinations of human P450s and UGTs might occur (i.e., 50 microsomal P450s $\times$ 19 UGTs). However, the number of functional combinations is restricted by the expression level and specificity for each isoform. The active site of microsomal P450s face toward the ER membrane from which the hydroxylated products can move to the cytosolic or luminal side of the membrane (Fig. 13). At the cytosolic side, the hydroxylated compounds are mainly conjugated by sulfotransferases, whereas at the lumi-nal side they are conjugated by UGTs. Although the sequential reactions catalyzed by P450s and UGTs are potentially very complicated, they are ultimately determined by kinetic parameters, such as the substrate specificity for each enzyme and the solubility of substrates and their corresponding metabolites.

B. Functional Interaction of P450s and UGTs in the ER

1. P450R and P450

a. Topology The topology of P450R and P450 and the formation of their complex on the ER membrane are important controlling factors for electron transfer. P450R is a 78-kDa flavoprotein associated with the cytoplasmic surface of the ER membrane. Two binding models have been proposed (Black and Coon, 1982). The first places the NH_2 and COOH termini on opposite sides (C_{cyt}-N_{lum}, type III topology) of the membrane with the hydrophobic segment spanning the lipid bilayer. An alternative model (C_{cyt}-N_{cyt}) proposes both termini to be located on the cytoplasmic side of the membrane. The latter model is supported by the fact that the NH_2-terminal anchor domain, which is not cleaved as a signal peptide, has hydrophobic characteristics and is acetylated (Haniu *et al.*, 1986). These observations indicate that the NH_2-terminal region of the domain is likely to be located on the cytosolic face (Fig. 13). This mode of binding facilitates more rapid movement across the surface of the ER than that of the type III topology. Furthermore, P450R is solubilized by trypsin treatment, indicating that the catalytic domain does not interact with ER membrane.

P450s that do not undergo posttranslational NH_2-terminal modification have an amino-terminal membrane-anchoring segment associated with the ER membrane with type III topology. In this case, the NH_2-terminus is found in the lumen and the COOH-terminus in the cytoplasm (Fig. 13). Furthermore, the hydrophobic tail and surface of the P450 enzyme can interact with the hydrophobic core region of the membrane. The basic residues are located above the hydrophobic region where they can interact favorably with the head group of phospholipids in the polar region of the membrane (Zhao *et al.*, 2006). The corresponding surface was identified in P450 17α (P45021A2) by a combination of chemical modifications and mass spectrometry (Izumi *et al.*, 2003). In this membrane-binding orientation, the P450 enzyme forms a channel for hydrophobic substrates in the lipid bilayer to access the active site. The channel also opens to the cytosol, providing access for less hydrophobic substrates. A hydrophobic compound might enter the substrate-binding site from the membrane surface (Zhao *et al.*, 2006). Comparison of the ligand-free and ligand-bound structure has identified structurally plastic regions that undergo conformational change in response to ligand binding. The most plastic regions are putative membrane-binding motifs involved in substrate access or substrate binding.

b. Interaction Between P450R and P450 Interaction between P450 and P450R molecules is required for electron transfer to occur (Hlavica *et al.*, 2003; Lewis and Hlavica, 2000; Peterson *et al.*, 1976; Taniguchi *et al.*, 1979).

Localization of these two proteins on the two dimensional (2-D) surface of the ER membrane serves to both concentrate reactants and increase the frequency of their interaction. In general, these processes include at least three elemental steps: (1) formation of an active P450R–P450 complex; (2) electron transfer between these complexes; and (3) dissociation of P450R and P450. The rate of P450 reduction by the first and second electron can be divided into two steps (Fig. 7):

$$\text{Reduction rate}^{\text{first electron}} = Ka\,k_{\text{ET}}^{1}(\text{P450R})(\text{P450}) \qquad (6)$$

$$\text{Reduction rate}^{\text{second electron}} = Ka\,k_{\text{ET}}^{2}(\text{P450R or } b_5)(\text{oxygenated P450}) \quad (7)$$

where Ka is the association constant between P450 or b_5 and reductase at concentrations represented by the terms in parentheses, and k_{ET}^{1} and k_{ET}^{2} are first and second electron transfer rate constants (Archakov and Bachmanova, 1990). The first and second electron is supplied from the P450R, but the second electron is also supplied via the cyt b_5 (Eq. 7) Transfer of the second electron is the rate-limiting step of the overall reaction (Imai et al., 1977). Therefore, the rate of formation of hydroxylated product (ROH) may be determined from Equation 7.

However, the reactions on the ER membrane are very complicated. In the Singer-Nicolson model (1972), it is believed that these proteins are distributed randomly in two dimensions, in which the movement and orientation of reactants are restricted. The ER membrane serves to concentrate the reactants and hence to increase the frequency of their interaction. As already discussed, the detergent-solubilized reductase has activity toward P450, whereas the protease-solubilized reductase, which lacks the membrane-binding domain, is not functional in the reduction of P450s. These observations suggest that the interaction of the reductase and P450 with the ER membrane is essential for efficient electron transfer.

Both b_5R, with an N-terminal myristoylated anchor, and b_5, with a C-terminal tail-anchored hydrophobic domain, are associated with the membrane and are exposed to the cytosolic compartment. Tonegawa et al. (2005) proposed that the interaction between b_5R and b_5 is described by a (2-D) random walk model.

The concentration of P450R in the membranes has been estimated to be 1/10 to 1/40 of total P450s (Estabrook et al., 1971; Watanabe et al., 1993). Therefore, the reductase must interact with all P450s. This raises the important question as to how the reductase can interact specifically with P450s. Two possible mechanisms are conceivable for functional interactions between the P450R and the P450 in microsomal membranes. One model suggests that the interactions are brought about by the lateral motion and subsequent collision of these proteins on the plane of the ER membrane

(Taniguchi *et al.*, 1979). Alternatively, the proteins may exist in the ER membrane as functional clusters in which the interactions can take place directly (Peterson *et al.*, 1976).

In addition to the interaction between P450 and P450R, P450–P450 interactions have also been observed in reconstituted systems (Kelley *et al.*, 2005). The presence of one P450 (P4501A2) enzyme can affect the function of another P450 (P4502B4). Interestingly, this interaction depends on ionic strength, indicating that P450–P450 complexes are formed by charge–pair interactions. Although electron transfer between two proteins, including the P450R/P450s, P450R/b_5, b_5/P450s and homo/hetero P450-P450 systems, have been studied *in vitro,* the interaction of these proteins on the natural membrane has yet to be fully addressed.

Kemper and coworkers (Ozalp *et al.*, 2005; Szczesna-Skorupa *et al.*, 2003) have used bimolecular fluorescence complementation techniques to study P450 interactions in a natural membrane context within living cells. Interactions of P450s with P450R were detected, as well as homo-oligomerization of P4502C2, but not P4502E1. The interaction of P4502C2 with P4502E1 is weak, but homo-oligomerization of P4502C2 is mediated by the signal anchor sequence. In contrast to self-oligomerization, the catalytic domain can mediate an interaction of P4502C2 with P450R. These data strongly suggest that interaction of reductase with P450 is mainly dependent on electrostatic interactions between the soluble catalytic domains of both enzymes. However, clustering of P450s on the ER membrane was detected. Studies of the rotational mobility of P450s indicate that P450 oligomers may dissociate when the enzyme binds to the reductase (Yamada *et al.*, 1995). The hetero-oligomerization of adrenal P450scc with P45011β (P45011B1) (Ikushiro *et al.*, 1992) and P4502B4 with P4501A2 (Kelley *et al.*, 2005) modulates the enzyme activity.

In addition to P450s, P450R can transfer an electron to cytochrome b_5, heme oxygenase and squalene monooxygenase. This raises the important question as to how the P450R interacts specifically with these electron acceptors, including P450. The highly conserved conformational motifs of the P450s may play a role in the molecular recognition process (Mestres, 2005). However, the structure of b_5 (Argos and Mathews, 1975) is significantly different from that of P450 (Johnson and Stout, 2005) and heme oxygenase (Lad *et al.*, 2003; Schuller *et al.*, 1999; Sugishima *et al.*, 2002) enzymes. It is well known that the soluble P450R domain, which lacks the N-terminal membrane-binding domain, cannot reduce b_5, which also lacks the N-terminal membrane-binding domain. Nevertheless, effective electron transfer occurs in detergent-solubilized enzymes, which retain the membrane-binding domain. Furthermore, the soluble domain of the reductase cannot directly reduce the microsomal bound P450s. These observations suggest that hydrophobic interactions between the membrane-binding domains of both

enzymes are necessary for effective electron transfer, whereas the electrostatic interactions between the soluble reductase and heme domain are less important. Thus, the hydrophobic region between the proteins ensures the correct orientation and juxtaposition of the binding sites at the proximal surface of the P450 and the dimethylbenzene ring of the FMN molecule. The functional complex formed between these proteins may only be transient, but movement of the FAD domain aids the orientation process (see Section II). The FMN domain as a flavodoxin-like carrier can donate an electron to several different electron acceptors. These proposals may explain why numerous P450s and other electron acceptors can be reduced by a single P450R molecule. However, both the protease solubilized b_5R and b_5, which lack a membrane-binding domain, can efficiently exchange an electron (Kimura et al., 2003), whereas protease solubilized P450R cannot transfer electrons to protease solubilized b_5 (Iyanagi and Mason, 1973).

2. P450 and UGT

a. Topology   As mentioned earlier, P450s are located on the cytosolic side of the ER, whereas UGTs are thought to be located within the lumen of the ER (Fig. 13). UGTs are synthesized as precursors of about 530 residues, which include a 20-amino acid signal peptide that mediates integration of the polypeptide chain into the ER (Fig. 8). The signal peptide is cleaved during protein maturation of the enzyme. The UGTs have a single 17-amino acid transmembrane segment and a 26-amino acid cytoplasmic tail at the C-terminal end of the molecule. The catalytic domain of the UGTs is localized on the luminal surface of the ER (Radominska-Pandya et al., 2005). On the other hand, microsomal aldehyde dehydrogenase, which lacks a signal sequence is a tail-anchored protein localized to the cytoplasmic face of the ER (Masaki et al., 2003).

A 45-amino acid C-terminal deletion mutant of UGT1A9, which includes the transmembrane segment, is water-soluble (Kurkela et al., 2004). However, the activity of this truncated UGT1A9 is significantly reduced suggesting that the membrane-binding segment is involved in the enzyme activity. A mutation within this region of UGT1A9, Y486D, causes Gilbert's and CN type II syndromes (Yamamoto et al., 1998). However, UGT1A1 isoform may contain a putative internal membrane-associated helix (Ciotti et al., 1998).

The microsomal UGTs have broad substrate specificity. Based on protein sequence analysis of UGT isoforms, it is generally accepted that the variable N-terminal domain binds substrate and therefore determines the substrate specificity, whereas the C-terminal domain binds the common substrate, UDP-GlcUA (Meech and Mackenzie, 1997). This analysis indicates that microsomal UGT enzymes consist of two domains. Compared with mammalian Golgi type II

membrane-associated UGT proteins (C_{lum}-N_{cyt} topology), which have relatively narrow substrate specificity and two tightly associated domains, the domains of microsomal UGT interact more loosely. The structure of plant UGT71G1, which has a GT-B fold, indicates that the active site is buried in the cleft region between the N- and C-terminal domains (Shao *et al.*, 2005). Furthermore, the two domains move in response to substrate binding. In microsomal UGT, the most variable amino acids are located in the N-terminal substrate-binding domain (Iyanagi, 1991). Photoaffinity labeling experiments have demonstrated that Phe90 and Phe93 in this region are directly involved in the catalytic activity of UGT1A10 isoform (Xiong *et al.*, 2006). It is likely that the active site of UGT is buried in the cleft region between the N- and C-terminal domains.

b. Interaction Between P450 and UGT   In general, membrane proteins containing a single transmembrane (TM) domain are able to interact at the catalytic and TM domains. However, interactions between P450 and UGT are mainly confined to the TM domains, although the interaction between the short N-terminal tail of the P450 and catalytic domain of UGT, or the short C-terminal tail of UGT and catalytic domain of P450 may also occur (Fig. 13). Two different TM helices, TM^{P450} and TM^{UGT}, in a lipid bilayer can interact to form three different dimers: TM^{P450}-TM^{P450}, TM^{P450}-TM^{UGT}, and TM^{UGT}-TM^{UGT}. The monomer-dimer equilibrium can be described by the individual equilibrium constants (Merzlyakov *et al.*, 2006). These constants may be determined from the specificity between isoforms of both enzymes, and their respective concentrations within the cell. To avoid the formation of a ternary complex, a P450 must dissociate from P450R before interaction with UGT. In this case, interactions between the TM domains and between catalytic domains must be considered within the homodimer or heterodimer of P450 or UGT.

   Taura *et al.* (2000) showed that rat UGTs coeluted with rat P4501A1 using a bovine serum albumin-conjugated Sepharose 4B column. Fremont *et al.* (2005) studied the formation of the complex using a coimmunoprecipitation method. The UGT2B7, UGT1A6, UGT1A1, and P4503A4 were immunoprecipitated with specific antibodies for each enzyme. Takeda *et al.* (2005) reported a coimmunoprecipitation of P4503A4 with UGT2B7. These data suggest that UGT isoforms may form complexes with each other, and UGT isoforms may interact with P450s.

   Ikushiro *et al.* (1997) demonstrated evidence for hetero-oligomers between UGT1A isoforms and UGT2B1. This complex was copurified using specific Sepharose-conjugated antibodies directed against either UGT1A or UGT2B1 isoforms and confirmed by crosslinking experiments. The effects of UGT complex formation on the stimulation of glucuronidation of testosterone and uptake of UDP-glucuronic acid (UDP-GlcUA) by UDP-N-acetylglucosamine

(UDP-GlcNAc) have also been examined. Alkaline pH-induced dissociation of the complex was associated with the loss of UDP-GlcNAc–dependent stimulation of glucuronidation, suggesting that two functional states of UGTs with different kinetic parameters correspond to the monomer and oligomer form of UGTs in the membrane. The UDP-GlcNAc–dependent stimulation of UDP-GlcUA uptake into the microsomal vesicles was also affected by the extent of complex formation. These results suggest that complex formation of the UGT isozymes affects the UDP-GlcNAc–dependent stimulation of glucuronidation via stimulation of UDP-GlcUA uptake.

Meech and Mackenzie (1997) engineered two forms of UGT2B1 that were catalytically inactive when expressed alone, but catalytically active when coexpressed. They further demonstrated that the N-terminal domain of UGT participates in dimer formation.

The interactions between P450/P450, P450/UGT, and UGT/UGT in the ER membrane may modulate the enzyme activity and substrate specificity. Kelley *et al.* (2005) reported P450-P450 interaction using a mixed reconstituted system containing P450R, P4502B4, and P4501A2. The enzyme activity decreased at high ionic strength, indicating disruption of the P450R-P450 and P450-P450 complexes. Additionally, they suggested a substrate-specific electrostatic interaction between P450 enzymes. Takeda *et al.* (2005) reported that the activity of morphine-3-glucuronide formation by UGT2B7 is reduced by addition of purified P4501A2 and P4502C9 in a concentration-dependent manner. Ishii *et al.* (2001) reported that morphine-6-glucuronide formation is enhanced by the UGT hetero-oligomer formation, indicating the change of substrate specificity.

The protein–protein interaction between P450 and UGT would permit reactions to proceed more efficiently in cells. The rat P4501A1 and UGT1A6 were coexpressed in yeast microsomes (Ikushiro *et al.*, 2004). However, efficient coupling of hydroxylation and glucuronidation in the sequential metabolism of 7-ethoxycoumarin was not observed in this combination. The data suggest that either a functional complex between these isoforms is not formed, or that the transfer of substrate from the active site of P450 to UGT is efficiently not coupled with the formation of complex.

Another example of the relationship between a UGT oligomer and its function has been reported for UGT1A1. In CN type II patients the interaction between the mutant forms of UGT1A1 and wild-type enzyme is dominant negative, and the activity toward bilirubin is reduced (Koiwai *et al.*, 1996). Further experimental studies support the homodimerization of recombinant UGT1A1 and may explain this dominant negative effect (Ghosh *et al.*, 2001).

However, it is very difficult to predict the interaction between enzymes on the ER membrane. A major question concerning the interaction between P450s and UGTs is how these enzymes interact with each other and how this

interaction modulates their activity. It is likely that contact between the TMs or the catalytic domains may induce a conformational change in the active site of the enzymes.

C. Broad Substrate Specificity

In general, enzymes have a high degree of substrate specificity. However, the phase I and phase II DMEs display broad, overlapping substrate specificities. Structural studies suggest that these enzymes have a highly plastic active site, which can accommodate a wide variety of substrates. Interestingly, the DNA repair enzymes, which recognize modified DNA as cytotoxic endobiotics, also have broad substrate specificity. It appears that these enzymes have acquired conformational plasticity, allowing them to recognize and metabolize multiple substrates. This may be a common feature of DMEs. Indeed, as described previously, protein–protein interactions may modify the activity and substrate specificity of the enzyme.

1. Microsomal Enzymes

a. P450/UGT   The substrate diversity of microsomal P450s suggests an easily accessible active site, whereas the mitochondrial P450s have a relatively narrow substrate specificity. The microsomal P450s can each bind and metabolize a number of substrates of different sizes, shapes, and stereochemistry (Clodfelter *et al.*, 2006; Johnson and Stout, 2005; Yanao *et al.*, 2005). The structures of P450s, including 2C5, 2C9, and 2B4 suggest that the ability of adjusting their binding sites to substrates that differ in size, shape, and polarity is to be responsible for the broad substrate specificity. After studying the structure of P4502B4, Zhao *et al.* (2006) proposed a model in which the most plastic regions of the enzyme are membrane-binding motifs involved in substrate access or substrate binding. The substrate binding site is largely hydrophobic, but polar interactions can contribute to selectivity for substrate binding and to the orientation of substrates. The relatively large active site cavities have the potential to bind two or more drug substrates simultaneously.

The Phe120, Asp301, Thr309, and Glu216 have been identified in microsomal P4502D6 substrate binding and catalysis. The Phe120 acts to control the orientation of the aromatic ring of substrates with respect to the heme moiety (Rowland *et al.*, 2006). The Thr309 is expected to be the conserved threonine (Thr) involved in proton delivery to the catalytic water, as proposed in bacterial P450cam (P450101) (Imai *et al.*, 1989; Nagano and Poulos, 2005). In addition to its potential role in molecular oxygen activation, Thr309 may play an important structural role within the active site crevice (Keizers *et al.*, 2005; van Waterschoot *et al.*, 2006).

The microsomal UGTs display broad, overlapping substrate specificities (King *et al.*, 2000; Radominska-Pandya *et al.*, 1999; Tukey and Strassburg, 2000), whereas the Golgi-type UGTs have a relatively narrow substrate specificity (Negishi *et al.*, 2003; Sugahara *et al.*, 2003). Although the structure of microsomal UGT is not known, it is likely that these enzymes contain the GT-B fold consisting of two domains. Control of conformational flexibility between the two domains is probably controlled in the same way as plant UGT71G1 (Shao *et al.*, 2005). Therefore, UGTs may also have a highly plastic active site due to the relative movement of the two domains, allowing the cavity to accommodate a wide variety of substrates. Because the active site of the P450 faces the ER membrane, the UGT may preferentially accept hydroxylated substrates from the ER membrane (Fig. 13).

b. Carboxylesterase (CE)   CEs, which are located on the luminal side of the ER, are typical phase I enzymes and play a major role in the metabolism, detoxification and elimination of xenobiotic and endobiotic esters (Imai, 2006; Satoh and Hosokawa, 1998). The enzymes also play a critical role in the activation of prodrugs and can hydrolyze a wide variety of ester, amide, and thioester substrates (Huang *et al.*, 2005b). The structure of rabbit and human enzymes is composed of a catalytic domain, αβ domain, and a regulatory domain (Bencharit *et al.*, 2002, 2003). The active site of this family shares a common mechanism of hydrolysis involving a catalytic trial composed of a serine, histidine, and either an aspartic acid or a glutamic acid residue. The enzymes contain a ''small rigid'' pocket, which recognizes the ester linkage, and a ''large flexible'' pocket, which recognizes a large region of the substrate. The anticancer prodrug CPT-11, which is a potent topoisomerase I inhibitor, is hydrolyzed by carboxyesterase (Slatter *et al.*, 1997) and the product, SN38, is conjugated by UGT1A1, UGT1A7, and UGT1A9 (Ando *et al.*, 2000; Ganng *et al.*, 2002; Iyer *et al.*, 1998; Tukey *et al.*, 2002; Villeneeuve *et al.*, 2003).

c. Epoxide Hydrolase (EH)   The epoxidation reaction of xenobiotics is catalyzed by P450s. The epoxide is then hydrolyzed by EHs to give the corresponding vicinal 1,2 diol (Arand *et al.*, 2003; Gomez *et al.*, 2006). The enzymes exist as microsomal and soluble isoforms. The microsomal EH contains an N-terminal membrane anchor, whereas soluble EH lacks this anchor. The structure of soluble EH suggests that the catalytic mechanism proceeds through a covalent alkylenzyme ester intermediate with an active site aspartate nucleophile. The hydrolysis of this intermediate requires that an oxygen atom of the enzyme is incorporated into the vicinal diol product. The microsomal EH also shares the same mechanism. Interestingly, the C-terminal catalytic domain is similar to that of haloalkane dehalogenase from *Xanthobacter autotrophicus,* which hydrolyzes carbon-halogen

bonds via a mechanism involving an aspartate nucleophile and an alkylen-zyme ester intermediate. Moreover, both these domains share a α/β hydro-lase fold. These findings suggest that the active site of EHs have diverged to accommodate a strikingly broad range of xenobiotic substrates (Argiriadi *et al.*, 1999).

2. Other Related Enzymes

a. NAD(P)H:Quinone Oxidoreductase (NQO1, DT-Diaphorase) NQO1 is a FAD-containing flavoprotein that catalyzes quinone. Detoxification is transcriptionally induced in response to various agents, including xenobiotics and oxidants (Talalay *et al.*, 1995). This enzyme catalyze the two electron reduction of a broad range of quinones to hydroquinones (Anusevicius *et al.*, 2002; Iyanagi and Yamazaki, 1970; Tedeschi *et al.*, 1995a,b). The structure of the enzyme has suggested a direct hydride transfer from reduced FAD to quinones (Li *et al.*, 1995). The duroquinone ring stacks 5 Å above the flavin ring with carbonyl oxygen atoms running almost parallel throughout the length of the isoalloxazine ring of the FAD cofactor. Steady-state kinetic and docking studies support a model in which quinones with aromatic rings in the quinone nucleus interact with the active site to optimize π-ring-stacking interactions with the isoalloxazine ring. Substrate binding is stabilized by hydrogen-bonding interactions with His161 in the active site (Zhou *et al.*, 2003). The larger quinones rotate along the quinone carbonyl axis, relative to the duroquinone position (Winski *et al.*, 2001). Thus, the enzyme modifies the shape of the active site to accommodate different substrates.

b. Sulfotransferase (SULT) SULTs catalyze the transfer reaction of the sulfate group from the donor 3′-phosphoadenosine 5′-phosphosulfate (PAPS) to an acceptor group of numerous substrates (Nagata and Yamazoe, 2000). The cytosolic SULTs transfer sulfate to small molecules, such as steroids, bioamines, and xenobiotics, whereas their counterparts in the Golgi membrane catalyze the transfer of sulfate to large molecules, such as glycosaminoglycans and proteins. Although the cytosolic- and Golgi-asso-ciated SULTs share a similar PAPS-binding site and catalytic core, the substrate-binding site is different (Negishi *et al.*, 2001). The binding site of membrane SULTs is a large open cleft with a hydrophilic surface, whereas a deep hydrophobic pocket provides the substrate-binding site in the cytosolic SULTs. The complementary structure of the substrate with the hydrophobic surface of the binding pocket appears to determine the substrate specificity.

c. DNA Repair Enzyme DNA damage caused by xenobiotic and endobiotic alkylation reagents creates lesions that are both mutagenic and cytotoxic (Mishina *et al.*, 2006; O'Brien, 2006). Although the DNA repair enzymes

are not DMEs, they can recognize modified DNA as a toxic endobiotic. Interestingly, the structure of the oxidative DNA/RNA repair enzyme AlkB suggests that the substrate-binding ''lid'' has a flexible conformation, which may enable docking of diverse alkylated nucleotide substrates in an optimal catalytic geometry (Yu *et al.*, 2006). Thus, AlkB appears to have developed an elegant molecular design in which these flexible protein segments recognize invariant nucleic acid backbone features to facilitate high-affinity docking of chemically diverse bases into a conserved catalytic core. The oxidative dealkylation is catalyzed by a dioxygen activation reaction involving a high-valent iron(IV)-oxo intermediate species that can function as an oxidant (Yu *et al.*, 2006), as discussed in Section II.

D. Biotransformation of Phenol Compounds

Aromatic hydrocarbons including benzene, benzo(α)pyrene and estrogens, are metabolized by phase I enzymes to give many metabolites. These metabolites, such as phenols, arene oxides, quinones, dihydrodiols, and diol epoxides, are conjugated by phase II enzymes to glucuronides, sulfate, and glutathione derivatives, which are water-soluble, detoxified products. The phenol derivatives are formed by P450 mediated hydroxylation or by the hydrolysis of epoxides. These compounds are converted to quinone derivatives by autoxidation or peroxidases, and their carbonyl groups may be enzymatically reduced to a hydroxyl moiety (Fig. 14). However, quinone compounds, including anticancer drugs, undergo one-electron reduction by flavoenzymes resulting in a semiquinone radical. The reaction of molecular oxygen with semiquinone radical generates an active oxygen species. In addition, the arylating quinones react with cellular nucleophiles such as thiols on cysteine residues of proteins, glutathione, and detoxifying agents such as N-acetyl cysteine (Fig. 14).

1. Hydroxylation of Aromatic Compounds and Their Biotransformation

Benzene, which is a highly toxic compound, is hydroxylated to phenol by P4502E1 and then converted to *p*-benzoquinone by autoxidation or peroxidases (Ross, 2005). In contrast, its epoxide is converted to diol by EH and oxidized to *o*-quinone. Glutathione (GSH) reacts directly with benzoquinone, whereas the hydroquinone is mainly conjugated by UGTs (King *et al.*, 2000) or SULTs (Shangari *et al.*, 2005), and it is readily excreted in bile or urine.

Benzo(α)pyrene is activated by P450s. P4501A1/1A2 and P4501B1 are responsible for the metabolic activation of this compound to epoxide
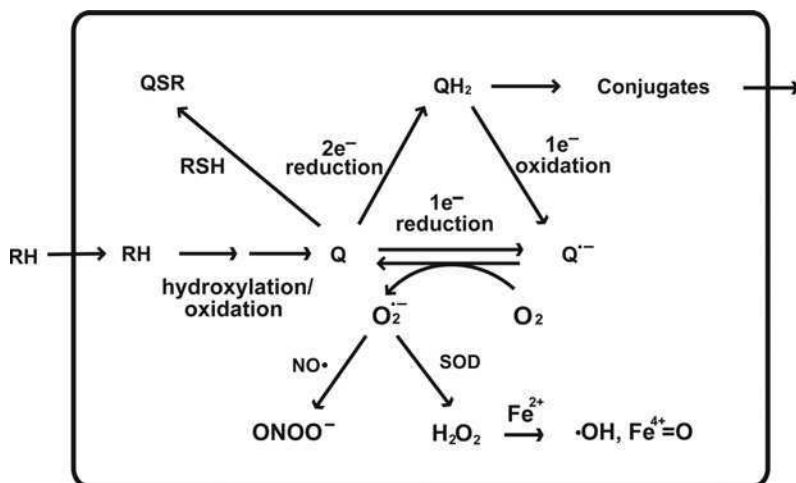
FIG. 14 The one ($1e^-$)- and two ($2e^-$)-electron oxidation-reduction reactions of quinone (Q) and active intermediates. RH and SOD indicate aromatic compound and superoxide dismutase, respectively.

intermediates, which are converted, with the aid of EH, to the powerful carcinogen, 7,8-diol-9,10-epoxide (Conney, 1982; Fujii-Kuriyama and Mimura, 2005; Miller, 1978; Shimada and Fujii-Kuriyama, 2004). The diol derivatives of benzo(α)pyrene are oxidized to o-quinone via semiquinone by autoxidation or peroxidases. However, aldo-keto reductase (AKR) catalyzes the formation of quinone derivatives by two-electron reduction. Fang et $al.$ (2002) suggest that several UGTs may play an important role in the overall glucuronidation of benzo(α)pyrene-$trans$-7,8-dihydrodiol, which is a precursor of the carcinogen derivatives. UGT1A1, 1A7, A8, 1A10, and potentially 1A8 play an important role in the glucuronidation of these compounds.

Estrogens are metabolized by oxidative and conjugative reactions (Samunio et $al.$, 2003). They are good substrates of P4501A1/1A2 and 1B1 that generate predominantly 2- and 4-hydroxy-catecholestrogen derivatives (2OHCE and 4OHCE), respectively. Both CEs are detoxified by several enzymatic processes, such as glucuronidation, sulfation, and methylation. UGT1A8, UGT1A9, and UGT2B7 are primarily involved in the inactivation of 4OHCEs (Thibaudeau et $al.$, 2006). UGT1A1, UGT1A3, UGT1A8, and UGT1A9 are also involved in the inactivation in 2OHCEs. The dihydrodiols are oxidized to o-quinones by autoxidation or peroxidases.

In addition to conjugation reactions, the quinone derivatives, which are derived from benzene, benzo(α)pyrene, and estrogens, react directly with the proteins and DNA (Bolton et $al.$, 2000; Zahid et $al.$, 2006).

2. One- and Two-Electron Oxidation and Reduction of Quinones

The flavoenzymes can reduce quinones (Qs) in one-electron, two-electron and mixed-type reduction (Anuservicius *et al.*, 2002; Cenas *et al.*, 2004; Iyanagi and Yamazaki, 1970; Matsuda *et al.*, 2000). Yamazaki (1971) proposed a tentative definition of the one-electron and two-electron transfer mechanism. Figure 15 illustrates the electron transfer between reduced flavin enzyme (E-FlH$_2$) and Q. When the reaction proceeds along route *a,* it is termed a two-electron mechanism regardless of the lifetime of the one-electron transfer intermediate (E-FlH$^{\bullet}$-QH$^{\bullet}$). Thus, a one-electron mechanism implies that the intermediate (E-FlH$^{\bullet}$-QH$^{\bullet}$) releases only semiquinone radical (QH$^{\bullet}$/Q$^{\bullet}$) via a reaction path indicated by route *b*. Anusevicius *et al.* (2005) proposed that the mechanism of quinone reduction by flavoenzymes may be determined by the stability of the intermediate, E-FlH$^{\bullet}$-QH$^{\bullet}$.

NQO1 catalyzes a typical two-electron transfer reaction, involving direct hydride transfer from FAD to quinones. In addition to NQO1, the short-chain dehydrogenase (SDR) and aldo-keto reductase (AKR), which do not contain the prosthetic group, catalyze the two-electron reduction of carbonyl compounds (Matsunaga *et al.*, 2006). These enzymes, which involve direct hydride transfer also mediate two-electron transfer reactions. In contrast, P450R, NADH:ubiquinone oxidoreductase (complex I), ferredoxin-NADP$^+$ reductase and NOSs are typical one-electron transfer enzymes (Cenas *et al.*, 2004; Fu *et al.*, 2004; Iyanagi and Yamazaki, 1969, 1970; Matsuda *et al.*, 2000). In P450R and NOS reductase domains, the fully reduced states (V and IX in Fig. 5) of FMN are the most active species with quinones (Yamamoto *et al.*, 2005). The rate of quinone reductions, including antitumor adriamycin and mitomycin C are stimulated by CaM (Fu *et al.*, 2004; Matsuda *et al.*, 2000).

However, hydroquinone compounds are oxidized in the one-electron reaction by peroxidases or autoxidation (Ohnishi *et al.*, 1969; Sawada *et al.*, 1975). The one-electron reduction of quinones or one-electron oxidation of hydroquinone results in the formation of semiquinone radicals, in which their cytotoxicity may depend on the reactivity with molecular oxygen (Cenas *et al.*, 2004).

The superoxide radical is formed from the direct reaction of oxygen with the semiquinone radical. Although this active oxygen radical dismutates to

$$\text{E-FlH}_2 \ + \ Q \rightarrow \text{E-FlH}_2\text{--Q} \rightarrow \text{EFlH}^{\bullet}\text{--QH}^{\bullet} \rightarrow \text{E-Fl--QH}_2 \xrightarrow{\ a\ } \text{El-F} \ + \ \text{QH}_2$$

$$\xrightarrow[\ b\ ]{} \text{EFlH}^{\bullet}+ \text{QH}^{\bullet}$$

FIG. 15   The mechanism of electron transfer in the overall bivalent oxidation-reduction. E-FlH$_2$ indicates enzyme-bound reduced flavin, and E-FlH$^{\bullet}$-QH$^{\bullet}$ corresponds to the principal formed one-electron transfer intermediate.

hydrogen peroxide and oxygen, the reaction is also catalyzed by superoxide dismutase (SOD). The superoxide radical reacts with nitric oxide (NO), resulting in the formation of peroxynitrite ($ONOO^-$) (Fig. 14). The peroxide also reacts with ferrous iron (Fenton reaction), resulting in a hydroxyl radical ($HO^{\cdot}$) and high-valent iron (IV)-oxo intermediates (FeO^{2+} or $Fe^{4+} = O$) (Groves, 2006; Yamazaki and Piette, 1990, 1991). The efficiency of hydroxyl radical formation depends on the nature of the iron chelator. The high-valent iron (IV)-oxo intermediates may be generated in the presence of a ligand such as ADP. As discussed in the activation of oxygen by P450 (see Section II.B.4.c), this active intermediate is also formed by one-electron reduction of ferrous oxygen complex. The P450R can efficiently donate electrons to ligand-bound $Fe^{2+}O_2$. The $HO^{\cdot}$ and $Fe^{4+} = O$ intermediates may also be involved in the complex formed from iron and anthracyclines (Zweier *et al.*, 1986) or bleomycins (Burger *et al.*, 1981, 1983).

The hydroxy radical ($HO^{\cdot}$) and high-valent iron intermediate ($Fe^{4+} = O$) can extract a hydrogen atom from the substrate (as discussed in Section II.B.4.c). Therefore, these may be a major cause of quinone-mediated toxicity in the presence of iron (Fe^{2+}), causing damage to lipids, proteins, and DNA (West and Marnett, 2006). For example, anthracyclines, which have quinone moieties in their structure, are potent antineoplastic drugs that cause apoptosis of breast cancer cells (Ravi *et al.*, 2005). The flavoenzymes catalyze one-electron reduction of anthracyclines (Bachur *et al.*, 1979; Fu *et al.*, 2004; Matsuda and Iyanagi, 1999; Powis, 1987; Vasquez-Vivar *et al.*, 1997). However, these compounds are glucuronized by UGT2B7, and their metabolites subsequently inactivated (Innocenti *et al.*, 2001).

All quinones are redox cycling agents that generate reactive oxygen (Fig. 14). In addition, the arylating quinones react with cellular nucleophiles such as thiols on cysteine residues of proteins, glutathione, and detoxifying agents such as N-acetyl cysteine, forming covalently linked quinone-thiol Michael adducts that retain the ability to function in redox cycling (Cadenas, 1989; Ollinger *et al.*, 1989). Wang *et al.* (2006) proposed that Michael adduct formation between arylating quinone and cysteine residues on secretory proteins can disrupt the formation of correct disulfide bonding, causing protein misfolding, inducing ER stress, and ultimately leading to cell toxicity.

In addition to xenobiotic compounds, physiological compounds are also important substrates in these pathways. For example, dopamine is oxidized to dopamine quinone, generating reactive oxygen radicals during the one-electron reduction (Paris *et al.*, 2005). The neurotoxicity of dopamine quinone is caused by the formation of a complex with iron. The NQO1 mediated two-electron reduction of aminochrome, which is derived from dopamine may reduce the toxicity (Segura-Aguilar and Lind, 1989). In addition to these events, dopamine quinone binds covalently to a variety of proteins via reduced cysteine residues (LaVoie *et al.*, 2005).

V. Concluding Remarks

It is interesting to consider the coordinate structure/function of the phase I and phase II DMEs in the ER membrane (Fig. 13). The P450s and UGTs display broad overlapping substrate specificities, which together constitute a general enzyme system within the organism. The DMEs including P450 and UGT have a highly plastic active site, which can accommodate a wide variety of substrates. Furthermore, P450R can donate electrons to 50 microsomal P450s. The microsomal electron transport systems facilitate the biotransformation and detoxification of xenobiotics with drastically different chemical structures. In addition, sequential biotransformation by both the P450R/ P450 system and UGTs constitute one of the major routes for drug metabolism. These reactions play a vital role in the metabolism and detoxification of xenobiotic (exogenous) and endobiotic (endogenous) compounds. The plant P450R/P450 system has a similar cellular organization to the mammalian system, although the GTs are soluble enzymes. The localization and functions of these enzymes strongly suggest that the DMEs are evolutionarily related to secondary metabolism of small molecules in plants. In addition, both the P450 and UGT are thought to acquire the diversity during the coevolution by ''animal-plant warfare'' (Holton *et al.*, 1993; Lewis, 2001; Lewis *et al.*, 1998).

The P450 genes are distributed on several chromosomes, although they are often found in clusters, but P450R is encoded by only one gene (Fig. 4). In contrast, UGTs are encoded by complex (UGT1A family) and cluster (UGT2 family) genes (Fig. 10A). UGT1 gene complex is unique, and not observed for other drug-metabolizing activities, including phase I, II, and III enzymes. This unique gene complex has not been found in plant and fish. A similar gene complex, which encodes the protocadherin proteins is expressed in distinct patterns in the nervous system. The gene organization of the UGT1 and protocadherin genes resembles that of the immunoglobulin and T-cell receptor gene clusters, with the tandemly arrayed variable region (V) exons followed by a diverse set of constant (C) exons (Fig. 10B). However, the diversity of the UGT1A and protocadherin proteins is due to alternative pre-mRNA splicing between different ''variable'' exons and ''constant'' exons. Furthermore, the phase I and II enzymes may have evolved synergistically for the metabolism of druglike molecules. The metabolic pathways for the hydrophobic compounds found in mammalian cells appear to necessitate compartmentalization in the hydrophobic ER membrane (Fig. 13). Finally, the P450R/P450 system and UGTs are now recognized as the principal enzymes involved in the detoxification of xenobiotics in the ER membrane.

Acknowledgments

References

Adachi, M., Tachibana, K., Asakura, Y., Yamamoto, T., Hanaki, K., and Oka, A. (2004). Compound heterozygous mutations of cytochrome P450 oxidoreductase gene (POR) in two patients with Antley-Bixler syndrome. *Am. J. Med. Genet. A.* **128,** 333–339.

Adak, S., Aulak, K. S., and Stuehr, D. J. (2002). Direct evidence for nitric oxide production by a nitric-oxide synthase-like protein from *Bacillus subtilis. J. Biol. Chem.* **277,** 16167–16171.

Albert, C., Vallee, M., Beaudry, A., Belanger, A., and Hum, D. W. (1999). The monkey and human uridine diphosphate-glucuronosyltransferase UGT1A9, expressed in steroid target tissues, are estrogen-conjugating enzymes. *Endocrinology* **140,** 3292–3302.

Allorge, D., Breant, D., Harlow, J., Chowdry, J., Lo-Guidice, J. M., Chevalier, D., Cauffiez, C., Lhermitte, M., Blaney, F. E., Tucker, G. T., Broly, F., and Ellis, S. W. (2005). Functional analysis of CYP2D6.31 variant: Homology modeling suggests possible disruption of redox partner interaction by Arg440His substitution. *Proteins* **59,** 339–346.

Ando, Y., Saka, H., Ando, M., Sawa, T., Muro, K., Ueoka, H., Yokoyama, A., Saitoh, S., Shimokata, K., and Hasegawa, Y. (2000). Polymorphisms of UDP-glucuronosyltransferase gene and irinotecan toxicity: A pharmacogenetic analysis. *Cancer Res.* **60,** 6921–6926.

Anusevicius, Z., Sarlauskas, J., and Cenas, N. (2002). Two-electron reduction of quinones by rat liver NAD(P)H:quinone oxidoreductase: Quantitative structure-activity relationships. *Arch. Biochem. Biophys.* **404,** 254–262.

Anusevicius, Z., Miseviciene, L., Medina, M., Martinez-Julvez, M., Gomez-Moreno, C., and Cenas, N. (2005). FAD semiquinone stability regulates single- and two-electron reduction of quinones by Anabaena PCC7119 ferredoxin:NADP+ reductase and its Glu301Ala mutant. *Arch. Biochem. Biophys.* **437,** 144–150.

Arand, M., Cronin, A., Oesch, F., Mowbray, S. L., and Jones, T. A. (2003). The telltale structures of epoxide hydrolases. *Drug Metab. Rev.* **35,** 365–383.

Archakov, A. I., and Bachmanova, G. T. (1990). "Cytochrome P450 and Active Oxygen." Taylor & Francis, London.

Argiriadi, M. A., Morisseau, C., Hammock, B. D., and Christianson, D. W. (1999). Detoxification of environmental mutagens and carcinogens: Structure, mechanism, and evolution of liver epoxide hydrolase. *Proc. Natl. Acad. Sci. USA* **96,** 10637–10642.

Argos, P., and Mathews, F. S. (1975). The structure of ferrocytochrome b5 at 2.8 A resolution. *J. Biol. Chem.* **250,** 747–751.

Arlt, W., Walker, E. A., Draper, N., Ivison, H. E., Ride, J. P., Hammer, F., Chalder, S. M., Borucka-Mankiewicz, M., Hauffa, B. P., Malunowicz, E. M., Stewart, P. M., and Shackleton, C. H. (2004). Congenital adrenal hyperplasia caused by mutant P450 oxidoreductase and human androgen synthesis: Analytical study. *Lancet* **363,** 2128–2135.

Auchus, R. J., Lee, T. C., and Miller, W. L. (1998). Cytochrome b5 augments the 17,20-lyase activity of human P450c17 without direct electron transfer. *J. Biol. Chem.* **273,** 3158–3165.

Axelrod, J. (1955). The enzymatic deamination of amphetamine. *J. Biol. Chem.* **214,** 753–763.

Axelrod, J. (2003). Journey of a late blooming biochemical neuroscientist. *J. Biol. Chem.* **278,** 1–13.

Axelrod, J., Schmid, R., and Hammaker, L. (1957). A biochemical lesion in congenital, nonobstructive, non-haemolytic jaundice. *Nature* **180,** 1426–1427.

Bach, R. D., and Dmitrenko, O. (2006). The ''somersault'' mechanism for the p-450 hydroxylation of hydrocarbons. The intervention of transient inverted metastable hydroperoxides. *J. Am. Chem. Soc.* **128,** 1474–1488.

Bachur, N. R., Gordon, S. L., Gee, M. V., and Kon, H. (1979). NADPH cytochrome P-450 reductase activation of quinone anticancer agents to free radicals. *Proc. Natl. Acad. Sci. USA* **76,** 954–957.

Backes, W. L., Batie, C. J., and Cawley, G. F. (1998). Interactions among P450 enzymes when combined in reconstituted systems: Formation of a 2B4-1A2 complex with a high affinity for NADPH-cytochrome P450 reductase. *Biochemistry* **37,** 12852–12859.

Black, S. D., and Coon, M. J. (1982). Structural features of liver microsomal NADPH-cytochrome, P-450 reductase. Hydrophobic domain, hydrophilic domain, and connecting region. *J. Biol. Chem.* **257,** 5929–5938.

Battaglia, E., and Gollan, J. (2001). A unique multifunctional transporter translocates estradiol-17beta-glucuronide in rat liver microsomal vesicles. *J. Biol. Chem.* **276,** 23492–23498.

Battaglia, E., Nowell, S., Drake, R. R., Mizeracka, M., Berg, C. L., Magdalou, J., Fournel-Gigleux, S., Gollan, J. L., Lester, R., and Radominska, A. (1996). Two kinetically-distinct components of UDP-glucuronic acid transport in rat liver endoplasmic reticulum. *Biochim. Biophys. Acta* **1283,** 223–231.

Belanger, A. (2003). Inactivation of androgens by UDP-glucuronosyltransferases. *Med. Sci. (Paris)* **19,** 931–936.

Bellodi-Privato, M., Aubert, D., Pichard, V., Myara, A., Trivin, F., and Ferry, N. (2005). Successful gene therapy of the Gunn rat by *in vivo* neonatal hepatic gene transfer using murine oncoretroviral vectors. *Hepatology* **42,** 431–438.

Bencharit, S., Morton, C. L., Xue, Y., Potter, P. M., and Redinbo, M. R. (2003). Structural basis of heroin and cocaine metabolism by a promiscuous human drug-processing enzyme. *Nat. Struct. Biol.* **10,** 349–356.

Bencharit, S., Morton, C. L., Howard-Williams, E. L., Danks, M. K., Potter, P. M., and Redinbo, M. R. (2002). Structural insights into CPT-11 activation by mammalian carboxylesterases. *Nat. Struct. Biol.* **9,** 337–342.

Bock, K. W. (2003). Vertebrate UDP-glucuronosyltransferases: Functional and evolutionary aspects. *Biochem. Pharmacol.* **66,** 691–696.

Bock, K. W., and Kohle, C. (2005). UDP-glucuronosyltransferase 1A6: Structural, functional, and regulatory aspects. *Meth. Enzymol.* **400,** 57–75.

Bock, K. W., Josting, D., Lilienblum, W., and Pfeil, H. (1979). Purification of rat-liver microsomal UDP-glucuronyltransferase. Separation of two enzyme forms inducible by 3-methylcholanthrene or phenobarbital. *Eur. J. Biochem.* **98,** 19–26.

Bolton, J. L., Trush, M. A., Penning, T. M., Dryhurst, G., and Monks, T. J. (2000). Role of quinones in toxicology. *Chem. Res. Toxicol.* **13,** 135–160.

Bosma, P. J., Seppen, J., Goldhoorn, B., Bakker, C., Oude Elferink, J., Roy Chowdhury, J., Roy Chowdhury, N., and Jansen, P. L. M. (1994). Bilirubin UDP-glucuronosyltransferase 1 is the only relevant bilirubin glucuronidating isoform in man. *J. Biol. Chem.* **269,** 17960–17964.

Bourne, Y., and Henrissat, B. (2001). Glycoside hydrolases and glycosyltransferases: Families and functional modules. *Curr. Opin. Struct. Biol.* **11,** 593–600.

Bowles, D., Isayenkova, J., Lim, E. K., and Poppenberger, B. (2005). Glycosyltransferases: Managers of small molecules. *Curr. Opin. Plant Biol.* **8,** 254–263.

Bowles, D., Lim, E. K., Poppenberger, B., and Vaistij, F. E. (2006). Glycosyltransferases of lipophilic small molecules. *Annu. Rev. Plant Biol.* **57,** 567–597.

Bossuyt, X., and Blanckaert, N. (1997). Carrier-mediated transport of uridine diphos-phoglucuronic acid across the endoplasmic reticulum membrane is a prerequisite for UDP-glucuronosyltransferase activity in rat liver. *Biochem. J.* **323,** 645–648.

Bredt, D. S., Hwang, P. M., Glatt, C. E., Lowenstein, C., Reed, R. R., and Snyder, S. H. (1991). Cloned and expressed nitric oxide synthase structurally resembles cytochrome P-450 reductase. *Nature* **351,** 714–718.

Breton, C., Snajdrova, L., Jeanneau, C., Koca, J., and Imberty, A. (2006). Structures and mechanisms of glycosyltransferases. *Glycobiology* **16,** 29R–37R.

Bridges, A., Gruenke, L., Chang, Y. T., Vakser, I. A., Loew, G., and Waskell, L. (1998). Identification of the binding site on cytochrome P450 2B4 for cytochrome b5 and cytochrome P450 reductase. *J. Biol. Chem.* **273,** 17036–17049.

Burchell, B. (1977). Studies on the purification of rat liver uridine diphosphate glucuronyl-transferase. *Biochem. J.* **161,** 543–549.

Burchell, B. (2003). Genetic variation of human UDP-glucuronosyltransferase: Implications in disease and drug glucuronidation. *Am. J. Pharmacogenomics* **3,** 37–52.

Burchell, B., Nebert, D. W., Nelson, D. R., Bock, K. W., Iyanagi, T., Jansen, P. L., Lancet, D., Mulder, G. J., Chowdhury, J. R., Siest, G., Tephly, T. R., and Mackenzie, P. I. (1991). The UDP glucuronosyltransferase gene superfamily: Suggested nomenclature based on evolu-tionary divergence. *DNA Cell Biol.* **110,** 487–494.

Burger, R. M., Peisach, S. B., and Horwitz, S. B. (1981). Activated bleomycin. A transient complex of drug, iron, and oxygen that degrades DNA. *J. Biol. Chem.* **256,** 11636–11644.

Burger, R. M., Kent, T. A., Horwitz, S. B., Munck, E., and Peisach, J. (1983). Mossbauer study of iron bleomycin and its activation intermediates. *J. Biol. Chem.* **258,** 1559–1564.

Cadenas, E. (1989). Biochemistry of oxygen toxicity. *Annu. Rev. Biochem.* **58,** 79–110.

Cenas, N., Anusevicius, Z., Nivinskas, H., Miseviciene, L., and Sarlauskas, J. (2004). Structure-activity relationships in two-electron reduction of quinones. *Meth. Enzymol.* **382,** 258–277.

Cetinbas, N., Macauley, M. S., Stubbs, K. A., Drapala, R., and Vocadlo, D. J. (2006). Identification of Asp174 and Asp175 as the key catalytic residues of human O-GlcNAcase by functional analysis of site-directed mutants. *Biochemistry* **45,** 3835–3844.

Chen, S., Beaton, D., Nguyen, N., Senekeo-Effenberger, K., Brace-Sinnokrak, E., Argikar, U., Remmel, R. P., Trottier, J., Barbier, O., Ritter, J. K., and Tukey, R. H. (2005). Tissue-specific, inducible, and hormonal control of the human UDP-glucuronosyltransferase-1 (UGT1) locus. *J. Biol. Chem.* **280,** 37547–37557.

Ciotti, M., Cho, J. W., George, J., and Owens, I. S. (1998). Required buried alpha-helical structure in the bilirubin UDP-glucuronosyltransferase, UGT1A1, contains a nonreplaceable phenylalanine. *Biochemistry* **37,** 11018–11025.

Ciotti, M., Werlin, S. L., and Owens, I. S. (1999). Delayed response to phenobarbital treatment of a Crigler-Najjar type II patient with partially inactivating missense mutations in the bilirubin UDP-glucuronosyltransferase gene. *J. Pediatr. Gastroenterol. Nutr.* **28,** 210–213.

Clarke, D. J., and Burchell, B. (1994). The uridine diphosphate glucuronosyltransferase multigene fanily; function and regulation. *Handb. Exp. Pharmacol.* **112,** 3–43.

Clarke, D. J., George, S. G., and Burchell, B. (1992a). Multiplicity of UDP-glucuronosyltransferases in fish. Purification and characterization of a phenol UDP-glucuronosyltransferase from the liver of a marine teleost, Pleuronectes platessa. *Biochem. J.* **284**(Pt 2), 417–423.

Clarke, D. J., Keen, J. N., and Burchell, B. (1992b). Isolation and characterisation of a new, hepatic bilirubin UDP-glucuronosyltransferase. Absence from Gunn rat liver. *FEBS Lett.* **299,** 183–186.

Clodfelter, K. H., Waxman, D. J., and Vojda, S. (2006). Computational solvent mapping reveals the importance of local conformational changes for broad substrate specificity in mammalian cytochromes P450. *Biochemistry* **45,** 9393–9407.

Colas, C., and Ortiz de Montellano, P. R. (2003). Autocatalytic radical reactions in physiological prosthetic heme modification. *Chem. Rev.* **103,** 2305–2332.

Conney, A. H. (1982). Induction of microsomal enzymes by foreign chemicals and carcinogenesis by polycyclic aromatic hydrocarbons: G. H. A. Clowes Memorial Lecture. *Cancer Res.* **42,** 4875–4917.

Craig, D. H., Chapman, S. K., and Daff, S. (2002). Calmodulin activates electron transfer through neuronal nitric-oxide synthase reductase domain by releasing an NADPH-dependent conformational lock. *J. Biol. Chem.* **277,** 33987–33994.

Crigler, J. F., and Najjar, V. A. (1952). Congenital familial nonhemolytic jaundice with kernicterus. *Pediatrics* **10,** 169–180.

Csala, M., Staines, A. G., Banhegyi, G., Mandl, J., Coughtrie, M. W., and Burchell, B. (2004). Evidence for multiple glucuronide transporters in rat liver microsomes. *Biochem. Pharmacol.* **68,** 1353–1362.

Danko, I., Jia, Z., and Zhang, G. (2004). Nonviral gene transfer into liver and muscle for treatment of hyperbilirubinemia in the Gunn rat. *Hum. Gene Ther.* **15,** 1279–1286.

Davydov, R. M., Yoshida, T., Ikeda-Saito, M., and Hoffman, B. M. (1999). Hydroperoxy-Heme Oxygenase Generated by Cryoreduction Catalyzes the Formation of -*meso*-Hydroxyheme as Detected by EPR and ENDOR. *J. Am. Chem. Soc.* **121,** 10656–10657.

Denosov, I. G., Makris, T. M., Sligar, S. G., and Schlichting, I. (2005). Structure and chemistry of cytochrome P450. *Chem. Rev.* **105,** 2253–2277.

Dutton, G. J., and Storey, I. D. (1951). Glucuronide synthesis in liver homogenates. *Biochem. J.* **48**(2), 29.

Dutton, G. J., and Storey, I. D. (1953). The isolation of a compound of uridine diphosphate and glucuronic acid from liver. *Biochem. J.* **53**(4), 37–38.

Dutton, G. J., and Storey, I. D. (1954). Uridine compounds in glucuronic acid metabolism. 1. The formation of glucuronides in liver suspensions. *Biochem. J.* **57,** 275–283.

Emi, Y., Ikushiro, S., and Iyanagi, T. (1995). Drug-responsive and tissue-specific alternative expression of multiple first exons in rat UDP-glucuronosyltransferase family 1 (UGT1) gene complex. *J. Biochem. (Tokyo).* **117,** 392–399.

Emi, Y., Ikushiro, S., and Iyanagi, T. (1996). Xenobiotic responsive element-mediated transcriptional activation in the UDP-glucuronosyltransferase family 1 gene complex. *J. Biol. Chem.* **271,** 3952–3958.

Emi, Y., Omura, S., Ikushiro, S., and Iyanagi, T. (2002). Accelerated degradation of mislocalized UDP-glucuronosyltransferase family 1 (UGT1) proteins in Gunn rat hepatocytes. *Arch. Biochem. Biophys.* **405,** 163–169.

Emi, Y., Ueda, K., Ohnishi, A., Ikushiro, S., and Iyanagi, T. (2005). Transcriptional enhancement of UDP-glucuronosyltransferase form 1A2 (UGT1A2) by nuclear factor I-A (NFI-A) in rat hepatocytes. *J. Biochem. (Tokyo).* **138,** 313–325.

ElAwady, M., Roy Chowdhury, J. R., Kesari, K., van Es, H., Jansen, P. L., Lederstein, M., Arias, I. M., and Roy Chowdhury, N. R. (1990). Mechanism of the lack of induction of UDP-glucuronosyltransferase activity in Gunn rats by 3-methylcholanthrene. Identification of a truncated enzyme. *J. Biol. Chem..* **265,** 10752–10758.

Estabrook, R. W., Cooper, D. Y., and Rosenthal, O. (1963). The light-reversible carbon monoxide inhibition of the steroid C-21 hydroxylation system of the adrenal cortex, *Biochem. Zeit.* **338,** 741–755.

Estabrook, R. W., Franklin, M. R., Cohen, B., Shigamatsu, A., and Hildebrandt, A. G. (1971). Biochemical and genetic factors influencing drug metabolism. Influence of hepatic microsomal mixed function oxidation reactions on cellular metabolic control. *Metabolism* **20,** 187–199.

Falany, C. N., and Tephly, T. R. (1983). Separation, purification and characterization of three isoenzymes of UDP-glucuronyltransferase from rat liver microsomes. *Arch. Biochem. Biophys.* **227,** 248–258.

Fang, J. L., Beland, F. A., Doerge, D. R., Wiener, D., Guillemette, C., Marques, M. M., and Lazarus, P. (2002). Characterization of benzo(a)pyrene-trans-7,8-dihydrodiol glucuronidation by human tissue microsomes and overexpressed UDP-glucuronosyltransferase enzymes. *Cancer Res.* **62,** 1978–1986.

Feng, C., Tollin, G., Holliday, M. A., Thomas, C., Salerno, J. C., Enemark, J. H., and Ghosh, D. K. (2006). Intraprotein electron transfer in a two-domain construct of neuronal nitric oxide synthase: The output state in nitric oxide formation. *Biochemistry* **45,** 6354–6362.

Fluck, C. E., Tajima, T., Pandey, A. V., Arlt, W., Okuhara, K., Verge, C. F., Jabs, E. W., Mendonca, B. B., Fujieda, K., and Miller, W. L. (2004). Mutant P450 oxidoreductase causes disordered steroidogenesis with and without Antley-Bixler syndrome. *Nat. Genet.* **36,** 228–230.

Fremont, J. J., Wang, R. W., and King, C. D. (2005). Coimmunoprecipitation of UDP-glucuronosyltransferase isoforms and cytochrome P450 3A4. *Mol. Pharmacol.* **67,** 260–262.

Fu, J., Yamamoto, K., Guan, Z. W., Kimura, S., and Iyanagi, T. (2004). Human neuronal nitric oxide synthase can catalyze one-electron reduction of adriamycin: Role of flavin domain. *Arch. Biochem. Biophys.* **427,** 180–187.

Fujii-Kuriyama, Y., and Mimura, J. (2005). Molecular mechanisms of AhR functions in the regulation of cytochrome P450 genes. *Biochem. Biophys. Res. Commun.* **338,** 311–317.

Gachon, C. M., Langlois-Meurinne, M., and Saindrenan, P. (2005). Plant secondary metabolism glycosyltransferases: The emerging functional analysis. *Trends Plant Sci.* **10,** 542–549.

Ganng, J. F., Montminy, V., Belanger, P., Journault, K., Gaucher, G., and Guillemette, C. (2002). Common human UGT1A polymorphisms and the altered metabolism of irinotecan active metabolite 7-ethyl-10-hydroxycamptothecin (SN-38). *Mol. Pharmacol.* **62,** 608–617.

Gao, Y. T., Smith, S. M., Weinberg, J. B., Montgomery, H. J., Guillemette, J. G., Ghosh, D. K., Roman, L. J., Martasek, P., and Salerno, J. C. (2004). Thermodynamics of oxidation-reduction reactions in mammalian nitric-oxide synthase isoforms. *J. Biol. Chem.* **279,** 18759–18766.

Garcin, E. D., Bruns, C. M., Lloyd, S. J., Hosfield, D. J., Tiso, M., Gachhui, R., Stuehr, D. J., Tainer, J. A., and Getzoff, E. D. (2004). Structural basis for isozyme-specific regulation of electron transfer in nitric-oxide synthase. *J. Biol. Chem.* **279,** 37918–37927.

Gardner-Stephen, D. A., Gregory, P. A., and Mackenzie, P. I. (2005). Identification and characterization of functional hepatocyte nuclear factor 1-binding sites in UDP-glucuronosyltransferase genes. *Meth. Enzymol.* **400,** 22–46.

Garfinkel, D. (1958). Studies on pig liver microsomes. I. Enzymic and pigment composition of different microsomal fractions. *Arch. Biochem. Biophys.* **77,** 493–509.

George, S. G., and Taylor, B. (2002). Molecular evidence for multiple UDP-glucuronosyltransferase gene families in fish. *Mar. Environ. Res.* **54,** 253–257.

Ghosh, D. K., and Salerno, J. C. (2003). Nitric oxide synthases: Domain structure and alignment in enzyme function and control. *Front Biosci.* **8,** 193–209.

Ghosh, D. K., Holliday, M. H., Thomas, C., Weinberg, J. B., Smith, S. M. E., and Salerno, J. C. (2006). Nitric-oxide synthase output state: Design and properties of nitric-oxide synthase oxygenase/FMN domain constructs. *J. Biol. Chem.* **281,** 14173–14183.

Ghosh, S. S., Sappal, B. S., Kalpana, G. V., Lee, S. W., Chowdhury, J. R., and Chowdhury, N. R. (2001). Homodimerization of human bilirubin-uridine-diphosphoglucuronate glucuronosyltransferase-1 (UGT1A1) and its functional implications. *J. Biol. Chem.* **276,** 42108–42115.

Gibbs, R. A., Weinstock, G. M., Metzker, M. L., Muzny, D. M., Sodergren, E. J., Scherer, S., Scott, G., Steffen, D., Worley, K. C., Burch, P. E., Okwuonu, G., Hines, S., *et al.* (2004). Rat Genome Sequencing Project Consortium. Genome sequence of the Brown Norway rat yields insights into mammalian evolution. *Nature* **428,** 493–521.

Gibson, G. G., and Skett, P. (2001). Introduction to drug metabolism, Third Edition, Nelson Thornes Publishers, United Kingdom.

Gillette, J. R., Brodie, B. B., and La Du, B. N. (1957). The oxidation of drugs by liver microsomes: On the role of TPNH and oxidase. *J. Pharmacol. Exp. Ther.* **119,** 532–540.

Gomez, G. A., Morisseau, C., Hammock, B. D., and Christianson, D. W. (2006). Human soluble epoxide hydrolase: Structural basis of inhibition by 4-(3-cyclohexylureido)-carboxylic acids. *Prot. Sci.* **15,** 58–64.

Gong, Q. H., Cho, J. W., Huang, T., Potter, C., Gholami, N., Basu, N. K., Kubota, S., Carvalho, S., Pennington, M. W., Owens, I. S., and Popescu, N. C. (2001). Thirteen UDP glucuronosyltransferase genes are encoded at the human UGT1 gene complex locus. *Pharmacogenetics* **11,** 357–368.

Gonzalez, F. J., and Kasper, C. B. (1981). Sequential translocation of two phenobarbital-induced polysomal messenger ribonucleic acids from the nuclear envelope to the endoplasmic reticulum. *Biochemistry* **20,** 2292–2298.

Groves, J. T. (2006). High-valent iron in chemical and biological oxidations. *J. Inorg. Biochem.* **100,** 434–447.

Guan, Z. W., and Iyanagi, T. (2003). Electron transfer is activated by calmodulin in the flavin domain of human neuronal nitric oxide synthase. *Arch. Biochem. Biophys.* **412,** 65–76.

Guan, Z. W., Kamatani, D., Kimura, S., and Iyanagi, T. (2003). Mechanistic studies on the intramolecular one-electron transfer between the two flavins in the human neuronal nitric-oxide synthase and inducible nitric-oxide synthase flavin domains. *J. Biol. Chem.* **278,** 30859–30868.

Guengerich, F. P. (2005). Human cytochrome P450 enzymes. *In* "Cytochrome P450: Structure mechanism and biochemistry" (P. R. Ortiz de Montellano, Ed.), pp. 377–530. Kluwer Academic/Plenum Publishers, New York.

Guillemette, C., Belanger, A., and Lepine, J. (2003). Metabolic inactivation of estrogens in breast tissue by UDP-glucuronosyltransferase enzymes: An overview. *Breast Cancer Res.* **6,** 246–254.

Gunn, C. H. (1938). Hereditary acholuric jaundice in a new mutant strain of rats. *J. Hered.* **29,** 137–139.

Gutierrez, A., Lian, L. Y., Wolf, C. R., Scrutton, N. S., and Roberts, G. C. (2001). Stopped-flow kinetic studies of flavin reduction in human cytochrome P450 reductase and its component domains. *Biochemistry* **40,** 1964–1975.

Gutierrez, A., Paine, M., Wolf, C. R., Scrutton, N. S., and Roberts, G. C. (2002). Relaxation kinetics of cytochrome P450 reductase: Internal electron transfer is limited by conformational change and regulated by coenzyme binding. *Biochemistry* **41,** 4626–4637.

Ha, S., Walker, D., Shi, Y., and Walker, S. (2000). The 1.9 A crystal structure of *Escherichia coli* MurG, a membrane-associated glycosyltransferase involved in peptidoglycan biosynthesis. *Prot. Sci.* **9,** 1045–1052.

Hall, A. V., Antoniou, H., Wang, Y., Cheung, A. H., Arbus, A. M., Olson, S. L., Lu, W. C., Kau, C. L., and Marsden, P. A. (1994). Structural organization of the human neuronal nitric oxide synthase gene (NOS1). *J. Biol. Chem.* **269,** 33082–33090.

Hall, D. A., Vander Kooi, C. W., Stasik, C. N., Stevens, S. Y., Zuiderweg, E. R., and Matthews, R. G. (2001). Mapping the interactions between flavodoxin and its physiological partners flavodoxin reductase and cobalamin-dependent methionine synthase. *Proc. Natl. Acad. Sci. USA* **98,** 9521–9526.

Haniu, M., Iyanagi, T., Legesse, K., and Shively, J. E. (1984). Structural analysis of NADPH-cytochrome P-450 reductase from porcine hepatic microsomes. Sequences of proteolytic fragments, cysteine-containing peptides, and a NADPH-protected cysteine peptide. *J. Biol. Chem.* **259,** 13703–13711.

Haniu, M., Iyanagi, T., Miller, P., Lee, T. D., and Shively, J. E. (1986). Complete amino acid sequence of NADPH-cytochrome P-450 reductase from porcine hepatic microsomes. *Biochemistry* **25,** 7906–7911.

Haniu, M., McManus, M. E., Birkett, D. J., Lee, T. D., and Shively, J. E. (1989). Structural and functional analysis of NADPH-cytochrome P-450 reductase from human liver: Complete sequence of human enzyme and NADPH-binding sites. *Biochemistry* **28,** 8639–8645.

Hanley, S. C., Ost, T. W., and Daff, S. (2004). The unusual redox properties of flavocytochrome P450 BM3 flavodoxin domain. *Biochem. Biophys. Res. Commun.* **325,** 1418–1423.

Hashimoto, Y., Yamano, T., and Mason, H. S. (1962). An electron spin resonance study of microsomal electron transport. *J. Biol. Chem.* **237,** 3843–3844.

Hauser, S. C., Ziurys, J. C., and Gollan, J. L. (1988). A membrane transporter mediates access of uridine 5′-diphosphoglucuronic acid from the cytosol into the endoplasmic reticulum of rat hepatocytes: Implications for glucuronidation reactions. *Biochim. Biophys. Acta* **967,** 149–157.

Hayaishi, O., Katagiri, M., and Rothberg, S. (1955). Mechanism of the pyrocatechase reaction. *J. Am.. Chem. Soc.* **77,** 5450–5451.

Hayano, M., Lindberg, M. C., Dorfman, R. I., Hancock, J. E., and Doering, W. E. (1955). On the mechanism of the C-11β-hydroxylation of steroids; a study with H_2O^{18} and O_2^{18}. *Arch. Biochem. Biophys.* **59,** 529–532.

Higashimoto, Y., Sakamoto, H., Hayashi, S., Sugishima, M., Fukuyama, K., Palmer, G., and Noguchi, M. (2005). Involvement of NADPH in the interaction between heme oxygenase-1 and cytochrome P450 reductase. *J. Biol. Chem.* **280,** 729–737.

Hirayama, T., and Yagi, T. (2006). The role and expression of the protocadherin-alpha clusters in the CNS. *Curr. Opin. Neurobiol.* **16,** 1–7.

Hlavica, P. (2004). Models and mechanisms of O-O bond activation by cytochrome P450. A critical assessment of the potential role of multiple active intermediates in oxidative catalysis. *Eur. J. Biochem.* **271,** 4335–4360.

Hlavica, P., Schulze, J., and Lewis, D. F. (2003). Functional interaction of cytochrome P450 with its redox partners: A critical assessment and update of the topology of predicted contact regions. *J. Inorg. Biochem.* **96,** 279–297.

Holton, T. A., Brugliera, F., Lester, D. R., Tanaka, Y., Hyland, C. D., Menting, J. G., Lu, C. Y., Farcy, E., Stevenson, T. W., and Cornish, E. C. (1993). Cloning and expression of cytochrome P450 genes controlling flower colour. *Nature* **366,** 276–279.

Horecker, B. L. (1950). Triphosphopyridine nucleotide-cytochrome c reductase in liver. *J. Biol. Chem.* **183,** 593–605.

Hu, Y., and Walker, S. (2002). Remarkable structural similarities between diverse glycosyl-transferases. *Chem. Biol.* **9,** 1287–1296.

Huang, N., Pandey, A. V., Agrawal, V., Reardon, W., Lapunzina, P. D., Mowat, D., Jabs, E. W., Van Vliet, G., Sack, J., Fluck, C. E., and Miller, W. L. (2005a). Diversity and function of mutations in p450 oxidoreductase in patients with Antley-Bixler syndrome and disordered steroidogenesis. *Am. J. Hum. Genet.* **76,** 729–749.

Huang, H., Fleming, C. D., Nishi, K., Redinbo, M. R., and Hammock, B. D. (2005b). Stereoselective hydrolysis of pyrethroid-like fluorescent substrates by human and other mammalian liver carboxylesterases. *Chem. Res. Toxicol.* **18,** 1371–1377.

Hubbard, P. H., Shen, A. L., Paschke, R., Kasper, C. B., and Kim, J. J. P. (2001). NADPH-cytochrome P450 oxidoreductase. Structural basis for hydride and electron transfer. *J. Biol. Chem.* **276,** 29163–29170.

Ichikawa, S., Sakiyama, H., Suzuki, G., Hidara, K. I., and Hirabayashi, Y. (1996). Expression cloning of a cDNA for human ceramide glucosyltransferase that catalyzes the first glycosylation step of glycosphingolipid synthesis. *Proc. Natl. Acad. Sci. USA* **93,** 4638–4643.

Ikushiro, S., Kominami, S., and Takemori, S. (1992). Adrenal P-450scc modulates activity of P-45011 beta in liposomal and mitochondrial membranes. Implication of P-450scc in zone specificity of aldosterone biosynthesis in bovine adrenal. *J. Biol. Chem.* **267,** 1464–1469.

Ikushiro, S., Emi, Y., and Iyanagi, T. (1997). Protein-protein interactions between UDP-glucuronosyltransferase isozymes in rat hepatic microsomes. *Biochemistry* **36,** 7154–7161.

Ikushiro, S., Emi, Y., Kimura, S., and Iyanagi, T. (1999). Chemical modification of rat hepatic microsomes with N-ethylmaleimide results in inactivation of both UDP-N-acetylglucos-amine-dependent stimulation of glucuronidation and UDP-glucuronic acid uptake. *Biochim. Biophys. Acta* **1428,** 388–396.

Ikushiro, S., Sahara, M., Emi, Y., Yabusaki, Y., and Iyanagi, T. (2004). Functional co-expression of xenobiotic metabolizing enzymes, rat cytochrome P450 1A1 and UDP-glucuronosyltransferase 1A6, in yeast microsomes. *Biochim. Biophys. Acta* **1672,** 86–92.

Imai, M., Shimada, H., Watanabe, Y., Matsushima-Hibiya, Y., Makino, R., Koga, H., Horiuchi, T., and Ishimura, Y. (1989). Uncoupling of the cytochrome P-450cam monooxygenase reaction by a single mutation, threonine-252 to alanine or valine: Possible role of the hydroxy amino acid in oxygen activation. *Proc. Natl. Acad. Sci. USA* **86,** 7823–7827.

Imai, T. (2006). Human carboxyesterase isozymes: Catalytic properties and rational drug design. *Drug Metab. Pharmacokinet.* **21,** 137–185.

Imai, Y., Sato, R., and Iyanagi, T. (1977). Rate-limiting step in the reconstituted microsomal drug hydroxylase system. *J. Biochem. (Tokyo)*. **82,** 1237–1246.

Inaba, N., Hiruma, T., Togayachi, A., Iwasaki, H., Wang, X. H., Furukawa, Y., Sumi, R., Kudo, T., Fujimura, K., Iwai, T., Gotoh, M., Nakamura, M., *et al.* (2003). A novel I-branching beta-1,6-N-acetylglucosaminyltransferase involved in human blood group I antigen expression. *Blood* **101,** 2870–2876.

Ingelman, M., Bianchi, V., and Eklund, H. (1997). The three-dimensional structure of flavodoxin reductase from *Escherichia coli* at 1.7 A resolution. *J. Mol. Biol.* **268,** 147–157.

Innocenti, F., Iyer, L., Ramirez, J., Green, M. D., and Ratain, M. J. (2001). Epirubicin glucuronidation is catalyzed by human UDP-glucuronosyltransferase 2B7. *Drug Metab. Dispos.* **29,** 686–692.

Ishii, Y., Oguri, K., and Yoshimura, H. (1993). Purification and characterization of a morphine UDP-glucuronyltransferase isoform from untreated rat liver. *Biol. Pharm. Bull.* **16,** 754–758.

Ishii, Y., Miyoshi, A., Watanabe, R., Tsuruda, K., Tsuda, M., Yamaguchi-Nagamatsu, Y., Yoshisue, K., Tanaka, M., Maji, D., Ohgiya, S., and Oguri, K. (2001). Simultaneous expression of guinea pig UDP-glucuronosyltransferase 2B21 and 2B22 in COS-7 cells enhances UDP-glucuronosyltransferase 2B21-catalyzed morphine-6-glucuronide formation. *Mol. Pharmacol.* **60,** 1040–1048.

Ishii, Y., Takeda, S., Yamada, H., and Oguri, K. (2005). Functional protein-protein interaction of drug metabolizing enzymes. *Front Biosci.* **10,** 887–895.

Isselbacher, K. J., Chrabas, M. F., and Quinn, R. C. (1962). The solubilization and partial purification of a glucuronyl transferase from rabbit liver microsomes. *J. Biol. Chem.* **237,** 3033–3036.

Iyanagi, T. (1977). Redox properties of microsomal reduced nicotinamide adenine dinucleotide-cytochrome b5 reductase and cytochrome b5. *Biochemistry* **16,** 2725–2730.

Iyanagi, T. (1991). Molecular basis of multiple UDP-glucuronosyltransferase isoenzyme deficiencies in the hyperbilirubinemic rat (Gunn rat). *J. Biol. Chem.* **266,** 24048–24052.

Iyanagi, T. (2005a). Interflavin one-electron transfer in the NADPH-cytochrome P450 reductase and nitric oxide synthase reductase domain. *In* "In Flavins and Flavoproteins" (T. Nishino R. Miura M. Tanokura, and K. Fukui, Eds.), pp. 453–464. ArchiTeck Inc., Tokyo.

Iyanagi, T. (2005b). Structure and function of NADPH-cytochrome P450 reductase and nitric oxide synthase reductase domain. *Biochem. Biophys. Res. Commun.* **338,** 520–528.

Iyanagi, T., and Mason, H. S. (1973). Some properties of hepatic reduced nicotinamide adenine dinucleotide phosphate-cytochrome *c* reductase. *Biochemistry* **12,** 2297–2308.

Iyanagi, T., and Yamazaki, I. (1969). One-electron-transfer reactions in biochemical systems. 1. One-electron reduction of quinones by microsomal flavin enzymes. *Biochim. Biophys. Acta* **172,** 370–381.

Iyanagi, T., and Yamazaki, I. (1970). One-electron-transfer reactions in biochemical systems. V. Difference in the mechanism of quinone reduction by the NADH dehydrogenase and the NAD(P)H dehydrogenase (DT-diaphorase). *Biochim. Biophys. Acta* **216,** 282–294.

Iyanagi, T., Makino, N., and Mason, H. S. (1974). Redox properties of the reduced nicotinamide adenine dinucleotide phosphate-cytochrome P-450 and reduced nicotinamide adenine dinucleotide-cytochrome b5 reductases. *Biochemistry* **13,** 1701–1710.

Iyanagi, T., Anan, F. K., Imai, Y., and Mason, H. S. (1978). Studies on the microsomal mixed function oxidase system: Redox properties of detergent-solubilized NADPH-cytochrome P-450 reductase. *Biochemistry* **17,** 2224–2230.

Iyanagi, T., Makino, R., and Anan, F. K. (1981). Studies on the microsomal mixed-function oxidase system: Mechanism of action of hepatic NADPH-cytochrome P-450 reductase. *Biochemistry* **31,** 1722–1730.

Iyanagi, T., Watanabe, S., and Anan, K. F. (1984). One-electron oxidation-reduction properties of hepatic NADH-cytochrome b5 reductase. *Biochemistry* **23,** 1418–1425.

Iyanagi, T., Haniu, M., Sogawa, K., Fujii-Kuriyama, Y., Watanabe, S., Shively, J. E., and Anan, K. F. (1986). Cloning and characterization of cDNA encoding 3-methylcholanthrene inducible rat mRNA for UDP-glucuronosyltransferase. *J. Biol. Chem.* **261,** 15607–15614.

Iyanagi, T., Watanabe, T., and Uchiyama, Y. (1989). The 3-methylcholanthrene-inducible UDP-glucuronosyltransferase deficiency in the hyperbilirubinemic rat (Gunn rat) is caused by a -1 frameshift mutation. *J. Biol. Chem.* **264,** 21302–21307.

Iyer, L., King, C. D., Whitington, P. F., Green, M. D., Roy, S. K., Tephly, T. R., Coffiman, B. L., Ratain, M. J. (1998). Genetic predisposition to the metabolism of irinotecan (CPT-11). Role of uridine diphosphate glucuronosyltransferase isoform 1A1 in the glucuronidation of its active metabolite (SN-38) in human liver microsomes. *J. Clin. Invest.* **101,** 847–854.

Izumi, S., Kaneko, H., Yamazaki, T., Hirata, T., and Kominami, S. (2003). Membrane topology of guinea pig cytochrome P450 17 alpha revealed by a combination of chemical modifications and mass spectrometry. *Biochemistry* **42,** 14663–14669.

Jachymova, M., Martasek, P., Panda, S., Roman, L. J., Panda, M., Shea, T. M., Ishimura, Y., Kim, J. J., and Masters, B. S. (2005). Recruitment of governing elements for electron transfer in the nitric oxide synthase family. *Proc. Natl. Acad. Sci. USA* **102,** 15833–15838.

Jackson, M. R., and Burchell, B. (1986). The full length coding sequence of rat liver androsterone UDP-glucuronyltransferase cDNA and comparison with other members of this gene family. *Nucl. Acids Res.* **14,** 779–795.

Jackson, M. R., McCarthy, L. R., Corser, R. B., Barr, G. C., and Burchell, B. (1985). Cloning of cDNAs coding for rat hepatic microsomal UDP-glucuronyltransferases. *Gene* **34,** 147–153.

Jackson, M. R., Nilsson, T., and Peterson, P. A. (1990). Identification of a consensus motif for retention of transmembrane proteins in the endoplasmic reticulum. *EMBO J.* **9,** 3153–3162.

Jenkins, C. M., Genzor, C. G., Fillat, M. F., Waterman, M. R., and Gomez-Moreno, C. (1997). Negatively charged anabaena flavodoxin residues (Asp144 and Glu145) are important for reconstitution of cytochrome P450 17alpha-hydroxylase activity. *J. Biol. Chem.* **272,** 22509–22513.

Jia, Z., and Danko, I. (2005a). Single hepatic venous injection of liver-specific naked plasmid vector expressing human UGT1A1 leads to long-term correction of hyperbilirubinemia and prevention of chronic bilirubin toxicity in Gunn rats. *Hun. Gene Ther.* **16,** 985–995.

Jia, Z., and Danko, I. (2005b). Long-term correction of hyperbilirubinemia in the Gunn rat by repeated intravenous delivery of naked plasmid DNA into muscle. *Mol. Ther.* **12,** 860–866.

Johnson, E. F., and Stout, C. D. (2005). Structural diversity of human xenobiotic-metabolizing cytochrome P450 monooxygenases. *Biochem. Biophys. Res. Commun.* **338,** 331–336.

Kakuda, S., Shiba, T., Ishiguro, M., Tagawa, H., Oka, S., Kajihara, Y., Kawasaki, T., Wakatsu, S., and Kato, R. (2004). Structural basis for acceptor substrate recognition of a human glucuronyltransferase, GlcAT-P, an enzyme critical in the biosynthesis of the carbohydrate epitope HNK-1. *J. Biol. Chem.* **279,** 22693–22703.

Kamisako, T., Kobayashi, Y., Takeuchi, K., Ishihara, T., Higuchi, K., Tanaka, Y., Gabazza, E. C., and Adachi, Y. (2000). Recent advances in bilirubin metabolism research: The molecular mechanism of hepatocyte bilirubin transport and its clinical relevance. *J. Gastroenterol.* **35,** 659–664.

Kaplan, M., Renbaum, P., Levy-Lahad, E., Hammerman, C., Lahad, A., and Beutler, E. (1997). Gilbert syndrome and glucose-6-phosphate dehydrogenase deficiency: A dose-dependent genetic interaction crucial to neonatal hyperbilirubinemia. *Proc. Natl. Acad. Sci. USA* **94,** 12128–12132.

Kaplan, M., Hammerman, C., and Maisels, M. J. (2003). Bilirubin genetics for the nongeneticist: Hereditary defects of neonatal bilirubin conjugation. *Pediatrics* **111,** 886–893.

Kapitonov, D., and Yu, R. K. (1999). Conserved domains of glycosyltransferases. *Glycobiology* **9,** 961–978.

Keizers, P. H., Schraven, L. H., de Graaf, C., Hidestrand, M., Ingelman-Sundberg, M., van Dijk, B. R., Vermeulen, N. P., and Commandeur, J. N. (2005). Role of the conserved threonine 309 in mechanism of oxidation by cytochrome P450 2D6. *Biochem. Biophys. Res. Commun.* **338,** 1065–1074.

Kelley, R. W., Reed, J. R., and Backes, W. L. (2005). Effects of ionic strength on the functional interactions between CYP2B4 and CYP1A2. *Biochemistry* **44,** 2632–2641.

Keppler, D. (2005). Uptake and efflux transporters for conjugates in human hepatocytes. *Meth. Enzymol.* **400,** 531–542.

Kessler, F. K., Kessler, M. R., Auyeung, D. J., and Ritter, J. K. (2002). Glucuronidation of acetaminophen catalyzed by multiple rat phenol UDP-glucuronosyltransferases. *Drug Metab. Dispos.* **30,** 324–330.

Kikuchi, A., Park, S. Y., Miyatake, H., Sun, D., Sato, M., Yoshida, T., and Shiro, Y. (2001). Crystal structure of rat biliverdin reductase. *Nat. Struct. Biol.* **8,** 221–225.

Kikuchi, G., Yoshida, T., and Noguchi, M. (2005). Heme oxygenase and heme degradation. *Biochem. Biophys. Res. Commun.* **338,** 558–567.

Kimura, S., Kawamura, M., and Iyanagi, T. (2003). Role of Thr(66) in porcine NADH-cytochrome b5 reductase in catalysis and control of the rate-limiting step in electron transfer. *J. Biol. Chem.* **278,** 3580–3589.

Kimura, T., and Suzuki, K. (1967). Components of the electron transport system in adrenal steroid hydroxylase. Isolation and properties of non-heme iron protein (adrenodoxin). *J. Biol. Chem.* **242,** 419–485.

King, C. D., Rios, G. R., Green, M. D., and Tephly, T. R. (2000). UDP-glucuronosyl-transferases. *Curr. Drug Metab.* **1,** 143–161.

Klingenberg, M. (1958). Pigments of rat liver microsomes. *Arch. Biochem. Biophys.* **75,** 376–386.

Knight, E., Jr., and Hardy, R. W. F. (1966). Isolation and characteristics of flavodoxin from nitrogen-fixing *Clostridium pasteurianum. J. Biol. Chem.* **241,** 2752–2756.

Kobayashi, K., Iyanagim, T., Ohara, H., and Hayashi, K. (1988). One-electron reduction of hepatic NADH-cytochrome b5 reductase as studied by pulse radiolysis. *J. Biol. Chem.* **263,** 7493–7499.

Kohara, A., Nakajima, C., Hashimoto, K., Ikenaka, T., Tanaka, H., Shoyama, Y., Yoshida, S., and Muranaka, T. (2005). A novel glucosyltransferase involved in steroid saponin biosynthesis in Solanum aculeatissimum. *Plant Mol. Biol.* **57,** 225–239.

Koiwai, O., Nishizawa, M., Hasada, K., Aono, S., Adachi, Y., Mamiya, N., and Sato, H. (1995). Gilbert's syndrome is caused by a heterozygous missense mutation in the gene for bilirubin UDP-glucuronosyltransferase. *Hum. Mol. Genet.* **4,** 1183–1186.

Koiwai, O., Aono, S., Adachi, Y., Kamisako, T., Yasui, Y., Nishizawa, M., and Sato, H. (1996). Crigler-Najjar syndrome type II is inherited both as a dominant and as a recessive trait. *Hum. Mol. Genet.* **5,** 645–647.

Konig, J., Nies, A. T., Cui, Y., Leier, I., and Keppler, D. (1999). Conjugate export pumps of the multidrug resistance protein (MRP) family: Localization, substrate specificity, and MRP2-mediated drug resistance. *Biochim. Biophys. Acta* **1461,** 377–394.

Kren, B. T., and Steer, C. J. (2002). The application of DNA repair vectors to gene therapy. *Curr. Opin. Biotechnol.* **13,** 473–481.

Kren, B. T., Parashar, B., Bandyopadhyay, P., Chowdhury, N. R., Chowdhury, J. R., and Steer, C. J. (1999). Correction of the UDP-glucuronosyltransferase gene defect in the Gunn rat model of Crigler-Najjar syndrome type I with a chimeric oligonucleotide. *Proc. Natl. Acad. Sci. USA* **96,** 10349–10354.

Kresge, N., Simoni, R. D., and Hill, R. L. (2006). The characterization of cytochrome P450 by Ryo Sato. *J. Biol. Chem.* **281,** e5–e6.

Krishnaswamy, S., Hao, Q., Von Moltke, L. L., Greenblatt, D. J., and Court, M. H. (2004). Evaluation of 5-hydroxytryptophol and other endogenous serotonin (5-hydroxytryptamine) analogs as substrates for UDP-glucuronosyltransferase 1A6. *Drug Metab. Dispos.* **32,** 862–869.

Kurisu, G., Kusunoki, M., Katoh, E., Yamazaki, T., Teshima, K., Onda, Y., Kimata-Ariga, Y., and Hase, T. (2001). Structure of the electron transfer complex between ferredoxin and ferredoxin-NADP(+) reductase. *Nat. Struct. Biol.* **8,** 117–121.

Kurkela, M., Morsky, S., Hirvonen, J., Kostiainen, R., and Finel, M. (2004). An active and water-soluble truncation mutant of the human UDP-glucuronosyltransferase 1A9. *Mol. Pharmacol.* **65,** 826–831.

La Du, B. N., Gaudette, L., Trousof, N., and Brodie, B. B. (1955). Enzymatic dealkylation of aminopyrine (Pyramidon) and other alkylamines. *J. Biol. Chem.* **214,** 741–752.

Lad, L., Schuller, D. J., Shimizu, H., Friedman, J., Li, H., Ortiz de Montellano, P. R., and Poulos, T. L. (2003). Comparison of the heme-free and -bound crystal structures of human heme oxygenase-1. *J. Biol. Chem.* **278,** 7834–7843.

Lamb, J. G., Straub, P., and Tukey, R. H. (1994). Cloning and characterization of cDNAs encoding mouse Ugt1.6 and rabbit UGT1.6: Differential induction by 2,3,7,8-tetrachlorodibenzo-p-dioxin. *Biochemistry* **33,** 10513–10520.

LaVoie, M. J., Ostaszewski, B. L., Weihofen, A., Schlossmacher, M. G., and Sekoe, D. J. (2005). Dopamine covalently modifies and functionally inactivates parkin. *Nat. Med.* **11,** 1214–1221.

Leung, Y. K., and Ho, J. W. (2002). Induction of UDP-glucuronosyltransferase 1A8 mRNA by 3-methylcholanthene in rat hepatoma cells. *Biochem. Pharmacol.* **63,** 767–775.

Lewis, D. F. V. (2001). "Guide to Cytochrome P450: Structure and Function." Taylor & Francis, London.

Lewis, D. F. V., and Hlavica, P. (2000). Interactions between redox partners in various cytochrome P450 systems: Functional and structural aspects. *Biochim. Biophys. Acta* **1460,** 3533–3574.

Lewis, D. F. V., Watson, E., and Lake, B. G. (1998). Evolution of the cytochrome P450 superfamily: Sequence alignments and pharmacogenetics. *Mutat. Res.* **410,** 245–270.

Li, R., Bianchet, M. A., Talalay, P., and Amezel, L. M. (1995). The three-dimensional structure of NAD(P)H: Quinone reductase, a flavoprotein involved in cancer chemoprotection and chemotherapy: Mechanism of the two-electron reduction. *Proc. Natl. Acad. Sci. USA* **92,** 8846–8850.

Li, Y., Baldauf, S., Lim, E. K., and Bowles, D. J. (2001). Phylogenetic analysis of the UDP-glycosyltransferase multigene family of *Arabidopsis thaliana*. *J. Biol. Chem.* **276,** 4338–4343.

Lu, A. Y., and Coon, M. J. (1968). Role of hemoprotein P-450 in fatty acid omega-hydroxylation in a soluble enzyme system from liver microsomes. *J. Biol. Chem.* **243,** 1331–1332.

Lu, A. Y., Junk, K. W., and Coon, M. J. (1969). Resolution of the cytochrome P-450-containing omega-hydroxylation system of liver microsomes into three components. *J. Biol. Chem.* **244,** 3714–3721.

Mackenzie, P. I. (1990). Structure and regulation of UDP-glucuronosyltransferases. *In* "Frontiers in Biotransformation: Principles, Mechanism and Biological Consequences of Induction" (K. Ruckpaul and H. Rein, Eds.), pp. 211–243. Akademie-Verlag, Berlin.

Mackenzie, P. I. (1986a). Rat liver UDP-glucuronosyltransferase. Sequence and expression of a cDNA encoding a phenobarbital-inducible form. *J. Biol. Chem.* **261,** 6119–6125.

Mackenzie, P. I. (1986b). Rat liver UDP-glucuronosyltransferase. cDNA sequence and expression of a form glucuronidating 3-hydroxyandrogens. *J. Biol. Chem.* **261,** 14112–14117.

Mackenzie, P. I., and Rodbourn, L. (1990). Organization of the rat UDP-glucuronosyltransferase, UDPGTr-2, gene and characterization of its promoter. *J. Biol. Chem.* **265,** 11328–11332.

Mackenzie, P. I., Gonzalez, F. J., and Owens, I. S. (1984). Cloning and characterization of DNA complementary to rat liver UDP-glucuronosyltransferase mRNA. *J. Biol. Chem.* **259,** 12153–12160.

Mackenzie, P. I., Joffe, M. M., Munson, P. J., and Owens, I. S. (1985). Separation of different UDP-glucuronosyltransferase activities according to charge heterogeneity by chromatofocusing using mouse liver microsomes. Three major types of aglycones. *Biochem. Pharmacol.* **34,** 737–746.

Mackenzie, P. I., Owens, I. S., Burchell, B., Bock, K. W., Bairoch, A., Belanger, A., Fournel-Gigleux, S., Green, M., Hum, D. W., Iyanagi, T., Lancet, D., Louisot, P., *et al.* (1997). The UDP glycosyltransferase gene superfamily: Recommended nomenclature update based on evolutionary divergence. *Pharmacogenetics* **7,** 255–269.

Mackenzie, P. I., Gregory, P. A., Gardner-Stephen, D. A., Lewinsky, R. H., Jorgensen, B. R., Nishiyama, T., Xie, W., and Radominska-Pandya, A. (2003). Regulation of UDP glucuronosyltransferase genes. *Curr. Drug Metab.* **4,** 249–257.

Mackenzie, P. I., Walter Bock, K., Burchell, B., Guillemette, C., Ikushiro, S., Iyanagi, T., Miners, J. O., Owens, I. S., and Nebert, D. W. (2005). Nomenclature update for the mammalian UDP glycosyltransferase (UGT) gene superfamily. *Pharmacogenet. Genom.* **15,** 677–785.

Maitland, M. L., Grimsley, C., Kuttab-Boulos, H., Witonsky, D., Kasza, K. E., Yang, L., Roe, B. A., and Di Rienzo, A. (2006). Comparative genomics analysis of human sequence variation in the UGT1A gene cluster. *Pharmacogen. J.* **6,** 52–62.

Maniatis, T., and Reed, R. (2002). An extensive network of coupling among gene expression machines. *Nature* **416,** 499–506.

Marcus, R. A., and Sutin, N. (1985). Electron transfer in chemistry and biology. *Biochim. Biophys. Acta* **811,** 265–322.

Masaki, R., Kameyama, K., and Yamamoto, A. (2003). Post-translational targeting of a tail-anchored green fluorescent protein to the endolpasmic reticulum. *J. Biochem. (Tokyo).* **134,** 415–426.

Marohnic, C. C., Bewley, M. C., and Barber, M. J. (2003). Engineering and characterization of a NADPH-utilizing cytochrome b5 reductase. *Biochemistry* **42,** 11170–11182.

Marohnic, C. C., Panda, S. P., Martasek, P., and Masters, B. S. (2006). Diminished FAD-binding in the Y459H and V492E antley-bixler syndrome mutants of human cytochrome P450 reductase. *J. Biol. Chem.* **281,** 35975–35982.

Mason, H. S. (1957). Mechanisms of oxygen metabolism. *Science* **125,** 1185–1188.

Mason, H. S., Fowlks, W. L., and Peterson, E. W. (1955). Oxygen transfer and electron transport by the phenolase complex. *J. Am. Chem. Soc.* **77,** 2914–2915.

Mason, H. S., North, J. C., and Vanneste, M. (1965). Microsomal mixed-function oxidations: The metabolism of xenobiotics. *Fed. Proc.* **24,** 1172–1180.

Masters, B. S. (2005). The journey from NADPH-cytochrome P450 oxidoreductase to nitric oxide synthases. *Biochem. Biophys. Res. Commun.* **338,** 507–519.

Matsuda, H., and Iyanagi, T. (1999). Calmodulin activates intramolecular electron transfer between the two flavins of neuronal nitric oxide synthase flavin domain. *Biochim. Biophys. Acta* **1473,** 345–355.

Matsuda, H., Kimura, S., and Iyanagi, T. (2000). One-electron reduction of quinones by the neuronal nitric-oxide synthase reductase domain. *Biochim. Biophys. Acta* **1459,** 106–116.

Matsunaga, T., Shintani, S., and Hara, A. (2006). Multiplicity of mammalian reductases for xenobiotic carbonyl compounds. *Drug Metab. Pharmacokinet.* **21,** 1–18.

Mayhew, S. G., and Ludwig, M. L. (1975). Flavodoxin and electron transfer flavoproteins. *Enzymes* **12,** 57–118.

Mayhew, S. G., Foust, G. P., and Massey, V. (1969). Oxidation-reduction properties of flavodoxin from Peptostreptococcus elsdenii. *J. Biol. Chem.* **244,** 803–810.

Mayoral, T., Martinez-Julvez, M., Perez-Dorado, I., Sanz-Aparicio, J., Gomez-Moreno, C., Medina, M., and Hermoso, J. A. (2005). Structural analysis of interactions for complex formation between Ferredoxin-NADP+ reductase and its protein partners. *Proteins* **59,** 592–602.

McDonagh, A. F., and Lightner, D. A. (1985). ''Like a shrivelled blood orange''—bilirubin, jaundice, and phototherapy. *Pediatrics* **75,** 443–455.

McMillan, K., Bredt, D. S., Hirsch, D. J., Snyder, S. H., Clark, J. E., and Masters, B. S. (1992). Cloned, expressed rat cerebellar nitric oxide synthase contains stoichiometric amounts of heme, which binds carbon monoxide. *Proc. Natl. Acad. Sci. USA* **89,** 11141–11145.

Meech, R., and Mackenzie, P. I. (1997). UDP-glucuronosyltransferase, the role of the amino terminus in dimerization. *J. Biol. Chem.* **272,** 26913–26917.

Merzlyakov, M., You, M., Li, E., and Hristova, K. (2006). Transmembrane helix heterodimerization in lipid bilayers: Probing the energetics behind autosomal dominant growth disorders. *J. Mol. Biol.* **358,** 1–7.

Mestres, J. (2005). Structure conservation in cytochromes P450. *Proteins* **58,** 596–609.

Miege, C., Marechal, E., Shimojima, M., Awai, K., Block, M. A., Ohta, H., Takamiya, K., Douce, R., and Joyard, J. (1999). Biochemical and topological properties of type A MGDG synthase, a spinach chloroplast envelope enzyme catalyzing the synthesis of both prokaryotic and eukaryotic MGDG. *Eur. J. Biochem.* **265,** 990–1001.

Miller, E. C. (1978). Some current perspectives on chemical carcinogenesis in humans and experimental animals: Presidential address. *Cancer Res.* **38,** 1479–1496.

Miller, W. L. (2005). Regulation of steroidogenesis by electron transfer. *Endocrinology* **146,** 2544–2550.

Mishina, Y., Duguid, E. M., and He, C. (2006). Direct reversal of DNA alkylation damage. *Chem. Rev.* **106,** 215–232.

Miyake, Y., Mason, H. S., and Langraf, W. (1967). An electron spin resonance study of liver and adrenal mixed function oxidases near the temperature of liquid helium. *J. Biol. Chem.* **242,** 393–397.

Miyake, Y., Gaylor, J. L., and Mason, H. S. (1968). Properties of a submicrosomal particle containing P-450 and flavoprotein. *J. Biol. Chem.* **243,** 5788–5797.

Moehs, C. P., Allen, P. V., Friedman, M., and Belknap, W. R. (1997). Cloning and expression of solanidine UDP-glucose glucosyltransferase from potato. *Plant J.* **11,** 227–236.

Muller, J. J., Lapko, A., Bourenkov, G., Ruckpaul, K., and Heinemann, U. (2001). Adrenodoxin reductase-adrenodoxin complex structure suggests electron transfer path in steroid biosynthesis. *J. Biol. Chem.* **276,** 2786–2789.

Munro, A. W., Noble, M. A., Robledo, L., Daff, S. N., and Chapman, S. K. (2001). Determination of the redox properties of human NADPH-cytochrome P450 reductase. *Biochemistry* **40,** 1956–1963.

Muraoka, M., Kawakita, M., and Ishida, N. (2001). Molecular characterization of human UDP-glucuronic acid/UDP-N-acetylgalactosamine transporter, a novel nucleotide sugar transporter with dual substrate specificity. *FEBS Lett.* **495,** 87–93.

Murataliev, M. B., Feyereisen, R., and Walker, F. A. (2004). Electron transfer by diflavin reductases. *Biochim. Biophys. Acta* **1698,** 1–26.

Nagai, F., Homma, H., Tanase, H., and Matsui, M. (1988). Studies on the genetic linkage of bilirubin and androsterone UDP-glucuronyltransferases by cross-breeding of two mutant rat strains. *Biochem. J.* **252,** 897–900.

Nagano, S., and Poulos, T. L. (2005). Crystallographic study on the dioxygen complex of wild-type and mutant cytochrome P450cam. Implications for the dioxygen activation mechanism. *J. Biol. Chem.* **280,** 31659–31663.

Nagano, S., Cupp-Vickery, J. R., and Poulos, T. L. (2005). Crystal structures of the ferrous dioxygen complex of wild-type cytochrome P450eryF and its mutants, A245S and A245T: Investigation of the proton transfer system in P450eryF. *J. Biol. Chem.* **280,** 22102–22107.

Nagata, K., and Yamazoe, Y. (2000). Pharmacogenetics of sulfotransferase. *Annu. Rev. Pharmacol. Toxicol.* **40,** 159–176.

Narayanan, R., LeDuc, B., and Williams, D. A. (2004). Glucuronidation of haloperidol by rat liver microsomes: Involvement of family 2 UDP-glucuronosyltransferases. *Life Sci.* **74,** 2527–2539.

Narhi, L. O., and Fulco, A. J. (1987). Identification and characterization of two functional domains in cytochrome P-450BM-3, a catalytically self-sufficient monooxygenase induced by barbiturates in *Bacillus megaterium*. *J. Biol. Chem.* **262,** 6683–6690.

Neeli, R., Girvan, H. M., Lawrence, A., Warren, M. J., Leys, D., Scrutton, N. S., and Munro, A. W. (2005). The dimeric form of flavocytochrome P450 BM3 is catalytically functional as a fatty acid hydroxylase. *FEBS Lett.* **579,** 5582–5588.

Negishi, M., Pederson, L. G., Petrotchenko, E., Shevtsov, S., Gorokhov, A., Kakuta, Y., and Pedesen, L. C. (2001). Structure and function of sulfotransferases. *Arch. Biochem. Biophys.* **390,** 149–157.

Negishi, M., Dong, J., Darden, T. A., Pedersen, L. G., and Pedersen, L. C. (2003). Glucosaminylglycan biosynthesis: What we can learn from the X-ray crystal structures of glycosyltransferases GlcAT1 and EXTL2. *Biochem. Biophys. Res. Commun.* **303,** 393–398.

Nelson, D. R., Zeldin, D. C., Hoffman, S. M., Maltais, L. J., Wain, H. M., and Nebert, D. W. (2004). Comparison of cytochrome P450 (CYP) genes from the mouse and human genomes, including nomenclature recommendations for genes, pseudogenes and alternative-splice variants. *Pharmacogenetics* **14,** 1–18.

Nguyen, T. H., and Ferry, N. (2004). Liver gene therapy: Advances and hurdles. *Gene Ther.* **11** (Suppl. 1), S76–S84.

Nguyen, T. H., Bellodi-Privato, M., Aubert, D., Prichard, V., Myara, A., Trono, D., and Ferry, N. (2005). Therapeutic lentivirus-mediated neonatal *in vivo* gene therapy in hyperbilirubinemic Gunn rats. *Mol. Ther.* **12,** 852–859.

Nikfarjam, L., Izumi, S., Yamazaki, T., and Kominami, S. (2006). The interaction of cytochrome P450 17alpha with NADPH-cytochrome P450 reductase, investigated using chemical modification and MALDI-TOF mass spectrometry. *Biochim. Biophys. Acta* **1764,** 1126–1131.

Nishida, C. R., and Ortiz de Montellano, P. R. (1998). Electron transfer and catalytic activity of nitric oxide synthases. Chimeric constructs of the neuronal, inducible, and endothelial isoforms. *J. Biol. Chem.* **273,** 5566–5571.

Nishino, Y., Yamamoto, K., Guan, Z.-W., Kimura, S., and Iyanagi, T. (2003). Human endothelial nitric oxide synthase reductase domain is activated by calmodulin and phosphorylation. *In* "Cytochromes P450, Biochemistry, Biophysics and Drug Metabolism" (P. Anzenbacher and J. Hudecek, Eds.), pp. 267–272. Monduzzi Editore, Bologna.

Noble, M. A., Munro, A. W., Rivers, S. L., Robledo, L., Daff, S. N., Yellowlees, L. J., Shimizu, T., Sagami, I., Guillemette, J. G., and Chapman, S. K. (1999). Potentiometric analysis of the flavin cofactors of neuronal nitric oxide synthase. *Biochemistry* **38,** 16413–16418.

Nogues, I., Perez-Dorado, I., Frago, S., Bittel, C., Mayhew, S. G., Gomez-Moreno, C., Hermoso, J. A., Mediana, M., Cortez, N., and Carrillo, N. (2005). The ferredoxin-NADP(H) reductase from Rhodobacter capsulatus: Molecular structure and catalytic mechanism. *Biochemistry* **44,** 11730–11740.

Noonan, J. P., Grimwood, J., Schmutz, J., Dickson, M., and Myers, R. M. (2004). Gene conversion and the evolution of protocadherin gene cluster diversity. *Genome Res.* **14,** 354–366.

O'Brien, P. J. (2006). Catalytic promiscuity and the divergent evolution of DNA repair enzymes. *Chem. Rev.* **106,** 720–752.

Offen, W., Martinerz-Fleites, C., Yang, M., Kiat-Lim, E., Davis, B. G., Tarling, C. A., Ford, C. M., Bowles, D. J., and Davies, G. J. (2006). Structure of a flavonoid glucosyltransferase reveals the basis for plant natural product modification. *EMBO J.* **25,** 1396–1405.

Ohnishi, T., Yamazaki, H., Iyanagi, T., Nakamura, T., and Yamazaki, I. (1969). One-electron-transfer reactions in biochemical systems. II. The reaction of free radicals formed in the enzymic oxidation. *Biochim. Biophys. Acta* **172,** 357–369.

Ollinger, K., Llopis, J., and Cadenas, E. (1989). Study of the redox properties of naphthazarin (5,8-dihydroxy-1,4-naphthoquinone) and its glutathionyl conjugate in biological reactions: One- and two-electron enzymatic reduction. *Arch. Biochem. Biophys.* **275,** 514–530.

Olteanu, H., and Banerjee, R. (2001). Human methionine synthase reductase, a soluble P-450 reductase-like dual flavoprotein, is sufficient for NADPH-dependent methionine synthase activation. *J. Biol. Chem.* **276,** 35558–35563.

Olteanu, H., Wolthers, K. R., Munro, A. W., Scrutton, N. S., and Banerjee, R. (2004). Kinetic and thermodynamic characterization of the common polymorphic variants of human methionine synthase reductase. *Biochemistry* **43,** 1988–1997.

Omura, T. (2005). Heme-thiolate proteins. *Biochem. Biophys. Res. Commun.* **338,** 404–409.

Omura, T., and Sato, R. (1962). A new cytochrome in liver microsomes. *J. Biol. Chem.* **237,** 1375–1376.

Omura, T., and Sato, R. (1964a). The carbon monoxide-binding pigment of liver microsomes. I. Evidence for its hemoprotein nature. *J. Biol. Chem.* **239,** 2370–2378.

Omura, T., and Sato, R. (1964b). The carbon monoxide-binding pigment of liver microsomes. II. Solubilization, purification, and properties. *J. Biol. Chem.* **239,** 2379–2385.

Omura, T., Sanders, E., Estabrook, R. W., Cooper, D. Y., and Rosenthal, O. (1966). Isolation from adrenal cortex of a nonheme iron protein and a flavoprotein functional as a reduced triphosphopyridine nucleotide-cytochrome P450 reductase. *Arch. Biochem. Biophys.* **117,** 660–673.

Oprian, D. D., and Coon, M. J. (1982). Oxidation-reduction states of FMN and FAD in NADPH-cytochrome P-450 reductase during reduction by NADPH. *J. Biol. Chem.* **257,** 8935–8944.

Orengo, C. A., and Thornton, J. M. (2005). Protein families and their evolution—A structural perspective. *Annu. Rev. Biochem.* **74,** 867–900.

Otto, D. M., Henderson, C. J., Carrie, D., Davey, M., Gundersen, T. E., Blomhoff, R., Adams, R. H., Tickle, C., and Wolf, C. R. (2003). Identification of novel roles of the cytochrome p450 system in early embryogenesis: Effects on vasculogenesis and retinoic acid homeostasis. *Mol. Cell Biol.* **23,** 6103–6116.

Ouzzine, M., Antonio, L., Burchell, B., Netter, P., Fournel-Gigleux, S., and Magdalou, J. (2000). Importance of histidine residues for the function of the human liver UDP-glucuronosyltransferase UGT1A6: Evidence for the catalytic role of histidine 370. *Mol. Pharmacol.* **58,** 1609–1615.

Owens, I. S., and Ritter, J. K. (1992). The novel bilirubin/phenol UDP-glucuronosyltransferase UGT1 gene locus: Implications for multiple nonhemolytic familial hyperbilirubinemia phenotypes. *Pharmacogenetics* **2,** 93–108.

Owens, I. S., Basu, N. K., and Banerjee, R. (2005). UDP-glucuronosyltransferases: Gene structures of UGT1 and UGT2 families. *Methods Enzymol.* **400,** 1–22.

Ozalp, C., Szczesna-Skorupa, E., and Kemper, B. (2005). Bimolecular fluorescence complementation analysis of cytochrome p450 2c2, 2e1, and NADPH-cytochrome p450 reductase molecular interactions in living cells. *Drug Metab. Dispos.* **33,** 1382–1390.

Palade, G. E. (1956). The endoplasmic reticulum. *J. Biophys. Biochem. Cytol* **2**(Suppl), 85–98.

Paris, I., Martinez-Alvarado, P., Cardenas, S., Perez-Pastene, C., Graumann, R., Fuentes, P., Olea-Azar, C., Caviedes, P., and Segura-Aguilar, J. (2005). Dopamine-dependent iron toxicity in cells derived from rat hypothalamus. *Chem. Res. Toxicol.* **18,** 415–419.

Pedersen, L. C., Tsuchida, K., Kitagawa, H., Sugahara, K., Darden, T. A., and Negishi, M. (2000). Heparan/chondroitin sulfate biosynthesis. Structure and mechanism of human glucuronyltransferase I. *J. Biol. Chem.* **275,** 34580–34585.

Peterson, J. A., Ebel, R. E., O'Keeffe, D. H., Matsubara, T., and Estabrook, R. W. (1976). Temperature dependence of cytochrome P-450 reduction. A model for NADPH-cytochrome P-450 reductase: Cytochrome P-450 interaction. *J. Biol. Chem.* **251,** 4010–4016.

Phillips, A. H., and Langdon, R. G. (1962). Hepatic triphosphopyridine nucleotide-cytochrome *c* reductase: Isolation, characterization, and kinetic studies. *J. Biol. Chem.* **237,** 2652–2660.

Porter, T. D., and Kasper, C. B. (1985). Coding nucleotide sequence of rat NADPH-cytochrome P-450 oxidoreductase cDNA and identification of flavin-binding domains. *Proc. Natl. Acad. Sci. USA* **82,** 973–977.

Porter, T. D., Beck, T. W., and Kasper, C. B. (1990). NADPH-cytochrome P-450 oxidoreductase gene organization correlates with structural domains of the protein. *Biochemistry* **29,** 9814–9818.

Powis, G. (1987). Metabolism and reactions of quinoid anticancer agents. *Pharmacol. Ther.* **35,** 57–162.

Radominska-Pandya, A., Czernik, P. J., Little, J. M., Battaglia, E., and Makenzie, P. I. (1999). Structural and functional studies of UDP-glucuronosyltransferases. *Drug Metab. Rev.* **31,** 817–899.

Radominska-Pandya, A., Ouzzine, M., Fournel-Gigleux, S., and Magdalou, J. (2005). Structure of UDP-glucuronosyltransferases in membranes. *Meth. Enzymol.* **400,** 116–147.

Ravi, D., Muniyappa, H., and Das, K. C. (2005). Endogenous thioredoxin is required for redox cycling of anthracyclines and p53-dependent apoptosis in cancer cells. *J. Biol. Chem.* **280,** 40084–40096.

Ritter, J. K., Chen, F., Sheen, Y. Y., Tran, H. M., Kimura, S., Yeatman, M. T., and Owens, I. S. (1992). A novel complex locus UGT1 encodes human bilirubin, phenol, and other UDP-glucuronosyltransferase isozymes with identical carboxyl termini. *J. Biol. Chem.* **267,** 3257–3261.

Roman, L. J., and Masters, B. S. (2006). Electron transfer by neuronal nitric oxide synthase is regulated by concerted interaction of calmodulin and two intrinsic regulatory elements. *J. Biol. Chem.* **281,** 23111–23118.

Roman, L. J., Martasek, P., Miller, R. T., Harris, D. E., de La Garza, M. A., Shea, T. M., Kim, J. J., and Masters, B. S. (2000). The C termini of constitutive nitric-oxide synthases control

electron flow through the flavin and heme domains and affect modulation by calmodulin. *J. Biol. Chem.* **275,** 29225–29232.

Roman, L. J., Martasek, P., and Masters, B. S. (2002). Intrinsic and extrinsic modulation of nitric oxide synthase activity. *Chem. Rev.* **102,** 1179–1190.

Ross, D. (2005). Functions and distribution of NQO1 in human bone marrow: Potential clues to benzene toxicity. *Chem. Biol. Interact.* **153–154,** 137–146.

Rowland, P., Blaney, F. E., Smyth, M. G., Jones, J. J., Leydon, V. R., Oxbrow, A. K., Lewis, J., Tennant, M. G., Modi, S., Eggleston, D. S., Chenery, R. J., and Bridges, A. M. (2006). Crystal structure of human cytochrome P450 2D6. *J. Biol. Chem.* **281,** 7614–7622.

Roy Chowdhury, J., Novikoff, P. M., Chowdhury, N. R., and Novikoff, A. B. (1985). Distribution of UDPglucuronosyltransferase in rat tissue. *Proc. Natl. Acad. Sci. USA* **82,** 2990–2994.

Roy Chowdhury, J., Wolkoff, A. W., Roy Chowdhury, N., and Arias, I. M. (2001). Hereditary jaundice and disorders of bilirubin metabolism. *In* "The Metabolic Basis of Inherited Disease" (C. R. Scriver A. L. Boudet, W. S. Sly, and D. Valle, Eds.), 8th ed., pp. 3063–3101. McGraw-Hill, New York.

Saeki, M., Saito, Y., Jinno, H., Sai, K., Ozawa, S., Kurose, K., Kaniwa, N., Komamura, K., Kotake, T., Morishita, H., Kamakura, S., Kitakaze, M., *et al.* (2006). Haplotype structures of the UGT1A gene complex in a Japanese population. *Pharmacogen. J.* **6,** 63–75.

Salerno, J. C., Harris, D. E., Irizarry, K., Patel, B., Morales, A. J., Smith, S. M., Martasek, P., Roman, L. J., Masters, B. S., Jones, C. L., Weissman, B. A., Lane, P., *et al.* (1997). An autoinhibitory control element defines calcium-regulated isoforms of nitric oxide synthase. *J. Biol. Chem.* **272,** 29769–29777.

Sampietro, M., Lupica, L., Perrero, L., Comino, A., Martinez di Montemuros, F., Cappellini, M. D., and Fiorelli, G. (1977). The expression of uridine diphosphate glucuronosyltransferase gene is a major determinant of bilirubin level in heterozygous beta-thalassaemia and in glucose-6-phosphate dehydrogenase deficiency. *Br. J. Haematol.* **99,** 437–439.

Samunio, A. M., Chuang, E. Y., Krishna, M. C., Stein, W., DeGraff, W., Russo, A., and Mitchell, J. B. (2003). Semiquinone radical intermediate in catecholic estrogen-mediated cytotoxicity and mutagenesis: Chemoprevention strategies with antioxidants. *Proc. Natl. Acad. Sci. USA* **100,** 5390–5395.

Satoh, T., and Hosokawa, M. (1998). The mammalian carboxylesterases: From molecules to functions. *Annu. Rev. Pharmacol. Toxicol.* **38,** 257–288.

Sawada, Y., Iyanagi, T., and Yamazaki, I. (1975). Relation between redox potentials and rate constants in reactions coupled with the system oxygen-superoxide. *Biochemistry* **14,** 3761–3764.

Sawada, S., Suzuki, H., Ichimaida, F., Yamaguchi, M. A., Iwashita, T., Fukui, Y., Hemmi, H., Nishino, T., and Nakayama, T. (2005). UDP-glucuronic acid: Anthocyanin glucuronosyltransferase from red daisy (Bellis perennis) flowers. Enzymology and phylogenetics of a novel glucuronosyltransferase involved in flower pigment biosynthesis. *J. Biol. Chem.* **280,** 899–906.

Schacter, B. A., Nelson, E. B., Marver, H. S., and Masters, B. S. (1972). Immunochemical evidence for an association of heme oxygenase with the microsomal electron transport system. *J. Biol. Chem.* **247,** 3601–3607.

Schmid, R., Harmmaker, L., and Axelrod, J. (1957). The enzymatic formation of bilirubin glucuronide. *Arch. Biochem. Biophys.* **70,** 285–288.

Schuller, D. J., Wilks, A., Ortiz de Montellano, P. R., and Poulos, T. L. (1999). Crystal structure of human heme oxygenase-1. *Nat. Struct. Biol.* **6,** 860–867.

Scott, E. E., White, M. A., He, Y. A., Johnson, E. F., Stout, C. D., and Halpert, J. R. (2004). Structure of mammalian cytochrome P450 2B4 complexed with 4-(4-chlorophenyl) imidazole at 1.9-A resolution: Insight into the range of P450 conformations and the coordination of redox partner binding. *J. Biol. Chem.* **279,** 27294–27301.

Segura-Aguilar, J., and Lind, C. (1989). On the mechanism of the Mn3(+)-induced neurotoxicity of dopamine: Prevention of quinone-derived oxygen toxicity by DT diaphorase and superoxide dismutase. *Chem. Biol. Interact.* **72,** 309–324.

Seppen, J., van der Rijt, R., Looije, N., van Til, N. P., Lamers, W. H., and Elferink, R. P. (2003). Long-term correction of bilirubin UDP-glucuronyltransferase deficiency in rats by *in utero* lentiviral gene transfer. *Mol. Ther.* **8,** 593–599.

Seppen, J., van Til, N. P., van der Rijt, R., Hiralall, J. K., Kunne, C., and Elferink, R. P. (2006). Immune response to lentiviral bilirubin UDP-glucuronosyltransferase gene transfer in fetal and neonatal rats. *Gene Ther.* **13,** 672–677.

Sevrioukova, I. F., Li, H., Zhang, H., Peterson, J. A., and Poulos, T. L. (1999). Structure of a cytochrome P450-redox partner electron-transfer complex. *Proc. Natl. Acad. Sci. USA* **96,** 1863–1868.

Shangari, N., Chan, T. S., and O'Brien, P. J. (2005). Sulfation and glucuronidation of phenols: Implications in coenzyme Q metabolism. *Meth. Enzymol.* **400,** 342–359.

Shao, H., He, X., Achnine, L., Blount, J. W., Dixon, R. A., and Wang, X. (2005). Crystal structures of a multifunctional triterpene/flavonoid glycosyltransferase from Medicago truncatula. *Plant Cell* **17,** 3141–3154.

Shelby, M. K., Cherrington, N. J., Vansell, N. R., and Klaassen, C. D. (2003). Tissue mRNA expression of the rat UDP-glucuronosyltransferase gene family. *Drug Metab. Dispos.* **31,** 326–333.

Shen, A. L., and Kasper, C. B. (1995). Role of acidic residues in the interaction of NADPH-cytochrome P450 oxidoreductase with cytochrome P450 and cytochrome c. *J. Biol. Chem.* **270,** 27475–27480.

Shen, A. L., and Kasper, C. B. (1996). Role of Ser457 of NADPH-cytochrome P450 oxidoreductase in catalysis and control of FAD oxidation-reduction potential. *Biochemistry* **35,** 9451–9459.

Shen, A. L., and Kasper, C. B. (2000). Differential contributions of NADPH-cytochrome P450 oxidoreductase FAD binding site residues to flavin binding and catalysis. *J. Biol. Chem.* **275,** 41087–41091.

Shen, A. L., Porter, T. D., Wilson, T. E., and Kasper, C. B. (1989). Structural analysis of the FMN binding domain of NADPH-cytochrome P-450 oxidoreductase by site-directed mutagenesis. *J. Biol. Chem.* **264,** 7584–7589.

Shen, A. L., Christensen, M. J., and Kasper, C. B. (1991). NADPH-cytochrome P-450 oxidoreductase. The role of cysteine 566 in catalysis and cofactor binding. *J. Biol. Chem.* **266,** 19976–19980.

Shen, A. L., Sem, D. S., and Kasper, C. B. (1999). Mechanistic studies on the reductive half-reaction of NADPH-cytochrome P450 oxidoreductase. *J. Biol. Chem.* **274,** 5391–5398.

Shen, A. L., O'Leary, K. A., and Kasper, C. B. (2002). Association of multiple developmental defects and embryonic lethality with loss of microsomal NADPH-cytochrome P450 oxidoreductase. *J. Biol. Chem.* **277,** 6536–6541.

Shen, S., and Strobel, H. W. (1994). Probing the putative cytochrome P450- and cytochrome c-binding sites on NADPH-cytochrome P450 reductase by anti-peptide antibodies. *Biochemistry* **33,** 8807–8812.

Shimada, T., and Fujii-Kuriyama, Y. (2004). Metabolic activation of polycyclic aromatic hydrocarbons to carcinogens by cytochromes P450 1A1 and 1B1. *Cancer Sci.* **95,** 1–6.

Shimomura, K., Kamata, O., Ueki, S., Ida, S., and Oguri, K. (1971). Analgesic effect of morphine glucuronides. *Tohoku J. Exp. Med.* **105,** 45–52.

Sibille, N., Blackledge, M., Brutscher, B., Coves, J., and Bersch, B. (2005). Solution structure of the sulfite reductase flavodoxin-like domain from *Escherichia coli*. *Biochemistry* **44,** 9086–9095.

Siest, G., Antoine, B., Fournel, S., Magdalou, J., and Thomassin, J. (1987). The glucuronosyl-transferases: What progress can pharmacologists expect from molecular biology and cellular enzymology? *Biochem. Pharmacol.* **36,** 983–989.

Singer, S. J., and Nicolson, G. L. (1972). The fluid mosaic model of the structure of cell membranes. *Science* **175,** 720–731.

Slatter, J. G., Su, P., Sams, J. P., Schaaf, L. J., and Wienkers, L. C. (1997). Bioactivation of the anticancer agent CPT-11 to SN-38 by human hepatic microsomal carboxylesterases and the *in vitro* assessment of potential drug interactions. *Drug Metab. Dispos.* **25,** 1157–1164.

Sligar, S. G., Cinti, D. L., Gibson, G. G., and Schenkman, J. B. (1979). Spin state control of the hepatic cytochrome P450 redox potential. *Biochem. Biophys. Res. Commun.* **90,** 925–932.

Smith, G. C., Tew, D. G., and Wolf, C. R. (1994). Dissection of NADPH-cytochrome P450 oxidoreductase into distinct functional domains. *Proc. Natl. Acad. Sci. USA* **9,** 8710–8714.

Smith, P. C., McDonagh, A. F., and Benet, L. Z. (1989). Irreversible binding of zomepirac to plasma protein *in vitro* and *in vivo. J. Clin. Invest.* **77,** 934–939.

Sprong, H., Degroote, S., Nilsson, T., Kawakita, M., Ishida, N., van der Sluijs, P., and van Meer, G. (2003). Association of the Golgi UDP-galactose transporter with UDP-galactose: ceramide galactosyltransferase allows UDP-galactose import in the endoplasmic reticulum. *Mol. Biol. Cell.* **14,** 3482–3493.

Storey, I. D. E., and Dutton, G. J. (1955). Uridine compounds in glucuronic acid metabolism. 1. The isolation and structure of uridine-diphosphate-glucuronic acid. *Biochem. J.* **59,** 279–288.

Strobel, H. W., and Dignam, J. D. (1978). Purification and properties of NADPH-cytochrome P-450 reductase. *Meth. Enzymol.* **52,** 89–96.

Strominger, J. L., Kalckar, H. M., Axelrod, J., and Maxwell, E. S. (1954). Enzymatic oxidation of uridine diphosphate glucose to uridine diphosphate glucuronic acid. *J. Am. Chem. Soc.* **76,** 6411–6412.

Strominger, J. L., Maxwell, E. S., Axelrod, J., and Kalckar, H. M. (1957). Enzymatic formation of uridine diphosphoglucuronic acid. *J. Biol. Chem.* **224,** 79–90.

Stuehr, D. J., Wei, C. C., Wang, Z., and Hille, R. (2005). Exploring the redox reactions between heme and tetrahydrobiopterin in the nitric oxide synthases. *Dalton Trans.* **7,** 3427–3435.

Sugahara, K., Mikami, T., Uyama, T., Mizuguchi, S., Nomura, K., and Kitagawa, H. (2003). Recent advances in the structural biology of chondroitin sulfate and dermatan sulfate. *Curr. Opin. Struct. Biol.* **13,** 612–620.

Sugatani, J., Kojima, H., Ueda, A., Kakizaki, S., Yoshinari, K., Gong, Q. H., Owens, I. S., and Negishi, M. (2001). The phenobarbital response enhancer module in the human bilirubin UDP-glucuronosyltransferase UGT1A1 gene and regulation by the nuclear receptor CAR. *Hepatology* **33,** 1232–1238.

Sugatani, J., Sueyoshi, T., Negishi, M., and Miwa, M. (2005). Regulation of the human UGT1A1 gene by nuclear receptors constitutive active/androstane receptor, pregnane X receptor, and glucocorticoid receptor. *Meth. Enzymol.* **400,** 92–104.

Sugishima, M., Sakamoto, H., Kakuta, Y., Omata, Y., Hayashi, S., Noguchi, M., and Fukuyama, K. (2002). Crystal structure of rat apo-heme oxygenase (HO-1): Mechanism of heme binding in HO-1 inferred from structural comparison of the apo and heme complex form. *Biochemistry* **41,** 7293–7300.

Swenson, R. P., and Krey, G. (1994). Site-directed mutagenesis of tyrosine-98 in the flavodoxin from Desulfovibrio vulgaris (Hildenborough): Regulation of oxidation-reduction properties of the bound FMN cofactor by aromatic, solvent, and electrostatic interactions. *Biochemistry* **33,** 8505–8514.

Szczesna-Skorupa, E., Mallah, B., and Kemper, B. (2003). Fluorescence resonance energy transfer analysis of cytochromes P450 2C2 and 2E1 molecular interactions in living cells. *J. Biol. Chem.* **278,** 31269–31276.

Takahashi, M., Ilan, Y., Chowdhury, N. R., Guida, J., Horwitz, M., and Chowdhury, J. R. (1996). Long term correction of bilirubin-UDP-glucuronosyltransferasedeficiency in Gunn rats by administration of a recombinant adenovirus during the neonatal period. *J. Biol. Chem.* **271,** 26539–26542.

Takeda, S., Ishii, Y., Mackenzie, P. I., Nagata, K., Yamazoe, Y., Oguri, K., and Yamada, H. (2005). Modulation of UDP-glucuronosyltransferase 2B7 function by cytochrome P450s *in vitro*: Differential effects of CYP1A2, CYP2C9 and CYP3A4. *Biol. Pharm. Bull.* **28,** 2026–2027.

Talalay, P., Fahey, J. W., Holtzclaw, W. D., Prestera, T., and Zhang, Y. (1995). Chemoprotection against cancer by phase 2 enzyme induction. *Toxicol. Lett.* **82–83,** 173–179.

Taniguchi, H., Imai, Y., Iyanagi, T., and Sato, R. (1979). Interaction between NADPH-cytochrome P-450 reductase and cytochrome P-450 in the membrane of phosphatidylcholine vesicles. *Biochim. Biophys. Acta* **19,** 341–356.

Taura, K. I., Yamada, H., Hagino, Y., Ishii, Y., Mori, M. A., and Oguri, K. (2000). Interaction between cytochrome P450 and other drug-metabolizing enzymes: Evidence for anassociation of CYP1A1 with microsomal epoxide hydrolase and UDP-glucuronosyltransferase. *Biochem. Biophys. Res. Commun.* **273,** 1048–1052.

Teasdale, R. D., and Jackson, M. R. (1996). Signal-mediated sorting of membrane proteins between the endoplasmic reticulum and the Golgi apparatus. *Annu. Rev. Cell Dev. Biol.* **12,** 27–54.

Tedeschi, G., Chen, S., and Massey, V. (1995a). DT-diaphorase. Redox potential, steady-state, and rapid reaction studies. *J. Biol. Chem.* **270,** 1198–1204.

Tedeschi, G., Chen, S., and Massey, V. (1995b). Active site studies of DT-diaphorase employing artificial flavins. *J. Biol. Chem.* **270,** 2512–2516.

Thibaudeau, J., Lepine, J., Tojcic, J., Duguay, Y., Pelletier, G., Plante, M., Brisson, J., Tetu, B., Jacob, S., Perusse, L., Belanger, A., and Guillemette, C. (2006). Characterization of common UGT1A8, UGT1A9, and UGT2B7 variants with different capacities to inactivate mutagenic 4-hydroxylated metabolites of estradiol and estrone. *Cancer Res.* **66,** 125–133.

Tiso, M., Konas, D. W., Panda, K., Garcin, E. D., Sharma, M., Getzoff, E. D., and Stuehr, D. J. (2005). C-terminal tail residue Arg1400 enables NADPH to regulate electron transfer in neuronal nitric-oxide synthase. *J. Biol. Chem.* **280,** 39208–39219.

Toietta, G., Mane, V. P., Norona, W. S., Finegold, M. J., Ng, P., McDonagh, A. F., Beaudet, A. L., and Lee, B. (2005). Lifelong elimination of hyperbilirubinemia in the Gunn rat with a single injection of helper-dependent adenoviral vector. *Proc. Natl. Acad. Sci. USA* **102,** 3930–3935.

Tonegawa, Y., Umeda, N., Hayakawa, T., and Ishibashi, T. (2005). Evaluation of data in terms of two-dimensional random walk model: Interaction between NADH-cytochrome b5 reductase and cytochrome b5. *Biomed. Res.* **26,** 207–212.

Tukey, R. H., and Strassburg, C. P. (2000). Human UDP-glucuronosyltransferases: Metabolism, expression, and disease. *Annu. Rev. Pharmacol. Toxicol.* **40,** 581–616.

Tukey, R. H., Strassburg, C. P., and Mackenzie, P. I. (2002). Pharmacogenomics of human UDP-glucuronosyltransferases and irinotecan toxicity. *Mol. Pharmacol.* **62,** 446–450.

Turgeon, D., Carrier, J. S., Levesque, E., Beatty, B. G., Belanger, A., and Hum, D. W. (2000). Isolation and characterization of the human UGT2B15 gene, localized within a cluster of UGT2B genes and pseudogenes on chromosome 4. *J. Mol. Biol.* **295,** 489–504.

Ullrich, V. (2003). Thoughts on thiolate tethering. Tribute and thanks to a teacher. *Arch. Biochem. Biophys.* **409,** 45–51.

Unligil, U. M., and Rini, J. M. (2000). Glycosyltransferase structure and mechanism. *Curr. Opin. Struct. Biol.* **10,** 510–517.

Usui, T., Kuno, T., Ueyama, H., Ohkubo, I., and Mizutani, T. (2006). Proximal HNF1 element is essential for the induction of human UDP-glucuronosyltransferase 1A1 by glucocorticoid receptor. *Biochem. Pharmacol.* **71,** 693–701.

van der Wegen, P., Louwen, R., Imam, A. M., Buijs-Offerman, R. M., Sinaasappel, M., Grosveld, F., and Scholte, B. J. (2006). Successful treatment of UGT1A1 deficiency in a rat model of Crigler-Najjar disease by intravenous administration of a liver-specific lentiviral vector. *Mol. Ther.* **13**, 374–381.

van Waterschoot, R. A., Keizers, P. H., de Graaf, C., Vermeulen, N. P., and Tschirret-Guth, R. A. (2006). Topological role of cytochrome P450 2D6 active site residues. *Arch. Biochem. Biophys.* **447**, 53–58.

Vanstapel, F., and Blanckaert, N. (1988). Carrier-mediated translocation of uridine diphosphate glucose into the lumen of endoplasmic reticulum-derived vesicles from rat liver. *J. Clin. Invest.* **82**, 1113–1122.

Vasquez-Vivar, J., Martasek, P., Hogg, N., Masters, B. S., Pritchard, K. A., Jr., and Kalyanaraman, B. (1997). Endothelial nitric oxide synthase-dependent superoxide generation from adriamycin. *Biochemistry* **36**, 11293–11297.

Vermilion, J., and Coon, M. J. (1974). Highly purified detergent-solubilized NADPH-cytochrome P-450 reductase from Phenobarbital-induced rat liver microsomes. *Biochem. Biophys. Res. Commun.* **60**, 1315–1322.

Vermilion, J. L., Ballou, D. P., Massey, V., and Coon, M. J. (1981). Separate roles for FMN and FAD in catalysis by liver microsomal NADPH-cytochrome P-450 reductase. *J. Biol. Chem.* **256**, 266–277.

Vessey, D. A., and Zakim, D. (1971). Regulation of microsomal enzymes by phospholipids. Activation of hepatic uridine diphosphate-glucuronyltransferase. *J. Biol. Chem.* **246**, 4649–4656.

Villeneeuve, L., Girard, H., Fortier, L. C., Gagne, J. F., and Guillemette, C. (2003). Novel functional polymorphisms in the UGT1A7 and UGT1A9 glucuronidating enzymes in Caucasian and African-American subjects and their impact on the metabolism of 7-ethyl-10-hydroxycamptothecin and flavopiridol anticancer drugs. *J. Pharmacol. Exp. Ther.* **307**, 117–128.

Wang, M., Roberts, D. L., Paschke, R., Shea, T. M., Masters, B. S., and Kim, J. J. (1997). Three-dimensional structure of NADPH-cytochrome P450 reductase: Prototype for FMN- and FAD-containing enzymes. *Proc. Natl. Acad. Sci. USA* **94**, 8411–8416.

Wang, X., Thomas, B., Sachdeva, R., Arterburn, L., Frye, L., Hatcher, P. G., Cornwell, D. G., and Ma, J. (2006). Mechanism of arylating quinone toxicity involving Michael adduct formation and induction of endoplasmic reticulum stress. *Proc. Natl. Acad. Sci. USA* **103**, 3604–3609.

Watanabe, J., Asaka, Y., Fujimoto, S., and Kanamura, S. (1993). Densities of NADPH-ferrihemoprotein reductase and cytochrome P-450 molecules in the endoplasmic reticulum membrane of rat hepatocytes. *J. Histochem. Cytochem.* **41**, 43–49.

Weatherill, P. J., and Burchell, B. (1980). The separation and purification of rat liver UDP-glucuronyltransferase activities towards testosterone and oestrone. *Biochem. J.* **189**, 377–380.

West, J. D., and Marnett, L. J. (2006). Endogenous reactive intermediates as modulators of cell signaling and cell death. *Chem. Res. Toxicol.* **19**, 173–194.

Wilke, R. A., Reif, D. M., and Moore, H. H. (2005). Combinatorial pharmacogenetics. *Nat. Drug Disc.* **4**, 911–918.

Wilkinson, G. R. (2001). The dynamics of drug absorption, distribution, and elimination. *In* "Goodman and Gilman's the Pharmacological Basis of Therapeutics" (J. G. Hardman and L. E. Limbird, Eds.), 10th ed., pp. 3–29. McGraw-Hill, New York.

Williams, C. H., Jr., and Kamin, H. (1962). Microsomal triphosphopyridine nucleotide-cytochrome *c* reductase of liver. *J. Biol. Chem.* **237**, 587–595.

Williams, P. A., Cosme, J., Sridhar, V., Johnson, E. F., and McRee, D. E. (2000). The crystallographic structure of a mammalian microsomal cytochrome P450 monooxygenase: Structural adaptations for membrane binding and functional diversity. *Mol. Cell.* **5**, 121–132.

Williams, R. T. (1959). "Detoxication Mechanisms," Wiley & Sons, New York.

Winski, S. L., Faig, M., Bianchet, M. A., Siegel, D., Swann, E., Fung, K., Duncan, M. W., Moody, C. J., Amwzel, L. M., and Ross, D. (2001). Characterization of a mechanism-based inhibitor of NAD(P)H:quinone oxidoreductase 1 by biochemical, X-ray crystallographic, and mass spectrometric approaches. *Biochemistry* **40,** 15135–15142.

Wolthers, K. R., Basran, J., Munro, A. W., and Scrutton, N. S. (2003). Molecular dissection of human methionine synthase reductase: Determination of the flavin redox potentials in full-length enzyme and isolated flavin-binding domains. *Biochemistry* **42,** 3911–3920.

Wu, Q. (2005). Comparative genomics and diversifying selection of the clustered vertebrate protocadherin genes. *Genetics* **169,** 2179–2188.

Wu, Q., and Maniatis, T. (1999). A striking organization of a large family of human neural cadherin-like cell adhesion genes. *Cell* **97,** 779–790.

Xiong, Y., Bernardi, D., Bratton, S., Ward, M. D., Battaglia, E., Finel, M., Drake, R. R., and Radominska-Pandya, A. (2006). Phenylalanine 90 and 93 are localized within the phenol binding site of human UDP-glucuronosyltransferase 1A10 as determined by photoaffinity labeling, mass spectrometry, and site-directed mutagenesis. *Biochemistry* **45,** 2322–2332.

Yamada, H., Ishii, K., Ishii, Y., Ieiri, I., Nishio, S., Morioka, T., and Oguri, K. (2003). Formation of highly analgesic morphine-6-glucuronide following physiologic concentration of morphine in human brain. *J. Toxicol. Sci.* **28,** 395–401.

Yamada, M., Ohta, Y., Bachmanova, G. I., Nishimoto, Y., Archakov, A. I., and Kawato, S. (1995). Dynamic interactions of rabbit liver cytochromes P450IA2 and P450IIB4 with cytochrome b5 and NADPH-cytochrome P450 reductase in proteoliposomes. *Biochemistry* **34,** 10113–10119.

Yamamoto, K., Sato, H., Fujiyama, Y., Doida, Y., and Bamba, T. (1998). Contribution of two missense mutations (G71R and Y486D) of the bilirubin UDP glycosyltransferase (UGT1A1) gene to phenotypes of Gilbert's syndrome and Crigler-Najjar syndrome type II. *Biochim. Biophys. Acta* **1406,** 267–273.

Yamamoto, K., Kimura, S., Shiro, Y., and Iyanagi, T. (2005). Interflavin one-electron transfer in the inducible nitric oxide synthase reductase domain and NADPH-cytochrome P450 reductase. *Arch. Biochem. Biophys.* **440,** 65–78.

Yamano, S., Aoyama, T., McBride, O. W., Hardwick, J. P., Gelboin, H. V., and Gonzalez, F. J. (1989). Human NADPH-P450 oxidoreductase: Complementary DNA cloning, sequence and vaccinia virus-mediated expression and localization of the CYPOR gene to chromosome 7. *Mol. Pharmacol.* **36,** 83–88.

Yamazaki, I. (1971). One- and two-electron transfer mechanism in enzymatic oxidation-reduction reaction. *Adv. Biophys.* **2,** 33–76.

Yamazaki, I., and Piette, L. H. (1990). ESR spin-trapping studies on the reaction of Fe2+ ions with H2O2-reactive species in oxygen toxicity in biology. *J. Biol. Chem.* **265,** 13589–13594.

Yamazaki, I., and Piette, L. H. (1991). EPR spin-trapping study on the oxidizing species formed in the reaction of the ferrousn ion with hydrogen peroxide. *J. Am. Chem. Soc.* **113,** 7588–7593.

Yanao, J. K., Hsu, M. H., Griffin, K. J., Stout, C. D., and Johnson, E. F. (2005). Structures of human microsomal cytochrome P450 2A6 complexed with coumarin and methoxsalen. *Nat. Struct. Mol. Biol.* **12,** 822–823.

Yasukochi, Y., and Masters, B. S. S. (1976). Some properties of a detergent-solubilized NADPH-cytochrome *c* (cytochrome P-450) reductase purified by biospecific affinity chromatography. *J. Biol. Chem.* **251,** 5337–5344.

Yokota, H., Yuasa, A., and Sato, R. (1988). Purification and properties of a form of UDP-glucuronyltransferase from liver microsomes of 3-methylcholanthrene-treated rats. *J. Biochem. (Tokyo).* **104,** 531–536.

Yoshida, T., Noguchi, M., Kikuchi, G., and Sano, S. (1981). Degradation of mesoheme and hydroxymesoheme catalyzed by the heme oxygenase system: Involvement of hydroxyheme in the sequence of heme catabolism. *J. Biochem. (Tokyo)*. **90,** 125–131.

Yoshimura, H., Oguri, K., and Tsukamoto, H. (1968). Metabolism of drugs. LX. The synthesis of codeine and morphine glucuronides. *Chem. Pharm. Bull. (Tokyo)*. **16,** 2114–2119.

Yoshioka, S., Tosha, T., Takahashi, S., Ishimori, K., Hori, H., and Morishima, I. (2002). Roles of the proximal hydrogen bonding network in cytochrome P450cam-catalyzed oxygenation. *J. Am. Chem. Soc.* **124,** 14571–14579.

Yu, B., Edstrom, W. C., Benach, J., Hamuro, Y., Weber, P. C., Gibney, B. R., and Hunt, J. F. (2006). Crystal structures of catalytic complexes of the oxidative DNA/RNA repair enzyme AlkB. *Nature* **439,** 879–884.

Yu, L. C., Twu, Y. C., Chou, M. L., Reid, M. E., Gray, A. R., Moulds, J. M., Chang, C. Y., and Lin, M. (2003). The molecular genetics of the human I locus and molecular background explain the partial association of the adult i phenotype with congenital cataracts. *Blood* **101,** 2081–2088.

Zahid, M., Kohli, E., Saeed, M., Rogan, E., and Cavalieri, E. (2006). The greater reactivity of estradiol-3,4-quinone vs estradiol-2,3-quinone with DNA in the formation of depurinating adducts: Implications for tumor-initiating activity. *Chem. Res. Toxicol.* **19,** 164–172.

Zakim, D., and Dannenberg, A. J. (1972). How does the microsomal membrane regulateUDP-glucuronosyltransferases? *Biochem. Pharmacol.* **43,** 1385–1393.

Zemojtel, T., Wade, R. C., and Dandekar, T. (2003). In search of the prototype of nitric oxide synthase. *FEBS Lett.* **554,** 1–5.

Zhang, H., Myshkin, E., and Waskell, L. (2005). Role of cytochrome b5 in catalysis by cytochrome P450 2B4. *Biochem. Biophys. Res. Commun.* **338,** 499–506.

Zhang, J., Martásek, P., Paschke, R., Shea, T. M., Masters, B. S. S., and Kim, J.-J. P. (2001). Crystal structure of the FAD/NADPH-binding domain of rat neuronal nitric-oxide synthase. Comparisons with NADPH-cytochrome P450 oxidoreductase. *J. Biol. Chem.* **276,** 37506–37513.

Zhang, T., Haws, P., and Wu, Q. (2004). Multiple variable first exons: A mechanism for cell- and tissue-specific gene regulation. *Genome Res.* **14,** 79–89.

Zhao, Q., Modi, S., Smith, G., Paine, M., McDonagh, P. D., Wolf, C. R., Tew, D., Lian, L. Y., Roberts, G. C., and Driessen, H. P. (1999). Crystal structure of the FMN-binding domain of human cytochrome P450 reductase at 1.93 A resolution. *Protein Sci.* **8,** 298–306.

Zhao, Y., White, M. A., Muralidhara, B. K., Sun, L., Halpert, J. R., and Stout, C. D. (2006). Structure of microsomal cytochrome P450 2B4 complexed with the antifungal drug bifonazole: Insight into P450 conformational plasticity and membrane interaction. *J. Biol. Chem.* **281,** 5973–5981.

Zhou, Z., Fisher, D., Spidel, J., Greenfield, J., Patson, B., Fazal, A., Wigal, C., Moe, O. A., and Madura, J. D. (2003). Kinetic and docking studies of the interaction of quinones with the quinone reductase active site. *Biochemistry* **42,** 1985–1994.

Zhu, H., Larade, K., Jackson, T. A., Xie, J., Ladoux, A., Acker, H., Berchner-Pfannschmidt, U., Fandrey, J., Cross, A. R., Lukat-Rodgers, G. S., Rodgers, K. R., and Bunn, H. F. (2004). NCB5OR is a novel soluble NAD(P)H reductase localized in the endoplasmic reticulum. *J. Biol. Chem.* **279,** 30316–30325.

Zweier, J. L., Gianni, L., Muindi, J., and Myers, C. E. (1986). Differences in O2 reduction by the iron complexes of adriamycin and daunomycin: The importance of the sidechain hydroxyl group. *Biochim. Biophys. Acta* **884,** 326–336.

Further Reading

Backes, W. L., and Kelley, R. W. (2003). Organization of multiple cytochrome P450s with NADPH-cytochrome P450 reductase in membranes. *Pharmacol. Ther.* **98,** 221–233.

Bock, K. W., and Kohle, C. (2004). Coordinate regulation of drug metabolism by xenobiotic nuclear receptors: UGTs acting together with CYPs and glucuronide transporters. *Drug Metab. Rev.* **36,** 595–615.

Bukowski, M. R., Koehntop, K. D., Stubna, A., Bominaar, E. L., Halfen, J. A., Munck, E., Nam, W., and Que, L., Jr., (2005). A thiolate-ligated nonheme oxoiron (IV) complex relevant to cytochrome P450. *Science* **310,** 1000–1002.

Caspersen, C. S., Reznik, B., Weldy, P. L., Abildskov, K. M., Stark, R. I., and Garland, M. (2007). Molecular cloning of the baboon UDP-glucuronosyltransferase 1A gene family: Evolution of the primate UGT1 locus and relevance for models of human drug metabolism. *Pharmacogenet. Genomics* **17,** 11–24.

Csala, M., Banhegyi, G., and Benedetti, A. (2006). Endoplasmic reticulum: A metabolic compartment. *FEBS Lett.* **580,** 2160–2165.

Guillemette, C. (2003). Pharmacogenomics of human UDP-glucuronosyltransferase enzymes. *Pharmacogenomics J.* **3,** 136–158.

Gutierrez, A., Grunau, A., Paine, M., Munro, A. W., Wolf, C. R., Roberts, G. C., and Scrutton, N. S. (2003). Electron transfer in human cytochrome P450 reductase. *Biochem. Soc. Trans.* **31,** 497–501.

Iyanagi, T., Emi, Y., and Ikushiro, S. (1998). Biochemical and molecular aspects of genetic disorders of bilirubin metabolism. *Biochim Biophys Acta* **1407,** 173–184.

Massey, V. (2000). The chemical and biological versatility of riboflavin. *Biochem. Soc. Trans.* **28,** 283–296.

Tasic, B., Nabholz, C. E., Baldwin, K. K., Kim, Y., Rueckert, E. H., Ribich, S. A., Cramer, P., Wu, Q., Axel, R., and Maniatis, T. (2002). Promoter choice determines splice site selection in protocadherin alpha and gamma pre-mRNA splicing. *Mol. Cell.* **10,** 21–33.

Wolkoff, A. W. (2005). The hyperbilirubinemias. *In* "Harison's Principles of Internal Medicine" (D. L. Kasper, E. B. Braunwald, A. S. Fauci, S. L. Hauser, D. L. Longo, and J. L. Jameson, Eds.), 16th ed., pp. 1817–1821. McGraw Hill, New York.

Yueh, M. F., Bonzo, J. A., and Tukey, R. H. (2005). The role of Ah receptor in induction of human UDP-glucuronosyltransferase 1A1. *Meth. Enzymol.* **400,** 75–91.

Effects of Growth Factors on Testicular Morphogenesis

Sarah Mackay and Robert A. Smith

Division of Neuroscience and Biomedical Systems, Institute of Biomedical and
Life Sciences, University of Glasgow, Glasgow, UK G12 8QQ

Since the discovery of the sex-determining gene *Sry* in 1990, research effort
has focused on the events downstream of its expression. A range of different
experimental approaches including gene expression, knocking-out and
knocking-in genes of interest, and cell and tissue culture techniques have been
applied, highlighting the importance of growth factors at all stages of testicular
morphogenesis. Migration of primordial germ cells and the mesonephric
precursors of peritubular myoid cells and endothelial cells to the gonad is under
growth factor control. Proliferation of both germ cells and somatic cells within the
gonadal primordium is also controlled by cytokines as is the interaction of Sertoli
cells (with each other and with the extracellular matrix) to form testicular cords.
Several growth factors/growth factor families (e.g., platelet-derived growth factor,
fibroblast growth factor family, TGFβ family, and neurotrophins) have emerged as
key players, exerting an influence at different time points and steps in
organogenesis. Although most evidence has emerged in the mouse, comparative
studies are important in elucidating the variety, potential, and evolution of control
mechanisms.

KEY WORDS: Testis development, Sex differentiation, Growth factors,
Morphogenesis, AMH, FGF9, PDGF, Neurotrophic factors.   © 2007 Elsevier Inc.

I. Introduction

In 1986 developmental biologist Rita Levi-Montalcini and biochemist Stanley
Cohen were awarded the Nobel Prize for Physiology or Medicine for their
discovery of nerve growth factor in the 1950s (see Levi-Montalcini, 1998).

It had taken over 3 decades for their work to be fully appreciated; moreover, the fundamental importance of growth factors in the control of proliferation and differentiation in both normal and abnormal development is still being elucidated. Morphogenesis of the testis provides a useful representative model system in which to study growth factor control of cell biological events as it involves, at various stages, cell migration, proliferation, differentiation, apoptosis, epithelial–mesenchymal interactions, cell–matrix interactions, and vasculogenesis (Brennan and Capel, 2004; Mackay, 2000; Ross and Capel, 2005). Growth factors have been implicated in the control of similar phenomena in other organ systems (Chen *et al.*, 2004; Lu *et al.*, 2006; Michael and Davies, 2004; Serls *et al.*, 2005; Shimogori *et al.*, 2004; Thisse and Thisse, 2005; Tickle, 2003; White *et al.*, 2006).

Over the last 15 to 20 years a considerable amount of research effort has been directed to investigate the role of growth factors at specific stages and on specific cell types during testis development (Abo-Elmaksoud and Sinowatz, 2005; Mackay, 2000). Both *in vivo* and *in vitro* approaches have been used (Cupp *et al.*, 2000; Ricci *et al.*, 2004). The application of genetic approaches, both knocking-in and knocking-out genes of interest, has also resulted in a wealth of new information (Behringer *et al.*, 1990; Brennan and Capel, 2004; Xia *et al.*, 2004).

The elucidation of the role of growth factors in testicular morphogenesis is key to understanding disorders of testicular function in adulthood, which may have their origins in the developmental period. For example, "testicular dysgenesis syndrome" in humans is a collection of common disorders (germ-cell cancer, cryptorchidism, hypospadias, and low sperm counts) thought to have a common origin during the developmental period related to abnormal functioning of Sertoli and Leydig cells (Sharpe *et al.*, 2003).

II. Comparative Testicular Morphogenesis

A considerable amount of research data on testicular morphogenesis has been accumulated using the mouse and the rat as experimental animals; these laboratory rodents are assumed to be representative mammals, although mouse development differs in several ways from that found in most mammals (Müller, 1997). Important developmental mechanisms tend to be conserved, but it is nonetheless desirable to widen the scope of observation and experimentation to a larger number of species to gain an insight into mammalian morphogenesis. Moreover, occasionally a species will come to light with a remarkable mode of development, which elucidates the potential of basic mechanisms.

Female moles belonging to several species of the genus *Talpa* are unique in having bilateral ovotestes (Barrionuevo *et al.*, 2004), with a smaller ovarian portion bearing normal follicles and a larger testicular part that lacks germ cells, but has abundant Leydig cells producing testosterone and spherical testicular cords composed of immature Sertoli cells surrounded by peritubular myoid cells. In contrast to other mammals, the first signs of sex differentiation appear in females rather than in males, with the appearance of the medulla and cortex in females before testis differentiation is seen in males. The authors speculate that the first role of the sex-determining gene, *SRY,* in male moles may be to avoid this regionalization. A further difference between moles and other mammals is that entry of female germ cells to meiosis is delayed with respect to testis differentiation and occurs after birth. Timing of entry to meiosis is known to be delayed in species where there are more well-defined ovarian cords which produce steroidal hormones during the delay period (Byskov, 1979). Importantly, this work shows key events of testicular differentiation (e.g., mesenchymal cell migration, medullary cord formation, development of the vascular system, and the tunica albuginea) can occur in the absence of SRY. Furthermore, given that the medullary cord cells lack morphological features of Sertoli cells and do not express their product, anti-Müllerian hormone (AMH), these elements of testicular differentiation can develop in female moles in the absence of typical pre-Sertoli or Sertoli cells. Follicular granulosa cells are known to have the potential to transform into Sertoli cells after oocyte loss (Taketo-Hosotani *et al.*, 1985), which might explain the development of testicular features in the medullary region of female moles where PGCs are largely absent (Barrionuevo *et al.*, 2004).

Insights into the evolution of the molecular genetics of vertebrate sex determination have been provided by studies on the chicken (Smith and Sinclair, 2004). Sex in birds is determined by a ZZ/ZW system rather than an XX/XY system and female is the heterogametic sex. Furthermore, only the left gonad becomes an ovary while the right regresses. The *SRY* gene is absent in birds, but several other genes important for mammalian sex determination are also expressed in the chicken, though with different expression patterns. These include the orphan nuclear receptor steroidogenic factor-1 (SF-1), the Wilm's Tumor-associated protein WT-1, and the LIM homeobox protein LHX; SF-1 and WT-1 activate SRY expression in mammals and presumably activate other sex determinants in the chicken (Smith and Sinclair, 2004). SF-1 and WT-1 also cooperate with *SOX9* to turn on expression of *AMH* in mammals, but in the chicken *AMH* expression precedes that of *SOX9*. These genes are not sex-linked in the chicken, but there are candidate sex-determining genes in birds and other organisms which are sex-linked: *Drosophila* Doublesex and *Caenorhabditis (C.) elegans* Mab-3–related transcription factor 1 *(DMRT1)* (Z-linked) and avian, sex-specific,

W-linked (ASW) and female-expressed transcript 1 (FET1), which are both W-linked. A further difference in birds is the importance of estrogens; evolutionary pressure in mammals, where there is a highly developed placenta and intrauterine development, has led to the establishment of other mechanisms so that testis differentiation can proceed in the presence of maternal sex steroids (Wolf, 1999). In the chicken, expression of the estrogen receptor is seen in both sexes prior to sex differentiation, but is later downregulated in males as well as in the right female gonad (Smith and Sinclair, 2004).

As in mammals, differentiation and proliferation of Sertoli cells within cords is a key step in testis differentiation, but there does not appear to be a prominent coelomic blood vessel (Smith and Sinclair, 2004), as seen at the time of cord formation in mouse testis differentiation (McLaren, 1983). The migration of mesonephric cells into the developing mouse testis is necessary for cord formation (Buehr *et al.*, 1993a; Martineau *et al.*, 1997; Tilmann and Capel, 1999). Incoming cells contribute to the endothelial (Martineau *et al.*, 1997), peritubular myoid cell (Nishino *et al.*, 2001), and Leydig cell populations (Merchant-Larios and Moreno-Mendoza, 1998). Mesonephric cell migration cannot be induced into XX mouse gonads after E12.5 unless the XX gonads are depleted of germ cells, which are by this stage meiotic and would otherwise antagonize mesonephric cell migration (Yao *et al.*, 2003). Investigation of the control of this process has shown that although mesonephric migration into XX gonads may be induced by addition of recombinant AMH in culture, no abnormalities are seen in *AMH*-deficient male mice (Ross *et al.*, 2003). It is also known that signaling by the receptor for platelet-derived growth factor (see Section III.B.1) acts on migrating mesonephric cells indirectly (Brennan *et al.*, 2003). In an elegant study using chicken–quail cocultures, no migration of QCPN[+] quail mesonephric cells was seen in cocultured male chicken gonads in the presence of the PDGFR inhibitor AG1296 (tyrphostin), though extensive immigration of QCPN^{+} cells occurred in controls (Smith *et al.*, 2005). Mouse cells migrated in chicken–mouse interspecific cocultures in the absence of *Sry* in the chicken; in the presence of inhibitor mesonephric cell migration was reduced. Results that *PDGFR-α* is expressed in the gonads rather than in the mesonephroi suggest the PDGF signaling necessary for mesonephric cell migration may be indirect. A component of the phosphatidylinositol 3-kinase pathway involved in PDGF signaling, the kinase P13KC2α is expressed in the chicken testis at the time of sex differentiation and concomitant with mesonephric cell migration. It remains to be seen whether this kinase is expressed at the time of mammalian gonadal development. In conclusion, *Sry* induces mouse mesonephric cell migration indirectly, via a conserved pathway shared with birds in which PDGFR signaling is implicated. There is no obvious effect on general cord formation when mesonephric cell migration is inhibited in the avian system, implying that promotion of cord

organization may not be the primary function of this migration in all verte-brates (Smith *et al.*, 2005).

Temperature-dependent sex determination is shown in many reptiles in-cluding all crocodilians, many turtles, and several lizards (Crews, 2003; Ferguson and Joanen, 1983; Western and Sinclair, 2001). Despite this major difference between reptiles and mammals, genetic mechanisms controlling gonadal morphological differentiation appear to be conserved: as in the mouse, *AMH* expression marks Sertoli cell differentiation in the alligator testis (Western and Sinclair, 2001). In the mouse, upregulation of *AMH* expression is controlled by SOX9, but in alligator and chicken gonads this *AMH* upregulation occurs before that of *SOX9* indicating a different control mechanism must operate (Western and Sinclair, 2001). Thus, although a similar repertoire of genes may be involved in gonadal differentiation during both genetic and environmental sex determination, a diversity of control mechanisms may operate (Yao and Capel, 2005).

Marsupial mammals are also of interest; for example, the tammar wallaby has been reported as showing extensive sexual dimorphisms preceding any morphological differentiation of the gonads (O *et al.*, 1988). This finding is at odds with the classical view of mammalian sexual differentiation that after the testis-determining gene triggers testis differentiation, androgen from Leydig cells promotes male reproductive tract development while AMH from Sertoli cells inhibits female tract development. Although such excep-tions to the rule are illuminating they may be very rare; evidence from another marsupial, *Monodelphus domestica,* suggests androgens play a role in development of the scrotum (Russell *et al.*, 2003). Furthermore, a study by Coveney *et al.* (2002) shows that treatment of tammar wallaby pouch young with estradiol benzoate from the day of birth results in profound effects on genital ducts and smaller scrota than those of controls; these effects appear to result from alteration of normal testicular production of both AMH and androgens as well as from direct effects of estrogen on target tissues indicating that androgens may play a role in this species.

A further puzzle in marsupials is the question of a mesonephric contribu-tion to the testis. As mentioned previously, in the mouse mesonephric cells contribute peritubular myoid cells, which are important in contributing fibronectin to the basal laminae of developing testicular cords, stabilizing their structure (Buehr *et al.*, 1993a; Capel *et al.*, 1999; Martineau *et al.*, 1997; Merchant-Larios *et al.*, 1993). In *M. domestica* the mesonephros is still acting as the functional kidney at the time of birth and so presumably cannot contribute cells during testicular differentiation around the time of birth (Mackay *et al.*, 2004a; Xie *et al.*, 1996). Testis cords will develop in sea turtle gonads cultured without adjacent mesonephroi (Moreno-Mendoza *et al.*, 2001) and no evidence for a mesonephric contribution to the testis of the red-eared slider turtle has been found (Yao and Capel, 2005).

A common denominator between the effects of sex-determining genes and environmental factors has been identified: control of metabolic rate (Kraak and de Looze, 1993; Mittwoch, 2004). Testis-determining genes may act by increasing metabolic rates rather than by directly determining Sertoli cell differentiation. Mittwoch proposes that the testis-determining genes *SRY* and *SOX9* bring about an increase in metabolic rate in tissues in which they are active, increasing cell proliferation and other developmental processes such as migration; similar effects are produced by a temperature rise in ectothermic vertebrates (Mittwoch, 2004).

III. Cell Migration

A. Germ Cells

In the male mammal there are four periods of germ cell movement, whether active or passive. The first occurs when the primordial germ cells (PGCs) migrate from the hindgut wall to the genital ridge. The second is when the germ cells relocate from the lumen of the testicular cord to the basement membrane in postnatal life. Thirdly, preleptotene and leptotene spermatocytes must translocate from the basal to the adlumenal compartment of the seminiferous tubule for further development in adult life (Lui *et al.*, 2003a). Lastly, the active motility of spermatozoa is important in fertilization. Growth factors are likely to be involved in control at all stages.

An elegant study was performed in which mice expressing green fluorescent protein (GFP) in early germ line cells were used to investigate migratory activity of PGCs (Molyneaux *et al.*, 2001). Slices of embryo at different stages of development were cultured and time-lapse recordings made, over periods from 8 to 10 h, using confocal microscopy. Observations showed active motility in PGCs from E9.0 to E12.5 occurring within four phases of behavior: (1) (E9–E9.5), PGCs are highly motile while they are within the gut wall; (2) (E9–E9.5), before the mesentery forms, they emerge rapidly from the gut; (3) (E10–E10.5) PGCs migrate into the genital ridges from the dorsal body wall; and (4) (E11.5) PGC movement slows; in females the PGCs move randomly, whereas in males most traced cells move in the medial-posterior direction (Molyneaux *et al.*, 2001). The authors suggest the long-held view that PGCs migrate up the dorsal mesentery is a misconception, because in these experiments the majority of PGCs had migrated from the gut into the dorsal body wall before the mesentery had formed.

Explanted E8.5 migratory PGCs will move preferentially toward E10.5 genital ridges in culture (Godin *et al.*, 1990); this chemotropic effect is

mediated by TGFβ_1 or a closely related molecule, as it can be abolished by anti-TGFβ_1 antibody (Godin and Wylie, 1991). The c-kit/stem cell factor signaling pathway (see Section V.A) is required for normal migration (McLaren, 2003). In mice homozygous for a mutation in the *W* gene (which encodes the c-kit ligand for stem cell factor; see Section V.A) migration of PGCs lags behind wild-type and heterozygotes with a larger proportion of germ cells remaining in the gut wall (Buehr *et al.*, 1993b).

Donovan and coworkers (1986) proposed that once PGCs reach the gonad anlage in the mouse they undergo major phenotypic changes resulting in a loss of motile capability. We have shown however, that in the female at least the potential for migration is not lost by oocytes because germ cells are shed from cultured mouse ovarian explants peaking at day 7 postnatally (Mackay *et al.*, 1992). This appears not to be just a mechanism for elimination of dying germ cells, as seen in humans to reduce the pool of oocytes (Motta and Makabe, 1986), because the germ cells in our study retained good cytoplasmic integrity (as evidenced by TEM) and SEM examination confirmed the presence of regular lamellipodia and filopodia. Oocytes displaying migratory phenotypes were also reported in a separate study of neonatal mice by Wordinger *et al.* (1990) with germ cells released at the surface from healthy nonarteritic primordial follicles indicative of retention of motility.

Stromal cell-derived factor 1 (SDF1) is a member of the CXC family of chemokines (i.e., cytokines which may activate or attract leucocytes). The normal migration of PGCs in zebrafish depends on the interaction between SDF1 and its G-protein–coupled receptor CXCR4 (Knaut *et al.*, 2003). This interaction is also required in the mouse, where the receptor is detected at E9.5 on migratory germ cells and its ligand in the entire dorsal body wall, with higher staining in the neural tube floorplate, the mesonephros, and adjacent mesenchyme (Molyneaux *et al.*, 2003). Migration of germ cells *in vitro* can be perturbed by adding high local concentrations of SDF1. In embryos with a targeted mutation for the receptor, germ cells do not colonize the genital ridges correctly, although PGCs do colonize the hindgut. In these mutant embryos a progressive reduction of germ cells occurs during and after colonization of the genital ridges. When tissue slices from E10.5 embryos were cultured in the presence or absence of SDF1, PGC numbers in SDF1-treated slices showed a statistically significant increase compared with controls, indicating that SDF1 acts as a growth or survival factor for PGCs in the mouse (Molyneaux *et al.*, 2003).

A role for FGF signaling in mouse germ cell migration has been shown (Takeuchi *et al.*, 2005). Evidence includes analysis by RT-PCR of cDNA which shows E10.5 germ cells express the FGF receptors *Fgfr1-IIIc* and *Fgfr2-IIIb* (see Section V.5) and results of gain-of-function experiments showing FGF2 (a ligand for FGFR1-IIIc) affects motility, whereas loss of

function causes inhibition of cell shape changes in migrating germ cells. Directionality of germ cell movement does not appear to be affected by FGFs (Takeuchi *et al.*, 2005).

Expression of *TGFβ3* has been found in adult rat germ cells in a stage-specific manner extending from the basal to the luminal compartment, being predominant in stages V–VIII of the cycle and diminished at stages IX and X (Lui *et al.*, 2003a,b). Evidence in the adult rat suggests that blood–testis barrier dynamics *in vivo* are regulated by TGFβ2 and TGFβ3 (Wong *et al.*, 2004). TGFβ3 plays a crucial role in the regulation of Sertoli cell tight junctions via the MEKK2/p38MAP kinase pathway (Lui *et al.*, 2003b), to open the blood–testis barrier to allow migration of preleptotene and leptotene spermatocytes.

B. Peritubular Myoid Cells/Endothelial Cells/ Mesonephric Cells

Migration of cells from the mesonephros to the gonad is a male-specific event (Martineau *et al.*, 1997). Migrating cells include peritubular myoid cells (PMCs) and other interstitial cells (Buehr *et al.*, 1993a; Nishino *et al.*, 2001) in addition to endothelial cells necessary for angiogenesis in the developing testis (Brennan *et al.*, 2002; Jeays-Ward *et al.*, 2003).

1. Platelet-Derived Growth Factor

Platelet-derived growth factor (PDGF) stimulates mitosis in cells of mesenchymal origin (Heldin and Westermark, 1990), it is involved in mesenchymal–epithelial interactions (Uzumcu *et al.*, 2002a), and it belongs to the PDGF-vascular endothelial growth factor family. Several biologically active PDGF molecules are known; four are homodimers (PDGF-AA, PDGF-BB, PDGF-CC, and PDGF-DD) and there is also a heterodimer, PDGF-AB (Mariani *et al.*, 2002). In a study of PDGF-AA and PDGF-BB and their receptors (PDGFRs), Gnessi and coworkers (1995) used a battery of techniques including immunohistochemistry, Northern blot analysis, and RNA isolation to elucidate the expression of these molecules in rats at various developmental stages from the late fetal stage, *in vivo* and *in vitro*. Expression of PDGF A-chain, B-chain, and PDGFR (both α and β subunits) was found from the earliest stage examined; expression rose postnatally, remaining high for the first 5 days of postnatal life and then declined to lower levels in 15-day animals, and had virtually disappeared in older animals. During prenatal and early postnatal stages expression of PDGFs was seen in Sertoli cells (PDGFs) and of PDGFRs in PMCs, whereas in adult animals expression of PDGFs and PDGFRs was only seen in Leydig cells. Postnatal production of PDGFs was

found to be controlled in a dose-dependent fashion by follicle-stimulating hormone (FSH) (Gnessi *et al.*, 1995). These authors were also able to show a chemotactic effect of all PDGF isoforms and of Sertoli cell-conditioned medium on isolated peritubular myoid cells, which was inhibited by anti-PDGF antibodies.

Brennan *et al.* (2003) carried out coculture experiments to investigate the effect of PDGF on recruitment of mesonephric cells in developing mouse gonads. In control experiments, although XY gonads recruited mesonephric cells, XX gonads did not. However, if 50 ng/ml of PDGF-AA, -BB, or -AB was added to the culture medium, cells were recruited into the XX gonad from GFP-expressing mesonephroi after 48 h *in vitro;* all migrating GFP cells were PECAM-positive endothelial cells. To investigate the possibility that mesonephric cell migration was abnormal in *Pdgfr-α*$^{-/-}$ XY gonads, cultures were established using different combinations of *Pdgfr-α*$^{-/-}$ mesonephroi or *Pdgfr-α*$^{-/-}$ gonads and wild-type/*Pdgfr-α*$^{+/-}$ XY mesonephroi or gonads (mesonephroi were GFP-positive). Two days later cultured gonads were examined for the presence of GFP-positive cells. Results showed *Pdgfr-α* expression is not required on mesonephric cells for migration; however, migration was severely impaired if the gonad was *Pdgfr-α*$^{-/-}$ and the mesonephros was *Pdgfr-α*$^{+/-}$. The authors interpreted this data to mean that PDGFR-α signaling acts on migrating mesonephric cells indirectly, activating a second signal in gonadal cells, which then promotes migration (Brennan *et al.*, 2003).

In the same year, similar experiments were carried out to investigate the expression and function of PDGF-BB and its receptor, PDGFR-β, during mouse testis morphogenesis (Puglianiello *et al.*, 2003). Immunoreactivity for PDGFR-β was found in the mesonephros, but not in the gonad at E11.5. However, at E12.5 and E13.5 PDGFR-β–expressing cells progressively appeared within the interstitial tissue of the male gonadal ridge. An earlier study by this group had shown mesenchymal cells migrating to the testis from the mesonephros are characterized by their expression of the p75 neurotrophin receptor (see Section III.B.4) and can be isolated by immunomagnetic sorting with anti-p75NTR antibody from total mesonephric cell suspensions (Campagnolo *et al.*, 2001). Virtually all of these selected cells were found to also express the PDGFβ receptor. At E12.5 and E13.5 Northern blot analysis showed PDGF-BB mRNA in gonads, with a higher content in males; *in situ* hybridization also showed a higher expression of PDGF-BB mRNA in the testis, mainly in the interstitial population. Exposure to PDGF-BB stimulated both mitosis (as indicated by a 2.5-fold increase in [^{3}H]-TdR incorporation) and migration of mesonephric mesenchymal cells, inducing shape changes associated with chemotaxis such as rearrangement of actin filaments and the development of edge ruffles. Although migration occurred at low PDGF-BB concentrations, higher concentrations were required for the

mitogenic effect. The authors suggest a gonadally released gradient might induce migration of mesonephric mesenchymal cells, which would then be exposed to higher levels once in the gonad, triggering proliferation. The possible signal transduction pathways involved in the PDGF-BB–induced stimulation of mitosis and migration were also investigated. Both mitogen-activated protein kinases (MAPK) and phosphatidylinositol-3 kinase (PI3K) pathways were found to be required, as both the MAPK inhibitor U0126 and the PI3K inhibitor Ly294002 were shown to inhibit migration and proliferation in assays *in vitro* (Puglianiello *et al.*, 2003).

Synthesis of PDGF-BB in the mouse testis was demonstrated by immuno-localization by Ricci *et al.* (2004): PDGF-BB was present at a low level in the male genital ridge at E11.5 and the interstitial compartment of the testis was weakly positive at E13.5. At E11.5 receptor immunolocalization was restricted to the coelomic epithelium and mesonephric mesenchyme, but not the gonad in the case of PDGFR-β. In the case of PDGFR-α, low level immunostaining was seen in some cells of the coelomic epithelium and at the boundary between the gonad and mesonephros and to a lesser extent in the mesonephric mesenchyme. By E13.5 the coelomic epithelium over the genital ridge was more positively stained for PDGFR-β as were the interstitial and peritubular cells, although staining for the α receptor chain was less evident. The role of PDGF-BB as a migratory factor for male mesonephric cells was investigated using Boyden's migration chambers to carry out an *in vitro* migration assay. Dissociated mesonephric cells were seeded in the upper side of the chambers whereas lower chambers were filled with medium alone or supplemented with 100-ng/ml PDGF-BB, which was found to strongly increase migratory activity as compared with controls. Conditioned medium (CM) from E13.5 testicular cell cultures also strongly increased migratory activity; this effect of CM was inhibited by the addition of an anti-PDGF-BB neutralizing antibody (Ricci *et al.*, 2004). An organ culture approach was used to investigate the role of the PI3K signaling pathway in testis differentiation. A high dose of the PI3K inhibitor Ly294002 totally inhibited cord formation in E11.5 male urogenital ridges cultured for 4 days *in vitro* (div) and also inhibited testicular cell reaggregation in a dose-dependent manner.

2. Hepatocyte Growth Factor

Hepatocyte growth factor (HGF), originally identified acting as a mitogenic factor for hepatocytes (Nakamura *et al.*, 1984), is a powerful angiogenic factor stimulating endothelial cell motility and growth (Bussolino *et al.*, 1992). HGF and its receptor c-met have been implicated in regulating the detachment and emigration of myogenic precursor cells in the dermomyotome (Birchmeier and Gherardi, 1998). Mesonephric cells isolated from E13.5 mouse embryos showed significantly increased ($p = < 0.001$) migratory

activity when cultured in the upper side of Boyden chambers whose lower chambers were filled with medium supplemented with HGF (100–400 U/ml), compared with cells cultured with medium alone (Ricci *et al.*, 2002).

3. Transforming Growth Factor β Superfamily

As well as the transforming growth factor (TGF)β family, this superfamily includes the activin/inhibin family, AMH and members of the bone morphogenetic protein (BMP) family (Lui *et al.*, 2003a) apart from BMP-1, which is a metalloproteinase (Kessler *et al.*, 1996). In mammals there are three homodimer isoforms of TGFβ: TGFβ1, TGFβ2, and TGFβ3 (Josso and di Clemente, 1999).

a. Transforming Growth Factor β3 In an immunohistochemical study on the expression and action of the three TGFβ isoforms during rat testis development, higher concentrations of TGFβ3 were found during embryonic development from E16 to the time of birth, with significantly lower concentrations postnatally. Although TGFβ1 was expressed in Sertoli cells, gonocytes and some interstitial cells during embryonic testis development, and TGFβ2 staining was specific for Sertoli cells at E14, TGFβ3 expression at this time was restricted to cells in the border region between the testis and mesonephros. Intensely staining cells appeared to be preperitubular, around testicular cords, although isolated interstitial cells were also positive. The authors speculate preperitubular cells may express TGFβ3 to induce migration or differentiation; further investigation should be directed to clarifying this potential role (Cupp *et al.*, 1999).

b. Anti-Müllerian Hormone Synthesized by, and released from pre-Sertoli cells (Josso, 1994), AMH, also known as Müllerian inhibiting substance (MIS), functions to induce Müllerian duct regression in the male. Additional roles for AMH include regulation of germ cell maturation and gonadogenesis, control of testicular descent, inhibition of lung maturation, and suppression of tumor growth (Lee and Donahoe, 1993). For many years there has been speculation about a possible role in testis development, because AMH produces the "freemartin" condition in nature, in which female bovine embryos can be masculinized if linked to a male twin by placental anastomoses, allowing the passage of AMH to the female (Jost *et al.*, 1972). Organ culture experiments have been carried out to determine whether AMH is involved in the control of mesonephric cell migration, specifically, whether AMH could induce migration of mesonephric cells into an XX mouse gonad (Ross *et al.*, 2003). Mouse gonads were detached from urogenital complexes of E11.5 and E12.5 embryos and cultured recombined with mesonephroi from ROSA 26 embryos which express a *lacZ* reporter gene. After 24 h

extensive mesonephric cell migration occurred into the E11.5 XY gonad but not the XX gonad. However, if the culture medium contained 15-µg/ml recombinant human AMH numerous cells did migrate into the female gonads, albeit in reduced numbers compared with the males. Migration could not be induced in the case of ovaries extracted at E12.5, suggesting a restricted time window during which differentiation may be influenced by AMH (Ross *et al.*, 2003). A further finding was that in E11.5 XX gonads cultured with AMH a coelomic blood vessel and coelomic epithelial thickening was seen as in normal XY gonads; these features are not normally seen in XX gonads, where follistatin acts downstream of Wnt4 to block mesonephric cell migration (see Section IV.B). No testis abnormality is seen in AMH null mutants. Therefore, if AMH does have a role in normal testis morphogenesis, its loss must be compensated by another factor or factors.

AMH exerts its effects by activating a BMP-like signaling pathway involving the phosphorylation of downstream Smad1 protein (Clarke *et al.*, 2001; Gouédard *et al.*, 2000; Visser *et al.*, 2001; Xavier and Allard, 2003). Signaling by TGFβ family cytokines is mediated through a complex of two serine/threonine kinase receptors (type I and type II) which then activate two cytoplasmic receptors, receptor-regulated Smads (R-Smad) and common Smad (Smad4). Type II is the primary receptor which binds the ligand, phosphorylating the type I receptor which then phosphorylates R-Smad, which in turn interacts with Smad4 (di Clemente *et al.*, 2003). The type I receptor for AMH is likely to be a BMP-specific type-I receptor: ALK-2 (also known as ActR-IA), ALK-3 (also known as BMPR-IA), and/or ALK-6 (also known as BMPR-IB); which is responsible for mediating the action of AMH and may vary under different conditions or in different cell types (Shimasaki *et al.*, 2004). Smad proteins are related to the protein product of the *Drosophila* gene *Mothers against decapentaplegic (Mad)* (Graff *et al.*, 1996). Mad-related proteins have been found in a variety of organisms and act as intracellular transducers of the TGFβ family. AMH induces the phosphorylation of the BMP-specific R-Smad, Smad1, and its association with Smad4; the complex moves to the nucleus (di Clemente *et al.*, 2003) where it presumably attaches to a Smad-binding element on the promoter of target genes (Massagué and Chen, 2000). In addition to the Smad pathway, AMH can also function via other signaling pathways such as β catenin/LEF-1, as in the case of Müllerian duct regression (Allard *et al.*, 2000) or NFkB in inhibition of breast cancer cell growth (Segev *et al.*, 2000).

To determine whether other members of the TGFβ family, which use the same Smad effector proteins as AMH, could substitute for it, XX gonads were cultured with beads coated with recombinant BMP2 or BMP4 protein (Ross *et al.*, 2003). Growth of vasculature was induced, but because neither gene is expressed in normal development, a different BMP may be involved in the regulation of mesonephric migration (Ross *et al.*, 2003).

4. Neurotrophic Factors

The neurotrophin family includes nerve growth factor (NGF), brain-derived neurotrophic factor (BDNF), neurotrophin (NT)-3, and NT-4/5 (Bothwell, 1995). All are able to bind to the low affinity receptor P75/NTR, but also have their own high-affinity receptors: trkA for NGF, trkC for NT3, and trkB for NT4/5 and BDNF (Barbacid, 1995; Cupp *et al.*, 2002). Cells that migrate from the mesonephros to the mouse gonad are characterized by the presence of the low-affinity NGF receptor (NGFR), p75 NT receptor (p75NTR) on their surface (Campagnolo *et al.*, 2001). A cluster of p75/NTR-positive cells can be identified in the mesonephros at E10.5 and in a region adjacent to the gonad from E11.25 (15–16 tail somites) where they spread into the gonad from E11.5, filling the testicular stroma by E12.5. Cells positive for p75/NTR can be isolated from the gonad by immunomagnetic selection; if cultured for up to 3 div on Matrigel nearly all cells express the peritubular myoid cell marker (Tung and Fritz, 1990), α-smooth muscle actin after 2 div (Campagnolo *et al.*, 2001). The specific ligand and its source remains to be identified for the mouse. No NT can be detected in the early mouse gonad until E14.5 when NT-3 is expressed by testicular mesenchymal cells (Russo *et al.*, 1999). It may be that NTs are active in the developing mouse gonad at concentrations below the limit at which we can currently measure their presence.

In the rat, a clearer story has emerged: immunohistochemistry shows migratory mesenchymal cell expression of high affinity trkC receptors, whereas embryonic Sertoli cells express NT3 (Cupp *et al.*, 2000; Levine *et al.*, 2000a). When signaling of NT3 through its trkC receptor is inhibited by a tyrphostin inhibitor (AG879), testicular cord formation is inhibited in E13 testis organ cultures and few to no cells migrate from labeled mesonephroi to testes. Furthermore, a reduction in *SOX-9* gene expression is seen in the differentiating testis (Cupp *et al.*, 2003). These findings show the importance of NT3 as a chemotactic signal attracting mesonephric cells necessary for the establishment of testicular cords.

The human fetal testis (at 14–19 weeks' gestation) shows expression of mRNA for NGF, NT3, NT4, BDNF, high-affinity receptors trkA, trkB, trkC, and low-affinity receptor p75. Expression of NT4 mRNA and protein and p75 is localized to the peritubular cells (Robinson *et al.*, 2003).

IV. Vascular Development

A differentiating mouse testis can first be identified on E12–E12.5 by its striped appearance, due to newly formed testicular cords and blood vessels in between (Fig. 1). Especially obvious is the peripheral vessel just below the coelomic
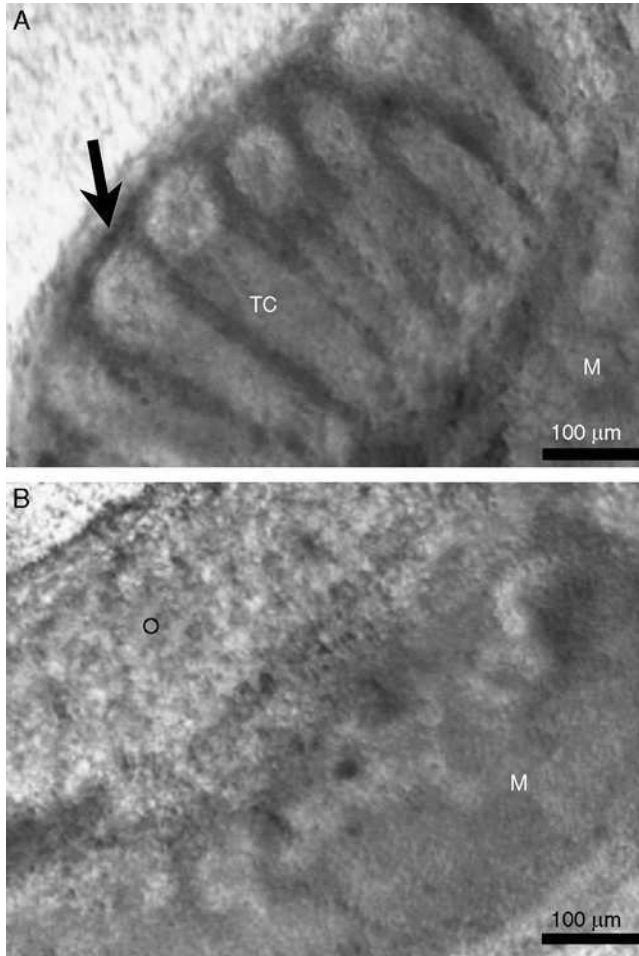
FIG. 1   Micrographs of E13.5 A male and B female urogenital complexes. TC, testicular cord, arrow indicates coelomic vessel; O, ovary; M, mesonephros.

surface, referred to by some authors as the coelomic vessel (Brennan *et al.*, 2002). The association in time between testicular cord formation and a new pattern of vasculature in the male has led authors to speculate on a possible role for vascular formation in testicular organogenesis (Brennan *et al.*, 2002; Martineau *et al.*, 1997; Merchant-Larios *et al.*, 1993). Incoming cells from the mesonephros discussed earlier (see Section III.B) include contributors to the endothelial population (Buehr *et al.*, 1993a; Martineau *et al.*, 1997; Merchant-Larios *et al.*, 1993). In fact, a large proportion of the male vasculature

(including the coelomic vessel) forms from cells that have migrated in from the mesonephros (Brennan *et al.*, 2002).

A. Vascular Endothelial Growth Factor

Despite the absence of mesonephric immigration, vascular growth occurs in the XX gonad at the same time as in the XY gonad. This does not appear to stem from assembly of new vessels from large numbers of vasculogenic precursors already present in the ovary or from increased endothelial cell proliferation (Brennan *et al.*, 2002). Expression of the endothelial-specific growth factor vascular endothelial growth factor (VEGF) shows similar levels of expression throughout the interstitial tissue of both XX and XY gonads, suggesting VEGF is involved in primary vascular growth in both sexes (Brennan *et al.*, 2002). These authors postulated that migration of endothelial cells into the XY gonad may function to increase complexity of the vasculature, perhaps to cater for rapid growth of the testis or to provide for export of testosterone. In fact, their studies with expression of the molecule Ephrin B2, which is expressed specifically in developing arteries, showed that the coelomic vessel is an artery.

B. Follistatin and *Bmp2*

The Wnt-4 gene encodes a signaling protein important in the female for suppression of Leydig cell differentiation, maintenance of postmeiotic oocyte development, and Müllerian duct development (Vainio *et al.*, 1999). In a study of $Wnt4^{-/-}$ mutant mice, the male pattern coelomic vessel was found to form by migration of endothelial cells from the mesonephros as in the male (Jeays-Ward *et al.*, 2003), indicating a function of *Wnt4* in blocking this migration in wild-type females. Two genes expressed downstream of *Wnt4* may be involved: the gene encoding the activin antagonist follistatin *(Fst)* and that encoding the bone morphogenetic protein *Bmp2*. In the XX gonad, both *Wnt4* and *Fst* are expressed in somatic cells several layers below the surface coelomic epithelium, whereas *Bmp2* is expressed in cells just below the coelomic epithelium. Neither *Fst* nor *Bmp2* are expressed in $Wnt4^{-/-}$ XX gonads between E12.5 and E14.5 (Yao *et al.*, 2004). Furthermore, in $Fst^{-/-}$ XX mutants a coelomic vessel is seen at E12.5 as in $Wnt4^{-/-}$ mutants (unfortunately $Bmp2^{-/-}$ mutants do not survive long enough to allow investigation of whether a coelomic vessel is present). These results show that although endothelial cell migration and formation of the coelomic vessel is normally XY-specific, it requires neither Sry expression nor Sertoli cell differentiation (Yao *et al.*, 2004). Although the coelomic vessel forms in

both $Wnt4^{-/-}$ and $Fst^{-/-}$ XX mutants, the branches that run from it between testicular cords in the XY gonad are not seen; this aspect of vascular development, which may play a part in testicular cord morphogenesis, must be separately controlled. A further finding of this study is that germ cells are lost by apoptosis from the ovarian cortex (as well as in the medullary region where it is normal) at E16.5 in $Fst^{-/-}$ XX mutants as in $Wnt4^{-/-}$ mutants (Vainio *et al.*, 1999). The authors suggest that the coelomic vessel could introduce new signals into the cortex which antagonize germ cell survival.

V. Proliferation

A. Germ Cells

In the past it has proved impossible to maintain isolated PGCs *in vitro* in the absence of somatic cell feeder layers (De Felici, 2000). However, a cocktail of growth factors and other compounds has been discovered which will allow the survival and proliferation of PGCs in the absence of feeder layers (Farini *et al.*, 2005). This mixture includes stem cell factor/kit ligand, leukemia inhibitory factor (LIF), FGF-2, BMP-4, and SDF-1 together with *N*-acetyl-L-cysteine, forskolin and retinoic acid.

1. Transforming Growth Factor β

Although the main effect of TGFβ is cell cycle arrest, TGFβ can either stimulate or inhibit proliferation of different cell types (Josso and di Clemente, 1999). Mouse E8.5 PGCs will increase in number during 5 div when cultured in serum-free medium conditioned by E10.5 genital ridges, but this increase in proliferation is inhibited in a dose-dependent manner when TGFβ1 is added to the medium (Godin and Wylie, 1991).

Isoforms TGFβ1, TGFβ2, and TGFβ3 are all present in the developing rat testis during fetal and neonatal life (Cupp *et al.*, 1999; Gautier *et al.*, 1994; Olaso *et al.*, 1997; Teerds and Dorrington, 1993). In a study in the rat, QRT-PCR was used to measure TGFβ expression in whole testes taken from rats ranging in age from E15 to PN30. Though the amount of mRNA for TGFβ1 was low at E15, it increased at E16, birth, and prepuberty before decreasing after puberty and into adulthood. Expression for TGFβ2 was raised at E15 then decreased through E16 and E18; there was a slight elevation from PN0 to PN4 but again expression decreased during pubertal and adult stages. TGFβ3 showed higher concentrations from E16 to PN0 and significantly lower concentrations in subsequent stages. The timing of expression of

TGFβ1 and TGFβ2 is consistent with a role in regulation of the mitotic arrest which occurs in gonocytes around E17–E18 (Cupp *et al.*, 1999).

When E13.5 rat testes were cultured for 2 div with or without TGFβ1 and TGFβ2, a concentration-dependent negative effect of TGFβ1 was exerted on the number of gonocytes (Olaso *et al.*, 1998). At 10 ng/ml the maximum reduction was reached; at this concentration TGFβ2 had the same effect as TGFβ1. TGFβs had no effect on BrdU incorporation index in either gonocytes or Sertoli cells. However, when the rate of apoptosis was measured by DNA fragmentation, using the terminal deoxynucleotidyl transferase-mediated dUTP nick end labeling (TUNEL) method, a statistically significant increase in the number of TUNEL positive gonocytes was apparent. There was no TGFβ1-induced reduction in the number of gonocytes in testes explanted on E17.5 (when germ cells were quiescent) but after mitosis had been resumed, on PN3, again a reduction was seen. Immunolocalization of type I and type II TGFβ receptors showed both receptors present in gonocytes from E13.5 through PN3 and in Leydig cells from E16.5 onward. TGFβs may directly increase apoptosis in gonocytes without affecting their mitotic activity (Olaso *et al.*, 1998).

2. Activin

Another member of the TGFβ superfamily, activin, is likely to control the coordinated development of germ cells and Sertoli cells at the onset of spermatogenesis. Gonocyte numbers are significantly increased in testis fragments from PN3 rats cultured with activin and a combination of FSH and follistatin increase the proportion of spermatogonia in the germ cell population after 3 div (Meehan *et al.*, 2000). *In situ* hybridization and immunohistochemistry on normal rat testis shows gonocytes (but not spermatogonia) express activin β_A subunit mRNA and protein. Follistatin mRNA and protein is first expressed at PN3, when gonocytes transform to spermatogonia. Germ cells may therefore regulate their own maturation by production of endogenous activin A and follistatin, aided by Sertoli cells which produce the activin/inhibin β_A subunit, the inhibin α subunit, and follistatin.

3. Stem Cell Factor

For many years it was known that two mutations in the mouse, for the *White spotting* and *Steel* genes decreased germ cell numbers (McCoshen and McCallion, 1975; McLaren, 1994; Mintz and Russell, 1957), but only comparatively recently was the reason for this discovered. The *White spotting* gene is now known to encode the c-kit tyrosine kinase receptor (Chabot *et al.*, 1988; Geissler *et al.*, 1988) and *Steel* encodes its ligand (Copeland *et al.*, 1990; Zsebo *et al.*, 1990), stem cell factor (SCF), which is also known as steel factor

and mast cell growth factor. The c-kit gene is expressed in PGCs (Orr-Urteger *et al.*, 1990) and the SCF gene along their migratory route and in the genital ridge (Matsui *et al.*, 1990). *In vitro,* SCF has been shown to be essential for survival (Dolci *et al.*, 1991) and/or proliferation of mouse PGCs (Godin *et al.*, 1991; Matsui *et al.*, 1991). It is possible that in White spotting and Steel mutants PGCs die by apoptosis (Pesce *et al.*, 1993). Proliferating PGCs die *in vitro* in the absence of somatic cell support, showing features characteristic of apoptosis, such as apoptotic bodies and high levels of tissue transglutaminase, an enzyme activated in apoptosis. Addition of SCF or LIF to cultures significantly reduced the amount of apoptosis after 4–5 h in culture although this effect was lost after longer times in culture (Pesce *et al.*, 1993).

4. Leukemia Inhibitory Factor

There is a direct stimulatory effect of LIF on PGC proliferation *in vitro* (Cheng *et al.*, 1994; Dolci *et al.*, 1993; Matsui *et al.*, 1991) and this growth factor will also aid survival of mouse PGCs cultured on feeder layers of the Sertoli cell line, TM4 (De Felici and Dolci, 1991). The low-affinity LIF receptor (LIFR) is present on the surface of PGCs and anti-LIFR antiserum abolishes PGC survival in culture (Cheng *et al.*, 1994).

5. Fibroblast Growth Factor Family

This family of heparin-binding polypeptides is composed of over 23 members (Nie *et al.*, 2006). Although SCF and LIF were found to support survival of PGCs and to allow their proliferation *in vitro,* rates of growth were only a fraction of those achieved *in vivo*. Three growth factors were found to be required for long-term culture of PGCs: SCF, LIF, and basic fibroblast growth factor (Matsui *et al.*, 1992; Resnick *et al.*, 1992), also known as fibroblast growth factor 2 (FGF2). Large multilayered clumps of cells resembling embryonic stem cells can be produced; these cells can form teratomas and contribute to chimeras (Matsui *et al.*, 1992). In a coculture system maintaining Sertoli cells and gonocytes from newborn or PN3 rats, addition of FGF2 from a concentration of 1 ng/ml significantly increased the number of gonocytes after 6 div, acting both as a survival and mitogenic factor (Van Dissel-Emiliani *et al.*, 1996).

   Localization of fibroblast growth factors and expression of their receptors has been investigated *in vivo* in the developing rat testis (Cancilla and Risbridger, 1998; Cancilla *et al.*, 2000). FGF receptors are encoded by four genes (*FGFR1*, *FGFR2*, *FGFR3*, and *FGFR4*). Each has an intracellular split tyrosine kinase domain and an extracellular domain with up to three immunoglobulin-like domains. Functional variants IIIb and IIIc arise by

alternative mRNA splicing of loop III (Cancilla *et al.*, 2000; Han *et al.*, 1993). Additional low-affinity receptors, heparin sulphate proteoglycans, are on the cell surface and form a complex with the high-affinity receptor for biological activity (Johnston *et al.*, 1995).

Expression of FGF1, FGF3, and FGF4, shown by immunohistochemistry, displays discrete cell- and stage-specific localization in the rat testis, which changes over development. Investigation of receptor expression by RT-PCR shows mRNAs for FGFR1 IIIb and IIIc (in whole testis and isolated Leydig cells), FGFR2 IIIc, FGFR3 IIIc, and FGFR4 in the fetal (E19.5), immature (PN20), and adult (PN90–PN100) rat testis (Cancilla *et al.*, 2000). Immunoreactivity for FGF1 and FGF4 is present in fetal gonocytes and Leydig cells, whereas FGF3 immunostaining is not seen in the fetal or immature testis.

Immunohistochemistry also shows FGFR2 IIIc in spermatocytes and spermatids of immature and adult testes and in Leydig cells. FGFR3 IIIb is not expressed, so the FGFR3 localized to fetal gonocytes, immature spermatocytes, and specific adult spermatocytes must be due to FGFR3 IIIc (Cancilla and Risbridger, 1998; Cancilla *et al.*, 2000). FGF3 is only found in adult testis and probably acts on elongating spermatids as does FGF4 in an autocrine fashion. The latter may also have an autocrine action on pachytene spermatocytes. Though FGF8 mRNA expression has been found at all stages examined, FGF8 protein may not be present in sufficient amounts to be immunolocalized, as it cannot be detected from E19.5 onward (Cancilla *et al.*, 2000).

In the mouse, FGF9, which plays a key role in Sertoli cell proliferation (see Section V.B.1) and differentiation (see Section VI.B.1), also acts independently to promote germ cell survival in XY but not XX gonads. Homozygous null mutant XY mice for *FGF9* show a significant reduction in gonocyte numbers by E12.5 compared with controls and E11.5 XX null mutants. Further, XY $FGF9^{-/-}$ gonads show greater numbers of dying germ cells than XY controls at E11.5, E12, and E12.5. They also fail to develop along the male pathway, subsequently expressing *follistatin* and *Bmp2* (markers of ovarian differentiation) and by E14.5 their germ cells enter meiosis as in the ovary (DiNapoli *et al.*, 2006).

6. Platelet-Derived Growth Factor

Rat testicular germ cells undergo two phases of proliferation: in the embryonic period and later at the time when they migrate from the center to the periphery of the seminiferous cord and differentiate into type A spermatogonia in early postnatal life (McGuiness and Orth, 1992). PDGF causes the proliferation of germ cells isolated from newborn and early postnatal rat testes in a dose-dependent fashion *in vitro* (Li *et al.*, 1997). A mitogenic effect

was also demonstrated in this study for 17β-estradiol, produced by Sertoli cells at high levels during the early postnatal period. However, the effects of PDGF and estradiol were not additive.

7. Neurotrophic Factors

Knockout mice for the high-affinity receptors trkA and trkC die at or shortly after birth. Heterozygotes can be mated to produce homozygote *trkA* knock-out mice that survive to PN19; these homozygotes null mutants show a 10-fold increase in germ cell apoptosis compared with germ cells in wild-type mice, although there are no differences in germ cell apoptosis during embryonic testis development (Cupp *et al.*, 2002). Testis germ cell numbers in trkA$^{-/-}$ and trkC$^{-/-}$ mice have been compared with those of wild-type mice at E13, E14, E17, and E19. When compared with wild-type testes, there are more germ cells in trkA$^{-/-}$ at E13 and E17, although numbers are lower than those in wild-type testes at E14 and E19. Germ cell numbers in trkC$^{-/-}$ mice are increased compared to wild-type mice at E17 but dramatically reduced at E19. These differences may result from changes in the expression pattern of genes controlling proliferation, apoptosis, or maturation of germ cells (Cupp *et al.*, 2002).

Experiments with human fetal testis explants cultured with the trk-specific kinase inhibitor K252a show a reduction in gonocyte and peritubular myoid cell number, but little effect on Sertoli cells (Robinson *et al.*, 2003), indicating a possible role for neurotropic factors in regulation of the proliferation and survival of germ cells and peritubular cells.

Glial cell line-derived neurotrophic factor (GDNF) is part of a family related to TGF-β now known also to include neurturin, persephin and artemin (Massagué, 1996). Both GDNF and neurturin are expressed in the developing mouse urogenital system (Golden *et al.*, 1999). Mice heterozy-gous for one GDNF null allele show a depletion of germ cell reserves (Meng *et al.*, 2000) although the gonads of *GDNF*$^{-/-}$ mice develop normally (Pichel *et al.*, 1996; Sánchez *et al.*, 1996) apart from one report of reversal in the orientation of the ovary in relation to abdominal viscera (Moore *et al.*, 1996). When a human GDNF gene is transfected to mouse Sertoli cells a dramatic amplification of germinal stem cells is seen (Meng *et al.*, 2000) and GDNF has been shown to enhance self-renewal and increase survival rates of bovine spermatogonial stem cells in culture (Aponte *et al.*, 2006).

B. Somatic Cells

A sex difference in gonadal size can be seen in E13.5 rat embryos, before histological differentiation has occurred (Mittwoch *et al.*, 1969). Similarly, after the onset of Sry expression in the mouse between E10.5 and E10.8

(Bullejos and Koopman, 2001; Hacker *et al.*, 1995) the male gonad doubles its size relative to the female within an 8-h time window (Schmahl and Capel, 2003; Schmahl *et al.*, 2000). This proliferation is critical to testis formation; when proliferation was blocked between 8 PM on E10 and 4 AM on E11, many XY gonads in each litter failed to develop testicular cords (Schmahl and Capel, 2003). Inhibition of proliferation before or after this critical period produces smaller gonads but does not block testis formation.

The male-specific increased proliferation occurs in at least two stages. Sertoli cells are produced by proliferation in SF-1 positive cells within the coelomic epithelium before the 18 tail somite stage, approximately equivalent to E11.5 (Karl and Capel, 1998; Schmahl *et al.*, 2000). Identification of cells produced during the second stage of proliferation (19–25 ts) has proved difficult, as they are not labeled with available markers, though many were labeled with the endothelial marker PECAM (Schmahl *et al.*, 2000).

Thyroid hormone plays an important role in controlling Sertoli cell number and the cyclin-dependent kinase inhibitors p27^{Kip1} and p21^{Cip1} (which regulate progression through the G1 checkpoint of the cell cycle) act as mediators of T3 effects on Sertoli cell proliferation (Holsberger and Cooke, 2005).

1. Fibroblast Growth Factor Family

Fibroblast growth factor 9 (FGF9) has been shown to be crucial to cord formation (Colvin *et al.*, 2001) and without it the gonad differentiates along the female pathway (see Section VI.B.1). *In situ* hybridization has shown a lack of expression of *Fgf9* in the developing gonad and mesonephros of E10.5 gonads of both sexes. However, by E11.5 and E12.5 *FGF9* is expressed in the XY gonad; by E12.5 it is expressed within testicular cords, whereas the region deep to the coelomic epithelium lacks expression (Colvin *et al.*, 2001).

In our laboratory an *in vitro* approach has been applied to determine the effect of FGF9 on isolated developing (E14.5) Sertoli cells in culture (Willerton *et al.*, 2004). Addition of FGF9 at a concentration of 10-ng/ml medium induces enhanced proliferation with an approximately twofold increase in cell number after 7 div. Significantly more cells were labeled with proliferating cell nuclear antigen (PCNA) in cultures treated with FGF9 compared with controls cultured in medium alone. Immunocytochemistry for the FGF9 receptor, FGFr3, showed its localization predominantly in the nucleus of cultured cells, with some cytoplasmic staining in both experimental and control cultures. *In vivo,* a temporal pattern of expression is seen with immunostaining in the E14.5 testicular cords (both Sertoli and germ cells) but is absent from interstitial tissue, mesonephros, and metanephros. By puberty, FGFr3 immunostaining is localized in spermatogonia and Sertoli cells closest to the tubule basement membrane whereas in the adult, in

which Sertoli cells do not divide, receptor expression is only seen in spermatogonia (Willerton *et al.*, 2004).

In a study of FGF9 function in mouse testis at the time of sex determination (E10.5–E12.5), *FGF9* transcripts were detected in XX and XY gonads and mesonephroi at E11.5 by both RT-PCR and *in situ* hybridization. Immunocytochemistry showed widespread expression of *FGFR1, FGFR2, FGFR3,* and *FGFR4* in most somatic cells at E11.5 in both sexes. However, *FGFR2* expression showed a sexually dimorphic pattern in that it showed nuclear localization only in XY gonads by E11, at the same time as the appearance of SOX9. Not only is SOX9 a marker of Sertoli cell differentiation, but its nuclear expression is the first sign of sex differentiation after Sry expression in the mouse (Schmahl *et al.*, 2004), so this puts FGFR2 nuclear expression at a key point in the early differentiation of Sertoli cells and male sex determination.

The nuclear expression of *FGFR3* and *FGFR2* found by Schmahl and coworkers and in our laboratory may seem anomalous at first. Traditionally the role of the receptor has been seen to transduce the signal (ligand binding) at the cell membrane into a cytosolic one, with subsequent communication involving nuclear translocation of signaling molecules such as kinases. However, there are additional mechanisms whereby ligands may be internalized with or without complexed receptors or signaling components and may translocate to the nucleus to modulate gene expression (Jans and Hassan, 1998). A number of ligands including FGF2 can associate with chromatin; nuclear ligands could alter chromatin structure and gene expression. Indeed, the induction of mitogenesis by FGF1α and FGF1β appears to be dependent on nuclear localization (Jans and Hassan, 1998). Immunofluorescence shows nuclear FGFr3 localization in cultured human breast epithelial cell lines (Johnston *et al.*, 1995) comparable to that shown in our study (Willerton *et al.*, 2004). FGFR3 may have a role in the nuclear function of FGF, a role in transporting it to the nucleus or in storage of FGF in an inactive form in the nucleus, or it may be more actively involved in mediating growth factor function (Johnston *et al.*, 1995).

FGF9 may play a part in the development of the chick gonad; there is an *FGF9* expression domain in the chick mesonephros adjacent to the gonadal primordium, where *FGFR3* is strongly expressed. At the time of gonadal differentiation *FGF9* expression decreases in the mesonephros, but appears in epithelial cells of gonads of both sexes. Misexpression of *FGF9* stimulates cell proliferation and gonadal expansion, whereas inhibition of FGFR3 causes a reduction in gonadal size (Yoshioka *et al.*, 2005).

In the perinatal rat, FGF2 is probably a survival factor for Sertoli cells. FGF2 at 1 ng/ml administered to E20, PN0, and PN3 Sertoli cells in coculture with gonocytes increases their number, but not their labeling index after 3 or 6 div (Van Dissel-Emiliani *et al.*, 1996). FGF2 from germ cells in the

adult rat can regulate Sertoli cell function, for example, in the secretion of transferrin (Han *et al.*, 1993). FGF4 from elongating spermatids may have paracrine interactions with Sertoli cells expressing FGFR4 (Cancilla and Risbridger, 1998; Cancilla *et al.*, 2000).

2. Platelet-Derived Growth Factor

PDGF is a major mitogen for mesenchymal and connective tissue cells (Gnessi *et al.*, 1997; Heldin and Westermark, 1999). Mesonephric mesenchymal cells immunomagnetically sorted by the presence of the p75 neurotrophin receptor from E12.5 male mouse embryos were shown to respond to PDGF-BB at concentrations of 50 and 100 ng/ml with a 2.5-fold increase in [^{3}H]-TdR incorporation (Puglianiello *et al.*, 2003).

Rat PMCs isolated at PN17 and treated with 1.6 nmol PDGF-AA, PDGF-BB, or PDGF-AB showed an increase in proliferation compared to controls (based on direct cell counts) with a rank order of potencies of PDGF-BB > PDGF-AB > PDGF-AA (Gnessi *et al.*, 1993). However, in a later study, cells isolated slightly later, from PN18 to PN20 rats, failed to show a proliferative response to PDGF-BB at the same dose when assessed by both direct cell counts and [^{3}H] thymidine incorporation (Chiarenza *et al.*, 2000). Rather than hyperplasia, PMCs in this study appeared to undergo initial contraction, followed by progressive hypertrophy when stimulated with PDGF-BB.

Disaggregated cells from E13.5 mouse testes showed a significant increase in both cell number and DNA synthesis when cultured for 16 h with PDGF-BB (100 ng/ml) compared with controls cultured in medium alone (Ricci *et al.*, 2004).

3. Hepatocyte Growth Factor

Cell proliferation is induced in dissociated E13.5 mouse testicular cells by HGF; a significant increase was seen in both cell number ($p < 0.001$) and DNA content ($p < 0.01$) compared with control cells cultured in medium alone (Ricci *et al.*, 2002). Because cell types were not separated in these experiments it is impossible to determine the extent of somatic cell and germ cell contribution to the proliferative effect, which was also found when cells were labeled with radioactive thymidine.

4. Transforming Growth Factor α

TGFα is a member of the epidermal growth factor family and signals through its receptor, epidermal growth factor receptor (EGFR), with effects on cell proliferation and tissue morphogenesis (Prigent and Lemoine, 1992). Growth of the embryonic rat testis is influenced by TGFα, as shown by

immunocytochemistry for proliferating cell nuclear antigen (PCNA), although cord formation is unaffected. Treatment of cultured testes with exogenous TGF-α leads to the proliferation of unorganized cells (Levine *et al.*, 2000a). In TGFα knockout mice there is no alteration in the phenotype of the testis, although when its receptor EGFR is targeted for deletion there is a transient decrease in the relative amount of interstitial cells occurs before birth. Testis growth can be inhibited by the inhibition of EGFR signaling by the EGFR kinase inhibitor. These results indicate that loss of TGFα can be compensated for by other factors (Levine *et al.*, 2000a).

5. Transforming Growth Factor β Family

a. Transforming Growth Factor β   In their study of TGFβ expression in rat testis development (see Section V.A.1), Cupp and coworkers found each isoform showed a different pattern of expression and suggested the three isoforms are differentially regulated (Cupp *et al.*, 1999). Testis organ cultures were used to investigate the functional significance of TGFβ1 in rat testis development. Urogenital complexes (each composed of a testis and attached mesonephros) were explanted at E13 and cultured on floating filters in the presence or absence of 40-ng/ml recombinant TGFβ1 over 3 days. Seminiferous cord formation was not inhibited in the presence of TGFβ1, but the overall size of the testis organ culture was reduced compared with controls cultured in medium alone. A similar reduction in testis growth was seen in E14 organ cultures. One major effect we had previously noted when explanted E12.5 and E13.5 testes were maintained for 2 or 7 days in the presence of 1-ng/ml TGFβ1, was the more spherical shape which the gonad assumed and which may have a bearing on this size reduction; microscopically there was a distinct increase in the number of cell layers of flattened fibroblasts in the tunica albuginea (Mackay *et al.*, 1995) (Figs. 2 and 3). We also observed good development of the testicular cords which showed an increase in the deposition of collagen fibrils in the extracellular matrix. To investigate the size effect further, Cupp and coworkers (1999) used a tritiated thymidine incorporation assay: PN0 testis cell cultures were treated with TGFβ alone or with positive regulators of PN0 testis growth (FSH, EGF, and 10% fetal calf serum). Treatment with 40-ng/ml TGFβ1 did not significantly alter thymidine incorporation into PN0 testis cultures compared with controls, but did inhibit EGF and FCS-stimulated thymidine incorporation into PN0 testis cultures, although not FSH-stimulated thymidine incorporation. Cultures were also subjected to quantitative RT-PCR to investigate the effects of EGF and FSH on expression of these TGFβ isoforms. Although FSH had no effect, EGF significantly stimulated expression of TGFβ1 and reduced expression of TGFβ3 compared with controls (Cupp *et al.*, 1999). In summary, TGFβ1 did not prevent cord formation but did inhibit growth of
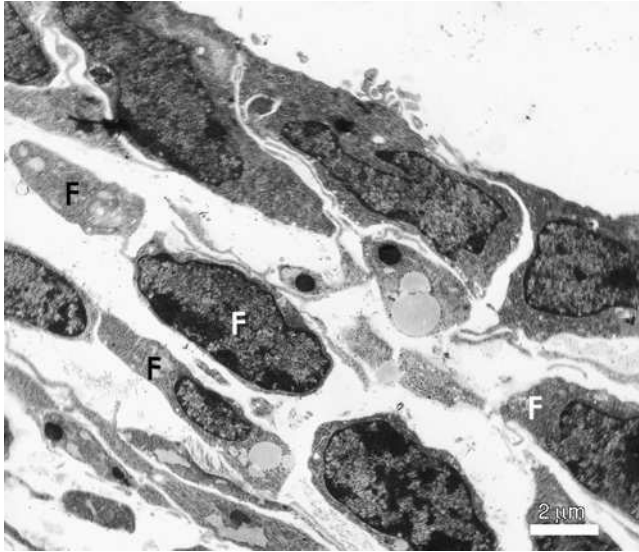
FIG. 2   Detail of tunica albuginea from control E13.5 male cultured for 7 div. Superficial layers of fibroblasts (F) are still quite rounded, below cuboidal surface epithelium.
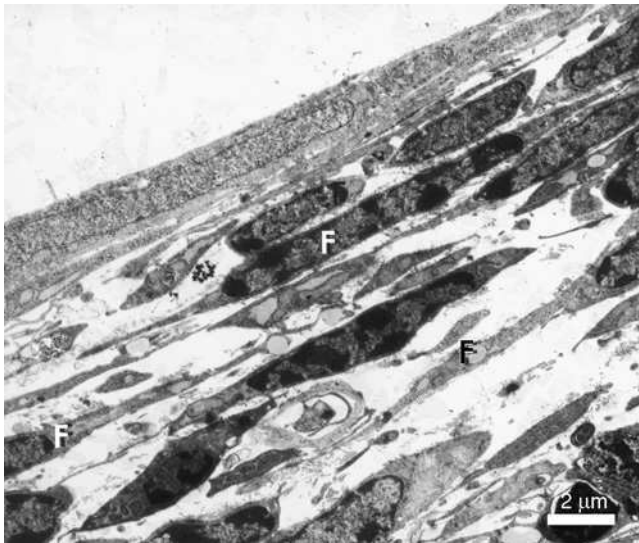
FIG. 3   Experimental male tunica is densely packed and multilayered, consisting of more flattened fibroblasts (F) below a very attenuated surface epithelium.

the testis in the embryonic and early postnatal periods indirectly, by inhibiting the effects of the positive growth factor, EGF, which in turn regulated TGFβ1 and TGFβ3 expression. It is unclear from this study which particular cell type is involved in this inhibition of growth, but the authors suggest that the dramatic reduction in testis size in cultures may result from a reduction in Leydig cell proliferation. Regulation of expression of TGFβ1 in the developing testis *in vivo* may be important both to regulate germ cell numbers initially and later to regulate somatic cell growth (Cupp *et al.*, 1999). In a subsequent study (Konrad *et al.*, 2000), the role of TGFβ2 in testicular cord formation has been highlighted (see Section VI.B.3.b).

b. Activin   Sertoli cell proliferation in cultured testis fragments from PN3 rats has been reported to be significantly increased when FSH is included in the culture medium, but reduced in the presence of activin and follistatin (Meehan *et al.*, 2000). A study using purified proliferating early postnatal rat Sertoli cells has shown that activin A acts directly on PN6 and PN9 (but not on PN3 Sertoli cells), both alone and with FSH to stimulate proliferation. *In vivo,* peritubular myoid cells may be the source of activin A, as it is secreted at high levels by cultured peritubular cells (Buzzard *et al.*, 2003).

6. Neurotrophic Factors

Glial cell line-derived neurotrophic factor (GDNF) is a distant relative of the TGF-β superfamily whose receptor GFRα1 lacks a transmembrane and cytoplasmic region and so requires a signaling component, the tyrosine kinase receptor Ret (Massagué, 1996). In the mouse, both GDNF and the related factor neurturin are expressed in the developing urogenital system from E10 to E14 (Golden *et al.*, 1999). Although both sexes express the Ret receptor and low-level expression of GFRα2, the GDFα1 receptor is highly expressed in the testis but undetectable in the ovary at E14. Although GDNF was highly expressed in the testis at E16 expression of its receptor was undetectable at that stage. Expression of GDNF in the rat testis increases during development reaching a peak at PN7 and declining thereafter (Trupp *et al.*, 1995). Because GDNF mRNA expression is also shown by the mouse Sertoli cell line, TM4 cells, the source of GDNF in the developing testis may be the Sertoli cells (Trupp *et al.*, 1995). In the rat, GDNF produces a marked stimulatory effect on Sertoli cell proliferation during the early postnatal period and an increase in ^{3}H thymidine incorporation in the presence of FSH (Hu *et al.*, 1999).

A proliferative effect on developing Sertoli cells is also seen in the mouse. Sertoli cells isolated at three stages, E12.5 (the time of cord formation), E13.5 (when gonocytes enter mitotic arrest), and E14.5 (when cords are stabilized)
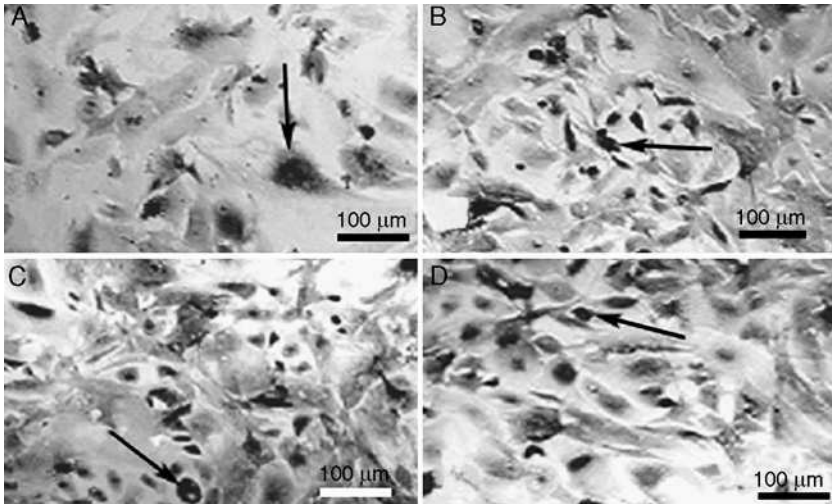
FIG. 4   Cultures of E14.5 Sertoli cells after 7 div showing immunopositive staining for PCNA: (A) DMEM alone, (B) DMEM + 1-ng/ml NGF, (C) DMEM + 10-ng/ml NGF, (D) DMEM + 100-ng/ml NGF. Arrows indicate PCNA immuno-positive cells.

and maintained for 2–7 div show a significant difference in proliferation in the presence of GDNF compared with controls (Wu *et al.*, 2005).

The neurotrophins, involved in germ cell proliferation (see Section V.A.7) may also play a part in the control of Sertoli cell proliferation. In a preliminary study in our laboratory, mouse E14.5 Sertoli cells were isolated and cultured for 7 div with or without NGF (Fig. 4). A significant increase ($p < 0.001$) in cell number was observed with NGF, at all concentrations (1 ng/ml, 10 ng/ml, and 100 ng/ml), compared with controls (Fig. 5A). Furthermore, a significant difference in proliferation as measured by PCNA immunocytochemistry was seen in cultures with NGF (at 1 ng/ml and 10 ng/ml, $p < 0.001$) (Fig. 5B).

VI. Control of Cell Phenotype/Differentiation

A. Germ Cell Control

One of the most tantalizing problems in germ cell control for many years has been the question of how entry to meiosis is controlled. An important paper has appeared on the role of retinoid signaling in this phenomenon. In an expression screen designed to identify key genes in mouse gonadogenesis, one

A   Total cell number
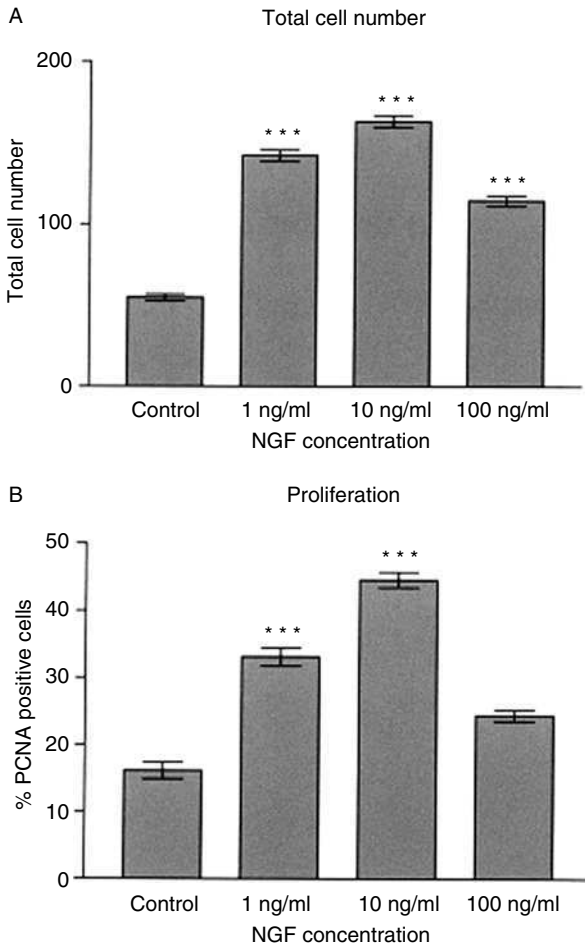
B   Proliferation

FIG. 5 Cell number estimates and percentages of proliferative cells with increasing NGF concentrations. (A) Total cell number in cultures with DMEM alone and increasing concentrations of NGF. (B) Percentage of proliferative cells in cultures with DMEM alone and increasing concentrations of NGF. *** $p = <0.001$.

gene *(Cyp26b1)* was found to become male sex-specific by E12.5 and is expressed in developing testicular cords by Sertoli cells and in some interstitial cells (Bowles *et al.*, 2006). The function of this gene is to encode a P450 cytochrome enzyme which degrades retinoic acid (RA), so the source of RA in the developing urogenital system was then investigated and found to be the mesonephroi of both male and female embryos. Using urogenital ridge organ cultures and a variety of molecular markers of meiotic progression,

exogenous RA was found to stimulate meiotic entry in germ cells, which express both RA receptors and retinoid X receptors at the right time. Evidence that CYP26B1 is the meiosis-inhibiting substance in males was provided by $Cyp26b1^{-/-}$ mouse embryos, in which testicular germ cells expressed $Sycp3$ (which encodes part of the synaptonemal complex) and $Stra8$, a premeiotic marker. Knockout ovaries showed an early meiotic progression, indicating early expression of $Cyp26b1$ may ensure female germ cells do not enter meiosis prematurely. Retinoic acid fulfills all necessary criteria to be identified as the meiosis-inducing substance; the meiosis-preventing substance appears to be an enzyme of retinoid metabolism rather than a secreted signaling molecule (Bowles *et al.*, 2006).

1. Transforming Growth Factor β Family

The importance of TGFβ family signaling in germ cell control is shown by the expression of its inhibitor, Bambi (Bmp and activin membrane-bound inhibitor). Significant expression of Bambi mRNA has been shown in the postnatal rat testis by Northern blotting and *in situ* hybridization. At birth gonocytes in the center of testicular cords show a weak or absent signal, but 5 days later spermatogonia show a readily detectable signal. In the adult rat *Bambi* mRNA and protein synthesis are predominantly seen in spermatocytes, although signal is also seen in type B spermatogonia and early elongating spermatids. Bambi is therefore likely to be involved in local regulation of TGFβ superfamily member activity in a broad spectrum of germ cell types. Sertoli cells of both immature and adult rat testis are also sources of *Bambi* mRNA (Loveland *et al.*, 2003).

a. Bone Morphogenetic Proteins Knockout mice homozygous for the null mutation of *Bmp4* have no primordial germ cells (PGCs) and heterozygotes show fewer PGCs than controls as a result of a smaller founding population. This is a result of failure of expression of *Bmp4* in the extraembryonic ectoderm prior to gastrulation, which is critical for the specification of the germ cell lineage (Lawson *et al.*, 1999). In addition, *Bmp8b* is also expressed in the extraembryonic ectoderm in pregastrula and gastrula stage mouse embryos and *Bmp8b* null mutants show a severe reduction in germ cell number (Ying *et al.*, 2000). Experiments *in vitro* have shown that BMP4 or BMP8b homodimers alone cannot induce PGC development in murine epiblasts, indicating that the two BMP pathways are required simultaneously for PGC induction. Induction of PGCs in *Bmp8b* mutants can be rescued by BMP8b homodimers but BMP4 homodimers cannot rescue PGC defects of Bmp4 null mutants; BMP4 proteins may be required for epiblast cells to gain germ-line competency before the synergistic action of BMP4 and BMP8B (Ying *et al.*, 2001).

The total number of PGCs is greatly reduced or absent in *Smad5* mutant embryos, as in *Bmp4* or *Bmp8b* mutant embryos, demonstrating that Smad5 is an important downstream signal mediator in PGC specification (Chang and Matzuk, 2001). It has also been shown that BMP4-induced PGC differentiation of PGCs from mouse epiblast *in vitro* is dependent on phosphorylated SMAD1 (Hayashi *et al.*, 2002). Although the role of BMP signaling has been shown to be essential for the differentiation of PGCs, the molecular mechanism involved is not fully elucidated. However, direct signaling from the extraembryonic ectoderm to the proximal epiblast is supplemented by an obligatory indirect BMP-dependent signal via the visceral endoderm (through ALK2, a type I BMP receptor) to induce PGC differentiation in the epiblast (Lopes *et al.*, 2004). In a study using recombinant human BMP4 on cultured mouse epiblasts *in vitro,* the ability to respond to BMP4 signals was acquired between E5.25 and E5.5. Fast acquisition of competence in the proximal epiblast may be controlled by increased expression of Smad1 and the onset of Smad5 expression induced by the extraembryonic ectoderm. Only proximal epiblast cells retain responsiveness to BMP4 for PGC formation at E6.0 and this is associated with expression of Smad5 by the proximal epiblast (Okamura *et al.*, 2005).

b. Transcription Growth Factor β   In an immunohistochemical study of TGFβ$_1$ and TGFβ$_2$ expression in rat testis development, from fetal (E19–E21) through neonatal (PN7) and prepubertal (PN21–PN35) to adult (12-week-old) stages, TGFβ$_1$ was found to predominate in spermatocytes and early round spermatids. However, as spermatids elongated, immunostaining for TGFβ$_1$ decreased and became undetectable. At the same time immunostaining for TGFβ$_2$, undetectable in spermatocytes and in round spermatids, was very intense as spermatids elongated (Teerds and Dorrington, 1993). The authors suggest two possible functions: First, TGFβ may be secreted by germ cells to act in an autocrine manner to control their differentiation. Secondly, TGFβ released from germ cells may influence neighboring Sertoli cells and may act as a chemotactic agent, either to maintain Sertoli cell cytoplasmic extensions around germ cells or to promote Sertoli cell/ peritubular myoid cell interactions (see Section VI.B.3.b). This study also showed that TGFβ$_1$ was present in Sertoli cells throughout development in the rat, with TGFβ$_1$ predominating in adult life and TGFβ$_2$ immunostaining declining after birth. A similar pattern of expression was seen in Leydig cells, but TGFβ immunoreactivity declined before puberty as TGFα immunostaining became intense. This may be related to the fact that TGFβ inhibits androgen production by Leydig cells whereas TGFα promotes steroidogenesis (Teerds and Dorrington, 1993).

c. Growth Differentiation Factor-9   This member of the TGFβ superfamily was identified using degenerate primers corresponding to conserved regions of known family members (McPherron and Lee, 1993). Although initially

reported to be absent from the testis, growth differentiation factor-9 (GDF-9) mRNA expression was subsequently discovered in the mouse, rat and human testis using Northern blot analysis, RT-PCR and *in situ* hybridization. Expression was seen specifically in large spermatocytes in the later pachytene stage of meiosis I and also in postmeiotic, immature, round spermatids (Fitzpatrick *et al.*, 1998). The role of GDF-9 in the testis is unclear; it may regulate growth and differentiation of other germ cells or Sertoli cells. However, GDF-9 knockout mice are fertile, so its activity may be compensated for by other TGFβ family members (Fitzpatrick *et al.*, 1998).

2. Leptin

A product of mature adipocytes, leptin is a 16-kd peptide hormone that acts as a growth factor in tissues from normal and diseased states (Frankenberry *et al.*, 2004). Expression of its receptor, Ob-R, was investigated in mouse testes from PN5 to PN30 and in adult testis and brain, using immunohistochemistry. In addition, RT-PCR and Southern and Western hybridization were used to investigate the presence of mRNA for Ob-R. At PN5 expression was mainly in type A spermatogonia, whereas at PN20 and PN30 expression was seen in spermatocytes. Only spermatocytes in Stages IX and X of the seminiferous epithelium cycle (stages following sperm release) showed positive expression. As leptin acts through induction of phosphorylation of STAT and mitogen-activating protein (MAP/ERK), isolated seminiferous tubules were treated with leptin and then phosphorylation of STAT3, ERK1, and ERK2 was examined. Results showed that leptin induces STAT3 phosphorylation in mouse seminiferous tubules and also ERK1, ERK2, and STAT3 phosphorylation in isolated mouse PN5 interstitial cells. The authors postulated that the different downstream results of leptin signaling in spermatogonia and spermatocytes are due to the different Ob-R isoforms expressed in these two cell types. In spermatogonial stem cells leptin may act through STS3 to prevent differentiation, allowing stem cell renewal. However, in the case of spermatocytes, leptin directs cells to full maturation into spermatids instead. The absence of Ob-R from germ cells in stages other than IX and X of the cycle in adults may be a result of negative feedback regulators from spermatids or other germ cells (El-Hefnawy *et al.*, 2000).

3. Vascular Endothelial Growth Factor

VEGF is involved in angiogenesis in embryonic development and in the mature ovary and uterus during the monthly cycle. Although there is no corresponding cyclical angiogenesis in the adult testis, a great amount of VEGF is produced by the developing testis, localized to Leydig and Sertoli cells (Ergun *et al.*, 1997; Nalbandian *et al.*, 2003). Two of three isoforms of

the VEGF receptor, VEGFR-1 and VEGFR-2 have been shown to be expressed on the surface of Leydig and Sertoli cells, suggesting an autocrine function of VEGF in the testis (Ergun *et al.*, 1997). In an immunohistochemical and RT-PCR study of the adult mouse testis, strong immunofluorescence for VEGF was seen in interstitial tissue and staining was also observed in Sertoli cells (Nalbandian *et al.*, 2003). In the immature (PN6) mouse testis strong expression of VEGF was observed in Sertoli cells and VEGFR-1 immunostaining was strong in the interstitial cell population, but was absent from Sertoli cells in this study. Expression of VEGFR-2 within tubules was localized to type A spermatogonia at this time. Interstitial tissue showed colocalization of VEGF and VEGFR-2. Immunostaining for VEGFR-2 was not maintained in the adult testis, although interstitial cells still showed strong immunofluorescence for VEGFR-2. However, the adult testis showed strong immunofluorescence for VEGFR-1 in round spermatids and spermatozoa. Although VEGFR-2 mRNA expression was seen in type A spermatogonia, there was none in pachytene spermatocytes and round spermatids. However, VEGFR-1 mRNA was expressed in the more advanced forms (pachytene spermatocytes and round spermatids) but not in type A spermatogonia. Moreover, expression of VEGFR-1 and VEGFR-2 is inversely correlated during postnatal development of the mouse testis; VEGF produced by Sertoli cells probably exerts a differential effect on proliferation or differentiation based on the receptor subtype expressed during spermatogenesis (Nalbandian *et al.*, 2003).

4. Neurotrophic Factors

GDNF is said to be essential for regulating the fate of stem cells during spermatogenesis (Sariola, 2001), contributing to the paracrine regulation of spermatogonial self-renewal in the mouse (Meng *et al.*, 2000). The spermatogonia of mice overexpressing GDNF are unable to differentiate, showing a spermatogonial phenotype (Creemers *et al.*, 2002; Meng *et al.*, 2000). Expression of the receptor *GFRα-1* could be used as a marker for undifferentiated type A spermatogonia (Dettin *et al.*, 2003).

B. Sertoli Cell Control/Testicular Cord Formation

1. Fibroblast Growth Factor 9

In a study of a targeted disruption of *FGF9* in the mouse embryo, of 24 E18.5 *FGF9*$^{-/-}$ embryos examined, 22 had female internal organs (although one showed epididymal-like tissue as well); of the two phenotypically male knockouts, both showed hypoplastic testes with reduced mesenchyme (Colvin *et al.*, 2001). Ten of 14 phenotypic females proved to be XY on sex genotyping.

Immunohistochemistry for AMH and *in situ* hybridization for cholesterol side-chain cleavage (SCC) cytochrome p450 showed that Sertoli and Leydig cells respectively failed to develop or were lost in most $FGF9^{-/-}$ XY gonads. Two $FGF9^{-/-}$ XY gonads examined in thin sections showed cell clusters rather than testicular cords; these lacked peritubular myoid cells and showed mesenchymal depletion (Colvin *et al.*, 2001). These results show a clear role for FGF9 in stimulating Sertoli cell differentiation and cord formation. Effects on cord formation may result from depletion of mesenchyme and peritubular myoid cells.

When isolated E14.5 mouse Sertoli cells are cultured with extracellular matrix (ECM) gel and Fgf9 at a concentration of 10-ng/ml culture medium, increased proliferation and cordlike aggregation of the cells is seen, with appositional contact of adjacent cell membranes (Willerton *et al.*, 2004). Extracellular matrix includes heparin sulphate proteoglycans that act as low-affinity receptors for FGFs and are required to activate FGFRs (Lin *et al.*, 1999; Rapraeger *et al.*, 1991; Schmahl *et al.*, 2004; Yayon *et al.*, 1991). Control cells cultured in medium alone proliferate and attach, but only show minor aggregations (Willerton *et al.*, 2004).

Proliferation may be induced in the coelomic epithelium in cultured E11.2–E11.5 XX gonads by FGF9 at 50 ng/ml for 36 h, but this is not sufficient for Sertoli cell differentiation and cord formation, indicating that increased proliferation alone is insufficient for Sertoli cell differentiation (Schmahl *et al.*, 2004).

2. Platelet-Derived Growth Factor

The receptor PDGFR-α can bind PDGF-A, PDGF-B, and PDGF-C homodimers and PDGF-AB heterodimers. In a study of *Pdgfr-α*$^{-/-}$ mice, E12.5 XY gonads failed to develop normal testis cords and interstitial tissue. A coelomic vessel was present, but showed fewer branches between forming testis cords compared with vessels in control gonads. In a quarter of *Pdgfr-α*$^{-/-}$ mice examined (n = 8), the coelomic vessel was also itself defective. Testis cord formation was delayed; cords had formed by E13.5 but were reduced in number and abnormal in shape (being large and dilated) in *Pdgfr-α*$^{-/-}$ mice (Brennan *et al.*, 2003). The role of PDGF-BB in testis cord formation was further investigated using a battery of techniques including immunolocalization of PDGF-BB and PDGF receptors α and β subunits; organ culture approaches utilizing laminin detection, cell migration assay, and reaggregation; Western blot analysis and DNA assay (Ricci *et al.*, 2004). Immunolocalization of PDGF-BB was seen at a low level in E11.5 male mouse urogenital ridges; at this time, PDGFR-β subunit positive staining was stronger and restricted to the coelomic epithelium and mesonephric mesenchyme. The PDGF-α subunit was seen at low levels in some coelomic

epithelial cells, at the mesonephros-gonad boundary and less strongly in the mesonephric mesenchyme. Two days later in development, PDGF-BB appeared in the interstitial compartment, though weakly positive in a large number of cells. Immunostaining for the PDGFR-β subunit was strong in the coelomic epithelium over the genital ridge, in interstitial cells, and in peritubular cells. Positive staining for the PDGFR-α subunit was less evident. Male E11.5 urogenital ridges were cultured in medium alone or medium supplemented with PDGF-BB or HGF. Undifferentiated male gonads formed cords in the presence of PDGF-BB, although these were smaller in size than cords formed in the presence of HGF (Ricci *et al*., 2004).

Immunohistochemistry demonstrated the presence of laminin in basement membranes around cords. High doses of the PI3K inhibitor LY294002 totally inhibited cord formation. When disaggregated E13.5 testes were plated on Matrigel-coated dishes and cultured in the presence or absence of PDGF-BB at 100 ng/ml, a different reorganization was seen in the presence of growth factor. Larger aggregates were formed, showing a star-shaped structure rather than the cordlike structures formed following HGF treatments as shown in previous experiments by the same group (Ricci *et al*., 2002). Once again LY29400 inhibited reaggregation in a dose-dependent manner. The role of this PI3K inhibitor was first investigated in the developing rat testis, where it was also shown to block cord formation or to reduce the number of testis cords in a dose-dependent manner in E13 testes *in vitro* (Uzumcu *et al*., 2002b). The rationale for its investigation was that the PI3K signal transduction pathway is common to growth factors implicated in testis cord formation, such as NT3, HGF, FGF-9, and PDGF.

3. Hepatocyte Growth Factor

HGF signaling acts via its receptor c-met to induce epithelial morphogenesis during lung development (Ohmichi *et al*., 1998). To investigate the role of HGF in mouse testis tubulogenesis (the transition from solid testicular cords to hollow seminiferous tubules), which normally occurs in postnatal life at the same time as the development of Sertoli-Sertoli tight junctions (Russell *et al*., 1989), culture experiments were carried out using both isolated primary Sertoli cells from prepubertal mice and an immortalized Sertoli cell line, SF7, established from a PN10 mouse testis (van der Wee and Hofmann, 1999). After 5 div on a Matrigel substrate in culture medium supplemented with 10% fetal calf serum, SF7 cells formed a three-dimensional (3-D) network, which proved to be tubular after sectioning. Various growth factors known to be present in Matrigel or serum were investigated; at a concentration of 5-ng/ml HGF both SF7 cells and primary Sertoli cells formed tubular structures, although higher concentrations caused detachment of cells. Immunocytochemistry showed strong expression of the c-*met* receptor in

both cultured SF7 cells and PG3 peritubular cells. A possible role *in vivo* was confirmed by reverse transcriptase-polymerase chain reaction (RT-PCR) which showed that the HGF gene is transcribed at low amounts in the postnatal and adult testis (van der Wee and Hofmann, 1999). These authors speculated that HGF might be itself regulated by basic fibroblast growth factor (bFGF) as in cultured human mesenchymal cells (Roletto *et al.*, 1996), and that TGF-β produced by PMCs might be involved in tubule formation by inhibiting HGF-stimulated branching morphogenesis as in cultured kidney-derived cell lines (Sakurai and Nigam, 1997).

Expression of the HGF receptor, c-*met*, was also shown by *in situ* hybridization in embryonic male gonads at E12.5, when testis cords first appear. A day earlier expression was restricted to the mesonephros, and at E13.5 higher expression was seen in testicular cords (Ricci *et al.*, 1999). In culture experiments, serum addition was found to be essential for testis differentiation from indifferent urogenital ridges, but HGF added alone to culture medium in the absence of serum was sufficient to allow cord development (Ricci *et al.*, 1999). However, others have found mouse testis differentiation can proceed in the absence of serum *in vitro* from the indifferent stage (Mackay and Smith, 1986, 1989).

Northern blot analysis showed strong male-specific expression of HGF in E13.5 and E15.5 mouse testes. Immunohistochemistry was used to determine the precise localization of expression, which was found in cells of the tunica albuginea, the interstitial compartment, and in peritubular myoid cells. Expression was seen in the coelomic epithelium and in small groups of cells within the genital ridge in E11.5 male urogenital complexes; strong expression was also seen in the mesonephric mesenchyme (Ricci *et al.*, 2002). Culture experiments showed that dissociated E13.5 testes formed cordlike structures in the presence of HGF (5–100 U/ml). At the highest dose of HGF 3-D networks were formed on the Matrigel substrate; these cords were longer and wider than those occasionally observed in control cultures (Ricci *et al.*, 2002).

4. Transforming Growth Factor β Superfamily

a. Anti-Müllerian Hormone   When rat prospective ovaries are explanted at E14 and cultured for 3–7 div with purified bovine AMH, there is a decrease in gonadal volume, germ cell depletion and differentiation of cells resembling rat fetal Sertoli cells (Vigier *et al.*, 1987). Sertoli cell differentiation may simply be a result of the germ cell depletion, because follicle cells can transdifferentiate as Sertoli cells if germ cells are lost after entry to meiosis (MacIntyre, 1956; McLaren, 1991). *In vivo,* AMH is first expressed in mouse pre-Sertoli cells at E12.5, when testicular cords are forming. Expression declines between 2 and 3 weeks postnatally, at the time when male germ

cells enter meiosis, suggesting a role for AMH in control of entry to meiosis (Münsterberg and Lovell-Badge, 1991). This is also the time of development of the blood-testis barrier, which results in a higher AMH concentration in the seminal plasma than in blood (Rey *et al.*, 2003). Further, laminin α-5 reappears at this time in the basement membrane of the seminiferous tubules (Pelliniemi and Fröjdman, 2001).

Transgenic "knock-in" mice have been produced that chronically express human AMH under the control of the mouse metallothionein-1 promoter (Behringer *et al.*, 1990). Müllerian duct differentiation was inhibited in females chronically expressing AMH, no uterus or oviducts were seen and at birth the ovaries had a reduced number of germ cells. These germ cells were subsequently lost over the first 2 postnatal weeks and the somatic cells reorganized into structures resembling seminiferous tubules, which had disappeared in adult females. Although the majority of transgenic males developed normally, in the two lines with the highest levels of AMH expression some males showed impairment of mesonephric duct development, undescended testes with no germ cells, and feminization of the external genitalia (a vaginal opening and mammary gland development). These results may be explained by the fact that high levels of AMH affect Leydig cell development in the testes of these animals, resulting in inhibition of androgen biosynthesis. Similarly, human recombinant AMH has been shown to inhibit LH-stimulated testosterone production by fetal rat Leydig cells *in vitro*, in a dose-dependent manner (Rouiller-Fabre *et al.*, 1998). Regarding failed testicular descent in AMH transgenic males, the first phase of testis descent is androgen-independent, controlled instead by AMH; high levels of AMH may lead to a downregulation of its receptor on cells controlling testis descent (Behringer *et al.*, 1990).

Ovarian development could occur when AMH levels were sufficient to inhibit Müllerian duct development, suggesting that a higher level of expression is required for the ovarian effect (Behringer *et al.*, 1990). Further evidence for this idea was provided earlier when E14.5 rat ovaries were cultured with medium conditioned by the preliminary culture of testes from young or fetal rats. In these ovaries follicles were rare, germ cell degenerated, and cords like seminiferous cords developed. Bioassay culture of genital ducts with transformed ovaries showed AMH was produced, but no germinostatic activity (i.e., suppression of oogonial proliferation) on cocultured E13.5 ovaries was seen (Prépin and Hida, 1989), as is exerted by isolated fetal testis seminiferous cords (Prépin *et al.*, 1985). Perhaps sufficient AMH was generated from transformed ovaries for the anti-Müllerian effect, but not enough for the germinostatic effect. In our own work in the mouse, we have observed a loss of germ cells in E12.5 ovaries cocultured with Sertoli cells isolated at the same age, with no evidence of the remaining germ cells entering meiosis (Mackay *et al.*, 2004b). If ovaries were explanted a day
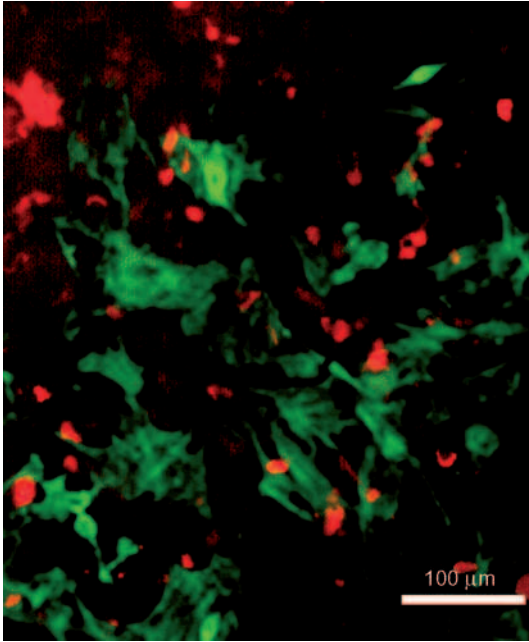
FIG. 6 Mouse Sertoli cell culture after 7 div in the presence of 10-ng/ml GDNF. Immunofluorescence for AMH (red), a marker for Sertoli cells and for α-smooth muscle actin (green), a marker for peritubular myoid cells.

later, however, meiotic germ cells survived when cultured together with Sertoli cells although the ovigerous cords did display signs of masculinization. The presence of AMH (Fig. 6) was demonstrated in our Sertoli cultures by immunocytochemical labeling (Mackay *et al.*, 2004b).

b. Transforming Growth Factor β To investigate the functional role and possible involvement of TGFβ2 in mediating epithelial/mesenchymal interactions in the developing rat testis, TGFβ2 secretion *in vitro* in monocultures and cocultures of PN19 (mesenchymal) peritubular cells and (epithelial) Sertoli cells has been determined, using a highly sensitive ELISA (Konrad *et al.*, 2000). Peritubular myoid cells and cocultures secreted increasing amounts of TGFβ2 in the first week of culture, although Sertoli cell secretion was only marginal. The total amount of TGFβ2 in cocultures on the first 2 days was similar to that of peritubular cell cultures, but became reduced from 3 div. Newly synthesized TGFβ cannot interact with TGFβ receptors until it has been activated by proteolytic cleavage. Secretion of bioactive TGFβ2 was highest in cocultures and showed a small peak on day 2,

probably preceding the formation of Sertoli cell aggregates, which appeared after 3 div. Sertoli cell aggregation or tubule formation was increased by a factor of two after stimulation with recombinant TGFβ2 in comparison with monocultures. These results, together with the fact that TGFβ2 has been found in other regions of active morphogenesis involving epithelial-mesenchymal interactions (Konrad *et al.*, 2000; Millan *et al.*, 1991), support a similar role in the developing testis; TGFβ2 may mediate the Sertoli cell/peritubular myoid cell interactions that underlie cord formation.

5. Neurotrophic Factors

A reduction in testicular cord number is seen in trkC knockout mice at E14 and in cord area at E19; similarly trkA knockouts show a reduction in cord number at E14. Further, in both trkA and trkC knockout mice development is delayed at E13 (Cupp *et al.*, 2002).

a. Neurotrophins   The role of neurotrophins in testicular morphogenesis has been investigated in the rat (Levine *et al.*, 2000a), in which organ cultures have been treated with an inhibitor (K252a) to the high-affinity receptor, trk. In cultures explanted at E13 (i.e., prior to cord formation in the rat), testicular cord formation is completely inhibited, whereas no alteration is seen in cultures explanted at E14 when cords are already present. Null mutant mice for *NT3* show normal morphology at both E15 and E17 as do *trkC* null mutants. However, both mutants show less interstitial tissue than wild-type animals, which may be a result of impaired migration from the mesonephros (see Section III.B.4). Expression of the low-affinity neurotrophin receptor p75/LNGFR is seen in E13 gonads of both sexes and then around cords in the testis alone at E14, although expression reappears in the ovary at the time of follicle development from E16 to E19 (Levine *et al.*, 2000a).

b. Glial Cell Line-Derived Neurotrophic Factor   Mouse Sertoli cells isolated at E13.5 and cultured in extracellular matrix-coated wells form obvious cordlike aggregations after 48 h; when cells are isolated at E12.5, the time of cord formation *in vivo,* aggregation of Sertoli cells (showing apposition of cell membranes at more than one surface) is observed after only 1 div. Fewer cordlike aggregations are seen in the absence of exogenous GDNF (Wu *et al.*, 2005).

C. Leydig Cell Control

The signaling molecule *Desert hedgehog (Dhh)* expressed by Sertoli cells is necessary for Leydig cell differentiation (Clark *et al.*, 2000; Yao *et al.*, 2002). Evidence from double mutants for the orphan nuclear receptors *Sf1/Dax 1*

suggests they function cooperatively to enhance *Dhh* expression (Park *et al.*, 2005). Fetal Leydig cell markers (*Cyp17* and *Cyp11a1*) show reduced expression in heterozygous *Sf1*-deficient mice at E13.5, consistent with dose-dependent effects of *Sf1*, similar to those seen in humans (Achermann *et al.*, 2002).

1. Platelet-Derived Growth Factor

Homozygous mutant mice for the gene encoding PDGF-A die postnatally of pulmonary failure, but some individuals survive long enough for effects on the testis to be studied. Null mutant mice weigh less than wild-type litter-mates and show an even more pronounced testicular size reduction. Numbers of Leydig cells are progressively reduced in the postnatal period, being almost completely absent by PN42. A lack of both bromodeoxyuridine (BrdU) labeling and TdT-mediated dUTP biotin nick end labeling (TUNEL) show the low number of Leydig cells is likely a result of proliferation arrest rather than an increase in apoptosis (Gnessi *et al.*, 2000). The authors suggest that in the absence of PDGF-A the normal pubertal replacement of the fetal Leydig cell population by adult cells is deranged as adult Leydig cell precursors fail to proliferate and differentiate. The ensuing reduction in testosterone would then cause the spermatogenic arrest and germ cell degeneration seen in the mutant mice.

In their study of *Pdgfr-α$^{-/-}$* mice (see earlier), Brennan *et al.* (2003) found that expression of the Leydig cell-specific marker P450 side chain cleavage (*Scc*) was at much lower levels (if expressed at all) in *Pdgfr-α$^{-/-}$* mice compared with wild-type controls, reflecting impaired development of the fetal Leydig cell population. In coculture experiments using gonads and GFP-labeled mesonephroi, when the gonad was *Pdgfr-α$^{-/-}$* there was no Leydig cell differentiation, even if the mesonephros was wild-type. Because *Dhh* signaling is necessary for fetal Leydig cell development (Yao *et al.*, 2002), *Dhh* and *Pdgfr-α* and *Pdgf-A* expression were investigated by *in situ* hybridization. Although wild-type E11.5 gonads show *Dhh* expression, none was seen in *Pdgfr-α$^{-/-}$* mice at this time. However, by E12.5 *Dhh* expression in *Pdgfr-α$^{-/-}$* mice was similar to that in controls although expression of the *Dhh* receptor *Ptch1* was still reduced at E13.5. Because *Ptch1* is upregulated in cells exposed to DHH, *Pdgfr-α* may act with *Dhh* to promote the expansion and/or differentiation of *Ptch1*-positive cells. This could be a result of defects in proliferation changing the number of *Ptch1* precursor cells, or less directly through structural and endothelial defects in *Pdgfr-α$^{-/-}$* gonads interfering with the cues needed to specify Leydig cell fate (Brennan *et al.*, 2003). An attempt was made in this study to alter the differentiation of XX gonads; although exogenous PDGF could induce migration and upregulation of *Pdgfr-α* in XX gonads *in vitro,* Leydig cell differentiation was not seen.

The authors speculate that this could be due to the presence of female factors repressing Leydig cell development such as WNT4, which has been shown to repress steroid cell development in the developing ovary (Vainio *et al.*, 1999).

2. Fibroblast Growth Factors

In an immunohistochemical study to investigate expression of FGF receptors (FGFRs) in the rat testis, a change in expression of FGFRs was found in the fetal Leydig cell and during development of the adult Leydig cell population. Both adult and fetal Leydig cells express FGFR-1, but immature adultlike Leydig cells differ in also expressing FGFR-2, FGFR-3, and FGFR-4. However, adult Leydig cells do not express FGFR-3, which may therefore be a specific functional requirement for the immature adultlike Leydig cell population (Cancilla and Risbridger, 1998).

D. Peritubular Myoid Cell Control

1. Platelet-Derived Growth Factor

When PMCs are isolated from 17-day-old rats and cultured *in vitro* in serum-free medium, they assume a round shape and are small in size, although they still express PMC markers such as desmin and vimentin. At isolation they do not show PDGF-binding sites, although after a day *in vitro* in serum-free conditions, high-affinity PDGF receptors induced by cell culturing can be detected. If then treated with 1.6-nmol PDGF-AA, PDGF-BB, or PDGF-AB, the cells show a fibroblast appearance with elongated slender processes and retracted cell bodies, that is, they regain their characteristic PMC phenotype. Expression of the PMC structural phenotype is accompanied by functional activity, because PDGF also increases the release of matrix components: type IV collagen and fibronectin (Gnessi *et al.*, 1993). Smooth muscle α-actin (Smα-actin) filaments become reorganized as stress fibers after 24 h stimulation with PDGF-BB; morphological changes and altered distribution of Smα-actin within PMCs are seen at a PDGF concentration as low as 10 ng/ml (Chiarenza *et al.*, 2000).

To test the hypothesis that PDGFs and PDGFRs are expressed during testicular cord formation and that inhibition of their action influences normal cord development, rat embryonic testis cultures were cultured for 3 days with PDGFR-specific tyrosine phosphorylation inhibitors (the tyrphostins, AG1295 or AG1296). Tyrphostin-treated testes formed abnormal swollen and fused cords, perhaps as a result of an alteration in mesonephric cell differentiation (Uzumcu *et al.*, 2002a), to form peritubular myoid cells.

2. Neurotrophins

Precursors of the peritubular myoid cell population can be identified by the presence of the low-affinity p75/NTR neurotrophin receptor. They can be isolated from E12.5 mouse mesonephroi and will differentiate *in vitro* to peritubular myoid cells. Immunohistochemistry shows a progressive occupation of the interstitial tissue by p75/NTR positive cells between E10.5 and E12.5 and postnatal testis sections show peritubular cells coexpressing p75/NTR and/or smooth muscle actin (Campagnolo *et al.*, 2001).

VII. Experimental Manipulations *In Vitro*

The existence and role of putative growth factors in testis differentiation has been investigated by a variety of experimental techniques *in vitro*. Culture systems allow continued development while environmental conditions are varied to investigate possible effects on differentiation. There are certain limitations however: if gonads are removed from a mouse embryo on E10 they will not differentiate, even with serum present (Taketo and Koide, 1981). If gonads are removed a day later on E11 serum must be added to the culture medium to allow differentiation *in vitro,* but from E12 onward gonads will continue to grow in culture medium without serum, differentiation being directed by their genetic sex (Taketo *et al.*, 1986). There is no qualitative morphological or functional difference between differentiation achieved *in vitro* compared with that *in vivo,* although there is a slight delay *in vitro,* presumably a result of the trauma of explantation (Mackay and Smith, 1989).

Different culture systems have been utilized to test the effect of male factors on female gonads and vice versa. Byskov and Saxén (1976) used a transfilter approach in an attempt to test the presence of diffusible factors. They reported the induction of meiosis in genetically male indifferent (E11) gonads by older (E14) ovaries separated from them by a Nuclepore filter. When older testes (E14) and ovaries of the same age were cultured together but separated by a filter, meiotic germ cells present in the ovary were arrested before entering the diplotene stage. The authors argued for the existence of meiosis-inducing and meiosis-preventing substances produced by the female and male gonads respectively. However, the interpretation of this experiment was qualified by a later demonstration that microscopical cell processes could cross the filter (Lehtonen *et al.*, 1975; Saxén *et al.*, 1976). Burgoyne and coworkers also used a transfilter approach to culture E11.5 XX and XY indifferent mouse gonads together, and concluded differentiation proceeded according to genotype. However, as these authors pointed out, the development of the embryonic

testes was poor, so the absence of a masculinizing influence was not entirely convincing (Burgoyne *et al.*, 1986). In our laboratory we cultured indifferent E11 mouse gonads together in mixed sex groups for up to a week and found no inhibition of one sex by the other; however, on the whole ovaries developed further in culture than testes (Mackay and Smith, 1986). This lack of either meiotic triggering or inhibiting effects may be explained by the fact that such factors act within a limited radius of activity.

More than thirty years have elapsed since Byskov and Saxén proposed the existence of meiosis-inducing and meiosis-preventing factors. A prevailing view has been that all germ cells are programmed to develop as oocytes, with the timing of meiotic entry a cell-autonomous event rather than an induced response (McLaren, 2003; McLaren and Southee, 1997; Ohkubo *et al.*, 1996), obviating the need for a meiotic-inducing factor. Female germ cells of E12.5 or younger can be inhibited from entering meiosis if aggregated with E12.5 male genital ridge cells, indicating that entry to the spermatogenic pathway is an induced response (Adams and McLaren, 2002), dependent on a meiotic inhibitor. When E11.5 mouse male genital ridges are cultured without their associated mesonephroi, germ cells develop as prespermatogonia even though the differentiated Sertoli cells do not enclose them in cords (Buehr *et al.*, 1993b). This finding suggests the meiotic-inhibiting factor may be produced by the Sertoli cells, but does not depend on enclosure of germ cells within cords. Possible candidates have been identified (McLaren, 2003) as prostaglandin D2 (Adams and McLaren, 2002) and the product of a novel gene, *Tdl* (testis-specific β-defensin–like gene). The latter shows Sertoli cell-specific expression and sequence homology to the antimicrobial peptides β-defensins (Yamamoto and Matsui, 2002). However, a paper cited earlier (see Section VI.A) shows that there is indeed a meiosis-inducing factor, retinoic acid, and it is controlled by an enzyme of retinoid metabolism, CYP26B1, the most likely meiosis-preventing substance (Bowles *et al.*, 2006).

A body of work has been carried out in the rat using a variety of *in vitro* techniques to investigate the role of AMH (see Section VI.B.3.a). When E14.5 rat ovaries are cultured on either side of a single E17.5 testis masculinization of the ovary is produced, with the presence of testicular cords and AMH production, but only if the gonads are in contact and only when E17.5 testes (which exhibit a strong Müllerian-inhibiting activity) are used (Charpentier and Magre, 1990). These results suggest a role for AMH in functional masculinization of fetal ovaries *in vitro* in the rat; however, the possibility that testicular cells have simply migrated into the ovaries cannot be excluded. A further finding to emerge is that a "germinostatic" factor different from AMH is produced by fetal or postnatal rat testes and reduces the number of germ cells in E13.5 ovaries after 4 div (Charpentier and Magre, 1989; Prépin *et al.*, 1986) or in E14.5 ovaries after 12 div (Prépin and Hida, 1989).

The culture environment of explanted gonads may be manipulated in a number of experimental paradigms. One with which we have generated some interesting results is the maintenance of either ovaries or testes, from a number of different developmental ages, in medium which has been previously conditioned by the presence of gonads from the opposite sex. When E13 ovaries were cultured for 4 days in medium which had been conditioned for 2 days previously by the presence of E13 testes (generating E13–E15 testis-CM) the mean number of oocytes in the explanted ovaries had dropped by nearly 50% (713 ± 177 as opposed to 1218 ± 166 in cultured control explanted ovaries, $p < 0.05$); this germinostatic effect, similar to that reported for the rat (see earlier) was eliminated if the testis-CM was heat-inactivated (Tavendale *et al.*, 1992). Germ cells were shown by TEM to have reached a meiotic equivalent to the E17 stage, so that although numbers were reduced those surviving continued to differentiate along the female path. It was proposed that AMH might be a candidate causing this, especially as our later work demonstrated that E12.5 (although not E13.5) ovaries maintained in the presence of Sertoli cells isolated at a time when they are producing AMH showed a similar effect (Mackay *et al.*, 2004b). Electrophoretic analysis of the testis-CM however, demonstrated the presence of proteins (absent from E13 to E15 ovary-CM) with molecular weights higher than that of AMH (140 kDa), indicative that other putative factors were responsible (Tavendale *et al.*, 1992). In parallel experiments testes were cultured in ovary-CM for similar time periods. In E13.5 and E14 testes maintained in E15–E17 ovary-CM there were no signs of germ cells entering meiosis (Fig. 7), but a significant reduction in the area occupied by the testicular cords in experimental, compared to control, cultured testes was evident (29.7 ± 1.32% in experimental testes compared to 22 ± 1.23 in gonads maintained in normal unconditioned medium $p < 0.05$). There was a concomitant increase in the amount of interstitial tissue, whereas in the cords small Sertoli cells with irregularly shaped nuclei were located peripherally enclosing the large pale germ cells (Figs. 8 and 9). The Wolffian Duct was well maintained in experimental E14 testes cultured in E15–E17 ovary-CM, however the Müllerian duct showed typical signs of involution (Fig. 10).

Another useful technique is that of disaggregation/reaggregation which can be applied to test the importance of control factors in differentiation. Cells have been disaggregated from newborn rat testes and allowed to reaggregate in rotation cultures where they reaggregated to form testicular tissue after 25 hours (Grund *et al.*, 1986). A disaggregation-reaggregation culture technique has also been used to show the E11.5 male genital ridge produces a factor inhibiting germ cell entry to meiosis; prior disaggregation of the genital ridge impairs cord formation at this stage (although not at E12.5) and disrupts its production (McLaren and Southee, 1997). Mouse gonads dissociated at
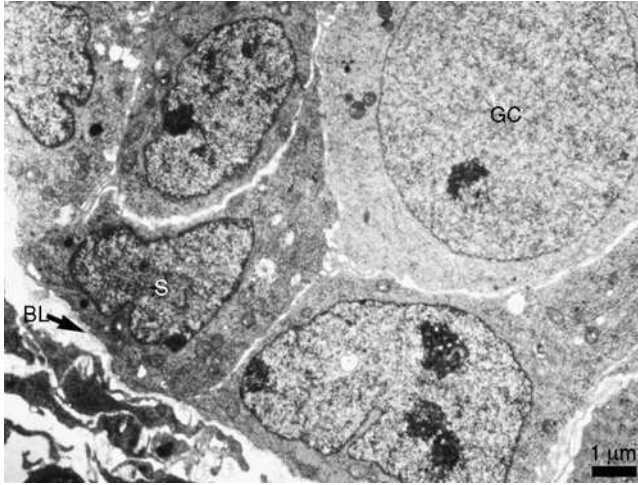
FIG. 7   Electron micrograph of experimental E14 testis cultured for 4 div in E15–E17 ovary-CM shows detail of testicular cord. Centrally located germ cell (G) shows no evidence of meiosis. A basal lamina (arrow) is present around the developing testicular cord.
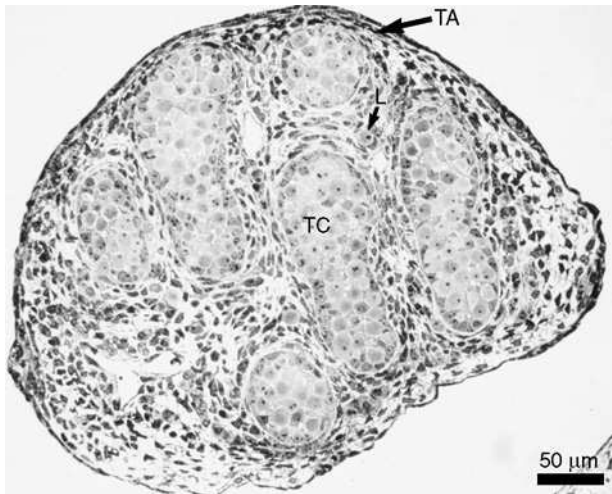
FIG. 8   E14.5 control testis cultured 4 div. Note tunica albuginea (TA), well-organized testicular cords (TC) with centrally placed germ cells and developing Leydig cells (L) within the interstitium.

E13.5–E14.5 will reorganize *in vitro* but their reaggregation is prevented by the inclusion of antibodies to laminin or the α6 subunit of its integrin receptor (Pesce *et al.*, 1994). In our laboratory a similar approach has been used to show
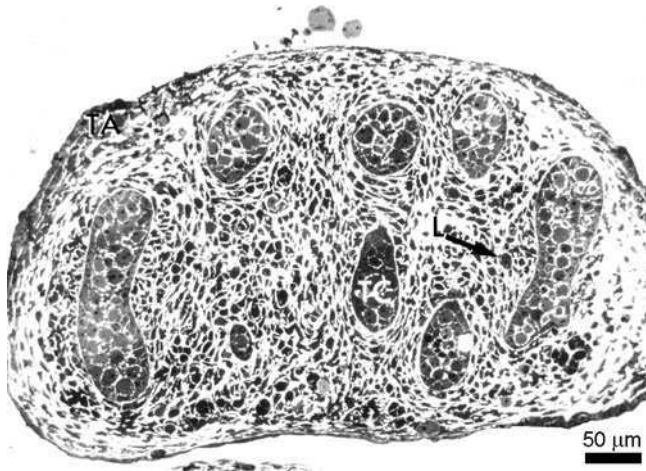
FIG. 9   Testis removed at E14 and cultured for 4 div in E15–E17 ovary-CM. Tunica albuginea is present (TA). Testicular cords appear reduced in size and interstitial tissue increased in volume. Differentiated Leydig cells (arrow) lie within the somatic tissue.
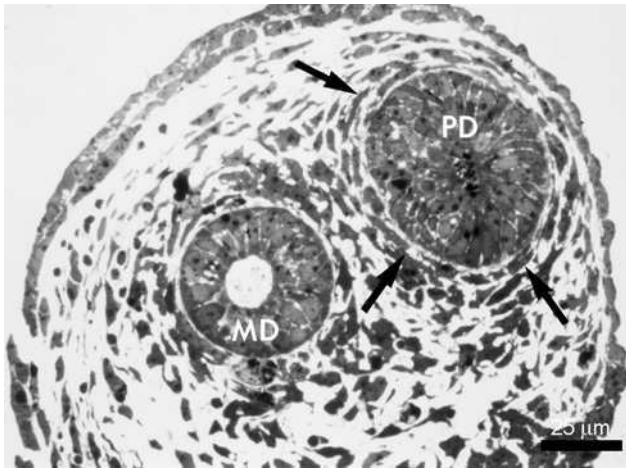
FIG. 10   Wolffian and Müllerian duct associated with one experimental E14.5 testis cultured 4 div in E15–E17 ovary-CM. The Wolffian duct (W) is well-maintained whereas the adjacent Müllerian duct (M) shows signs of involution such as an epithelial cuff (arrows).

the functional importance of E-cadherin in gonadal development, dissociating and culturing E17 gonads in the presence and absence of antibody to E-cadherin (Mackay *et al.*, 1999). This *in vitro* technique (dissociation followed by reaggregation in the presence or absence of neutralizing antibodies against

the factor of interest) offers a useful adjunct to the mouse knockout model, especially if the gene in question has housekeeping functions when overall development may be compromised (Mackay *et al.*, 2004b).

VIII. Concluding Remarks

Different approaches have been applied to investigate the role of growth factors in testis development. One is to screen knockout gene mutants for effects on testis development, another is to examine the developmental steps involved in testicular morphogenesis and to hypothesize which growth factors might be involved, based on findings in other systems. Culture approaches provide a means of creating knockout equivalents, by culturing in the presence of neutralizing antibodies. Possible cell and tissue interactions can be investigated *in vitro* and occasionally diffusible signals are found by this approach which can then be identified, although in the case of the meiosis-inducing and meiosis-preventing substances this has taken 30 years. Genes encoding growth factors of interest can be silenced by means of small interfering RNAs (siRNAs), a relatively new technique that has proved to be a powerful and widely used tool for the analysis of gene function in mammalian cells (Haraguchi *et al.*, 2004). Viral-mediated delivery of siRNA specifically reduces expression of targeted genes in various cell types, both *in vitro* and *in vivo* (Xia *et al.*, 2002); siRNA technology can also be applied in organ culture experiments (Davies *et al.*, 2004). Other genetic approaches include expression screens which can be applied to discover new genes that are sex-specifically expressed during mouse gonadal organogenesis (Bowles *et al.*, 2006; Nordqvist and Tohonen, 1997; O'Shaughnessy *et al.*, 2003). Such tools will prove useful in the future as alternatives to creating null mutant mice.

Summarizing the evidence presented here for the importance of growth factors in morphogenesis of the testis, some can be seen as key players, active in several different roles at different times (Table I). The PDGF/PDGFR system has been highlighted as a major factor in testis morphogenesis (Brennan *et al.*, 2003; Mariani *et al.*, 2002; Puglianiello *et al.*, 2003), mediating testis cord development and fetal Leydig cell development, with a possible role in the proliferation and migration of PMC precursors from the interstitial tissue to the peritubular area. PDGF-A/PDGFR-α interactions also drive precursors to commit to the adult Leydig cell phenotype (Mariani *et al.*, 2002). FGF9 is a key factor acting downstream of Sry controlling mesonephric migration, and the proliferation, aggregation and differentiation of Sertoli cells as well as promoting XY germ cell survival (Colvin *et al.*, 2001; DiNapoli *et al.*, 2006; Willerton *et al.*, 2004). Furthermore, there is increasing evidence for a significant role for neurotrophic factors in testis development (Cupp *et al.*, 2000, 2002, 2003; Levine *et al.*, 2000b; Wu *et al.*, 2005).

TABLE I

Summary of Growth Factors Involved in Testicular Morphogenesis

Event	Growth factor	Function, species
Migration		
Germ cells	$TGF\beta_1$	Chemotropic factor, mouse
	SCF	Migration, mouse
	SDF1	Migration, mouse
	FGF2	Shape changes during migration, mouse
Mesonephric cells including PMCs, endothelial cells	$TGF\beta_3$	Induces migration, rat
	PDGF	Shape changes during migration, mouse, rat
	HGF	Increases migratory activity, mouse
	AMH	Induces migration in XX, E11.5 mouse
	Neurotrophins	Migration, mouse, rat
Vascular Development		
	VEGF	Mouse, blocked in XX gonad by Fst and Bmp2 acting downstream of *Wnt4*
Proliferation		
Germ cells	TGFβ	↑ Apoptosis or↓ proliferation, mouse, rat
	Activin (+FSH, Fst)	↑ Spermatogonia, rat
	SCF	↑ Proliferation and survival, mouse
	LIF	↑ Proliferation, mouse
	FGF2	↑ Proliferation, mouse, rat
	PDGF	↑ proliferation, PN rat
	GDNF	↑ Survival, proliferation, mouse
	Neurotrophin	↑ Survival, rat
Somatic cells	$TGF\beta_1$	Leydig cell growth inhibitor, rat
	FGF2	Survival factor, rat Sertoli cells
	FGF9	Sertoli cell proliferation, mouse
	PDGF	PMCs proliferation, rat
	Activin (+FSH)	↑ proliferation, PN Sertoli cells, rat
	GDNF	↑ proliferation, Sertoli cells, rat, mouse
	NGF	↑ proliferation, Sertoli cells, mouse
Control of Cell Phenotype		
Germ cells	BMP4, BMP8b	Specification of germ cell lineage
	$TGF\beta_1$	Expressed in spermatocytes, early round spermatids, rat
	$TGF\beta_2$	Intense expression as spermatids elongate
	Leptin	?Stem cell renewal, mouse
	VEGF	Proliferation or differentiation, mouse
	GDNF	Stem cell renewal, mouse

(*continued*)

TABLE I   *(continued)*

Event	Growth factor	Function, species
Sertoli cells/cord formation	TGFβ₂	Sertoli cell/PMC interaction in cord formation, rat
	AMH	? Cord formation, mouse
	FGF9	Sertoli cell differentiation, cord formation, mouse
	PDGF	Cord formation, mouse
	HGF	Cord formation, mouse
	GDNF	Cordlike aggregation of Sertoli cells, mouse
	Neurotrophins	Cord formation in e13 rat
Leydig cells	Pdgf-a	Leydig cell differentiation and proliferation, mouse
PMCs	Pdgf	Phenotype
	Neurotrophin	Mouse PMC precursors express receptor p75/ntr

TGF, transforming growth factor; SCF, stem cell factor; SDF1, stromal cell-derived factor 1; FGF, fibroblast growth factor; PDGF, platelet-derived growth factor; HGF, hepatocyte growth factor; AMH, anti-Müllerian hormone; VEGF, vascular endothelial growth factor; *Wnt4,* gene controling female differentiation; FSH, follicle stimulating hormone; Fst, follistatin; LIF, leukemia inhibitory factor; GDNF, glial cell line-derived neutrotrophic factor; PN, postnatal; PMC, peritubular myoid cells; NGF, nerve growth factor; BMP, bone morphogenetic hormone; p75/ntr, neurotrophin receptor; ?, possible role in; ↑, increases; ↓, decreases.

It looks as if there is not just one key growth factor involved in testis development but several interchangeable growth factors and their family members, which is not surprising as this would provide a fail-safe mechanism in the event of gene damage. Ricci *et al.* (2004) suggest some of the factors involved in the regulation of migration of cells from the mesonephros and testicular cord formation converge to a common signaling pathway, the P1–3K pathway. This could explain the lack of a severe testicular phenotype in knockouts for c-met (Bladt *et al.*, 1995; Ricci *et al.*, 2002), PDGFR-β (Soriano, 1994), trkA, and trkC neurotrophin receptors (Cupp *et al.*, 2002).

Although little sequence similarity is found between the growth factors, when a comparison is made of the crystal structures of TGF-β2, PDGF-BB, and NGF, a common structural motif is seen involving two pairs of β-strands and six conserved cysteine residues arranged as a "cysteine knot" (McDonald and Hendrickson, 1992). One other cysteine residue forms a single disulfide bridge between the two subunits, forming a covalently linked dimer, critical for biological activity (Shimasaki *et al.*, 2004). Therefore, although these growth factors show little sequence similarity and different dimerization, they nevertheless have a similar protomeric organization (Wall and Hogan, 1994).

Much remains to be elucidated about the events downstream of Sry expression. Problems remaining to be solved at the time of writing include
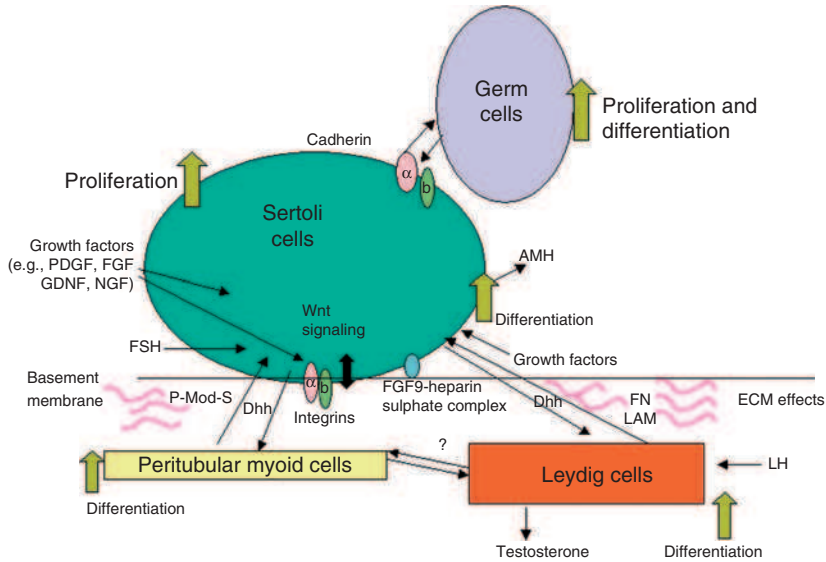
FIG. 11 Somatic and germ cell interactions in the developing testis.

the origin of the Leydig cell population and the significance of the different timing of tunica albuginea development in the two sexes. However, our understanding of the way in which the indifferent gonad is influenced to develop along male lines has been greatly improved since the discovery of *Sry*. Deciphering the role of growth factors and the other extrinsic developmental cues, together with the resulting signaling cascades which potentially regulate cell proliferation and further differentiation, has increased our appreciation of how the interactions between the respective cell types within the testis ensure development proceeds successfully (Fig. 11).

Acknowledgments

References

Abo-Elmaksoud, A., and Sinowatz, F. (2005). Expression and localization of growth factors and their receptors in the mammalian testis. Part I: Fibroblast growth factors and insulin-like growth factors. *Anat. Histol. Embryol.* **34,** 319–334.

Achermann, J. C., Ozisik, G., Ito, M., Orun, U. A., Harmanci, K., Gurakan, B., and Jameson, J. L. (2002). Gonadal determination and adrenal development are regulated by the orphan

nuclear receptor steroidogenic factor-1, in a dose-dependent manner. *J. Clin. Endocr. Metab.* **87,** 1829–1833.

Adams, I. R., and McLaren, A. (2002). Sexually dimotrophic development of mouse primordial germ cells: Switching from oogenesis to spermatogenesis. *Development* **129,** 1155–1164.

Allard, S., Adin, P., Gouédard, L., di Clemente, N., Josso, N., Orgebin-Crist, M. C., Picard, J. Y., and Xavier, F. (2000). Molecular mechanisms of hormone-mediated Müllerian duct regression: Involvement of β-catenin. *Development* **127,** 3349–3360.

Aponte, P. M., Soda, T., van de Kant, H. J. G., and de Rooij, D. G. (2006). Basic features of bovine spermatogonial culture and effects of glial cell line-derived neutrotrophic factor. *Theriogenology* **65,** 1828–1847.

Barbacid, M. (1995). Neurotrophic factors and their receptors. *Curr. Opin. Cell Biol.* **7,** 148–155.

Barrionuevo, F. J., Zurita, F., Burgos, M., and Jiménez, R. (2004). Testis-like development of gonads in female moles. New insights on mammalian gonad organogenesis. *Dev. Biol.* **268,** 39–52.

Behringer, R. R., Cate, R. L., Froelick, G. J., Palmiter, R. D., and Brinster, R. L. (1990). Abnormal sexual development in transgenic mice chronically expressing Müllerian inhibiting substance. *Nature* **345,** 167–170.

Birchmeier, C., and Gherardi, E. (1998). Developmental roles of HGF/SF and its receptor, the c-Met tyrosine kinase. *Trends Cell Biol.* **8,** 404–410.

Bladt, F., Riethmacher, D., Isenmann, S., Aguzzi, A., and Birchmeier, C. (1995). Essential role for the c-met receptor in the migration of myogenic precursor cells into the limb bud. *Nature* **376,** 768–771.

Bothwell, M. (1995). Functional interactions of neurotrophins and neurotrophic receptors. *Annu. Rev. Neurosci.* **18,** 223–253.

Bowles, J., Knight, D., Smith, C., Wilhelm, D., Richman, J., Mamiya, S., Yashiro, K., Chawengsaksophak, K., Wilson, M. J., Rossant, J., Hamda, H., and Koopman, P. (2006). Retinoid signaling determines germ cell fate in mice. *Science* **312,** 596–600.

Brennan, J., and Capel, B. (2004). One tissue, two fates: Molecular genetic events that underlie testis versus ovary development. *Nat. Rev. Genet.* **5,** 509–521.

Brennan, J., Karl, J., and Capel, B. (2002). Divergent vascular mechanisms downstream of *Sry* establish the arterial system in the XY gonad. *Dev. Biol.* **244,** 418–428.

Brennan, J., Tilmann, C., and Capel, B. (2003). *Pdgfr-α* mediates testis cord organization and fetal Leydig cell development in the XY gonad. *Genes Dev.* **17,** 800–810.

Buehr, M., Gu, S., and McLaren, A. (1993a). Mesonephric contribution to testis differentiation in the fetal mouse. *Development* **117,** 273–281.

Buehr, M., McLaren, A., Bartley, A., and Darling, S. (1993b). Proliferation and migration of primordial germ cells in W^e/W^e mouse embryos. *Dev. Dyn.* **198,** 182–189.

Bullejos, M., and Koopman, P. (2001). Spatially dynamic expression of Sry in mouse genital ridges. *Dev. Dyn.* **221,** 201–205.

Burgoyne, P. S., Ansell, J. D., and Tournay, A. (1986). Can the indifferent mammalian XX gonad be sex-reversed by interaction with testicular tissue? *In* "Serono Symposia Review No. 11, Development and Function of Reproductive Organs" (A. Eshkol, N. Dekel, B. Eckstein, H. Peters, and A. Tsafriri, Eds.), pp. 23–39. Ares-Serono Symposia, Rome.

Bussolino, F., Direnzo, M. F., Ziche, M., Bocchietto, E., Olivero, M., Naldini, L., Gaudino, G., Tamagone, L., Coffer, A., and Comoglio, P. M. (1992). Hepatocyte growth-factor is a potent angiogenic factor which stimulates endothelial-cell motility and growth. *J. Cell Biol.* **119,** 629–641.

Buzzard, J. J., Farnworth, P. G., de Kretser, D. M., O'Connor, A. E., Wreford, N. G., and Morrison, J. R. (2003). Proliferative phase Sertoli cells display a developmentally regulated response to activin *in vitro*. *Endocrinology* **144,** 474–483.

Byskov, A. G. (1979). Regulation of meiosis in mammals. *Ann. Biol. Anim. Bioch. Biophys.* **19,** 1251–1261.

Byskov, A. G., and Saxén, L. (1976). Induction of meiosis in fetal mouse testis *in vitro*. *Dev. Biol.* **52,** 193–200.

Campagnolo, L., Russo, M. A., Puglianiello, A., Favale, A., and Siracusa, G. (2001). Mesenchymal cell precursors of peritubular smooth muscle cells of the mouse testis can be identified by the presence of the p75 neurotrophin receptor. *Biol. Reprod.* **64,** 464–472.

Cancilla, B., and Risbridger, G. P. (1998). Differential localization of fibroblast growth factor receptor-1, -2, -3 and -4 in fetal, immature and adult rat testes. *Biol. Reprod.* **58,** 1138–1145.

Cancilla, B., Davies, A., Ford-Perris, M., and Risbridger, G. P. (2000). Discrete cell- and stage-specific localisation of fibroblast growth factors and receptor expression during testis development. *J. Endocrinol.* **164,** 149–159.

Capel, B., Albrecht, K. H., Washburn, L. L., and Eicher, E. M. (1999). Migration of mesonephric cells into the mammalian gonad depends on *Sry*. *Mech. Dev.* **84,** 127–131.

Chabot, B., Stephenson, D. A., Chapman, V. M., Besmer, P., and Bernstein, A. (1988). The proto-oncogene c-kit encoding a transmembrane receptor maps to the mouse W locus. *Nature* **335,** 88–89.

Chang, H., and Matzuk, M. M. (2001). Smad5 is required for mouse primordial germ cell development. *Mech. Dev.* **104,** 61–67.

Charpentier, G., and Magre, S. (1989). La réduction du nombre de cellules germinales induite *in vitro* par le testicule dans l'ovaire foetal de rat pourrait être due à un facteur distinct de l'hormone anti-Müllérienne. *C. r. hebd. Séanc. Acad. Sci (Paris)* **309,** 35–42.

Charpentier, G., and Magre, S. (1990). Masculinizing effect of testes on developing rat ovaries in organ culture. *Development* **110,** 839–849.

Chen, D., Zhao, M., and Mundy, G. R. (2004). Bone morphogenetic proteins. *Growth Factors* **22,** 233–241.

Cheng, L. Z., Gearing, D. P., White, L. S., Compton, D. L., Schooley, K., and Donovan, P. J. (1994). Role of leukemia inhibitory factor and its receptor in mouse primordial germ-cell growth. *Development* **120,** 3145–3153.

Chiarenza, C., Filippini, A., Tripiciano, A., Beccari, E., and Palombi, F. (2000). Platelet-derived growth factor-BB stimulates hypertrophy of peritubular smooth muscle cells from rat testis in primary cultures. *Endocrinology* **141,** 2971–2981.

Clark, A. M., Garland, K. K., and Russell, L. D. (2000). *Desert hedgehog (Dhh)* gene is required in the mouse testis for formation of adult-type Leydig cells and normal development of peritubular cells and seminiferous tubules. *Biol. Reprod.* **63,** 1825–1838.

Clarke, T. R., Hoshiya, Y., Yi, S. E., Liu, X., Lyons, K. M., and Donahoe, P. K. (2001). Mullerian inhibiting substance signaling uses a bone morphogenetic protein (BMP)-like pathway mediated by ALK2 and induces SMAD6 expression. *Mol. Endocrinol.* **15,** 946–959.

Colvin, J. S., Gree, R. P., Schmahl, J., Capel, B., and Ornitz, D. M. (2001). Male-to-female sex reversal in mice lacking fibroblast growth factor 9. *Cell* **104,** 875–889.

Copeland, N. G., Gilbert, D. J., Cho, B. C., Donovan, P. J., Jenkins, N. A., Cosman, D., Anderson, D., Lyman, S. D., and Williams, D. E. (1990). Mast cell growth factor maps near the steel locus on mouse chromosome 10 and is deleted in a number of steel alleles. *Cell* **63,** 175–183.

Coveney, D., Shaw, G., and Renfree, M. B. (2002). Effects of estrogen treatment on testicular descent, inguinal closure and prostatic development in a male marsupial, *Macropus eugenii*. *Reproduction* **124,** 73–83.

Creemers, L. B., Meng, X., den Ouden, K., van Pelt, A. M. M., Izadyar, F., Santoro, M., Sariola, H., and de Rooij, D. G. (2002). Transplantation of germ cells from glial cell line-derived neurotrophic factor-overexpressing mice to host testes depleted of endogenous spermatogenesis by fractionated irradiation. *Biol. Reprod.* **66,** 1579–1584.

Crews, D. (2003). Sex determination: Where environment and genetics meet. *Evol. Dev.* **5,** 50–55.

Cupp, A. S., Kim, G., and Skinner, M. K. (1999). Expression and action of transforming growth factor beta (TGFβ1, TGFβ2, and TGFβ3) during embryonic rat testis development. *Biol. Reprod.* **60,** 1304–1313.

Cupp, A. S., Kim, G., and Skinner, M. K. (2000). Expression and action of neurotrophin-3 and nerve growth factor in embryonic and early postnatal rat testis development. *Biol. Reprod.* **63,** 1617–1628.

Cupp, A. S., Tessarollo, L., and Skinner, M. K. (2002). Testis developmental phenotypes in neurotrophin receptor trkA and trkC null mutations: Role in formation of seminiferous cords and germ cell survival. *Biol. Reprod.* **66,** 1838–1845.

Cupp, A. S., Uzumcu, M., and Skinner, M. K. (2003). Chemotactic role of neurotropin 3 in the embryonic testis that facilitates male sex determination. *Biol. Reprod.* **68,** 2033–2037.

Davies, J. A., Ladomery, M., Hohenstein, P., Michael, L., Shafe, A., Spraggon, L., and Hastie, N. (2004). Development of an siRNA-based method for repressing specific genes in renal organ culture and its use to show that the Wt1 tumour suppressor is required for nephron differentiation. *Hum. Mol. Genet.* **13,** 235–246.

De Felici, M. (2000). Regulation of primordial germ cell development in the mouse. *Int. J. Dev. Biol.* **44,** 575–580.

De Felici, M., and Dolci, S. (1991). Leukemia inhibitory factor sustains the survival of mouse primordial germ cells cultured on TM4 feeder layers. *Dev. Biol.* **147,** 281–284.

Dettin, L., Ravindranath, N., Hofmann, M.-C., and Dym, M. (2003). Morphological characterization of the spermatogonial subtypes in the neonatal mouse testis. *Biol. Reprod.* **69,** 1565–1571.

di Clemente, N., Josso, N., Gouédard, L., and Belville, C. (2003). Components of the anti-Müllerian hormone signaling pathway in gonads. *Mol. Cell. Endocrinol.* **211,** 9–14.

DiNapoli, L., Batchvarov, J., and Capel, B. (2006). FGF9 promotes survival of germ cells in the fetal testis. *Development* **133,** 1519–1527.

Dolci, S., Williams, D. E., Ernst, M. K., Resnick, J. L., Brannan, C. L., Fock, L. F., Lyman, S. D., Boswell, S. H., and Donovan, P. J. (1991). Requirements for mast cell growth factor for primordial germ cell survival in culture. *Nature* **352,** 809–811.

Dolci, S., Pesce, M., and De Felici, M. (1993). Combined action of stem-cell factor, leukemia inhibitory factor, and CAMP on *in vitro* proliferation of mouse primordial germ-cells. *Mol. Reprod. Dev.* **35,** 134–139.

Donovan, P. J., Stott, D., Cairns, L. A., Heasman, J., and Wylie, C. C. (1986). Migratory and postmigratory mouse primordial germ cells behave differently in culture. *Cell* **44,** 831–838.

El-Hefnawy, T., Ioffe, S., and Dym, M. (2000). Expression of the leptin receptor during germ cell development in the mouse testis. *Endocrinology* **141,** 2624–2630.

Ergun, S., Kilic, N., Fiedler, W., and Mukhopadhyay, A. K. (1997). Vascular endothelial growth factor and its receptors in normal testicular tissue. *Mol. Cell. Endocrinol.* **131,** 9–20.

Farini, D., Scaldaferri, M. L., Iona, S., La Sala, G., and De Felici, M. (2005). Growth factors sustain primordial germ cell survival, proliferation and entering into meiosis in the absence of somatic cells. *Dev. Biol.* **285,** 49–56.

Ferguson, M. W. J., and Joanen, T. (1983). Temperature-dependent sex determination in *Alligator mississippiensis. J. Zool.* **200,** 143–177.

Fitzpatrick, S. L., Sindoni, D. M., Shughrue, P. J., Lane, M. V., Merchenthaler, I. J., and Frail, D. E. (1998). Expression of growth differentiation factor-9 messenger ribonucleic acid in ovarian and nonovarian rodent and human tissues. *Endocrinology* **139,** 2571–2578.

Frankenberry, K. A., Somasundar, P., McFadden, D. W., and Vona-Davis, L. C. (2004). Leptin induces cell migration and the expression of growth factors in human prostate cancer cells. *Am. J. Surg.* **188,** 560–565.

Gautier, C., Levacher, C., Avallet, O., Vigier, M., Rouiller-Fabre, V., Lecerf, L., Saez, J., and Habert, R. (1994). Immunohistochemical localization of transforming growth factor β in the fetal and neonatal testis. *Mol. Cell. Endocrinol.* **99,** 55–61.

Geissler, E. N., Ryan, M. A., and Housman, D. E. (1988). The dominant-white spotting (W) locus of the mouse encodes the c-kit proto-oncogene. *Cell* **55,** 185–192.

Gnessi, L., Emidi, A., Scarpa, S., Palleschi, S., Ragano-Caracciolo, M., Silvestroni, I., Modesti, A., and Spera, G. (1993). Platelet-derived growth factor effects on purified testicular peritubular myoid cells: Binding, cytosolic Ca^{2+} increase, mitogenic activity, and extracellular matrix production enhancement. *Endocrinology* **133,** 1880–1890.

Gnessi, L., Emidi, A., Jannini, E. A., Carosa, E., Maroder, M., Arizzi, M., Ulisse, S., and Spera, G. (1995). Testicular development involves the spatiotemporal control of PDGFs and PDGF receptors gene expression and action. *J. Cell Biol.* **131,** 1105–1121.

Gnessi, L., Fabbri, A., and Spera, G. (1997). Gonadal peptides as mediators of development and functional control of the testis: An integrated system with hormones and local environment. *Endocr. Rev.* **18,** 541–609.

Gnessi, L., Basciani, S., Mariani, S., Arizzi, M., Spera, G., Wang, C., Bondjers, C., Karlsson, L., and Betsholtz, C. (2000). Leydig cell loss and spermatogenic arrest in platelet-derived growth factor (PDGF)-A-deficient mice. *J. Cell Biol.* **149,** 1019–1025.

Godin, I., and Wylie, C. (1991). $TGF\beta_1$ inhibits proliferation and has a chemotropic effect on mouse primordial germ cells in culture. *Development* **113,** 1451–1457.

Godin, I., Wylie, C., and Heasman, J. (1990). Genital ridges exert long-range effects on mouse primordial germ cell numbers and direction of migration in culture. *Development* **108,** 357–363.

Godin, I., Deed, R., Cooke, J., Zsebo, K., Dexter, M., and Wylie, C. C. (1991). Effects of the *Steel* gene product on mouse primordial germ cells in culture. *Nature* **352,** 807–809.

Golden, J. P., DeMaro, J. A., Osborne, P. A., Milbrandt, J., and Johnson, E. M., Jr. (1999). Expression of neurturin, GDNF and GDNF family-receptor mRNA in the developing and mature mouse. *Exp. Neurol.* **158,** 504–528.

Gouédard, L., Chen, Y. G., Thevenet, L., Racine, C., Borie, S., Lamarre, I., Josso, N., Massagué, J., and di Clemente, N. (2000). Engagement of bone morphogenetic protein type 1B receptor and Smad1 signaling by anti-Mullerian hormone and its type II receptor. *J. Biol. Chem.* **275,** 27973–27978.

Graff, J. M., Bansal, A., and Melton, D. A. (1996). *Xenopus* Mad proteins transduce distinct subsets of signals for the TFGβ superfamily. *Cell* **85,** 479–487.

Grund, S. K., Pelliniemi, L. J., Paranko, J., Müller, U., and Lakkala-Paranko, T. (1986). Reaggregates of cells from rat testis resemble developing gonads. *Differentiation* **32,** 135–143.

Hacker, A., Capel, B., Goodfellow, P., and Lovell-Badge, R. (1995). Expression of Sry, the mouse sex determining gene. *Development* **121,** 1603–1614.

Han, I. S., Sylvester, S. R., Kim, K. H., Schelling, M. E., Venkateswaran, S., Blankaert, V. D., McGuiness, M. P., and Griswold, M. D. (1993). Basic fibroblast growth factor is a testicular germ cell product which may regulate Sertoli cell function. *Mol. Endocrinol.* **7,** 889–897.

Haraguchi, S., Saga, Y., Naito, K., Inoue, H., and Seto, A. (2004). Specific gene silencing in the pre-implantation stage mouse embryo by an siRNA expression vector system. *Mol. Reprod. Dev.* **68,** 17–24.

Hayashi, K., Kobayashi, T., Umino, T., Goitsuka, R., Matsui, Y., and Kitamura, D. (2002). SMAD1 signaling is critical for initial commitment of germ cell lineage from mouse epiblast. *Mech. Dev.* **118,** 99–109.

Heldin, C.-H., and Westermark, B. (1990). Platelet-derived growth factor: Mechanisms of action and possible *in vivo* function. *Cell Reg.* **1,** 555–566.

Heldin, C.-H., and Westermark, B. (1999). Mechanism of action and *in vivo* role of platelet-derived growth factor. *Physiological Rev.* **79,** 1283–1316.

Holsberger, D. R., and Cooke, P. S. (2005). Understanding the role of thyroid hormone in Sertoli cell development: A mechanistic hypothesis. *Cell Tissue Res.* **322,** 133–140.

Hu, J., Shima, H., and Nakagawa, H. (1999). Glial cell line-derived neurotrophic factor stimulates Sertoli cell proliferation in the early postnatal period of rat testis development. *Endocrinology* **140,** 3416–3421.

Jans, D. A., and Hassan, G. (1998). Nuclear targeting by growth factors, cytokines, and their receptors: A role in signaling? *BioEssays* **20,** 400–411.

Jeays-Ward, K., Hoyle, C., Brennan, J., Dandonneau, M., Alldus, G., Capel, B., and Swain, A. (2003). Endothelial and steroidogenic cell migration are regulated by WNT4 in the developing mammalian gonad. *Development* **130,** 3663–3670.

Johnston, C. L., Cox, H. C., Gomm, J. J., and Coombes, R. C. (1995). Fibroblast growth factor receptors (FGFRs) localize in different cellular compartments. *J. Biol. Chem.* **270,** 30643–30650.

Josso, N. (1994). Anti-Müllerian hormone: A masculinizing relative of TGF-β. *In* ''Oxford Reviews of Reproductive Biology'' (H. M. Charlton, Ed.), Vol. 16, pp. 139–163. Oxford University Press, Oxford.

Josso, N., and di Clemente, N. (1999). TGF-β family members and gonadal development. *Trends Endocrin. Met.* **10,** 211–254.

Jost, A., Vigier, B., and Prépin, J. (1972). Freemartins in cattle: The first steps of sexual organogenesis. *J. Reprod. Fert.* **29,** 349–379.

Karl, J., and Capel, B. (1998). Sertoli cells of the mouse testis originate from the coelomic epithelium. *Dev. Biol.* **203,** 323–333.

Kessler, E., Takahara, K., Biniaminov, L., Brusel, M., and Greenspan, D. S. (1996). Bone morphogenetic protein-1: The type 1 procollagen C-proteinase. *Science* **271,** 360–362.

Konrad, L., Albrecht, M., Renneberg, H., and Aumüller, G. (2000). Transforming growth factor-β2 mediates mesenchymal-epithelial interactions of testicular somatic cells. *Endocrinology* **1451,** 3679–3686.

Knaut, H., Werz, C., Geisler, R., and Nusslein-Volhard, C. (2003). A zebrafish homologue of the chemokine receptor Cxcr4 is a germ-cell guidance receptor. *Nature* **421,** 279–282.

Kraak, S. B. M., and de Looze, E. M. A. (1993). A new hypothesis on the evolution of sex determination in vertebrates — big females ZW, big males XY. *Neth. J. Zool.* **43,** 260–273.

Lawson, K. A., Dunn, N. R., Roelen, B. A. J., Zeinstra, L. M., Davis, A. M., Wright, C. V. E., Korving, J. P. W. F. M., and Hogan, B. L. M. (1999). *Bmp4* is required for the generation of primordial germ cells in the mouse embryo. *Genes Dev.* **13,** 424–436.

Lee, M. M., and Donahoe, P. K. (1993). Mullerian inhibiting substance: A gonadal hormone with multiple functions. *Endocr. Rev.* **14,** 152–164.

Lehtonen, E., Wartiovaara, J., Nordling, S., and Saxén, L. (1975). Demonstration of cytoplasmic processes in millipore filters permitting kidney tubule induction. *J. Embryol. Exp. Morph.* **33,** 187–203.

Levine, E., Cupp, A. S., and Skinner, M. K. (2000a). Role of neurotropins in rat embryonic testis morphogenesis (cord formation). *Biol. Reprod.* **62,** 132–142.

Levine, E., Cupp, A. S., Miyashiro, L., and Skinner, M. K. (2000b). Role of transforming growth factor-α and the epidermal growth factor receptor in embryonic rat testis development. *Biol. Reprod.* **62,** 477–490.

Levi-Montalcini, R. (1998). The saga of the nerve growth factor. *NeuroReport* **9,** R71–R83.

Li, H., Papadopoulos, V., Vidic, B., Dym, M., and Culty, M. (1997). Regulation of rat testis gonocyte proliferation by platelet-derived growth factor and estradiol: Identification of signaling mechanisms involved. *Endocrinology* **138,** 1289–1298.

Lin, X., Buff, E. M., Perrimon, N., and Michelson, A. M. (1999). Heparan sulfate proteoglycans are essential for FGF receptor signaling during *Drosophila* embryonic development. *Development* **126,** 3715–3723.

Lopes, S. M. C. D., Roelen, B. A. J., Monteiro, R. M., Emmens, R., Lin, H. Y., Li, E., Lawson, K. A., and Mummery, C. L. (2004). BMP signaling mediated by ALK2 in the visceral endoderm is necessary for the generation of primordial germ cells in the mouse embryo. *Genes Dev.* **18,** 1838–1849.

Loveland, K. L., Bakker, M., Meehan, T., Christy, E., von Schönfeldt, V., Drummond, A., and de Kretser, D. (2003). Expression of Bambi is widespread in juvenile and adult rat tissues and is regulated in male germ cells. *Endocrinology* **144,** 4180–4186.

Lu, P. F., Minowada, G., and Martin, G. R. (2006). Increasing Fgf4 expression in the mouse limb bud causes polysyndactyly and rescues the skeletal defects that result from loss of Fgf8 function. *Development* **133,** 33–42.

Lui, W.-Y., Lee, W. M., and Cheng, C. Y. (2003a). TGF-βs: Their role in testicular function and Sertoli cell tight junction dynamics. *Int. J. Androl.* **26,** 147–160.

Lui, W.-Y., Lee, W. M., and Cheng, C. Y. (2003b). Transforming growth factor-β3 regulates the dynamics of Sertoli cell tight junctions via the p38 mitogen-activated protein kinase pathway. *Biol. Reprod.* **68,** 1597–1612.

MacIntyre, M. N. (1956). Effect of fetal testis on ovarian differentiation in heterosexual embryonic rat gonad transplants. *Anat. Rec.* **124,** 27–46.

Mackay, S. (2000). Gonadal development in mammals at the cellular and molecular levels. *Int. Rev. Cytol.* **200,** 47–99.

Mackay, S., and Smith, R. A. (1986). The differentiation of mouse gonads *in vitro*: A light and electron microscopical study. *J. Embryol. Exp. Morph.* **97,** 189–199.

Mackay, S., and Smith, R. A. (1989). Mouse gonadal differentiation *in vitro* in the presence of fetal calf serum. *Cell Diff. Dev.* **27,** 19–28.

Mackay, S., Smith, R. A., and Haig, T. (1992). An investigation of the migratory potential of mouse oocytes *in vitro*. *J. Anat.* **181,** 437–446.

Mackay, S., Smith, R. A., Campbell, R. J., and McLeod, L. E. (1995). The effect of TGF-β1 on developing mouse gonads *in vitro*. *J. Anat.* **187,** 238.

Mackay, S., Nicholson, C. L., Lewis, S. P., and Brittan, M. (1999). E-cadherin in the developing mouse gonad. *Anat. Embryol.* **200,** 91–102.

Mackay, S., Xie, Q., Ullmann, S. L., Gilmore, D. P., and Payne, A. P. (2004a). Postnatal development of the reproductive system in the grey short-tailed opossum, *Monodelphis domestica*. *Anat. Embryol.* **208,** 121–133.

Mackay, S., Willerton, L., Ballingall, C. J., Henderson, N. J. S., and Smith, R. A. (2004b). Developing mouse Sertoli cells *in vitro*: Effects on developing ovaries in co-culture and production of AMH. *Cells Tiss. Organs* **177,** 79–86.

Mariani, S., Basciani, S., Arizzi, M., Spera, G., and Gnessi, L. (2002). PDGF and the testis. *Trends Endocrin. Met.* **13,** 11–17.

Martineau, J., Nordqvist, K., Tilmann, C., Lovell-Badge, R., and Capel, B. (1997). Male-specific cell migration into the developing gonad. *Curr. Biol.* **7,** 958–968.

Massagué, J. (1996). Crossing receptor boundaries. *Nature* **382,** 29–30.

Massagué, J., and Chen, Y. G. (2000). Controlling TGF-β signaling. *Gene. Dev.* **14,** 627–644.

Matsui, Y., Zsebo, K., and Hogan, B. (1990). Embryonic expression of a hemopoietic growth factor encoded by the *Steel* locus and the ligand for c-kit. *Nature* **347,** 667–669.

Matsui, Y., Toksoz, D., Nishikawa, S. I., Williams, D., Zsebo, K., and Hogan, B. (1991). Effect of *Steel* factor and leukaemia inhibitory factor on murine primordial germ cells in culture. *Nature* **353,** 750–752.

Matsui, Y., Zsebo, K., and Hogan, B. (1992). Derivation of pluripotential embryonic stem cells from murine primordial germ cells in culture. *Cell* **70,** 841–847.

McCoshen, J. A., and McCallion, D. J. (1975). A study of the primordial germ cells during their migratory phase in *Steel* mutant mice. *Experientia* **81,** 589–590.

McDonald, N. Q., and Hendrickson, W. A. (1992). A structural superfamily of growth factors containing a cystine knot motif. *Cell* **73,** 421–424.

McGuiness, M. P., and Orth, J. M. (1992). Reinitiation of gonocyte mitosis and movement of gonocytes to the basement membrane in testes of newborn rats *in vivo* and *in vitro*. *Anat. Rec.* **233,** 527–537.

McLaren, A. (1983). Studies on mouse germ cells inside and outside the gonad. *J. Exp. Zool.* **228,** 167–171.

McLaren, A. (1991). Development of the mammalian gonad: The fate of the supporting cell lineage. *BioEssays* **13,** 151–156.

McLaren, A. (1994). Germline and soma: Interactions during early mouse development. *Semin. Dev. Biol.* **5,** 43–49.

McLaren, A. (2003). Primordial germ cells in the mouse. *Dev. Biol.* **262,** 1–15.

McLaren, A., and Southee, D. (1997). Entry of mouse embryonic germ cells into meiosis. *Dev. Biol.* **187,** 107–113.

McPherron, A. C., and Lee, S.-J. (1993). GDF-3 and GDF-9: Two new members of the transforming growth factor-β superfamily containing a novel pattern of cysteines. *J. Biol. Chem.* **268,** 3444–3449.

Meehan, T., Schlatt, S., O'Bryan, M. K., de Kretser, D. M., and Loveland, K. L. (2000). Regulation of germ cell and Sertoli cell development by activin, follistatin and FSH. *Dev. Biol.* **220,** 225–237.

Meng, X., Lindahl, M., Hyvönen, M. E., Parvinen, M., de Rooij, D. G., Hess, M. W., Raatikainen-Ahokas, A., Sainio, K., Rauvala, H., Lakso, M., Pichel, J. G., Westphal, H., *et al.* (2000). Regulation of cell fate decision of undifferentiated spermatogonia by GDNF. *Science* **287,** 1489–1493.

Merchant-Larios, H., and Moreno-Mendoza, N. (1998). Mesonephric stromal cells differentiate into Leydig cells in the mouse fetal testis. *Exp. Cell Res.* **244,** 230–238.

Merchant-Larios, H., Moreno-Mendoza, N., and Buehr, M. (1993). The role of the mesonephros in cell differentiation and morphogenesis of the mouse fetal testis. *Int. J. Dev. Biol.* **37,** 407–415.

Michael, L., and Davies, J. A. (2004). Pattern and regulation of cell proliferation during murine ureteric bud development. *J. Anat.* **204,** 241–255.

Millan, F. A., Denhez, F., Kondaiah, P., and Akhurst, R. J. (1991). Embryonic gene expression patterns of TGF-β1, β2 and β3 suggest different developmental functions *in vivo*. *Development* **111,** 131–144.

Mintz, B., and Russell, E. S. (1957). Gene-induced embryological modifications of primordial germ cells in the mouse. *J. Exp. Zool.* **134,** 207–230.

Mittwoch, U. (2004). The elusive action of sex-determining genes: Mitochondria to the rescue? *J. Theoret. Biol.* **228,** 359–365.

Mittwoch, U., Delhanty, J. D. A., and Beck, F. (1969). Growth of differentiating testes and ovaries. *Nature* **224,** 1323–1325.

Molyneaux, K. A., Stallock, J., Schaible, K., and Wylie, C. (2001). Time-lapse analysis of living mouse germ cell migration. *Dev. Biol.* **240,** 488–498.

Molyneaux, K. A., Zinszner, H., Kunwar, P. S., Schaible, K., Stebler, J., Sunshine, M. J., O'Brien, W., Raz, E., Littman, D., Wylie, C., and Lehmann, R. (2003). The chemokine SDF1/CXCL12 and its receptor CXCR4 regulate mouse germ cell migration and survival. *Development* **130,** 4279–4286.

Moore, M. W., Klein, R. D., Fariñas, I., Sauer, H., Armanini, M., Phillips, H., Reichardt, L. F., Ryan, A. M., Carver-Moore, K., and Rosenthal, A. (1996). Renal and neuronal abnormalities in mice lacking GDNF. *Nature* **382,** 76–79.

Moreno-Mendoza, N., Harley, V. R., and Merchant-Larios, H. (2001). Temperature regulates SOX9 expression in cultured gonads of *Lepidochelys olivacea,* a species with temperature sex determination. *Dev. Biol.* **229,** 319–326.

Motta, P. M., and Makabe, S. (1986). Elimination of germ cells during differentiation of the human embryo: An electron microscopic study. *Europ. J. Ob. Gyaenecol. Reprod. Biol.* **22,** 271–286.

Müller, W. A. (1997). Model organisms in developmental biology. "Developmental Biology," p. 101. Springer-Verlag, New York.

Münsterberg, A., and Lovell-Badge, R. (1991). Expression of the mouse anti-Müllerian hormone gene suggests a role in both male and female sexual differentiation. *Development* **113,** 613–624.

Nakamura, T., Nawa, K., and Ichihara, A. (1984). Partial purification and characterization of hepatocyte growth factor from serum of hepatectomized rats. *Biochem. Biophys. Res. Commun.* **122,** 1450–1459.

Nalbandian, A., Dettin, L., Dym, M., and Ravindranath, N. (2003). Expression of vascular endothelial growth factor receptors during male germ cell differentiation in the mouse. *Biol. Reprod.* **69,** 985–994.

Nie, X., Luukko, K., and Kettunen, P. (2006). FGF signaling in craniofacial development and developmental disorders. *Oral Dis.* **12,** 102–111.

Nishino, K., Yamanouchi, K., Naito, K., and Tojo, H. (2001). Characterization of mesonephric cells that migrate into the XY gonad during testis differentiation. *Exp. Cell Res.* **267,** 225–232.

Nordqvist, K., and Tohonen, V. (1997). An mRNA differential display for cloning genes expressed during mouse gonad development. *Int. J. Dev. Biol.* **41,** 627–638.

O., W.-S., Short, R. V., Renfree, M. B., and Shaw, G. (1988). Primary genetic control of somatic sexual differentiation in a mammal. *Nature* **331,** 716–717.

Ohkubo, Y., Shirayoshi, Y., and Nakatsuji, N. (1996). Autonomous regulation of proliferation and growth arrest in mouse primordial germ cells studied by mixed and clonal cultures. *Exp. Cell Res.* **222,** 291–297.

Ohmichi, H., Koshimizu, U., Matsumoto, K., and Nakamura, T. (1998). Hepatocyte growth factor acts as a mesenchymal-derived morphogenic factor during fetal lung development. *Development* **125,** 1315–1324.

Okamura, D., Hayashi, K., and Matsui, Y. (2005). Mouse epiblasts change responsiveness to BMP4 signal required for PGC formation through functions of extraembryonic ectoderm. *Mol. Reprod. Dev.* **70,** 20–29.

Olaso, R., Gautier, C., Levacher, C., Saez, J. M., and Habert, R. (1997). The immuno-histochemical localization of transforming growth factor-β2 in the fetal and neonatal rat testis. *Mol. Cell. Endocrinol.* **126,** 165–172.

Olaso, R., Pairault, C., Boulogne, B., Durand, P., and Habert, R. (1998). Transforming growth factor β1 and β2 reduce the number of gonocytes by increasing apoptosis. *Endocrinology* **139,** 733–740.

Orr-Urteger, A., Avivi, A., Zimmer, Y., Givol, D., Yarden, Y., and Lonai, P. (1990). Developmental expression of *c-kit*, a protooncogene encoded at the *W* locus of the mouse. *Development* **109,** 911–923.

O'Shaughnessy, P. J., Fleming, L., Baker, P. J., Jackson, G., and Johnston, H. (2003). Identification of developmentally regulated genes in the somatic cells of the mouse testis using serial analysis of gene expression. *Biol. Reprod.* **69,** 797–808.

Park, S. Y., Meeks, J. J., Raverot, G., Pfaff, L. E., Weiss, J., Hammer, G. D., and Jameson, J. L. (2005). Nuclear receptors Sf1 and Dax1 function cooperatively to mediate somatic cell differentiation during testis development. *Development* **132,** 2415–2423.

Pelliniemi, L. J., and Fröjdman, K. (2001). Structural and regulatory macromolecules in sex differentiation of gonads. *J. Exp. Zool.* **290,** 523–528.

Pesce, M., Farrace, M. G., Piacentini, M., Dolci, S., and De Felici, M. (1993). Stem cell factor and leukemia inhibitory factor promote primordial germ cell survival by suppressing programmed cell death (apoptosis). *Development* **118,** 1089–1094.

Pesce, M., Siracusa, G., Giustiniani, Q., and De Felici, M. (1994). Histotypic *in vitro* reorganization of dissociated cells from mouse fetal gonads. *Differentiation* **56,** 137–142.

Pichel, J. G., Shen, L., Sheng, H. Z., Granholm, A.-C., Drago, J., Grinberg, A., Lee, E. J., Huang, S. P., Saarma, M., Hoffer, B. J., Sariola, H., and Westphal, H. (1996). Defects in enteric innervation and kidney development in mice lacking GDNF. *Nature* **382,** 73–76.

Prépin, J., and Hida, N. (1989). Influence of age and medium on formation of epithelial cords in the rat fetal ovary *in vitro. J. Reprod. Fert.* **87,** 375–382.

Prépin, J., Charpentier, G., and Jost, A. (1985). Action du testicule foetal sur le nombre des cellules germinales de l'ovaire de foetus de rat, *in vitro. C. r. hebd. Séanc. Acad. Sci., Paris* **300,** 43–47.

Prépin, J., Charpentier, G., Hida, N., Jost, A., and Maingourd, M. (1986). Isolement par liaison à des membranes d'ultrafiltration, d'un facteur testiculaire limitant le nombre de cellules germinales dans l'ovaire du foetus de rat, *in vitro. C. r. hebd. Séanc. Acad. Sci. (Paris)* **303,** 123–126.

Prigent, S. A., and Lemoine, N. R. (1992). The type 1 (EGFR-related) family of growth factor receptors and their ligands. *Prog. Growth Factor Res.* **4,** 1–24.

Puglianiello, A., Campagnolo, L., Farini, D., Cipollone, D., Russo, M. A., and Siracusa, G. (2003). Expression and role of PDGF-BB and PDGFR-β during testis morphogenesis in the mouse embryo. *J. Cell Sci.* **117,** 1151–1160.

Rapraeger, A. C., Krufka, A., and Olwin, B. B. (1991). Requirement of heparan sulfate for bFGF-mediated fibroblast growth and myoblast differentiation. *Science* **252,** 1705–1708.

Resnick, J. L., Bixler, L. S., Cheng, L., and Donovan, P. J. (1992). Long-term proliferation of mouse primordial germ cells in culture. *Nature* **359,** 550–551.

Rey, R., Lukas-Croisier, C., Lasala, C., and Bedecarrás, P. (2003). AMH/MIS: What we already know about the gene, the protein and its regulation. *Mol. Cell. Endocrinol.* **211,** 21–31.

Ricci, G., Catizone, A., Innocenzi, A., and Galdieri, M. (1999). Hepatocyte growth factor (HGF) receptor expression and role of HGF during embryonic mouse testis development. *Dev. Biol.* **216,** 340–347.

Ricci, G., Catizone, A., and Galdieri, M. (2002). Pleiotropic activity of hepatocyte growth factor during embryonic mouse testis development. *Mech. Dev.* **118,** 19–28.

Ricci, G., Catizone, A., and Galdieri, M. (2004). Embryonic mouse testis development: Role of platelet derived growth factor (PDGF-BB). *J. Cell. Physiol.* **200,** 458–467.

Robinson, L. L. L., Townsend, J., and Anderson, R. A. (2003). The human fetal testis is a site of expression of neurotrophins and their receptors: Regulation of the germ cell and peritubular cell population. *J. Clin. End. Metab.* **88,** 3943–3951.

Roletto, F., Galvani, A. P., Cristiani, C., Valsasina, B., Landonio, A., and Bertolero, F. (1996). Basic fibroblast growth factor stimulates hepatocyte growth factor/scatter factor secretion by human mesenchymal cells. *J. Cell Physiol.* **166,** 105–111.

Ross, A. J., and Capel, B. (2005). Signaling at the crossroads of gonad development. *Trends Endocrin. Met.* **16,** 19–25.

Ross, A. J., Tilman, C., Yao, H., MacLaughlin, D., and Capel, B. (2003). AMH induces mesonephric cell migration in XX gonads. *Mol. Cell. Endocrinol.* **211,** 1–7.

Rouiller-Fabre, V., Carmona, S., Abou Merhi, R., Cate, R., Habert, R., and Vigier, B. (1998). Effect of anti-Mullerian hormone on Sertoli and Leydig cell functions in fetal and immature rats. *Endocrinology* **139,** 1213–1220.

Russell, A. J., Gilmore, D. P., Mackay, S., Ullmann, S. L., Baker, P. J., and Payne, A. P. (2003). The role of androgens in development of the scrotum of the grey short–tailed Brazilian opossum (*Monodelphis domestica*). *Anat. Embryol.* **206,** 381–389.

Russell, L. D., Bartke, A., and Goh, J. C. (1989). Postnatal development of the Sertoli cell barrier, tubular lumen and cytoskeleton of Sertoli and myoid cells in the rat, and their relationship to tubular fluid secretion and flow. *Am. J. Anat.* **184,** 179–198.

Russo, M. A., Giustizieri, M. L., Favale, A., Fantini, M. C., Campagnolo, L., Konda, D., Germano, F., Farini, D., Manna, C., and Siracusa, G. (1999). Spatiotemporal patterns of expression of neurotrophin and neurotrophin receptors in mice suggest functional roles in testicular and epididymal morphogenesis. *Biol. Reprod.* **61,** 1123–1132.

Sakurai, H., and Nigam, S. K. (1997). Transforming growth factor-β selectively inhibits branching morphogenesis but not tubulogenesis. *Am. J. Physiol.* **272,** F139–F146.

Sariola, H. (2001). The neurotrophic factors in non-neuronal tissues. *Cell. Mol. Life Sci.* **58,** 1061–1066.

Saxén, L., Lehtonen, E., Karkinenjaaskelainen, M., Nordling, S., and Wartiovaara, J. (1976). Are morphogenetic tissue interactions mediated by transmissable signal substances or through cell contacts? *Nature* **259,** 662–663.

Schmahl, J., and Capel, B. (2003). Cell proliferation is necessary for the determination of cell fate in the gonad. *Dev. Biol.* **258,** 264–276.

Schmahl, J., Eicher, E. M., Washburn, L. L., and Capel, B. (2000). *Sry* induces cell proliferation in the mouse gonad. *Development* **127,** 65–73.

Schmahl, J., Kim, Y., Colvin, J. S., Ornitz, D. M., and Capel, B. (2004). *Fgf9* induces proliferation and nuclear localization of FGFR2 in Sertoli precursors during male sex determination. *Development* **131,** 3627–3636.

Segev, D. L., Ha, T. U., Tran, T. T., Kenneally, M., Harkin, P., Jung, M., MacLaughlin, D. T., Donahoe, P. K., and Maheswaran, S. (2000). Mullerian inhibiting substance inhibits breast cancer cell growth through an NF kappa B-mediated pathway. *J. Biol. Chem.* **275,** 28371–28379.

Serls, A. E., Doherty, S., Parvatiyar, P., Wells, J. M., and Deutsch, G. H. (2005). Different thresholds of fibroblast growth factors pattern the ventral foregut into liver and lung. *Development* **132,** 35–47.

Sharpe, R. M., McKinnell, C., Kivlin, C., and Fisher, J. (2003). Proliferation and functional maturation of Sertoli cells, and their relevance to disorders of testis function in adulthood. *Reproduction* **125,** 769–784.

Shimasaki, S., Moore, R. K., Otsuka, F., and Erickson, G. F. (2004). The bone morphogenetic protein system in mammalian reproduction. *Endocr. Rev.* **25,** 72–101.

Shimogori, T., Banuchi, V., Ng, H. Y., Strauss, J. B., and Grove, E. A. (2004). Embryonic signaling centers expressing BMP, WNT and FGF proteins interact to pattern the cerebral cortex. *Development* **131,** 5639–5647.

Smith, C. A., and Sinclair, A. (2004). Sex determination: Insights from the chicken. *BioEssays* **26,** 120–132.

Smith, C. A., McClive, P. J., Hudson, Q., and Sinclair, A. H. (2005). Male-specific cell migration into the developing gonad is a conserved process involving PDGF signaling. *Dev. Biol.* **284,** 337–350.

Soriano, P. (1994). Abnormal kidney development and hematological disorders in PDGF β-receptor mutant mice. *Genes Dev.* **8,** 1888–1896.

Taketo, T., and Koide, S. S. (1981). *In vitro* development of testis and ovary from indifferent fetal mouse gonads. *Dev. Biol.* **84,** 61–66.

Taketo, T., Seen, C. D., and Koide, S. S. (1986). Requirement of serum components for the preservation of primordial germ cells in testis cords during early stages of testicular differentiation *in vitro* in the mouse. *Biol. Reprod.* **34,** 919–924.

Taketo-Hosotani, T., Merchant-Larios, H., Thau, R. B., and Koide, S. S. (1985). Testicular cell differentiation in fetal mouse ovaries following transplantation into adult male mice. *J. Exp. Zool.* **236,** 229–237.

Takeuchi, Y., Molyneaux, K., Runyan, C., Schaible, K., and Wylie, C. (2005). The roles of FGF signaling in germ cell migration in the mouse. *Development* **132,** 5399–5409.

Tavendale, S. J., Mackay, S., and Smith, R. A. (1992). Oocyte numbers are reduced in developing mouse ovaries cultured in testis-conditioned medium. *J. Anat.* **180,** 289–296.

Teerds, K. J., and Dorrington, J. H. (1993). Localization of transforming growth factor β$_1$ and β$_2$ during testicular development in the rat. *Biol. Reprod.* **48,** 40–45.

Thisse, B., and Thisse, C. (2005). Functions and regulations of fibroblast growth factor signaling during embryonic development. *Dev. Biol.* **287,** 390–402.

Tickle, C. (2003). Patterning systems—from one end of the limb to the other. *Dev. Cell* **4,** 449–458.

Tilmann, C., and Capel, B. (1999). Mesonephric cell migration induces testis cord formation and Sertoli cell differentiation in the mammalian gonad. *Development* **126,** 2883–2890.

Trupp, M., Rydén, M., Jörnvall, H., Funakoshi, H., Timmusk, T., Arenas, E., and Ibáñez, C. F. (1995). Peripheral expression and biological activities of GDNF, a new neurotrophic factor for avian and mammalian peripheral neurons. *J. Cell Biol.* **130,** 137–148.

Tung, P. S., and Fritz, I. B. (1990). Characterisation of rat testicular myoid cells in culture: α-smooth muscle isoactin is a specific differentiation marker. *Biol. Reprod.* **42,** 351–365.

Uzumcu, M., Dirks, K. A., and Skinner, M. K. (2002a). Inhibition of platelet-derived growth factor actions in the embryonic testis influences normal cord development and morphology. *Biol. Reprod.* **66,** 745–753.

Uzumcu, M., Westfall, S. D., Dirks, K. A., and Skinner, M. K. (2002b). Embryonic testis cord formation and mesonephric cell migration requires the phosphatidyl 3-kinase signaling pathway. *Biol. Reprod.* **67,** 1927–1935.

Vainio, S., Heikkilä, M., Kispert, A., Chin, N., and McMahon, A. P. (1999). Female development in mammals is regulated by Wnt-4 signaling. *Nature* **397,** 405–409.

van der Wee, K., and Hofmann, M.-C. (1999). An *in vitro* tubule assay identifies HGF as a morphogen for the formation of seminiferous tubules in the postnatal mouse testis. *Exp. Cell Res.* **252,** 175–185.

Van Dissel-Emiliani, F. M. F., de Boer-Brouwer, M., and de Rooij, D. G. (1996). Effect of fibroblast growth factor-2 on Sertoli cells and gonocytes in coculture during the perinatal period. *Endocrinology* **137,** 647–654.

Vigier, B., Watrin, F., Magre, S., Tran, D., and Josso, N. (1987). Purified bovine AMH induces a characteristic freemartin effect in fetal rat prospective ovaries exposed to it *in vitro*. *Development* **100,** 43–55.

Visser, J. A., Olaso, R., Verhoef-Post, M., Kramer, P., Themmen, A. P., and Ingraham, H. A. (2001). The serine/threonine transmembrane receptor ALK2 mediates Mullerian inhibiting substance signaling. *Mol. Endocrinol.* **15,** 936–945.

Wall, N. A., and Hogan, B. L. M. (1994). TGF-β related genes in development. *Curr. Opin. Genet. Dev.* **4,** 517–522.

Western, P. S., and Sinclair, A. H. (2001). Sex, genes and heat: Triggers of diversity. *J. Exp. Zool.* **290,** 624–631.

White, A. C., Xu, J. S., Yin, Y. L., Smith, C., Schmid, G., and Ornitz, D. M. (2006). FGF9 and SHH signaling coordinate lung growth and development through regulation of distinct mesenchymal domains. *Development* **133,** 1507–1517.

Willerton, L., Smith, R. A., Russell, D., and Mackay, S. (2004). Effects of FGF9 on embryonic Sertoli cells proliferation and testicular cord formation in the mouse. *Int. J. Dev. Biol.* **48,** 637–643.

Wolf, U. (1999). Reorganization of the sex-determining pathway with the evolution of placentation. *Hum. Genet.* **105,** 288–292.

Wong, C.-H., Mruk, D. D., Lui, W.-Y., and Cheng, C. Y. (2004). Regulation of blood-testis barrier dymanics: An *in vivo* study. *J. Cell Sci.* **117,** 783–798.

Wordinger, R., Sutton, J., and Brun-Zinkernagel, A. (1990). Ultrastructure of oocyte migration through the mouse ovarian surface epithelium during neonatal development. *Anat Rec.* **227,** 187–198.

Wu, Z., Templeman, J. L., Smith, R. A., and Mackay, S. (2005). Effects of glial cell line-derived neurotrophic factor on isolated developing mouse Sertoli cells *in vitro*. *J. Anat.* **206,** 175–184.

Xavier, F., and Allard, S. (2003). Anti-Müllerian hormone, β-catenin and Müllerian duct regression. *Mol. Cell. Endocrinol.* **211,** 115–121.

Xia, H., Mao, Q., Paulson, H. L., and Davidson, B. L. (2002). siRNA-mediated gene silencing *in vitro* and *in vivo*. *Nat. Biotechnol.* **20,** 1006–1010.

Xia, Y., Sidis, Y., and Schneyer, A. (2004). Overexpression of follistatin-like 3 in gonads causes defects in gonadal development and function in transgenic mice. *Mol. Endocrinol.* **18,** 979–994.

Xie, Q., Mackay, S., Ullmann, S. L., Gilmore, D. P., and Payne, A. P. (1996). Testis development in the opossum Monodelphis domestica. *J. Anat.* **189,** 393–406.

Yamamoto, M., and Matsui, Y. (2002). Testis-specific expression of a novel mouse defensin-like gene, *Tdl. Mech. Dev.* **116,** 217–221.

Yao, H. H.-C., and Capel, B. (2005). Temperature, genes and sex: A comparative view of sex determination in *Trachemys scripta* and *mus musculus*. *J. Biochem.* **138,** 5–12.

Yao, H. H.-C., Whoriskey, W., and Capel, B. (2002). Desert Hedgehog/Patched 1 signaling specifies fetal leydig cell fate in testis organogenesis. *Genes Dev.* **16,** 1433–1440.

Yao, H. H.-C., DiNapoli, L., and Capel, B. (2003). Meiotic germ cells antagonize mesonephric cell migration and testis cord formation in mouse gonads. *Development* **130,** 5895–5902.

Yao, H. H.-C., Matzuk, M. M., Jorgez, C. J., Menke, D. B., Page, D. C., Swain, A., and Capel, B. (2004). *Follistatin* operates downstream of *Wnt4* in mammalian ovary organogenesis. *Dev. Dyn.* **230,** 210–215.

Yayon, A., Klagsbrun, M., Esko, J. D., Leder, P., and Ornitz, D. M. (1991). Cell surface, heparin-like molecules are required for binding of basic fibroblast growth factor to its high affinity receptor. *Cell* **64,** 841–848.

Ying, Y., Liu, X. M., Marble, A., Lawson, K. A., and Zhao, G. Q. (2000). Requirement of *Bmp8b* for the generation of primordial germ cells in the mouse. *Mol. Endocrinol.* **14,** 1053–1063.

Ying, Y., Qi, X. X., and Zhao, G. Q. (2001). Induction of primordial germ cells from murine epiblasts by synergistic action of BMP4 and BMP8B signaling pathways. *Proc. Natl. Acad. Sci. USA* **98,** 7858–7862.

Yoshioka, H., Ishimaru, Y., Sugiyama, N., Tsunekawa, N., Noce, T., Kasahara, M., and Morohashi, K. (2005). Mesonephric FGF signaling is associated with the development of sexually indifferent gonadal primordium in chick embryos. *Dev. Biol.* **280,** 150–161.

Zsebo, K. M., Williams, D. A., Geissler, E. N., Broudy, V. C., Martin, F. H., Atkins, H. L., Hsu, R. Y., Birkett, N. C., Okino, K. H., Murdock, D. C., Jacobsen, F. W., Langley, K. E., *et al*. (1990). Stem cell factor is encoded at the Sl locus of the mouse and is the ligand for the c-kit tyrosine kinase receptor. *Cell* **63,** 213–224.

Further Reading

Meng, X., Pata, I., Pedrono, E., Popsueva, A., de Rooij, D. G., Jänne, M., Rauvala, H., and Sariola, H. (2001). Transient disruption of spermatogenesis by deregulated expression of neurturin in testis. *Mol. Cell Endocrinol.* **184,** 33–39.

Sánchez, M. P., Silos-Santiago, I., Frisén, J., He, B., Lira, S. A., and Barbacid, M. (1996). Renal agenesis and the absence of enteric neurons in mice lacking GDNF. *Nature* **382,** 70–73.

This page intentionally left blank

Flagellar Length Control in *Chlamydomonas*—A Paradigm for Organelle Size Regulation

Kimberly A. Wemmer and Wallace F. Marshall

Department of Biochemistry, University of California,
San Francisco, San Francisco, California 94158

A fundamental unsolved question in cell biology is how the cell controls the size of its organelles. Cilia and flagella are an ideal test case to study the mechanism of organelle size control, because their size is easily measured and can be represented by a single number—length. Moreover, the involvement of cilia in many developmental and physiological processes suggests an understanding of their size control system is critical for understanding ciliary diseases, many of which (e.g., autosomal recessive polycystic kidney disease) are known to involve abnormally short cilia. The flagella of the model organism *Chlamydomonas reinhardtii* provide the best genetic and cell-biological system to study length control of cilia. Studies in this organism using genetics, biochemistry, imaging, and mathematical modeling have revealed many genes involved in length control of cilia and flagella, and have suggested several testable models for length regulation.

KEY WORDS: Primary cilia, Feedback control, Intraflagellar transport, IFT, Organelle abundance, Homeostasis, Noise, Nanotechnology. © 2007 Elsevier Inc.

I. Introduction

Great leaps in understanding cell biology have been occurring, yet we have only begun to understand the importance of organelle size control for the optimal functioning of cells. The organelles of a cell must be the correct size to perform their required functions or the biology of the cell will break down. In addition, organelle size also plays an important role in cell differentiation

and identity, with different cell types varying a great deal in their requirement for and use of organelles to perform their specific functions. The study of organelle size control will be crucial to a complete understanding of how cells function.

In addition to being able to regulate the overall size of the cell body (Morris, 2002; Umen, 2005), cells must have a way to control the abundance or quantity of each organelle within the cell. For most organelles, the abundance in a given cell will be a function of the number of individuals of each organelle present, and the size of each organelle. Depending on how size and number affect function, the cell might be more interested in controlling the size of individuals, or alternatively it might be more important to control the total abundance regardless of how this material is apportioned among the multiple copies of the organelle found within one cell. Flagella and the centrioles that nucleate them provide a very convenient approach to the study of organelle abundance, because they separate the two factors of number and size. The number of flagella in the cell is determined entirely by the number of centrioles that become active as basal bodies, and so flagellar abundance can be expressed strictly in terms of the size of the flagella. Conversely, centrioles are always the same size, and hence their abundance can be expressed strictly in terms of the number of centrioles present. Taken together, the centriole-flagella system allows the general problem of organelle abundance to be reduced into two distinct problems of size and number. It also turns out that flagella have special advantages as a system for the study of size, even apart from the fact that number need not be taken directly into consideration as it would for other organelles. To see this advantage, we first discuss an overview of organelle size control systems, before moving on to a summary of the specialized features of flagella that relate to size.

II. Size of Organelles

A. Size Control

1. Examples of Studies of Organelle Size Control

Very few studies of the mechanisms that determine size in eukaryotic organelles have been done. Size control has been studied for several viral and prokaryotic systems, especially bacteriophage tails, bacterial flagella, and flagellar hook structures. In these cases, identification of mutants affecting length has played a key role in suggesting possible mechanisms for length control. For instance, in bacteriophage, mutants in specific proteins result in defined reductions in length proportional to the size of the deleted region,

suggesting the gene products function as molecular rules (Katsura, 1990). In bacteria, length control of hooks and flagellar filaments has been studied by both genetic and math modeling approaches (Keener, 2006), resulting in a fairly detailed understanding of size control. However, these structures are exceedingly small, and one can legitimately ask whether the types of control systems that have evolved to regulate such small sizes can also work in the much larger organelles of eukaryotes.

The majority of cellular organelles are membrane-bound compartments with potentially complex three-dimensional (3-D) structures. The size of organelles tends to be consistent within a given cell type, and moreover is under a degree of cell-cycle dependent regulation (reviewed in Blank *et al.*, 2006). The endoplasmic reticulum (ER) serves as an excellent example. Although the structure is challenging to measure, an important insight has been gained from studies of the unfolded protein response (UPR), a molecular pathway that becomes activated when the ER is unable to properly fold proteins within its lumen. Activation of the UPR pathways causes induction of a large number of genes, some of which encode chaperones and other response proteins that directly cope with the unfolded proteins, but more interestingly, some of the UPR targets appear to be genes involved in ER biogenesis. Research has suggested UPR plays a normal role in controlling ER size, using folding of proteins effectively as a size sensor (Bernales *et al.*, 2006). The idea is, assuming secreted proteins are produced at a constant rate, then if the ER were to become too small to cope with these proteins, the UPR would trigger additional ER synthesis until the organelle became large enough to perform its task. This is an interesting system in which the organelle does not necessarily attempt to reach a defined size, but just a defined level of functionality depending on the particular requirements of the cell. This model suggests many interesting surprises may await us as we probe more deeply into the mechanisms controlling organelle size.

2. Flagella as a Model System for Size Control

However, this fascinating problem can be technically difficult to study, as determining the size of organelles is a very difficult problem. The organelles are complex 3-D structures contained within cell bodies and the simple act of measuring the dimensions of the organelles can be extremely challenging. Traditionally, measurement of size would require laborious serial-section electron microscopy (EM), followed by stereometric techniques to infer size descriptors such as volume and surface area based on the edges of the structure observed in individual sections. Use of electron tomography can simplify the task of measuring volume by directly acquiring the entire organelle, and the ability of tomography to be automated (Fung *et al.*, 1996) is gradually helping this approach to become more routine. However, it is still quite difficult, requiring substantial technical skills, and the thickness of sections that can be

imaged puts a strong upper limit on the size of an individual organelle that can be imaged entirely in a single tomographic data set. The fact that organelles in general have complex 3-D structures also creates a challenge for mathematical analysis—which number should one use to describe size? Surface area and volume are obvious measures, but other shape descriptors may also be necessary such as Gaussian curvature. We thus see that the inherent three dimensionality of most organelles makes the study of size control extremely challenging, both from a technical point of view and from a mathematical point of view.

By focusing attention on a single dimension, length, the problem of organelle size control can be vastly simplified. Although length control has been studied in a variety of structures, including bacteriophage tails and sarcomere spacing (reviewed in Marshall, 2004), we feel that flagella and cilia represent a particularly tractable situation for studying the mechanisms of biological length control. Flagella present an elegant solution to this problem as they protrude from the cell, away from the cell body, and thus are easy to image and observe. They are significantly larger than bacteriophage tails or bacterial hooks, obviating the need for EM—indeed it is easy to measure flagellar lengths even in living cells using the very simplest of light microscopes. They are also very easy to describe as their size changes in only one dimension, length, making this the only dimension in which measurements must be made to observe differences in total organelle size.

3. Studying Length Control in *Chlamydomonas*—the Green Yeast

This review focuses on studies of flagellar length control in the unicellular green alga *Chlamydomonas,* which is without question the most convenient model organism in which to study flagella. *Chlamydomonas* is sometimes referred to as green yeast because it has many of the same practical advantages for doing genetics as yeast, such as the ability to work with both haploid and diploid cells, tetrad analysis, growth as colonies on plates, and a rapid life cycle. However, unlike yeast, *Chlamydomonas* has flagella that are virtually indistinguishable from cilia and flagella in animal cells. This allows the powerful genetics of this organism to be brought to bear on questions of flagellar assembly and function, and for this reason most of what we know about flagellar assembly, including the polarity of assembly and the process of IFT, was first discovered in *Chlamydomonas* (see reviews by Dutcher, 1995; Silflow and Lefebvre, 2001). Consequently, there is a rich legacy of pre-existing mutants in *Chlamydomonas,* which affect flagellar assembly and length. These include *fla* mutants, which cannot assemble flagella at the restrictive temperature (Adams *et al.*, 1982), *lf* (long-flagella) mutants, which have abnormally long flagella (Asleson and Lefebvre, 1998; Barsel *et al.*, 1988; McVittie, 1972), and *shf* (short-flagella) mutants, which have abnormally short flagella (Jarvik *et al.*, 1984; Kuchka and Jarvik, 1987). Most of these mutants are

available from the NSF-sponsored Chlamydomonas Genetics Center stock collection. In addition to its genetic advantages, *Chlamydomonas* is also an excellent system for molecular biology, as it is easy to transform with DNA using simple methods (e.g., by electroporation), protein localization can be visualized using green fluorescent protein fusions, and gene expression profiles can be obtained using cDNA microarrays that have just become available. Completion of the *Chlamydomonas* genome, as well as establishment of a large database of EST sequences, has solidified this organism's position as the premier model system for studying flagellar structure and function.

B. Flagella and Cilia

The terms flagella and cilia refer to essentially identical organelles, and we will use the two terms interchangeably. Historically, *Chlamydomonas* researchers have used the term flagella exclusively, so we will use this term in this review. However, we urge the reader to use the term cilia whenever possible, to avoid confusion with bacterial flagella, which bear no relation whatsoever to eukaryotic flagella.

1. Structure and Composition

Flagella and cilia are microtubule-based structures consisting of nine doublet microtubules nucleated by modified centrioles known as basal bodies. The microtubule doublets extend from the cell, and are surrounded by an extension of the plasma membrane. These doublets are all oriented with the microtubule plus-ends located at the distal tip of the flagellum, and the minus-ends located at the basal body located at the cell surface (Fig. 1). The term axoneme describes the microtubule doublets themselves along with the structural components that hold them together. Cilia and flagella are highly conserved throughout evolution, appearing in virtually identical forms in vertebrates, invertebrates, algae, lower plants, and protists.

Although flagella and cilia are generally thought of as motile structures, many cells contain immotile cilia likely to play a sensory role (Marshall and Nonaka, 2006). For instance, a class of somatostatin receptors (Handel *et al.*, 1999) is located on immotile cilia in the brain. Indeed, most sensory input to an animal is provided via sensory cilia, including both olfaction and vision (rods and cones being, in essence, highly modified cilia).

2. Human Diseases Involving Length Control Defects

Given the near ubiquity of cilia and flagella in various tissues, it should not be surprising that many human diseases and their animal models appear to involve defects in cilia or flagella (Pazour and Rosenbaum, 2002). Examples include
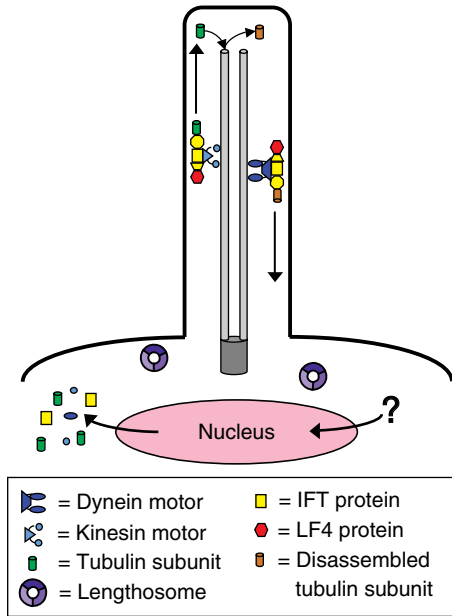
FIG. 1 Diagram of flagellum showing components involved in length control. Intraflagellar transport (IFT) proteins capture flagellar protein precursors from the cytoplasm and transport them to the tip of the flagellum, the site of turnover. This movement is driven by kinesin-II, and the retrograde movement of the IFT complexes back to the cytoplasm is driven by cytoplasmic dynein. IFT also transports the length-regulating kinase LF4, although the function of this protein in the length control system is not yet fully understood. Three other length control proteins, LF1–LF3, localize within the cytoplasm in a structure called the lengthosome. This complex somehow regulates length, but its mechanism is not known. Genes encoding flagellar proteins are upregulated when flagellar regeneration is triggered by deflagellation, implying that some sort of signal reaches the nucleus, but the nature of this signal is not known. Thus, although many of the key players are identified, the systems level question of how they act together to produce a well-defined length remains unanswered.

polycystic kidney disease (Haycraft *et al.*, 2001; Pazour *et al.*, 2000), biliary cystogenesis (Masyuk *et al.*, 2003), male infertility (Chemes *et al.*, 1990; Toyama *et al.*, 1996), situs inversus, chronic sinusitis (Toskala *et al.*, 1995), nephronophthisis (Otto *et al.*, 2003), and Bardet-Biedl syndrome (Ansley *et al.*, 2003). In many cases, disease pathology involves the presence of abnormally short cilia or flagella (Chemes *et al.*, 1990; Masyuk *et al.*, 2003; Ortug, 2003; Pazour *et al.*, 2000; Toskala *et al.*, 1995; Toyama *et al.*, 1996). This suggests that to understand, and possibly develop treatments for such diseases, we will need to understand not only what functions these cilia and flagella provide in human physiology, but also the mechanisms that specify their assembly and length determination. Because human cilia are highly homologous to *Chlamydomonas* flagella, both at the

level of ultrastructure as well as in terms of their molecular composition, it is to be expected that lessons learned from flagellar length control will be directly applicable to the study of human ciliary disease.

3. Intraflagellar Transport and Flagellar Assembly

Flagellar assembly is a particularly fascinating biosynthetic process because it occurs in a highly polarized manner (Johnson and Rosenbaum, 1992; Rosenbaum and Child, 1967). When flagella assemble, addition of new subunits (e.g., tubulin) occurs exclusively at the tip. In contrast, all protein synthesis occurs in the cell body, the flagellum being completely devoid of ribosomes. Therefore, flagellar precursor proteins must be transported to the distal tip of the flagellum where they are assembled. This transport is achieved by a process called intraflagellar transport (IFT, see Fig. 1) in which a pair of protein complexes (IFT complex A and IFT complex B) are moved from the cell body out to the tip by a kinesin motor and then returned to the cell body by cytoplasmic dynein (Cole, 2003; Scholey, 2003; Sloboda, 2002). The IFT protein complexes directly bind to flagellar precursor proteins in order to bring them to the tip (Qin *et al.*, 2004, 2005). At the tip, the A and B subcomplexes undergo a rearrangement ultimately activating cytoplasmic dynein 1b, which then brings the IFT proteins back to the base of the flagellum (Pedersen *et al.*, 2006). The process of IFT can be broken down into four distinct phases, that is, initiation of movement from the base, movement out to the tip, reversal of direction at the tip (accompanied by rearrangement of complexes), and then movement back to the base. These four phases can be measured in kymograph analyses, and it has been shown that mutants exist that differentially affect various phases (Iomini *et al.*, 2001). The molecules that regulate the switching between these phases remain unknown.

Although IFT and its role in flagellar assembly were first discovered in the green alga *Chlamydomonas,* the process is highly conserved and involves the same set of molecules in all organisms that have cilia or flagella, including humans.

Flagellar assembly at the tip not only occurs when the flagellum first grows, but also continues even after the flagellum has reached its final length (Marshall and Rosenbaum, 2001; Song and Dentler, 2001; Stephens, 1999). This steady-state assembly is necessary to balance a continuous removal of subunits from the tip of the flagellum that occurs even once the flagellum has reached its final length. The continuous assembly and disassembly at the flagellar tip result in continuous turnover at a steady state. The teleological purpose of this turnover is unclear, but it may have first evolved as a mechanism to allow disassembly of cilia and flagella prior to cell division (Grimes and Gavin, 1987; Parker and Quarmby, 2003). Flagella are normally present in cells during the G1 growth phase and are resorbed prior to mitosis.

Resorption can also be triggered by various chemical agents, and the mechanisms that mediate this resorption are currently the object of intense study (Pan and Snell, 2005; Parker and Quarmby, 2003), but one possibility is that it involves an upregulation of the underlying steady-state turnover rate. The steady-state assembly requires IFT to provide subunits for assembly (Adams *et al.*, 1982; Piperno *et al.*, 1996), and when IFT is turned off in full-length flagella, the flagellum immediately begins to resorb. Another interesting question is the mechanism of turnover. Flagellar axonemal microtubules are completely stable when isolated, suggesting they are not simply disassembling via conventional microtubule depolymerization. Instead, it appears tubulin turnover may involve exchange of tubulin at the junction between the two microtubules of the doublet (Stephens, 1999, 2000), via an unknown mechanism. It would be of great interest to identify the proteins that catalyze axonemal microtubule turnover, but so far there is no information about their identity. Given that the turnover occurs at the tip of the flagellum (Marshall and Rosenbaum, 2001), the disassembly machinery must be localized to the tip. It is known that the tip contains a morphologically distinct structure known as the "tip structure" (Dentler and Rosenbaum, 1977) but its composition or function is unclear. The microtubule plus-end tracking protein EB1 also localizes to the tip (Pedersen *et al.*, 2003), and this may play a role in regulating turnover, either directly or by recruiting other factors.

C. Phenomenological Studies of Flagellar Length Control

1. Measurement of Flagellar Length Distributions

Because flagella are so easy to observe, there is a wealth of quantitative information concerning flagellar length variations under different conditions. These experiments set the boundary conditions that any length control model must satisfy. Flagella are roughly 10- to 14-microns long, although their average length depends on time of day and cell cycle progression (Tuxhorn *et al.*, 1998). The fact that flagellar length is in a size range easy to measure using simple methods of light microscopy is one of the main reasons why this organelle is so useful as a model system to study size control.

The first fact established by observations of flagella is that length appears to be under tight control. Specifically, measurements of the distribution of lengths in a population of *Chlamydomonas* cells appear to indicate length must be actively adjusted. What, exactly, does this statement mean? Careful measurements on synchronized cells (gametes, for instance) show flagellar lengths have an approximately Gaussian distribution with an average length around 10 microns and standard deviation in length of approximately 1 micron. Similar distributions of ciliary lengths are seen in other organisms

(Wheatley and Bowser, 2000). The low coefficient of variation of these length distributions provide a visual impression that length control is somehow "tight" in the sense that the variation in lengths is less than what we might expect in the absence of a control system. Why is this? Consider the length distribution that would be expected if there was NO length control. Suppose flagellar precursor subunits were assembled randomly into the flagella. What length distribution would result? Simple calculations show the length distribution for a simple single-stranded linear equilibrium polymer should follow an exponential distribution, with the majority of the polymers having a short length (Nossal and Lecar, 1991). This would obviously not fit the Gaussian distribution seen in actual flagella. On the other hand, it is highly questionable whether a structure as complex as the flagellum should be considered a simple equilibrium polymer at all. Certainly a better approximation might be a multistranded dynamic polymer such as a microtubule, especially given experimental data that flagella are dynamic structures undergoing continuous turnover (Marshall and Rosenbaum, 2001; Stephens, 1999). Multistranded equilibrium polymers still show an exponential length distribution (Howard, 2001), as do dynamic polymers undergoing dynamic instability when confined within a cell, as judged by both experimental measurements and theoretical modeling (Dogterom and Leibler, 1993; Verde *et al.*, 1992). If a dynamic polymer is allowed to grow without bounds, the length distribution can begin to approach a Gaussian (Verde *et al.*, 1992), but theoretical models require such a distribution to have a constantly increasing average length over time (Verde *et al.*, 1992). The fact that *Chlamydomonas* cells arrested in their growth cycle (e.g., gametes), can maintain a Gaussian distributed length with a constant average length, indicates that the length distribution cannot simply be accounted for by the same mechanism that functions in individual microtubules. To summarize this discussion, our naive visual impression that length is somehow restricted in its variation by a specific mechanism is likely to be correct.

Two other important results are obtained from simple length measurements. First, although there is a certain degree of variability in lengths among a population of cells, the two flagella within a single cell are always more similar to each other than they are to the population in general. This suggests there might be an additional mechanism for equalizing lengths within one cell, above and beyond that involved in setting the length in the general population. It also suggests the dominant source of length variation in a population may be caused by cell–cell variation, as opposed to random temporal fluctuations within the activity of the length control system itself. Length variation is thus dominated by so-called "extrinsic" noise (Elowitz *et al.*, 2002). Second, flagellar lengths do not noticeably fluctuate in wild-type cells during a normal observation period. Upon extended observation, it can be seen that lengths gradually increase over the course of a day. It would be

interesting to know whether this is due to a simple increase in cell mass or biosynthetic capacity as the *Chlamydomonas* cell grows during the light phase, or whether instead this is due to a more direct influence of the cell cycle or circadian clock machinery on the length control system. Careful measurement of variation (i.e., noise) in flagellar lengths in *Chlamydomonas* cells grown under various conditions shows that there is a large reduction in the length variance when gametes are compared to asynchronously growing wild-type cells (our unpublished data). Because gametes are arrested in a G0-like stage of the cell cycle, this difference suggests variation in progression through the cell cycle is a major contributor to the extrinsic noise in flagellar length. Further evidence flagellar length is under specific control is obtained from other types of algal cells in which flagellar length varies reproducibly depending on the age of the basal body and cell cycle progression (Beech and Wetherbee, 1990; Lechtreck *et al.*, 1997). Such results indicate flagellar length must be under active control, and the basal body is able to exert an influence *in cis* on its associated flagellum.

2. Flagellar Regeneration

Much can be learned about a structure by watching how it is assembled. For most organelles, this is quite challenging because one cannot induce the organelle to form in a controlled fashion. Usually, the cell decides when it wants to build an organelle. One major advantage of flagella as a model system for organelle assembly is that one can, in *Chlamydomonas,* induce flagellar assembly in a highly defined and synchronous manner. This is because *Chlamydomonas* cells are able to sever their own flagella in response to a transient reduction in extracellular pH, a phenomenon known as flagellar autotomy. When cells are exposed to a pH shock, a complex signaling cascade is set in motion that ultimately leads to a katanin-mediated severing of flagellar axonemal microtubules. The flagellum is then shed into the media, and a new flagellum begins to grow. The flagellum generally shows a lag of up to 10 min before growth begins, and growth typically reaches full length in less than 2 h. An alternative way to induce flagella to grow is to start with cells grown on a plate of agar media. For unknown reasons, *Chlamydomonas* cells grown on plates have flagella that are extremely short or even lacking entirely. Once the cells are washed off into liquid media, they rapidly grow flagella reaching full length in less than half an hour.

The first insight one gains from observing flagellar regeneration is that flagella do not grow at a uniform speed. Plots of growth curves show flagella grow at their maximum speed when they first start growing, and then continuously slow down, so that they asymptotically approach their final length. Most of the growth is over within the first hour. This type of kinetics has given rise to several different interpretations. One interpretation is that

the slowdown in growth shows that flagella grow under the control of a negative feedback loop such that the growth rate is highest when the length is maximally far from the desired set-point, and then slows down as the set-point is reached. This interpretation seems unlikely to be true for the following reason. If cells are pretreated with cycloheximide, which blocks new protein synthesis, and then induced to shed their flagella, the new flagella that regenerate only grow to approximately half of the wild-type length. Thus, they are far from their normal set-point when they stop growing. Yet they show the same type of kinetics as normal flagella, with a rapid growth early on and a gradual approach to the final length over a roughly 1–2 hour period (Rosenbaum *et al.*, 1969). If the growth rate were simply set by a feedback control that measured distance from the set-point, then the slowdown in growth should only be observed when the flagella reach the set-point length, which they never do in the cycloheximide experiment. A second possible explanation for the observed kinetics might be that the induction of flagellar assembly activates a defined intracellular signaling program, which directly determines growth rate as a function of time. This also seems unlikely because when cells with half-length flagella, formed by regeneration in cycloheximide, are fused to wild-type cells, the wild-type cytoplasm allows the half-length flagella to grow to the wild-type length. When the growth kinetics in such experiments are compared to those in wild-type flagellar regeneration, the growth rate at any given point in the elongation process correlates exactly with the length reached at the point, and not with the time elapsed since induction of growth (Marshall *et al.*, 2005). The third interpretation is that growth rate is inherently length-dependent due to a length-dependence of intraflagellar transport. This possibility will be discussed in detail in the section on models for length control.

Interestingly, when cells first form flagella, they do so with a dramatically different type of kinetics. Madey and Melkonian (1990) measured flagellar outgrowth in *Chlamydomonas* cells after mitosis, before hatching from the mother cell wall would normally have occurred. They found in such cells, flagellar growth was completely linear, occurring at a constant, slow rate of 28 nm/min. This constant linear growth contrasts sharply with the decelerating growth seen during regeneration, and suggests a different assembly mechanism might be at work. One possibility would be flagellar assembly at this stage might be strictly rate-limited by a lack of a pre-existing pool of precursor protein. In this case, the assembly rate is never able to become large enough for the length-dependent effects of IFT to become apparent. Consistent with this idea, Madey and Melkonian (1990) found that the postmitotic flagellar growth phase could be completely arrested by addition of cycloheximide. Thus, there are two types of flagellar assembly kinetics, apparently depending on the degree to which a cell has accumulated a precursor pool. The presence of these same two types of growth kinetics has also been reported in the closely

related alga Volvox carteri (Coggin and Kochert, 1986) and is therefore probably a general phenomenon. It has been shown that flagellar growth in a related green alga, Spermatozopsis similis, occurs exclusively via an extremely slow linear kinetics (Schoppmeier and Lechtreck, 2003), suggesting that in this organism, unlike *Chlamydomonas,* IFT may either not be involved, or else be under dramatically different regulation. At the very least, the fact that the flagella grow so slowly in Spermatozopsis (about 1 micron/h, compared to *Chlamydomonas* in which a flagellum can grow to 10 microns in 20 min) suggests the growth mechanism in Spermatozopsis occurs via a distinct process. Although this means results in this organism cannot be directly used to test the mechanism of length control in *Chlamydomonas* (Beech, 2003), it suggests a careful analysis of what is actually occurring in Spermatozopsis, using genetic and biochemical methods, might eventually provide some extremely useful insights into length control.

   The second insight resulting from studies of flagellar regeneration is that when flagella elongate, they do so by adding new protein exclusively at their distal ends (Johnson and Rosenbaum, 1992; Rosenbaum and Child, 1967). This conclusion, reached by pulse-labeling cells undergoing elongation, would have been difficult to obtain had it not been so easy to induce flagellar growth at the time of ones choosing. Similarly, studies of mRNA levels as a function of time after flagellar regeneration begins, have revealed cells execute a complex program of transcriptional activation, with several hundred genes upregulated (Lefebvre *et al.*, 1980; Stolc *et al.*, 2005) leading to concomitant increases in protein levels of flagellar precursor proteins (Lefebvre *et al.*, 1978). Interestingly, when *Chlamydomonas* flagella are induced to elongate by addition of the drug lithium, this elongation also triggers induction of flagellar genes (Pena, 2005). Although the molecular pathway that regulates this gene induction program is unknown, mutants have been identified in which induction no longer occurs (Lefebvre *et al.*, 1988). It will be extremely interesting to learn the precise nature of the pathway that drives flagellar gene expression. Because most current methods used to study gene expression are based on analysis of whole populations of cells, the ability to induce synchronous flagellar regeneration in a whole population of *Chlamydomonas* cells has been invaluable for these studies. The role of this transcriptional program in length control remain unclear, given that cells in which protein synthesis is blocked are still able to reach a defined length, albeit one that is shorter than normal.

3. Flagellar Length Equalization

One of the most dramatic phenomena pertaining to flagellar length control is the equalization of flagellar lengths following a transient perturbation. This is observed experimentally by removing one of the two flagella from a cell,

and then observing the behavior in real time. Technically, the challenge to this experiment is how to remove just one of the two flagella. In some organisms with very large flagella, this can be done by direct micromanipulation (Tamm, 1967). In *Chlamydomonas,* this has been accomplished by blending a suspension of cells in a Waring blender. If the shear forces are adjusted properly, a significant fraction of the cells will shear off just one flagellum. After shearing, cells are examined under a microscope, and once a cell is found that has only one flagellum, it can be tracked over time to observe the behavior.

The behavior of cells from which one flagellum has been removed is quite remarkable, and has had a major impact on our conceptual view of flagellar length control as an active process. In such cells, the severed flagellum begins to regenerate, following similar kinetics to those seen in flagellar regeneration as previously described. However, while this growth is occurring, the other flagellum begins to shorten! The long flagellum continues to shorten while the regenerating flagellum grows, until they reach the same length. At that point, the two flagella grow out together. If cells are treated with cycloheximide, to poison new protein synthesis, then the two flagella will converge on the same length but will not undergo further growth. In some cases, the long flagellum overshoots the short flagellum transiently, but in such cases it eventually returns to the same length.

This ability of cells to equalize the lengths of their flagella has been taken to indicate the long flagellum somehow "knows" it is too long, or it is "instructed" by the cell to shorten. To some extent, this view was a byproduct of a mistaken idea of flagellar stability. Before studies of flagellar protein turnover were performed (Marshall and Rosenbaum, 2001; Stephens, 1999), it was generally assumed flagellar microtubules were perfectly stable (Tilney and Gibbins, 1968). This was thought to be the case because flagella do not disassemble when isolated *in vitro,* nor do they shorten when microtubule depolymerizing drugs are applied. If flagella are in fact stable, then the length equalization process would necessarily entail an activation of some disassembly machinery. However such a disassembly would not, or so the reasoning went, be active in the regenerating flagellum, or else it would not be able to grow. For this machinery to be activated in the long flagellum, but not in the short one, there must be a regulatory pathway differentially activated in the long versus the short flagellum. In other words, the long flagellum must know it is too long.

However this argument is based entirely on the mistaken view that flagella are static structures. The fact that flagella are dynamic structures, undergoing continual turnover, provides an alternative explanation for the length equalization. In a cell with two flagella, these two flagella are competing for a common pool of precursor protein. During flagellar regeneration, flagella grow extremely quickly when they are short, and grow with a decelerating kinetics such that their growth rate decreases as length increases. Because turnover continues even after flagella reach full length, the assembly rate

never quite becomes zero, but attains some small finite value to balance the ongoing removal during turnover. If one flagellum is suddenly shortened, it will grow with a much faster assembly rate than the full-length flagellum. Because when a flagellum grows, it incorporates precursor protein from the cytoplasmic pool, the rapid growth of the regenerating flagellum will necessarily choke off the supply of precursor from the longer flagellum. In essence, the short flagellum will be able to take more than its fair share of the cytoplasmic protein pool. This will then cause the assembly rate in the long flagellum to decrease to the point that it no longer balances disassembly during turnover, and as a result the flagellum will begin to shorten. The disparity in assembly rates will hold as long as the two flagella are of unequal length. Numerical simulations have shown that this type of mechanism can account for the length equalization seen in experiments (Marshall and Rosenbaum, 2001). Therefore, it can no longer be claimed that flagella know how long they are, in the sense of having regulatory pathways whose activity depends on length, simply on the basis of the flagellar length equalization experiments.

Another example of flagellar length equalization has been reported using mutant cells having recessive mutation that cause their flagella to be longer than wild-type. These mutants are discussed in detail in Section D. When these long flagella cells are fused to wild-type cells, it has been observed that the abnormally long flagella shorten until they reach the same length as the original wild-type flagella from the wild-type cell. In this case the length equalization is simply due to the fact that the mutations causing the abnormally long flagellar length are recessive, so that when mixed with wild-type cytoplasm, the recessive mutation is rescued and the length reverts to normal. This experiment, therefore, tells us something about the nature of the mutations, but certainly does not constitute evidence for an active length-change– inducing regulatory pathway within flagella. As with the length equalization experiments discussed in the preceding paragraph, the length equalization response in cell fusion experiments with long-flagella mutant cells has also been recapitulated using numerical simulations that rely only on turnover and do not invoke any specific signaling pathway (Marshall and Rosenbaum, 2001).

To summarize this section, we can say that flagellar length equalization is now understood to reflect that flagella are dynamic structures, undergoing continual turnover, and that their assembly rate depends on length.

D. Genetic Analysis of Flagellar Length Control

Whenever attempting to learn about a new biological system, one way to shine light into the "black box" is genetics. Genetic screens in *Chlamydomonas* have revealed a set of genes affecting flagellar length control.

1. Identifying Length Mutants in *Chlamydomonas* Genetic Screens

Because flagella drive *Chlamydomonas* cell motility, flagellar length defects can be isolated in motility screens. The general procedure is to mutagenize cells, pick individual colonies into tubes or microwells, and then examine cell movements under a dissecting microscope. This method has been used to identify both short-flagella mutants (Kuchka and Jarvik, 1987) and long-flagella mutants (Asleson and Lefebvre, 1998; Jarvik *et al.*, 1976, 1980; McVittie, 1972). Because this screening strategy requires each mutagenized colony to be individually examined by a human observer using a microscope, it is exceedingly tedious and difficult to perform on a large scale. Thus it seems likely the screens conducted to date are far from saturation, and many more long- and short-flagella mutants could be obtained if screening methods with higher throughput could be devised.

The difficulty of identifying long-flagella mutants by visual genetic screens has therefore prompted a search for more efficient strategies. In a very clever approach, Lefebvre's group noticed many long-flagella mutants also show reduced rates of flagellar regeneration after pH-induced flagellar autotomy. Based on this observation, they reasoned that long-flagella mutants could be enriched by first screening for mutants defective in flagellar regeneration, followed by a secondary visual screen for length alteration. Using this approach, coupled with a high-throughput screen for flagellar regeneration mutants, they were able to identify long-flagella alleles of a new gene, *LF3* (Barsel *et al.*, 1988). We note, however, that not all long-flagella mutants show such a delay in flagellar regeneration, indicating that a screen based on this criterion will not be able to identify all potential long-flagella mutants, but only those that have this additional phenotype. Therefore, a need still exists for a rapid and scalable screening method based on automated measurement of either flagellar length directly or of motility.

2. Phenotypic and Genetic Analysis of Long-Flagella Mutants

It is also important to consider phenotypes other than an overall increase or decrease in length. Indeed, if one considers that length is maintained by a control system, if the system were to be truly broken by a mutation, then one might expect that the predominant phenotype would be failure to maintain a unique consistent length. If a mutation causes all cells to shift to a new, longer length, this indicates that the length control system is still functioning, but has simply been reset to a new set-point. Such mutations would therefore reveal genes involved in setting the control point of the system, but not in the functioning of the system itself. Thus, the most interesting mutants would be those resulting in a randomization or increased fluctuation in length from cell to cell.

In fact, such mutations have been found, and interestingly, they appear to represent alleles of previously identified length genes. The original *lf2* and *lf3* alleles were all induced by chemical mutagenesis or UV and may not have resulted in null alleles. It turns out null mutations in the LF2 and LF3 genes result in a phenotype in which the average flagellar length is not particularly long. Instead, the main defect observed is that the flagellar lengths within a given cell are unequal, a phenotype known as unequal flagellar length (ULF). This was discovered in insertional mutagenesis screens for mutations that gave the *ulf* phenotype. Two ulf mutants identified in this screen, *ulf1* and *ulf3,* were found by genetic analysis to be alleles of LF3 (Tam *et al.*, 2003). These mutant cells mostly lacked flagella, and when flagella were present, they were of unequal lengths and, interestingly, shorter than the average wild-type length. It may at first seem puzzling or paradoxical that null alleles of a long-flagella gene have abnormally short flagella, but bear in mind that the main phenotype of *lf1, lf2,* and *lf3* mutants is the increased variability in length—the average length is actually not that much more than wild-type, and in a population of *lf* mutant cells, many flagella are quite short while others have unusually long flagella. This is true even in many original *lf* alleles. These results imply that the LF genes are affecting flagellar dynamics in a subtle way.

3. Intraflagellar Transport in Length Mutants

Given that intraflagellar transport is required to maintain flagellar length, it is obvious to ask whether any length mutants affect the process of IFT. Certainly, partial reductions in IFT do in fact result in shorter flagella, for instance *fla2* mutant cells, which have a reduced velocity of IFT particle motion at the permissive temperature (Iomini *et al.*, 2001) have flagella that are significantly shorter than wild-type (our unpublished observations). What about long-flagella mutants? In this case the evidence is much less clear, but IFT is so obviously a candidate for involvement in length control, that it makes sense to check whether known lf mutants might increase the rate of IFT. To some extent, this is like a drunk looking for his keys under the street lamp for the sole reason that this is where the light is brightest. Because we know more about IFT than we do about most aspects of flagellar assembly, it makes a good starting point for analyzing the effects of lf mutations. In any case, detailed information about how distinct alleles of the lf genes affect transport and turnover within the flagellum is likely to yield new insights into the length control machinery.

It has been demonstrated that flagella in LF3 null mutants show an increase in the quantity of IFT proteins relative to wild-type (Tam *et al.*, 2003). This result seems at first glance to explain the lf3 mutant phenotype: *lf3* mutant flagella have increased IFT, allowing them to grow more rapidly

to a longer final length. Unfortunately, this cannot be the whole story because the increased IFT protein levels were measured in an insertional allele of LF3 *(lf3–5)* in which flagella are actually shorter on average than wild-type. If increased IFT protein leads to a longer flagellum, why are the *lf3–5* flagella shorter? In actuality, the apparent increase in IFT proteins in lf3 mutants is potentially misleading. It has previously been shown, both by immunofluorescence and Western blotting (Marshall and Rosenbaum, 2001; Marshall *et al.*, 2005) that the quantity of IFT protein within the flagellum is independent of length, such that very short flagella contain the same total quantity of IFT protein as very long flagella. Consequently, in cells with short flagella such as those seen in *lf3–5,* the IFT proteins will always represent a disproportionate fraction of the total protein simply because their quantity per flagellum remains constant regardless of length whereas the total axonemal protein content per flagellum is reduced in shorter flagella, so that if Western blots are run loading the same total protein, as was done by Tam *et al.* (2003), one would expect any short flagella will show an increase in IFT. Therefore, the increased fraction of total protein represented by IFT proteins in the LF3 null mutant does NOT indicate that the LF3 gene product regulates IFT. Quite the contrary, this result suggests IFT levels are normal in the LF3 null mutant. It thus remains unclear how the lf3 mutation affects length. An interesting clue comes from extensive ultrastructural analysis of lf3 which revealed linear aggregates of material accumulating at the tips of the short flagella, like a bag full of toothpicks. Although the authors who conducted the study interpreted this material as IFT protein aggregates, it is equally possible that these linear structures represent defective assembly of axonemal components, suggesting a role for LF3 in regulation of assembly.

4. Length Control Proteins—Localization and Function

In addition to serving as tools to probe the behavior of the length control system, length mutants also allow us to identify the protein components of the system itself, once the genes are cloned. A major ongoing effort by the Lefebvre laboratory has resulted in the identification of all four LF genes. Both LF1 and LF3 are apparently novel genes (Nguyen *et al.*, 2005; Tam *et al.*, 2003). However, identification of the genes provides a foot in the door. For instance, epitope tagging has led to new and interesting information about subcellular localization. Both LF1 and LF3 appear to localize in the cell body rather than the flagellum, and both localize in a number of punctate foci. This suggests that LF1 and LF3, and possibly other length control proteins, colocalize together in a cytoplasmic substructure which has been dubbed the "lengthosome" (see Fig. 1). How the activity of the lengthosome functions to regulate flagellar length remains unknown.

LF4 was found to encode a protein kinase of the MAP kinase family (Berman *et al.*, 2003). LF4p localizes both to the cytoplasm and also within the flagellum and is apparently regulated by a phosphatase located within the flagellum (Wilson and Lefebvre, 2005). The fact that LF4 is a kinase indicates a signal transduction pathway is involved in length control. It is tempting to speculate that this might represent a feedback control pathway, in which a length sensor reads flagellar length, modifies the activity LF4 accordingly, and then LF4 signals to a downstream pathway that adjusts length. There is, however, no evidence so far that LF4 actually functions within a feedback loop. It is just as likely, a priori, that LF4 acts in an input pathway to the length control system, by which the cell can specify how long the flagella ought to be. The only evidence in favor of a feedback function, so far, is the presence of LF4 protein within the flagellum. This might seem hard to reconcile with a purely input-pathway function for LF4, unless LF4 has to carry its signal to the flagellar tip, for example, to provide its input to the pathway. It is clear further investigation of LF4 will be of great interest.

To summarize the genetic analyses of flagellar length control, four long-flagella genes have been cloned, LF1 through LF4, of which LF1–LF3 appear to localize together in cytoplasmic "lengthosome" complexes of unknown function, whereas LF4 is a MAP kinase that can be found within the flagellum. These genes provide a starting point to dissect the molecular pathway of length control. They also provide invaluable tools for testing potential models for the length-control mechanism.

III. Models for Flagellar Length Control System

Given the extensive set of genetic and phenomenological data that exist concerning flagellar length control in *Chlamydomonas,* this system represents a best-case situation for developing and testing mechanistic models for length control. In this section we consider five broad classes of theoretical length-control mechanisms that have been suggested to account for length control in various cellular systems (Marshall, 2004). We will consider which of these may be applicable to the specific problem of flagellar length control in *Chlamydomonas*.

A. Molecular Ruler

One mechanism used in length control is a molecular rule, in which a protein molecule is produced whose physical length matches the length of the structures whose size is to be controlled. One end of the ruler molecule is anchored at the point where the polymeric structure begins its self-assembly, and then

the other end tracks the growing end of the polymeric structure, either promoting assembly directly or acting as a protective cap to block access of the growing end to diffusible growth-inhibiting factors. This type of mechanism is clearly at work in the case of bacteriophage tail fibers (Katsura, 1990) and is also implicated in the control of actin filament length within striated muscles (Fowler *et al.*, 2006). The key prediction of a molecular ruler model is that a protein must be identified whose length matches the assembling structure. Such a protein has not yet been identified for the flagellum, although we must admit failure to discover something hardly constitutes proof of its nonexistence. In general, though, molecular rulers tend to be employed for size control in small structures less than a micron long, which makes sense given that the size has to be set by a single protein, and there is a limit to how long a protein can be. Again, though, we do not strictly know what this limit is. Moreover, there are ways to get around the need for a single long protein— one can theorize vernier-type mechanisms where a pair of proteins of slightly different length assemble alongside one another and only when their two ends line up flush with each other can they recruit a factor to define the assembly termination point. In this case, the length is set by the least common multiple of the lengths of the individual elements. In such a vernier system, it might be very hard to know a priori that a given protein is part of the vernier system, because it would assemble alongside the axoneme and to all intents and purposes be part of it. Because the component proteins of a vernier ruler would not have to be particularly long, there is no obvious feature that would reveal them to us.

Is there any conceivable way to rule out a ruler model then, given that we cannot rest on the absence of direct demonstration of the ruler itself? One approach is theoretical, as described by mathematical analyses of the ruler mechanism (Wagenknecht and Bloomfield, 1975); the distribution of lengths produced by a ruler shows a very skewed distribution. Conceptually this can be understood because a protein has a certain degree of flexibility, hence the ruler protein can sometimes flex to a shorter end-to-end length, allowing structures of a reduced length to form with some probability. There is a hard cut-off at longer lengths, however, because there is a limit to how far the ruler can stretch. This leads to a distribution skewed to shorter lengths. Our own measurements (W. Marshall, unpublished data) show flagellar length distributions in wild-type *Chlamydomonas* cells show an essentially Gaussian distribution, based on statistical calculations of skew and kurtosis. This would seem to rule out ruler models of the simplest type based on a single long flexible ruler protein.

However, for a vernier system that coassembles alongside the highly rigid axoneme, it is unlikely that shorter structures can be produced. Moreover, if the ruler acts by interacting with a diffusible effector, it might simply set the mean value of a Gaussian distribution of sizes whose variance is determined by the diffusion constant of the diffusing effector. It is thus not possible to completely rule out a ruler model by this type of measurement.

A better argument against rulers is the fact that in a population of cells, flagellar lengths can vary by 1–2 microns. Moreover, even in a single cell, the length varies during the course of the day. Length is also reduced when cells regenerate in the absence of protein synthesis as discussed earlier in the chapter. It is quite hard to reconcile these results with a single fixed-ruler mechanism. One would have to propose that a ruler or vernier undergoes changes from cell to cell, throughout the day, and in response to changes in protein levels. While a suitably baroque model could probably be devised to incorporate all of these effects, Occam's razor suggests our time is better spent evaluating alternative length control methods.

B. Quantal Production

The second type of mechanism we consider is the quantal production of limiting precursor. In this model, there is one (or possibly more) key structural protein constituent of the flagellum whose quantity is limiting. When a cell initiates formation of a flagellum, a certain quantity of this precursor is synthesized, and then it is incorporated into the growing flagellum. In this model, flagellar growth ceases when the quantity of this limiting precursor is exhausted. Supporting evidence for this type of model comes from experiments in sea urchin cells (Norrander *et al.*, 1995; Stephens, 1989) in which the level of tektin synthesis was found to correlate with the length of cilia in various cells. However, correlation does not prove causality and from this data alone it would be equally plausible that protein production is sensitive to the length or growth of the flagellum.

Direct evidence against the limiting precursor model comes from experiments in *Chlamydomonas* in which cells regenerate flagella in the presence of cycloheximide. In such experiments, flagella do in fact regenerate, albeit to approximately half the normal length. This demonstrates that even after flagellar assembly is completed, the cytoplasm retains a sufficient quantity of all precursor proteins to produce two half-length flagella. Therefore, there cannot be a limiting precursor whose consumption sets the final flagellar length.

Further evidence against the quantal production of limiting precursor model comes from experiments with *Chlamydomonas* mutants having variable numbers of flagella (Kuchka and Jarvik, 1982). Such mutants are called *vfl,* which stands for "variable flagella." In the Kuchka and Jarvik study (1982), vfl2 mutant cells having a variable flagellar number between 1 and 4 were examined. If cells produced a fixed limiting quantity of a key precursor that was completely consumed during the process of flagellar growth, then the combined lengths of all flagella in a single cell must add up to the length of a flagellum that could be constructed from this limiting precursor quantity

in a cell with a single flagellum. Hence, cells with two flagella should have flagella half as long as cells with a single flagellum. Flagella would be one third as long in cells with three flagella, and one quarter as long in cells with four flagella. This geometric dependence of length on flagellar number was not, however, observed. Instead, the lengths of the flagella decreased only slightly as their copy number increased. More extensive measurements on three different vfl mutants *(vfl1, vfl2,* and *vfl3),* including measurements under different fixation conditions and in living cells, have confirmed that the dependence of flagellar length on number does not match the geometric dependence predicted by the limiting precursor model (Marshall *et al.*, 2005).

Finally, one can ask whether a limiting precursor model can account for altered lengths in shf or lf mutants. In the context of this model, an lf mutant would increase length by generating increased levels of precursor protein. Such an increase has not been detected by Western blot analysis with known flagellar proteins. It could be argued that one might only see a major increase in protein quantity in those particular cells that make long flagella within a mixed population of lf cells showing a high variance in length, some short, some long. Because standard biochemical analyses are population-based, they could not detect such a phenomenon at the level of the single cell and might fail to see a significant difference at the population level. We can, however, rule out this possibility by another experiment. If an lf mutant makes a drastically larger quantity of a key precursor protein, then if such cells were fused to wild-type cells, the increased precursor levels in the combined cytoplasm should result in a cell with four longer-than-normal flagella. In fact, when lf mutants and wild-type are fused, the two long flagella rapidly revert to wild-type length (Barsel *et al.*, 1988). This argues against the idea of a dramatically increased level of a specific precursor protein in such mutants, even if the increase is only seen in a few individual cells. It thus appears the quantal precursor model is not compatible with the observed genetic and phenomenological data.

C. Cumulated Strain Model

A model has been proposed for bacteriophage tail length control, which theorizes that as additional subunits polymerize onto the growing structure, they undergo an increasingly great conformation alteration, such that the free energy of binding is gradually reduced by a constant increment (Kellenberger, 1972). This model, known as the "cumulated strain model," has been investigated mathematically by Wagenknecht and Bloomfield (1975), who demonstrate that it can lead to an extremely tight distribution around some defined length, using biologically realistic parameters. Their model indicates that for a given precision of length control, the free energy change needed to explain that

control becomes less and less as the number of subunits increases. Their model can account for length control in a phage tail with fewer than 100 subunits without invoking an unreasonable change in binding energy. Therefore, the change in energetics needed to fit length control in flagella, which contain tens or hundreds of thousands of subunits (depending on whether one considers a subunit a tubulin dimer or a whole 96-nm repeating unit of axonemal structure) will be even less, and therefore certainly within a physically possible realm.

The cumulated strain model is thus capable, in theory, of producing the degree of length regulation (in terms of the standard deviation of the length) observed in real flagella, at least in the sense that the change in free energy of binding that would have to be invoked will be extremely small. So, the model will not violate the laws of physics, which is of course important. But a somewhat more stringent test is to ask whether this model can account for all phenomenological and genetic data discussed in Sections II.C and II.D. The cumulated strain model predicts that if the ratio between the total quantity of monomer and the number of initiation sites (basal bodies, in our case) is altered, the length should change in defined ways (Wagenknecht and Bloomfield, 1975). Specifically, when the ratio drops, the length should decrease in proportion to the change in the ratio. This predicts cells with two basal bodies should have flagella twice as long as those with four, a prediction that is not borne out by experiments with vfl mutants (Kuchka and Jarvik, 1982; Marshall *et al.*, 2005). Thus, this model fails the same test that excluded the quantal production model.

We can also consider whether the cumulated strain model can account for the known *shf* and *lf* mutants. The only parameters that can really be changed in the model are the free energy change during successive polymerization steps, and the total quantity of monomer present. Therefore, if a length mutant is to result in altered length, it must change one or the other of these quantities. It is not obvious how proteins such as lf3, whose products localize to the cell body and are not components of the flagellum itself, could alter the binding energy of flagellar protein subunits. This leaves the alternative, that the lf and shf mutants alter the quantity of one or more key flagellar protein subunits. An interesting result of the analysis of the cumulated strain model, as shown by Wagenknecht and Bloomfield, is that although reductions in monomer quantity lead to pro-portional reductions in length, increases do not. The cumulated strain model is highly resistant to length increases beyond the normal length, such that to generate a detectable increase in average length, concentrations of monomer must be increased by several orders of magnitude. Such increases are simply not seen in lf mutants for flagellar proteins in general—for instance, tubulin does not appear to be made in significantly larger quantities in lf mutants. Strictly speaking, however, it is possible one or more unknown proteins are playing a key role in limiting length, and without a specific antibody to detect them, we might have no way of knowing whether they are suddenly produced in much greater

quantities in an lf mutant. But as with the quantal precursor model, the fact that lf mutant cells with long flagella undergo rapid flagellar shortening to wild-type length when fused with wild-type cells, strongly suggests they do not contain elevated precursor levels. Therefore, it seems difficult to make the cumulated strain model work out in the context of long-flagella mutants.

Overall, the cumulated strain model is difficult to reconcile with specific experimental details of flagellar length control, at least in its simplest form. Whether a more generalized version of the model, perhaps with a different dependence of binding energy as a function of polymerization extent, could overcome these problems, remains to be seriously explored.

D. Feedback Model

A fourth type of length control system one could envision is a feedback control system. In this mechanism, a signal transduction pathway somehow senses the length of the flagellum, and then acts to modulate the assembly process to attain the correct length. For instance, a length-sensing pathway could inhibit IFT when the flagellum is too long, or upregulate IFT when the flagellum is too short. For such a system to produce a flagellum of a defined length, the feedback would have to be negative. Thus, a length-sensing pathway, if it acted upon IFT, would have to inhibit IFT as length increases. Feedback control systems are common in man-made devices, and are known to confer desirable properties of stability and robustness.

Feedback control requires a length sensor to provide the initial input into a signal transduction cascade that ultimately impinges on flagellar assembly machinery. How might length be sensed by a molecular mechanism? One proposal (Rosenbaum, 2003) is that flagella may contain a length-dependent number of calcium channels, so that the total calcium current through the flagellar membrane would be length dependent. How calcium fluxes might lead to changes in flagellar length is unclear but could involve one or more of the known calcium-dependent phosphorylation events that occur within flagella (Bloodgood, 1992). This model is consistent with measurements showing that the number of calcium channels in the flagellar membrane of *Chlamydomonas* is proportional to flagellar length (Beck and Uhl, 1994). However, as with the studies of tektin levels, correlation does not prove causality, and so it is just as likely that length affects channel number rather than vice versa. An alternative model for measuring length would be to attach a molecular timer, such as a G-protein, to the IFT complexes, load it with GTP using a GEF at the basal body region, and then check the nucleotide state of the G-protein upon the return of the IFT complex from the flagellum. If the round-trip time for a wild-type length flagellum is comparable to the GTPase rate of the G-protein, then deviations in length would result

in measurable changes in the GTP/GDP ratio which could in turn modulate the activity of a length-sensitive signal transduction cascade. Many other such models can be easily proposed, but the problem is finding a way to test them.

Ultimately, the only way to determine whether a feedback control loop is involved in length control is to identify the potential signaling pathway and then test whether it is activated in a manner consistent with overall negative feedback. The most likely candidate for a length-responsive signaling molecule is the LF4 kinase (Berman *et al.*, 2003). As discussed earlier, lf4 mutants have abnormally long flagella. The mere fact that a kinase like LF4 results in a length change when mutated, does not by any means prove it is part of a feedback loop. For example, one could speculate the LF4 kinase might instead be present to allow the cell to alter the length of its flagellum in response to various environmental or developmental cues. The feedback control model does, however, make some simple predictions about LF4 that can be tested. Loss-of-function mutations in LF4 lead to increased flagellar length, hence the normal function of LF4 must be to oppose net flagellar assembly. Therefore, for this molecule to act in a negative feedback loop, its own activity must be an increasing function of flagellar length. In other words, LF4 kinase must be activated when flagella are too long, and inactivated when flagella are too short. It is thus conceptually straightforward to test whether LF4 is part of a length-sensing feedback loop—one has only to measure the activation state of LF4 as a function of flagellar length. However, this measurement has not yet been reported. If the activity of LF4 is not in fact length-dependent, then it cannot be acting in a feedback loop. Other possible signaling molecules involved in length control have been revealed by pharmacological studies (Wilson and Lefebvre, 2004). However the same caveats apply to these studies as to LF4—the detection of a signaling molecule does not prove it acts in a feedback pathway. To support such a claim, the pharmacological drug targets must be definitively identified (not a simple task in most cases) and then the activation state of these targets measured as a function of flagellar length and compared to the behavior required by the negative-feedback constraint. Nevertheless, the identification of signaling molecules that impinge upon length control, primarily due to the groundbreaking work of Wilson and Lefebvre, is a major step forward because it leads to readily testable hypotheses about the molecular mechanism of length control.

E. Balance Point Model

A simple model for length control has been proposed that does not require an explicit length sensor or signaling pathway (as in the feedback model). This model is based on the observation in *Chlamydomonas* showing axonemal microtubules undergo continuous turnover at their distal tip, and this turnover is balanced by new assembly, which in turn requires intraflagellar

transport (Marshall and Rosenbaum, 2001). The rate of disassembly at the tip appears to be independent of length. Further analysis of IFT particles revealed the number of IFT particles per flagellum is independent of length (Marshall and Rosenbaum, 2001; Marshall *et al.*, 2005). If a fixed number of transport particles are forced to move over a greater and greater length, the rate at which they can drop off cargo to the tip and return for another load will decrease. Eventually, when the flagellum gets long enough, transport will no longer be efficient enough to balance disassembly, and the flagellum will have to shorten. It has previously been remarked that the deceleratory kinetics of flagellar regrowth in *Chlamydomonas* require a reduction in IFT as elongation progresses (Beech, 2003). In our model, this reduction occurs via simple physics—when a fixed number of IFT complexes, traveling at a fixed velocity, then it takes them longer and longer to complete a transport cycle as the flagellum elongates. No special signaling or regulation is required apart from the obvious fact it takes longer for a moving object to travel a greater distance. The model as formulated is a macroscopic model, phrased in terms of lengths and rates. A more detailed microscopic model that describes the behavior of individual molecular components, has been evaluated and shown capable of producing a stable steady-steady state length (Bressloff, 2006), confirming the balance point model is at least theoretically reasonable.

This model predicts that the flagellum will reach a unique length defined by a balance-point between length-independent disassembly and length-dependent assembly. This model can account for many observed aspects of length control, for instance the dependence of flagellar length on number in vfl mutants, the growth kinetics upon resumption of growth in half-length flagella, the ability of flagella to equalize their lengths when one flagellum on a biflagellate cell is severed, and the shortening kinetics of long-flagella mutant cells when fused to wild-type cells (Marshall, 2005; Marshall and Rosenbaum, 2001). For two of these experiments, previous publications had presented data that appeared to be inconsistent with the balance-point model. A previous study (Kuchka and Jarvik, 1982) reported flagellar length does not depend on number, however the data reported in that paper actually show just the opposite and confirm a report (Marshall *et al.*, 2005) that cells with more than two flagella have a reduced flagellar length. Kuchka and Jarvik's data suggested cells with one flagellum and cells with two flagella had equal lengths, but additional data suggests this is not generally the case (Marshall *et al.*, 2005). A previous study suggested that when flagella arrested at half-length resume growth by restoration of wild-type gene function to a shf mutant, that these flagella initially grow with the same rate as a wild-type flagellum growing starting at zero length (Jarvik *et al.*, 1984). This suggests that growth rate is a function of time after growth induction, and not a function of length as predicted by the balance-point model. However, re-examination of the published data suggested an erroneous value for

wild-type growth rates, and when these experiments were repeated in two different ways, in all cases the results support the model that growth rate depends strictly on length (Marshall *et al.*, 2005). Thus, we conclude that the balance point model is compatible with all known phenomenological experiments on flagellar length regulation.

The balance point model also accounts for the possibility of shf and lf mutants. In this model, shf mutants can arise in either of two ways: either the rate of turnover is increased, or the rate of transport is decreased. Confirmation of this latter possibility has been obtained by creating a partial reduction in IFT. This partial IFT reduction was achieved by growing temperature-sensitive fla10 mutants cells, carrying a conditional mutation in the fla10 kinesin that drives IFT, at a temperature intermediate between fully permissive and fully nonpermissive. It was confirmed by western blot analysis that such flagella contain a reduced quantity of IFT protein (Marshall *et al.*, 2005). This reduction in IFT was observed to produce a stable, persistent shift in length to a new length roughly half that of wild-type cells (Marshall and Rosenbaum, 2001). This directly demonstrates that the shf phenotype can be obtained by reduction in intraflagellar transport, which is a prediction of the balance point model but NOT of any of the other models. We especially note that feedback control systems, when present, are able to maintain a stable set-point even when the underlying process is perturbed (e.g., a thermostat can maintain room temperature even if the radiator is partially blocked by furniture, because it will lead to increased furnace activity to compensate). The fact that reduction in IFT levels leads to a decreased length is thus compatible with the balance point model but not the feedback control model.

The lf phenotype can also be explained by the balance point model. Again there are two possibilities: a long flagellum can be generated either by a reduction in the rate of turnover or an increase in intraflagellar transport. The first possibility is potentially the case for lf2 mutants based on experimental measurements of tubulin dynamics in such mutants having shown them to have a reduced rate of turnover at steady state (Marshall and Rosenbaum, 2001). Similarly, the NIMA kinase Cnk2 exerts an influence on flagellar length apparently, at least in part, by modulating the disassembly rate (Bradley and Quarmby, 2005). In contrast, the long-flagella mutant lf4 does not appear to alter its rate of turnover compared to wild-type (Song and Dentler, 2001) suggesting lf4 flagella are long for some other reason.

This model therefore seems capable of explaining all known experimental data concerning flagellar length control. However, the model faces one serious problem. The balance point model of length control requires the number of IFT particles active in the cilium be held constant. This prediction raises two questions: first, is it actually the case that the number of IFT proteins is constant, and second, by what possible mechanism could this constant quantity be achieved? Direct measurements, including both biochemical analysis of protein levels on Western blots (Marshall *et al.*, 2005),

quantitative measurements of immunofluorescence intensity (Marshall and Rosenbaum, 2001), and counting of IFT particles by immunofluorescence microscopy (Marshall *et al.*, 2005), all show the quantity of IFT protein complexes within the flagellum is independent of length. Particle counting analysis indicates the number of particle aggregates is roughly eight on average, with a range of between seven and nine from cell to cell. How can an organelle count the number of particles within it? Kymograph data suggests a remarkably simple model for particle counting. As indicated in Fig. 2B, William Dentler (Dentler, 2005) has shown beautiful kymographs of IFT particle aggregates moving up and down within the flagellum in *Chlamydomonas*. His images strongly suggest that individual IFT particle aggregates move up and down within the flagellum without leaving it, because all of the kymograph traces of a particle moving upwards begin at the end of a trace of a particle moving downwards. Traces indicative of new particles being injected into the flagellum, which would not originate at the end of a downwards trace, were not observed in his images. These considerations suggest IFT might resemble a subway, in which passengers (cargo) come and go to and from the station (basal body) to ride on the trains, but the trains themselves simply go back and forth between stations, never leaving the tracks (flagellar outer doublets). It is also possible the exit of retrograde IFT particles from the base of the flagellum is tightly coupled with the entry of new IFT particles, such that an uninterrupted kymograph trace results. Distinguishing these two possibilities will require photobleaching analysis of particle turnover in live cells. These kymograph results have many caveats, the most serious being that one cannot tell precisely what a given DIC trace actually represents. We would most especially like to know what fraction of the total IFT proteins in the flagellum are present in the large visible traces, and what fraction are invisible to the method. Nevertheless, taking this data at face value, it is at least suggestive of a rather tight association of IFT complexes with outer doublet microtubules *in vivo*.

Electron micrographs of cross sections through *Chlamydomonas* flagella invariably reveal the IFT particle aggregates as long chains of protein tightly apposed to the B tubule of the outer doublet. Given this intimate association of IFT particles with the outer doublets, data showing that particles move back and forth without leaving the doublet to which they are attached, and the fact that the number of IFT particle aggregates observed by immunofluorescence is approximately equal to the number of outer doublets in the flagellum, we propose a simple mechanism to control particle number.

As illustrated in Fig. 2B, we suggest that each outer doublet interacts with a single IFT particle raft. This raft moves back and forth within the flagellar compartment, picking up new cargo at the base and depositing cargo at the tip, without ever leaving the flagellum. The IFT rafts thus behave analogously to elevators moving up and down in an elevator shaft. The entire flagellum thus behaves like an elevator core with nine elevator shafts. To keep the number of IFT particle rafts constant at nine per flagellum, it is only necessary

A

B
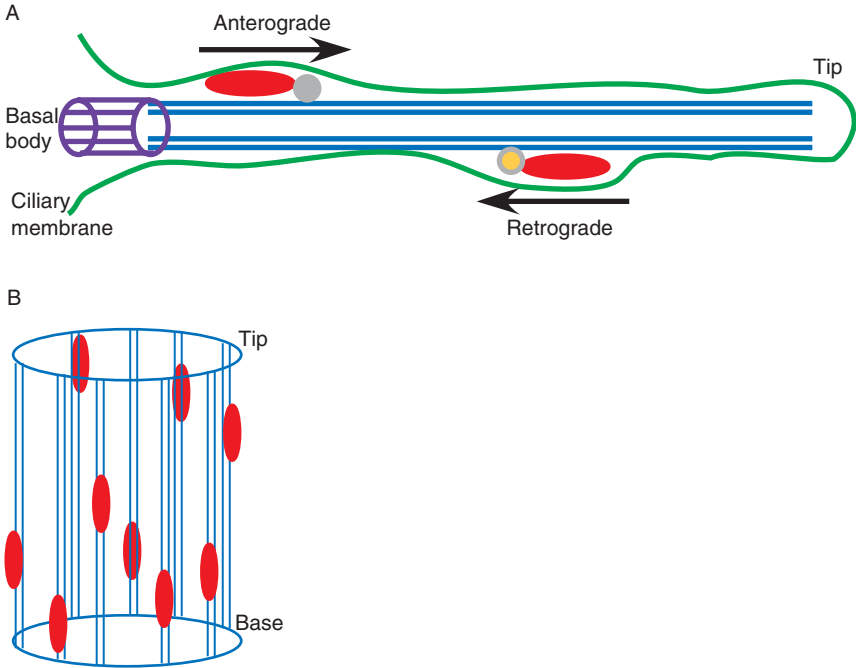
FIG. 2 Length-independent regulation of intraflagellar transport—the elevator model. (A) Schematic of cilium, showing basal body embedded in cell cortex (purple) and ciliary membrane (green), which is topologically contiguous with plasma membrane but with a distinct lipid composition. IFT particles (red) are pulled by heterotrimeric kinesin-II (gray) in the anterograde direction, and by cytoplasmic dynein (orange) in the retrograde direction. Cargo proteins such as tubulin are bound by the IFT particles and brought to the tip, where they are assembled onto the growing end of the axoneme. (B) Elevator model. Each outer doublet has a single IFT particle aggregate attached to it, which moves up and down from base to tip and back, like an elevator moving between floors. A defined copy number of nine aggregates per flagellum is thus attained if each doublet recruits exactly one aggregate. This could either be established during initial assembly or maintained by a timer that injects new particles onto unoccupied doublets.

for the flagellar pores (Deane *et al.*, 2001) at the base of each doublet to monitor the presence or absence of an IFT particle raft on the doublet. A doublet lacking a raft would signal the pore to inject another IFT particle raft. The main feature of this model is that it solves the problem of how a flagellum can count to nine—it simply has to count to one, nine times. How does the flagellar pore recognize when it needs to inject an IFT particle? The simplest way would be for retrograde particles to interact with the pore in such a way as to inhibit further introduction of new IFT particles. This would explain why IFT particles accumulate in retrograde IFT mutants—although particles enter the flagellum, because they cannot return to the base, the

flagellar pore "thinks" there is no particle raft on its corresponding outer doublet, so it lets in another bolus of IFT protein. This model easily accounts for the fact that retrograde IFT mutants accumulate IFT proteins in their flagella—the lack of returning retrograde particles would be interpreted by the flagellar pore as a lack of active IFT, and in response the pore would inject additional IFT particles, leading to an eventual accumulation.

As previously mentioned, it is also possible IFT particles enter and exit the flagellum, but that entry and exit are coupled, and in this case the elevator model still works, because if entry of a new particle is coupled to exit of an old particle, the number of particles would never change. This alternate form of the model would, however, have difficulty accounting for the accumulation of IFT particles in a retrograde mutant. This model, which we emphasize is purely speculative at the moment, makes the prediction that length-altering mutations could occur in components of the flagellar pore apparatus.

One conceptual advantage of the balance-point model is that the constant ongoing turnover could potentially allow rapid readjustment of length in response to cellular signaling cues. For instance, cells resorb their flagella prior to division. Studies in *Chlamydomonas* suggest that this resorption involves intraflagellar transport, either as a trigger for increased disassembly or severing (Parker and Quarmby, 2003) or as part of the disassembly machinery itself (Pan and Snell, 2005). We also note that in the balance-point model, the basal body plays a key role, potentially controlling the entry of both IFT proteins and flagellar precursor proteins into the flagellum. Thus, modifications or regulation of activities localized to the basal body would be expected to result in changes in flagellar length. This could provide a simple explanation for the fact that many cell types can possess flagella of different lengths depending on the maturation age of the corresponding basal bodies (Schoppmeier and Lechtreck, 2003).

IV. Conclusion: What Have We Learned from Flagellar Length Control?

Although flagellar length control in the green alga *Chlamydomonas* is a fascinating biological puzzle, we anticipate that the lessons learned from studying this simple and tractable system will be readily extendible to other contexts.

A. Length Control as Pharmacological Target for Ciliary Disease

As noted in the first section of this review, ciliary diseases in humans are often characterized by short cilia, rather than a complete absence of cilia. The degree to which an abnormally short cilium is detrimental may depend on the function of

the cilia in a particular tissue. For motile cilia, that need to move fluid via their own motility, reduced length is obviously a severe problem. The same is true of mechanosensory cilia, such as those of the kidney—a shorter cilium will have different mechanical properties, and is likely to produce less bending at the base in response to a given rate of fluid flow. For chemosensory cilia, short or stumpy cilia may have less surface area into which receptors may embed. They may thus lack the sensitivity of a longer cilium. In all cases, shorter cilia are likely to have reduced, but not eliminated function. This partial function may be the reason the disease results in symptoms at all—a disease mutation resulting in a complete loss of cilia is most likely to be lethal in early development.

Given that abnormal ciliary length may underlie many human ciliary diseases, what can we do about it? The fact that mutants with abnormally long cilia exist suggests that if pharmacological interventions can be devised to induce an increase in ciliary length, these could be used to treat ciliary diseases with short cilia. For instance, assuming the balance point is correct, a disease caused by a partial reduction in IFT, which would tend to cause a shortening of cilia, could be compensated by a chemical therapy that inhibits turnover. Similarly, the molecular signaling pathways that lead to increased length, such as the LF4 pathway, provide potential targets for drug development—a chemical inhibitor of LF4 ought to lead to an increase in ciliary length.

To implement this general scheme for treating ciliary disease, there are two major requirements. First, it is important to determine the extent to which the length-control machinery in human cells matches that of *Chlamydomonas*. This is simply a question of repeating, in human cells, the types of experiments described earlier in algae. It will be especially interesting to see whether reverse genetic knockdown of the human homologs of the LF genes will produce a similar increase in length of primary cilia. Second, efficient and highly parallelizable assays will be needed to allow high throughput screening of compounds for a potential effect on length. By combining green fluorescent protein (GFP) constructs specifically targeted to cilia, with automated high throughput imaging devices, it should be possible to rapidly screen through hundreds of thousands of compounds to identify candidates for further study.

B. Flagellar Length Control as Paradigm for General Organelles

A major reason for studying flagellar length control is that the ease of analysis provided by this organelle makes it possible to do large numbers of simple experiments. The hope, however, is that the general models for length control derived from experiments in *Chlamydomonas* flagella will ultimately be applicable to size control of other types of organelles. First, we consider other organelles whose size can be described entirely by length. The most obvious is

the microvillus. Microvilli contain parallel bundles of actin filaments. We have previously presented a simple model, analogous to the balance-point model of flagellar length control, to account for length regulation in microvilli (Marshall, 2004). It is known that actin in microvilli undergoes continuous treadmilling, with retrograde movement of the filaments toward the cytoplasm balanced by continuous addition of new actin at the tip. It is also known that actin monomer reaches the tip via diffusion. Solution of the diffusion equation for a one-dimensional system at steady state with a constant rate of addition at the tip balancing constant treadmilling, results in a system that can achieve a unique, stable steady-state value for its length (Marshall, 2004). This model is, in an abstract sense, very similar to the balance point model for flagellar length control. The only real difference is that the inherent length dependence of assembly derives not from the details of IFT, but rather from the dependence of monomer concentration on length at steady state. So far, this type of model has not yet been tested for microvilli, but there is no reason why it could not be tested. In fact, the very same methods that have been used to test the mechanism of flagellar length control in *Chlamydomonas* (Marshall and Rosenbaum, 2001; Marshall *et al.*, 2005) can be directly applied to microvilli: specifically one would like to measure the assembly kinetics, resorption kinetics when assembly is blocked, and the dependence of length on number when multiple microvilli are forced to compete for a common pool of precursor. Genetics can also be used to probe the mechanism of length control in microvilli, by identifying partial loss-of-function alleles in, for instance, the motors that drive treadmilling, and then comparing the observed phenotype with results of simulations.

It remains to be seen how many other linear structures will have their length controlled by similar processes. For instance it now seems likely that the sarcomere size in striated muscle uses a very different mechanism that may be based on a molecular ruler (Fowler *et al.*, 2006). To ultimately conduct the same types of length control studies in other cellular systems, a major challenge is the fact that flagella are so much longer than most other linear structures. Fortunately, several clever new imaging and image processing methods have greatly facilitated precise and accurate length measurement for very small structures (Littlefield and Fowler, 2002), and it seems likely the development and application of these measuring tools, combined with reverse genetics and mathematical modeling, will soon lead to a clear understanding of length control in general, at which point it will be interesting to see what overall patterns emerge in the types of mechanisms that biology has evolved to control length.

What about organelles that are not simple linear structures? So far, size control in such structures remains very poorly understood. We have previously proposed an abstract version of the balance point model which frees it from a single dimension (Marshall, 2002). To formulate such a model, which is really a schema for generating models rather than a specific model per se, we note that the balance-point model for length control hinges on two

features. First, the model requires the structure to be dynamic, such that size control works by setting the assembly and disassembly rates equal at a single value of size. Second, the model requires that assembly is inherently length dependent, due to the properties of IFT. To generalize from this specific model, we say that size control of an organelle can work by a balance-point type of mechanism if two features are present: first, the organelle must be dynamic such that its size (surface area, volume, etc.) is constantly changing slightly as the result of ongoing assembly (e.g., via fusion of vesicles onto the organelle surface and budding of vesicles off of the surface), and second, that either the assembly or disassembly rate, or both, is inherently size-dependent. For instance, if a membrane-bound organelle is exchanging vesicles with the ER (or any other large reservoir of material), then we can assume the rate of vesicles traveling to the organelle and fusing with its surface will depend only on the rate of vesicle formation at the ER and transit to the organelle, and not on the surface area of the organelle (because we presume the ER has no way of knowing how big the distant organelle actually is). If we further assume the rate of vesicle budding from the surface is proportional to the surface area, we immediately obtain a simple balance-point model for size control. If we let the rate of vesicle fusion onto the surface be represented by the variable α, and the rate of budding be equal to βS, then the instantaneous rate of change of the surface area S is given by $dS/dt = \alpha - \beta S$. If we solve for the steady state solution by setting $dS/dt = 0$, we find that the system only can maintain a steady-state surface area when $S = \alpha/\beta$. This steady-state solution is stable, because if the surface area were to increase, now the budding rate would go up, leading to a reduction in area back down to the steady-state solution. Similarly, if the area were to somehow be reduced, now assembly (fusion) would predominate and restore the organelle to its steady-state size. This simple generalization of the balance-point model seems reasonable but it has never been tested for any membrane-bound organelle so far. Testing the model can proceed using the same methods developed for probing the mechanism of flagellar length control, such as measuring growth kinetics or the dependence of size on the number of organelles present in a given cell.

We conclude that flagellar length control continues to serve as a valuable paradigm for studying the problem of organelle size control in general. The types of length control models resulting from the study of flagellar size provide insights into possible models that could regulate size in other systems. The experimental strategies that have been devised to study flagellar length can likewise be used to devise similar approaches for the study of other organelles. More generally, the fact that flagellar length control studies give us easy access to quantitative information which can be used for mathematical modeling, suggests that flagella will be a paradigm not just for size control, but for a more general systems-biology approach to cellular structure.

C. Length Control in Nanotechnology

Current efforts to build more complex and miniaturized machines using the methods of nanotechnology are faced with the same problems that the cell faces in building its substructures. How does one specify the size of the structure, or its position, or the number of copies to be made? Much current effort in nanotechnology solves these problems using the type of fabrication processes used in building man-made machines—a blueprint is developed that explicitly encodes all spatial information (size, position, etc.), and then this blueprint is used to direct the activity of a fabrication device, such as a lithographic process. Such methods reach a hard limit on size scale, imposed by the physics of the fabrication process. For instance, photolithography is limited in the size of the features it can produce, by the wavelength of the light used. An alternative method, currently under consideration, is self-organization (Ewaschuk and Turney, 2006). In this paradigm, components of a nano-machine would put themselves together. This type of fabrication gets around the normal physics-imposed constraints, because there is no need to convert a macroscopic blueprint or image into a microscopic structure.

Because self-assembly of the type currently being considered for nanotechnology applications is precisely the fabrication principle used by cells, it makes sense to ask whether the methods employed by cells can be applied to human-designed nanomachines. Controlling the length of polymeric structures is a major issue in nanotechnology (Graveland-Bikker *et al.*, 2006). The same mechanisms employed for length control within cells (molecular rules, cumulative strain, quantal production, feedback, and balance-point regulation) are all potentially applicable to length control in nanotechnology.

Further, the axoneme itself is promising as a potential platform for the fabrication of very small machines. With its precise symmetry, and 96-nm repeating arrangement of dynein arms, it provides a highly structured lattice on which other small components could be positioned. Pursuit of this specific approach to nano-biotechnology will obviously require a very deep quantitative understanding of how the flagellum is put together. Length control is just one part of this understanding.

References

Adams, G. M. W., Huang, B., and Luck, D. J. L. (1982). Temperature-sensitive assembly-defective flagella mutants of *Chlamydomonas reinhardtii*. *Genetics* **100,** 579–586.

Ansley, S. J., Badano, J. L., Blacque, O. E., Hill, J., Hoskins, B. E., Leitch, C. C., Kim, J. C., Ross, A. J., Eichers, E. R., Teslovich, T. M., Mah, A. K., Johnsen, R. C., *et al.* (2003). Basal body dysfunction is a likely cause of pleiotropic Bardet-Biedl syndrome. *Nature* **425,** 628–633.

Asleson, C. M., and Lefebvre, P. A. (1998). Genetic analysis of flagellar length control in *Chlamydomonas reinhardtii*: A new long-flagella locus and extragenic suppressor mutations. *Genetics* **148,** 693–702.

Barsel, S. E., Wexler, D. E., and Lefebvre, P. A. (1988). Genetic analysis of long-flagella mutants of *Chlamydomonas reinhardtii*. *Genetics* **118,** 637–648.

Beck, C., and Uhl, R. (1994). On the localization of voltage-sensitive calcium channels in the flagella of *Chlamydomonas reinhardtii*. *J. Cell Biol.* **125,** 1119–1125.

Beech, P. L. (2003). The long and the short of flagellar length control. *J. Phycol.* **39,** 837–839.

Beech, P. L., and Wetherbee, R. (1990). Direct observations on flagellar transformation in *Mallomonas splendens* (synurophyceae). *J. Phycol.* **26,** 90–95.

Berman, S. A., Wilson, N. F., Haas, N. A., and Lefebvre, P. A. (2003). A novel MAP kinase regulates flagellar length in *Chlamydomonas*. *Curr. Biol.* **13,** 1145–1149.

Bernales, S., Papa, F. R., and Walter, P. (2006). Intracellular signaling by the unfolded protein response. *Ann. Rev. Cell Dev. Biol.* **22,** 487–508.

Blank, H. M., Totten, J. M., and Polymenis, M. (2006). CDK control of membrane-bound organelle homeostasis. *Cell Cycle* **5,** 486–488.

Bloodgood, R. A. (1992). Calcium-regulated phosphorylation of proteins in the membrane-matrix compartment of the *Chlamydomonas flagellum*. *Exp. Cell Res.* **198,** 228–236.

Bradley, B. A., and Quarmby, L. M. (2005). A NIMA-related kinase, Cnk2p, regulates both flagellar length and cell size in *Chlamydomonas*. *J. Cell Sci.* **118,** 3317–3326.

Bressloff, P. C. (2006). Stochastic model of intraflagellar transport. *Phys. Rev. E.* **73,** 061916.

Chemes, H. E., Morero, J. L., and Lavieri, J. C. (1990). Extreme asthenozoospermia and chronic respiratory disease: A new variant of the immotile cilia syndrome. *Int. J. Androl.* **13,** 216–222.

Coggin, S. J., and Kochert, G. (1986). Flagellar development and regeneration in *Volvox carteri* (Chlorophyta). *J. Phycol.* **22,** 370–381.

Cole, D. G. (2003). The intraflagellar transport machinery of *Chlamydomonas reinhardtii*. *Traffic* **4,** 435–442.

Deane, J. A., Cole, D. G., Seeley, E. S., Diener, D. R., and Rosenbaum, J. L. (2001). Localization of intraflagellar transport protein IFT52 identifies basal body transitional fibers as the docking site for IFT particles. *Curr. Biol.* **11,** 1586–1590.

Dentler, W. (2005). Intraflagellar transport (IFT) during assembly and disassembly of *Chlamydomonas flagella*. *J. Cell Biol.* **170,** 649–659.

Dentler, W. L., and Rosenbaum, J. L. (1977). Flagellar elongation and shortening in *Chlamydomonas*. III. Structures attached to the tips of flagellar microtubules and their relationship to the directionality of flagellar microtubule assembly. *J. Cell Biol.* **74,** 747–759.

Dogterom, M., and Leibler, S. (1993). Physical aspects of the growth and regulation of microtubule structures. *Phys. Rev. Lett.* **70,** 1347–1350.

Dutcher, S. K. (1995). Flagellar assembly in two hundred and fifty easy-to-follow steps. *Trends Genet.* **11,** 398–404.

Elowitz, M. B., Levine, A. J., Siggia, E. D., and Swain, P. S. (2002). Stochastic gene expression in a single cell. *Science* **297,** 1183–1186.

Ewaschuk, R., and Turney, P. D. (2006). Self-replication and self-assembly for manufacturing. *Artif. Life* **12,** 411–433.

Fowler, V. M., McKeown, C. R., and Fischer, R. S. (2006). Nebulin: Does it measure up as a ruler? *Curr. Biol.* **16,** R18–R20.

Fung, J. C., Liu, W., de Ruijter, W. J., Chen, H., Abbey, C. K., Sedat, J.W, and Agard, D. A. (1996). Toward fully automated high-resolution electron tomography. *J. Struct. Biol.* **116,** 181–189.

Graveland-Bikker, J. F., Schaap, I. A., Schmidt, C. F., and de Kruif, C. G. (2006). Structural and mechanical study of a self-assembling protein nanotube. *Nano. Lett.* **6,** 616–621.

Grimes, G. W., and Gavin, R. H. (1987). Ciliary protein conservation during development in the ciliated protozoan, Oxytricha. *J. Cell Biol.* **105,** 2855–2859.

Handel, M., Schulz, S., Stanarius, A, Schreff, M., Erdtmann-Vourliotis, M., Schmidt, H., Wolf, G., and Hollt, V. (1999). Selective targeting of somatostatin receptor 3 to neuronal cilia. *Neuroscience* **89,** 909–926.

Haycraft, C. J., Swoboda, P., Taulman, P. D., Thomas, J. H., and Yoder, B. K. (2001). The *C. elegans* homolog of the murine cystic kidney disease gene Tg737 functions in a ciliogenic pathway and is disrupted in osm-5 mutant worms. *Development* **128,** 1493–1505.

Howard, J. (2001). "Mechanics of Motor Proteins and the Cytoskeleton." Sinauer Associates, Sunderland, MA.

Iomini, C., Babaev-Khainov, V., Sassaroli, M., and Piperno, G. (2001). Protein particles in *Chlamydomonas flagella* undergo a transport cycle consisting of four phases. *J. Cell Biol.* **153,** 13–24.

Jarvik, J., Lefebvre, P. A., and Rosenbaum, J. L. (1976). A cold-sensitive mutant of *Chlamydomonas* with aberrant control of flagellar length. *J. Cell Biol.* **70,** 149a.

Jarvik, J., Reinhart, F., and Adler, S. (1980). Length control in the *Chlamydomonas flagellum*. *J. Cell Biol.* **87,** 38a.

Jarvik, J. W., Reinhart, F. D., Kuchka, M. R., and Adler, S. A. (1984). Altered flagellar size-control in shf-1 short-flagella mutants of *Chlamydomonas reinhardtii*. *J. Protozool.* **31,** 199–204.

Johnson, K. A., and Rosenbaum, J. L. (1992). Polarity of flagellar assembly in *Chlamydomonas*. *J. Cell Biol.* **119,** 1605–1611.

Katsura, I. (1990). Mechanism of length determination in bacteriophage lambda tails. *Adv. Biophys.* **26,** 1–8.

Keener, J. P. (2006). How Salmonella typhimurium measures the length of flagellar filaments. *Bull. Math. Biol.* **26,** in press..

Kellenberger, E. (1972). Polymerization in Biological Systems. *Ciba Found. Symp.* **7,** 295–299.

Kuchka, M. R., and Jarvik, J. W. (1982). Analysis of flagellar size control using a mutant of *Chlamydomonas reinhardtii* with a variable number of flagella. *J Cell Biol.* **92,** 170–175.

Kuchka, M. R., and Jarvik, J. W. (1987). Short-flagella mutants of *Chlamydomonas*. *Genetics* **115,** 685–691.

Lechtreck, K. F., Reize, I. B., and Melkonian, M. (1997). The cytoskeleton of the naked green flagellate *Spermatozopsis similis* (chlorophyta): Flagellar and basal body developmental cycle. *J. Phycol.* **33,** 254–265.

Lefebvre, P. A., Nordstrom, J. E., Moulder, J. E., and Rosenbaum, J. L. (1978). Flagellar elongation and shortening in *Chlamydomonas*. IV. Effects of flagellar detachment, regeneration, and resorption on the induction of flagellar protein synthesis. *J. Cell Biol.* **78,** 8–27.

Lefebvre, P. A., Silflow, C. D., Widen, E. D., and Rosenbaum, J. L. (1980). Increased levels of messenger RNA species for tubulin and other flagellar proteins after amputations or shortening of *Chlamydomonas flagella*. *Cell* **20,** 469–578.

Lefebvre, P. A., Barsel, S. E., and Wexler, D. E. (1988). Isolation and characterization of *Chlamydomonas reinhardtii* mutants with defects in the induction of flagellar protein synthesis after deflagellation. *J. Protozool.* **35,** 559–564.

Littlefield, R., and Fowler, V. M. (2002). Measurement of thin filament lengths by distributed deconvolution analysis of fluorescence images. *Biophys. J.* **82,** 2548–2564.

Madey, P., and Melkonian, M. (1990). Flagellar development during the cell cycle in *Chlamydomonas reinhardtii*. *Botanica Acta* **103,** 97–102.

Marshall, W. (2002). Size control in dynamic organelles. *Trends Cell Biol.* **12,** 414–419.

Marshall, W. F. (2004). Cellular length control systems. *Annu. Rev. Cell Dev. Biol.* **20,** 677–693.

Marshall, W. F., and Nonaka, S. (2006). Cilia: Tuning in to the Cell's Antenna. *Curr. Biol.* **16,** R604–R614.

Marshall, W. F., and Rosenbaum, J. L. (2001). Intraflagellar transport balances continuous turnover of outer doublet microtubules: Implications for flagellar length control. *J. Cell Biol.* **155,** 405–414.

Marshall, W. F., Qin, H., Rodrigo Brenni, M., and Rosenbaum, J. L. (2005). Flagellar length control system: Testing a simple model based on intraflagellar transport and turnover. *Mol. Biol. Cell* **16,** 270–278.

Masyuk, T. V., Huang, B. Q., Ward, C. J., Masyuk, A. I., Yuan, D., Splinter, P. L., Punyashthiti, R., Ritman, E. L., Torres, V. E., Harris, P. C., and LaRusso, N. F. (2003). Defects in cholangiocyte fibrocystin expression and ciliary structure in the PCK rat. *Gastroenterology* **125,** 1303–1310.

McVittie, A. C. (1972). Flagellum mutants of *Chlamydomonas reinhardtii. J. Gen. Microbiol.* **71,** 525–540.

Morris, E. C. (2002). How did cells get their size? *Anat. Rec.* **268,** 239–251.

Norrander, J. M., Linck, R. W., and Stephens, R. E. (1995). Transcriptional control of tektin A mRNA correlates with cilia development and length determination during sea urchin embryogenesis. *Development* **121,** 1615–1623.

Nossal, R., and Lecar, H. (1991). "Molecular & Cell Biophysics." Addison-Wesley, Redwood City, CA.

Nguyen, R. L., Tam, L. W., and Lefebvre, P. A. (2005). The LF1 gene of *Chlamydomonas reinhardtii* encodes a novel protein required for flagellar length control. *Genetics* **169,** 1415–1424.

Ortug, C. (2003). Scanning electron microscopic findings in respiratory nasal mucosa following cigarette smoke exposure in rats. *Ann. Anat.* **185,** 207–210.

Otto, E. A., Schermer, B., Obara, T., O'Toole, J. F., Hiller, K. S., Mueller, A. M., Ruf, R. G., Hoefele, J., Beekmann, F., Landau, D., Foreman, J. W., Goodship, J. A., *et al.* (2003). Mutations in INVS encoding inversin cause nephronophthisis type 2, linking renal cystic disease to the function of primary cilia and left-right axis determination. *Nat. Genet.* **34,** 355–356.

Pan, J., and Snell, W. J. (2005). *Chlamydomonas* shortens its flagella by activating axonemal disassembly, stimulating IFT particle trafficking, and blocking anterograde cargo loading. *Dev. Cell* **9,** 431–438.

Parker, J. D., and Quarmby, L. M. (2003). *Chlamydomonas* fla mutants reveal a link between deflagellation and intraflagellar transport. *BMC Cell Biol.* **4,** 11.

Pazour, G. J., and Rosenbaum, J. L. (2002). Intraflagellar transport and cilia-dependent diseases. *Trends Cell Biol.* **12,** 551–555.

Pazour, G. J., Dickert, B. L., Vucica, Y., Seeley, E. S., Rosenbaum, J. L., Witman, G. B., and Cole, D. G. (2000). *Chlamydomonas* IFT88 and its mouse homologue, polycystic kidney disease gene Tg737, are required for assembly of cilia and flagella. *J. Cell Biol.* **151,** 709–718.

Pedersen, L. B., Geimer, S., Sloboda, R. D., and Rosenbaum, J. L. (2003). The microtubule plus end tracking protein EB1 is localized to the flagellar tip and basal bodies in *Chlamydomonas reinhardtii. Curr. Biol.* **13,** 1969–1974.

Pedersen, L. B., Geimer, S., and Rosenbaum, J. L. (2006). Dissecting the molecular mechanisms of intraflagellar transport in *Chlamydomonas. Curr. Biol.* **16,** 450–459.

Pena, J. (2005). Correlation of flagellar length and flagellar gene expression in *Chlamydomonas reinhardtii.* (Undergraduate Honors Major Thesis) *Florida State University D-Scholarship Repository Article #95.*

Piperno, G., Mead, K., and Henderson, S. (1996). Inner dynein arms but not outer dynein arms require the activity of kinesin homologue protein KHP1 (FLA10) to reach the distal part of flagella in *Chlamydomonas. J. Cell Biol.* **133,** 371–379.

Qin, H., Diener, D. R., Geimer, S., Cole, D. G., and Rosenbaum, J. L. (2004). Intraflagellar transport (IFT) cargo: IFT transports flagellar precursors to the tip and turnover products to the cell body. *J. Cell Biol.* **164,** 255–266.

Qin, H., Burnette, D. T., Bae, Y. K., Forscher, P., Barr, M. M., and Rosenbaum, J. L. (2005). Intraflagellar transport is required for the vectorial movement of TRPV channels in the ciliary membrane. *Curr. Biol.* **15,** 1695–1699.

Rosenbaum, J. (2003). Organelle size regulation: Length matters. *Curr. Biol.* **13,** R506–R507.

Rosenbaum, J. L., and Child, F. M. (1967). Flagellar regeneration in protozoan flagellates. *J. Cell Biol.* **34,** 345–364.

Rosenbaum, J. L., Moulder, J. E., and Ringo, D. L. (1969). Flagellar elongation and shortening in *Chlamydomonas*. The use of cycloheximide and colchicine to study the synthesis and assembly of flagellar proteins. *J. Cell Biol.* **41,** 600–619.

Scholey, J. M. (2003). Intraflagellar transport. *Annu. Rev. Cell Dev. Biol.* **19,** 423–443.

Schoppmeier, J., and Lechtreck, K. F. (2003). Flagellar regeneration in *Spermatozopsis similis* (Chlorophyta). *J. Phycol.* **39,** 918–922.

Silflow, C. D., and Lefebvre, P. A. (2001). Assembly and motility of eukaryotic cilia and flagella. Lessons from *Chlamydomonas reinhardtii*. *Plant Physiol.* **127,** 1500–1507.

Sloboda, R. D. (2002). A healthy understanding of intraflagellar transport. *Cell Motil. Cytoskel.* **52,** 1–8.

Song, L., and Dentler, W. L. (2001). Flagellar protein dynamics in *Chlamydomonas*. *J. Biol. Chem.* **276,** 29754–29763.

Stephens, R. E. (1989). Quantal tektin synthesis and ciliary length in sea-urchin embryos. *J. Cell Sci.* **92,** 403–413.

Stephens, R. E. (1999). Turnover of tubulin in ciliary outer doublet microtubules. *Cell Struct. Funct.* **24,** 413–418.

Stephens, R. E. (2000). Preferential incorporation of tubulin into the junctional region of ciliary outer doublet microtubules: A model for treadmilling by lattice dislocation. *Cell Motil. Cytoskel.* **47,** 130–140.

Stolc, V., Samanta, M. P., Tongprasit, W., and Marshall, W. F. (2005). Genome-wide transcriptional analysis of flagellar regeneration in *Chlamydomonas reinhardtii* identifies orthologs of ciliary disease genes. *Proc. Natl. Acad. Sci. USA* **102,** 3703–3707.

Tam, L. W., Dentler, W. L., and Lefebvre, P. A. (2003). Defective flagellar assembly and length regulation in LF3 null mutants in *Chlamydomonas*. *J. Cell Biol.* **163,** 597–607.

Tamm, S. L. (1967). Flagellar development in the protozoan *Paranema trichophorum*. *J. Exp. Zool.* **164,** 163–186.

Tilney, L. G., and Gibbins, J. R. (1968). Differential effects of antimitotic agents on the stability and behavior of cytoplasmic and ciliary microtubules. *Protoplasma* **65,** 167–179.

Toskala, E., Nuutinen, J., and Rautiainen, M. (1995). Scanning electron microscope findings of human respiratory cilia in chronic sinusitis and in recurrent respiratory infections. *J. Laryngol. Otol.* **109,** 509–514.

Toyama, Y., Sumiya, H., Fuse, H., and Shimazaki, J. (1996). A case of an infertile man with short-tailed spermatozoa. *Andrologia* **28,** 81–87.

Tuxhorn, J., Daise, T., and Dentler, W. L. (1998). Regulation of flagellar length in *Chlamydomonas*. *Cell Motil. Cytoskel.* **40,** 133–146.

Umen, J. G. (2005). The elusive sizer. *Curr. Opin. Cell Biol.* **17,** 435–441.

Verde, F., Dogterom, M., Stelzer, E., Karsenti, E., and Leibler, S. (1992). Control of microtubule dynamics and length by cyclin A- and cyclin B-dependent kinases in *Xenopus* egg extracts. *J. Cell Biol.* **118,** 1097–1108.

Wagenknecht, T., and Bloomfield, V. A. (1975). Equilibrium mechanisms of length regulation in linear protein aggregates. *Biopolymers* **14,** 2297–2309.

Wheatley, D. N., and Bowser, S. S. (2000). Length control of primary cilia: Analysis of monociliate and multiciliate PtK1 cells. *Biol. Cell* **92,** 573–582.

Wilson, N. F., and Lefebvre, P. A. (2004). Regulation of flagellar assembly by glycogen synthase kinase 3 in *Chlamydomonas reinhardtii*. *Eukaryote Cell* **3,** 1307–1319.

Wilson, N. F., and Lefebvre, P. A. (2005). LF4p, a regulator of flagellar length in *Chlamydomonas*, is a cargo for transport by IFT. *American Society for Cell Biology annual meeting*, Abstract #1019.

Molecular Mechanism and Evolutional Significance of Epithelial–Mesenchymal Interactions in the Body- and Tail-Dependent Metamorphic Transformation of Anuran Larval Skin

Katsutoshi Yoshizato

Department of Biological Science, Graduate School of Science,
Hiroshima University, Higashihiroshima, 739-8526, Japan

The epidermis of an anuran larva is composed of apical and skein cells that are both mitotically active and self-renewed through larval life. In contrast, the epidermis of an adult frog, with typical stratified squamous epithelium composed of germinative basal, spinous, granular, and cornified cells, is histologically identical to the mammalian epidermis. Two important issues have not yet been addressed in the study of the development of anuran skin. One is the origin of adult basal cells in the larval epidermis and the other is the mechanism by which larval basal cells are transformed into adult basal cells in a region- (body- and tail-) dependent manner. The cell lineage relationship between the larval and adult epidermal cells was determined by examining the expression profiles of several genes that are expressed specifically in larval and/or adult epidermal cells and differentiation profiles of larval basal cells cultured in the presence of thyroid hormone (TH). Histological analyses using several markers led to the identification of the skin transformation center (STC) where the conversion of larval skin to the adult counterpart is taking place. The STC emerges at a specific place in the body skin and at a specific stage of larval development. The STC progressively "moves" into and "invades" the adjacent larval region of the trunk skin as a larva develops, converting the larval skin into the preadult skin, but never into the tail region. The larva to preadult skin conversion requires an epidermal–mesenchymal interaction. The genesis of preadult basal cells is suppressed in the tail epidermis due to the influence of underlying mesenchyme in the tail region. PDGF signaling is one of the molecular cues of epidermal–mesenchymal interactions. In addition, a unique feature of

anuran skin metamorphosis is presented referring to the skin of other vertebrates. Histological comparisons of the skin among vertebrate species strongly suggested a similarity between the anuran larval skin and the teleost fish adult skin and between the anuran adult skin and the adult skin of other tetrapod species. Based on these similarities, the evolutional significance of anuran skin metamorphosis is proposed. Finally, studies are reviewed that reveal the molecular mechanism of anuran metamorphosis in relation to TH-TR-TRE signaling. The results of these studies suggest new aspects of the biological significance of TH, and also enable us to envision concerted regulations of the expression of a gene in the frame of the gene network responsible for metamorphic remodeling of larval tissues. The present review will contribute to an understanding of the molecular mechanism of region-dependent skin development of anurans from not only a metamorphic but also from an evolutional point of view, and will provide a new way to understand the biological significance of TH in anurans.

I. Introduction

After fertilization, anurans undergo embryogenesis, larval development, and metamorphosis to adults. To meet the change in habitation from the aquatic to terrestrial environment, the larva undergoes extensive postembryonic remodeling of most of its tissues in which the cells required only for larval life undergo apoptosis. In contrast, the cells required for adult life differentiate into adult cells. A larval tissue composed of larval cells develops into an intermediate and transient tissue in which adult progenitor cells (preadult cells) newly emerge (Fig. 1). Thus, the tissue becomes chimeric in that preadult cells and larval cells coexist. Preadult cells differentiate into adult cells, whereas larval cells undergo apoptosis and disappear from the tissue during metamorphosis. Therefore, there are two populations of larval cells: one (larva-proper cells) that terminates its lineage at metamorphosis and the other whose lineage is maintained as adult cells.

A. Region-Dependent Progression of Skin Remodeling in Anuran Metamorphosis

The larval epidermis is one of the tissues that has been extensively studied in terms of the mechanism underlying such a metamorphic transformation of larval cells. The epidermis has an additional uniqueness that attracts us:
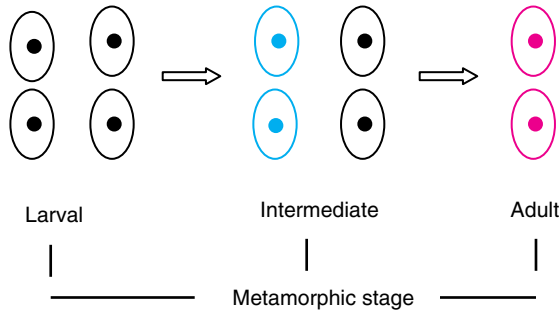
FIG. 1   Two types of larval cells with different differentiation potentials. Cellular events are shown that take place during larval to adult development. A larval tissue at an early developmental stage (premetamorphic stage) contains cells with different differentiation potentials and develops into an intermediate tissue, in which some cells are committed to differentiate into preadult cells (adult progenitor cells) in a middle stage of development (pro- and premetamorphic stage), whereas other cells remain as larval cells. The preadult cells differentiate into adult cells that form adult tissue in a late stage of development (climax stage of metamorphosis). Larval cells undergo apoptosis, thus their lineage is being terminated.

the metamorphic program of the epidermis is quite different between the cephalic part (head and trunk region and then the body) and the caudal part (tail region). Among epidermal cells, basal cells that attach themselves to the basement membrane play prime roles in constructing the epidermis. The body and tail basal epidermal cells undergo a "transformation program" and an "apoptosis program," respectively. Common larval cells construct larval epidermis in both the body and the tail regions of a tadpole in an early stage of development (Fig. 2). Then, the epidermis in the body becomes chimeric containing both larval and preadult cells, which then follows the two different metamorphic programs (transformation and apoptosis) under the same hormonal (thyroid hormone, TH) cue. In contrast, the tail epidermal cells do not differentiate into preadult cells, but remain larval in nature through the end of metamorphosis, and undergo apoptosis. This apoptotic event in the tail is really massive and of a large scale, because the tail region just before the onset of metamorphosis occupies 33% and 25% of the total length and the volume of a tadpole of *Xenopus laevis,* respectively.

The major aim of this review is to present a current view of how the originally homogeneous epidermal basal cell population becomes heterogeneous in its differentiation potential in a region- and TH-dependent manner. The studies accumulated in our laboratory on skin metamorphosis have led us to hypothesize the presence of a metamorphic skim transformation center (STC) where interactions between the epidermis and the subepidermal connective tissue induce the larval skin to transform into its adult counterpart. STC is not formed in the tail region.
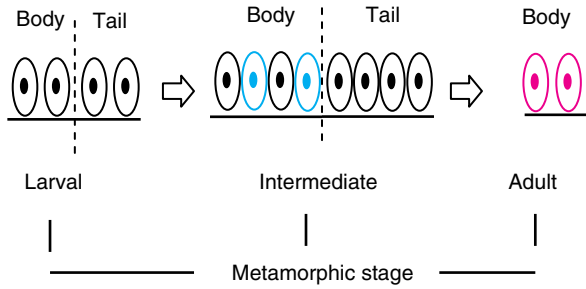
FIG. 2   Two types of epidermal basal cells with regional differences. There are no differences in phenotypes of basal cells in the larval epidermis between the body and tail regions. Some basal cells in the body transform into preadult basal cells (adult progenitor cells) in the intermediate stage, but those in the tail do not show such a transformation. The preadult cells differentiate into adult basal cells and construct the adult epidermis. Larval cells in both regions undergo apoptosis. The symbols in the illustration are as in Fig. 1. The horizontal bar underneath the cells represents the basement membrane. The dotted vertical line represents the boundary between the body and the tail regions. The symbols for the cells are used as in Fig. 1.

B. Evolutional Significance of Anuran Skin Metamorphosis

When skin histology was compared among the teleost, the anura, and the mammal, we noticed the similarity between the anuran larva and the fish adult and between the anuran adult and the amniote adult. These similarities appear to be correlated with the environmental differences in the habitation of these animal species. Therefore, we speculate that anuran skin metamorphosis is a process that might have taken place when ancestral anurans evolved from fish approximately 350 million years ago. It could be said that the metamorphic process of the anuran skin recapitulates the evolutionary process from the aquatic life of teleost fish to the terrestrial life of tetrapods.

C. Regulation of Metamorphosis by Thyroid Hormone

TH triggers metamorphosis of an anuran larva and induces its transformation to the adult. Larval cells receive TH with the nuclear TH receptor (TR). TR acts as a transcription factor by binding to the TH response element (TRE) of metamorphosis-associated and TH-direct responsive genes. This flow of the TH-TR-TRE signal in larval cells plays a key role in anuran metamorphosis. It has generally been considered that the biological significance of TH in anurans resides solely in its metamorphosis-inducing activity (metamorphosis hormone), because TH in serum is detectable only during

climactic stages of metamorphosis. Studies have been accumulated in which the molecular mechanism of anuran metamorphosis was examined in relation to TH-TR-TRE signaling. We obtained evidence that suggests that TH plays roles not only in metamorphosis, but also in embryogenesis and in physiological processes of adult tissues. Studies on amphibian metamorphosis at the molecular level have revealed the regulation of the expression of individual metamorphosis-associated genes. Accumulation of these studies will permit us to envision concerted regulation of gene expression in the frame of gene networks that govern the metamorphic remodeling of larval tissues.

II. Anuran Skin Remodeling and Metamorphosis

A. Development of Anuran Skin from the Late Embryonic Stage to the Adult

The skin of *Rana catesbeiana* and *Xenopus laevis* larva is homologous in histological structures, but develops differently in chronology as shown in Fig. 3A and B, respectively. The larva to preadult skin conversion takes place early (at a premetamorphic stage) in larval life around stage IV (TK-IV), defined by Taylor and Kollros (1946) in *R. catesbeiana* (Kawai *et al.*, 1994; Suzuki *et al.*, 2001, 2002; Utoh *et al.*, 2000), but much later (at a prometamorphic stage) around stage 58–59 (NF-58–59) defined by Nieuwkoop and Faber (1967) in *X. laevis* (Utoh *et al.*, 2003; Watanabe *et al.*, 2001, 2002). Various epidermal cell species are involved in the development and metamorphosis: basal skein, suprabasal skein, larval basal, preadult basal, adult basal cells, and differentiated descendants of adult basal cells (Izutsu *et al.*, 1993; Suzuki *et al.*, 2001, 2002; Utoh *et al.*, 2000, 2003; Watanabe *et al.*, 2001, 2002; Yoshizato, 1996). Apical cells are located at the outermost layer. Skein cells are defined as the larval epidermal cells that contain in the cytoplasm conspicuous spirally wound tonofilaments taking the appearance of huge bundles of intermediate filaments called "Figures of Eberth" (Eberth, 1866; Fox, 1992; Fox and Whitear, 1986). These cells are so called because this unique keratin bundle possesses "skein," a loosely coiled length of thread wound on a reel. Skein cells are a major cell type of anuran larval epidermis (Yoshizato, 1989). *Rana* larval keratin (RLK) is a component of keratin bundles and thus a useful biochemical indicator of skein cells (Suzuki *et al.*, 2001). *Xenopus* larval keratin (XLK) is a *Xenopus* homologue of RLK (Watanabe *et al.*, 2001). There are two types of skein cells: basal and suprabasal skein cells. Electron microscopic observations showed that basal skein cells apparently resemble larval basal cells (Izutsu *et al.*, 1993). However,

these two types of cells are morphologically quite different from each other in that the basal skein cells, but not the larval basal cells, do contain keratin bundles. Apical and suprabasal skein cells undergo TH-induced apoptosis, whereas larval basal cells proliferate in response to the stimulus of the same hormone (Nishikawa *et al.*, 1989; Yoshizato, 1996). Larval basal cells are present in the trunk (hereafter, body), but rarely in the tail (Izutsu *et al.*, 1993). Orthogonally arranged multilayered collagen fibers (collagen layer or lamella) beneath the basement membrane feature the amphibian subepidermal connective tissue (Utoh *et al.*, 2000; Weiss and Ferris, 1954; Yoshizato, 1989). These collagen lamellae are formed by type I collagen originally synthesized by basal skein cells and later also by subepidermal fibroblasts (Utoh *et al.*, 2000).
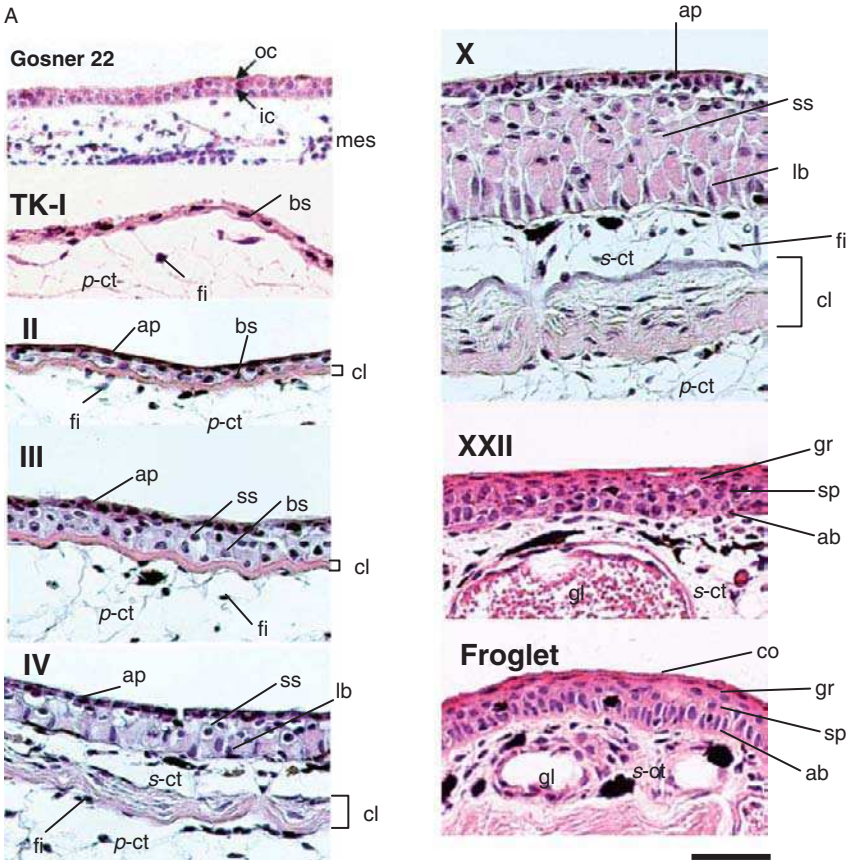
B
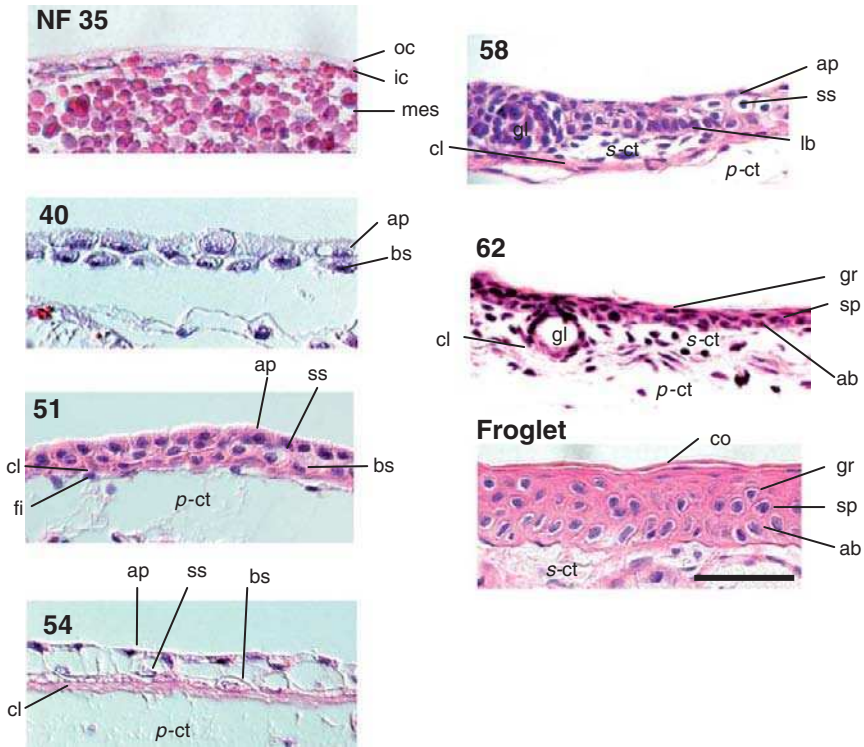
FIG. 3 Comparison of the development of skin between *Rana catesbeiana* and *Xenopus laevis*. Histology of skin of *Rana catesbeiana* (A) and *Xenopus laevis* (B) at the indicated developmental stages, sectioned, and stained with hematoxylin and eosin. oc, outer cell; ic, inner cell; mes, mesenchyme; bs, basal skein cell; *p*-ct, *p*-connective tissue; fi, fibroblast; ap, apical cell; cl, collagen lamella; ss, suprabasal skein cell; lb, larval basal cell; *s*-ct, *s*-connective tissue; gr, granular cell; sp, spinous cell; co, cornified cell; ab, adult basal cell; gl, gland. Bars, 50 μm.

The epidermis of *Rana* embryos at a late embryonic stage, stage 22 after Gosner (1960), is composed of two-cell layers, outer and inner layers (Fig. 3A). The epidermis of larvae just after hatch (TK-I) is one-cell layered (Utoh *et al.*, 2000) and then becomes two-cell layered at late TK-I, with apical and basal skein cells in the upper and inner layer, respectively. It becomes three-cell layered at TK-III, the upper, middle, and lower layer consisting of apical, suprabasal skein, and basal skein cells, respectively (Suzuki *et al.*, 2001; Utoh *et al.*, 2000). The larval basal cells first emerge at around TK-IV (Utoh *et al.*, 2000), a critical event because the larval basal cells were considered to be a progenitor of adult basal cells (Robinson and Heintzelman, 1987; Yoshizato, 1996).

Initially (TK-I to -III), the subepidermal basement membrane directly contacts the acellular collagen layer that is associated with ''primary connective tissues'' (*p*-connective tissues, Fig. 3A). Concomitantly with the emergence of larval basal cells ''secondary connective tissues'' (*s*-connective tissues) are formed between the basement membrane and the collagen lamella at a late early premetamorphic stage (around TK-IV; Utoh *et al.*, 2000). Collagen lamellae are populated with fibroblasts. This event takes place in the STC as detailed in Section V. Through these changes, the larval skin transforms into the ''preadult skin,'' the skin containing larval basal cells and *s*-connective tissue. The preadult skin develops, increasing the number of intermediate cell layers and the area of *s*-connective tissues until the onset of the climax stage (TK-XX). During the climax stages, the preadult skin is transformed into the adult skin, deleting suprabasal skein and apical cells, and differentiating larval basal cells to their adult counterparts.

Xenopus larvae have a two-cell layered epidermis from the late embryonic stage through the hatching stage (NF-stage 35): the outer and the inner layer (Fig. 3B). The epidermis then develops into a larval type composed of apical and basal skein cells around NF-40. Suprabasal skein cells have appeared at NF-51. Collagen lamellae become prominent around NF-54. Drastic changes in the skin take place at NF-58, a late prometamorphic stage. The larval skin converts to the preadult skin. Preadult basal cells emerge and the *s*-connective tissues are formed between the basement membrane and the acellular collagen layer. Thus, the skin at NF-58 of *Xenopus* larvae corresponds to that at TK-IV of *R. catesbeiana*. The preadult skin is eventually transformed into the adult skin at the completion of metamorphosis.

B. Molecular Probes for Anuran Epidermal Cells

Appropriate molecular markers have been sought for or newly identified to investigate the lineage relationship among these different types of anuran epidermal basal cells. For this, the following four genes/proteins are particularly useful: integrin β1, collagen α1(I) (COLα1), RLK, and *Rana* adult keratin (RAK). Integrin β1 is expressed in mammalian epidermal stem cells located in the basal layer and controls the differentiation of keratinocytes (Jones and Watt, 1993; Jones *et al.*, 1995; Watt, 2001). *Rana* epidermal basal cells commonly express this gene from larval to adult life (Suzuki *et al.*, 2002). Collagen type I is usually expressed in mesoderm-derived tissues such as bones and dermis of adult mammals. However, interestingly, it was found that its gene *(colα1)* is expressed in the inner layer of epidermis during *Xenopus* embryonic development (Goto *et al.*, 2000). We cloned bullfrog COLα1cDNA (Asahina *et al.*, 1997) and showed that this unique expression continued to early larval development (Suzuki *et al.*, 2002; Utoh *et al.*, 2000).

The inner epidermal cells at Gosner stage 23 expressed the *colα1*. The epidermis at the early TK-I is one-cell layered and these cells expressed it. These single-layered epidermal cells produce two types of cells: apical cells and basal skein cells. Only the latter cells express *colα1*. The basal skein cells yield suprabasal skein cells at TK-III that do not express the gene. Larval basal cells do not express *colα1*. Thus, *colα1* is a specific and unique gene marker of embryonic to early-larval basal epidermal cells.

RLK and XLK are of type II keratin and each is a member of the proteins consisting of Figures of Eberth of *Rana* (Suzuki *et al.*, 2001) and *Xenopus* (Watanabe *et al.*, 2001), respectively. XLK was originally found as a protein on two-dimensional electrophoretic gels for the larval skin proteins (Kobayashi *et al.*, 1996); it was sequenced and its cDNA was cloned (Watanabe *et al.*, 2001). RLK cDNA *(rlk)* was cloned using specific antisera against XLK (Suzuki *et al.*, 2001). A subtractive cloning between the body and the tail skin of bullfrog tadpole yielded a cDNA *(rak)* of RAK (Suzuki *et al.*, 2001). Adult-type keratin cDNAs of *X. laevis* were screened from an adult skin cDNA library using probes that were designed from the highly conserved N-terminal of the rod domain of type I keratin, which resulted in yielding three types of *xak, xak-a, -b,* and *-c* (Watanabe *et al.*, 2001, 2002). Among them, *xak-c* is expressed in basal cells (Watanabe *et al.*, 2002). The other two keratins are present in granular and spinous cells (Watanabe *et al.*, 2001). RAK and XAK are of type I keratin. Granular cells of *Rana* species also express specific cell surface antigens that react with antihuman blood group A antigen (hbA) antibodies (Izutsu *et al.*, 1993). Table I summarizes the distributions of these markers among epidermal cells of anurans together with mammals for the sake of comparison.

TABLE I

Molecular Probes for Anuran and Mammalian Epidermal Cells

	Rana catesbeiana	*Xenopus laevis*	*Homo sapiens*
Apical cell (periderm)	RK8	XLK19[a]	CK8, CK18[b]
Skein cell	RLK	XLK	–
Basal skein cell	RLK, COLα1, SPARC, integrin β	XLK, SPARC	–
Larval basal cell	RLK, RAK, integrin β	XLK, XAK-C	–
Adult basal cell	RAK, integrin β, SPARC	XAK-C, SPARC	CK5, CK14, integrin β
Spinous/granular cell	hbA	XAK-A, XAK-B	CK1, CK10

[a]Furlow *et al.* (1997).
[b]Moll *et al.* (1982).

Figure 4 shows the expression of *colα1, rlk,* and *rak* in respective cells during the metamorphosis of bullfrog tadpole, at early TK-II, -III, -X, and adult. Fluorescent views of Bouin-fixed sections are also presented to identify Figures of Eberth (Kawai *et al.*, 1994). Basal skein cells at early TK-II express COLα1 (Fig. 4A) and RLK (Fig. 4B), but not RAK mRNAs (Fig. 4C). Basal skein cells have not developed keratin bundles (Fig. 4D). The skin at TK-III shown in Fig. 4E contains suprabasal skein cells and the fibroblast-populated collagen lamella. Fibroblasts are concentrated near the lamella. These fibroblasts intensely express *colα1*. The basal cells well develop keratin bundles (Fig. 4H) and intensely express *colα1* (Fig. 4E) and *rlk* (Fig. 4F). Importantly, these cells do express RAK mRNA, an adult basal marker gene (Fig. 4G), indicating that basal skein cells proceed to the next step of basal cell differentiation. We call the basal skein cells at this step "*rak*$^+$ basal skein cells" to emphasize that the basal skein cells begin to express an adult gene. Thus, the *rak*$^+$ basal skein cells are defined as the cells that express genes of *colα1, rlk,* and *rak*, and contain keratin bundles. The suprabasal skein cells express *rlk* (Fig. 4F). The dermis at TK-X contains *s*-connective tissues (Fig. 4I–L). Basal cells cease to express *colα1* (Fig. 4I) and *rlk* (Fig. 4J), and do not contain keratin bundles (Fig. 4L), indicating that the basal cells drastically change their characteristics. They discard several larval traits, but continue to express *rlk* and *rak* (Fig. 4K). We call these basal cells "larval basal cells" or "preadult basal cells," and propose using the term "preadult skin" as the skin that contains larval basal cells in the epidermis and the *s*-connective tissue in the dermis. Supra-basal skein cells at TK-X abundantly propagate and form multilayers, and their keratin bundles are conspicuous (Fig. 4L). The adult basal cells do not express *colα1* (Fig. 4M) and *rlk* (Fig. 4N), but do express *rak* (Fig. 4O). The epidermis does not contain suprabasal skein cells (Fig. 4P).

The previously mentioned expression profiles of the molecular markers for various types of basal cells strongly suggest a pathway of their development and differentiation during metamorphosis as shown in Fig. 5. Presently, at least four types of basal cells have been distinguished in the epidermis during larval and metamorphic development. These cells sequentially emerge on the basement membrane during development of a tadpole as follows: basal skein cells, *rak*$^+$ basal skein cells, larval (or preadult) basal cells, and adult basal cells. They are considered to be on the same lineage (Suzuki *et al.*, 2002). Skein cells are the cells that contain keratin bundles (kb$^+$) and express *colα1* and *rlk,* but not *rak* (kb$^+$, *colα1*$^+$, *rlk*$^+$, *rak*$^-$). *Rak*$^+$ basal skein cells are of kb$^+$, *integrin β1*$^+$, *colα1*$^+$, *rlk*$^+$, and *rak*$^+$. Larval basal cells are of kb$^-$, *integrin β1*$^+$, *colα*$^-$, *rlk*$^+$, and *rak*$^+$. Adult basal cells are of *integrin β1*$^+$, *colα1*$^-$, *rlk*$^-$, and *rak*$^+$.
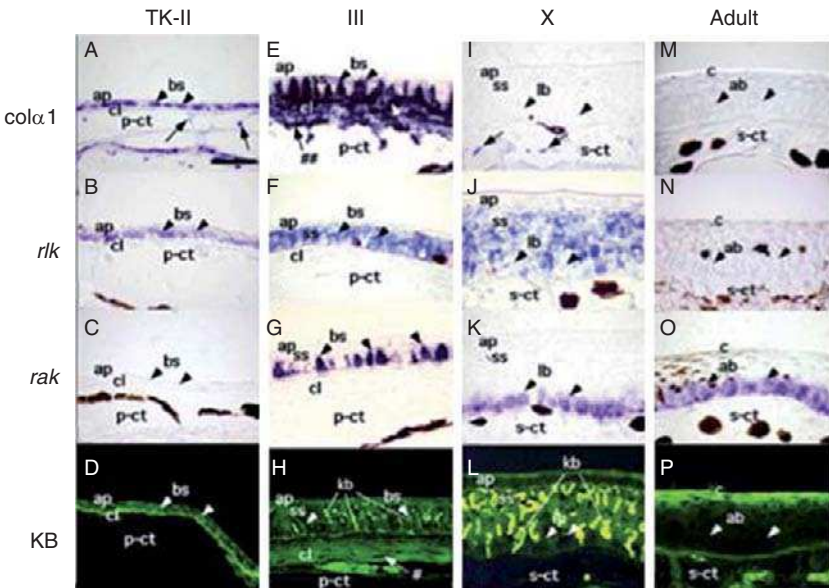
FIG. 4 Distribution of mRNAs of COLα1, RLK, and RAK in the epidermis. *In situ* hybridization was performed with cRNA probes of COLα1 *(colα1)* (A, E, I, M), RLK *(rlk)* (B, F, J, N), and RAK *(rak)* (C, G, K, O) for the *Rana* epidermis at TK-II (A, B, C), III (E, F, G), X (I, J, K), and adult (M, N, O). Bouin-fixed skin sections (KB) are shown for TK-II (D), III (H), X (L), and adults (P). Arrowheads in the figures point to some of the basal cells. (A) The COLα1 gene is expressed in basal skein cells (bs), but not in apical cells (ap). Fibroblasts in *p*-connective tissues (*p*-ct) also weakly express the gene (arrows). No fibroblasts are in the collagen lamella (cl). (B) The RLK gene is expressed in basal skein cells, but not in apical cells. (C) RAK mRNA is not detected in any cells. Brown and red colors represent pigment cells. (D) Strong fluorescence is seen in the collagen lamella (cl). The two-layer structure of the epidermis is clearly recognized and basal skein cells do not develop keratin bundles. (E) Basal cells intensively express *colα1* (arrowheads). Collagen lamellae are invaded by fibroblasts (#). These fibroblasts and the fibroblasts (##) approaching the lower side of the collagen lamella strongly express *colα1*. (F) RLK mRNA is detected in both suprabasal skein (ss) and *rak+* basal skein cells but not in apical cells. (G) RAK mRNA is observed only in *rak+* basal skein cells (arrowheads). (H) The three-layer structure is clearly seen in the epidermis. Keratin bundles (kb) are well developed in two types of skein cells, *rak+* basal skein cells and suprabasal skein cells. (I) Laval basal cells (lb) do not express *colα1*. The *s*-connective tissue (*s*-ct) is formed between the basement membrane and the collagen lamella. The collagen lamella and *p*-connective tissue (*p*-ct) are not seen here and in (J) through (P). (J) Suprabasal skein cells, but not apical and larval basal cells, express *rlk*. (K). Larval basal cells, but not apical and suprabasal skein cells, express *rak*. (L) Suprabasal skein cells fully develop fluorescent keratin bundles. (M) No signals of COLα1 mRNA are seen in the adult epidermis. c, cornified cells; ab, adult basal cells. (N) RLK mRNA is not detected in the adult epidermis. (O) RAK mRNA is exclusively and intensively expressed in adult basal cells (ab). (P) Keratin bundles are not observed in adult epidermal cells. Bar, 50 μm.
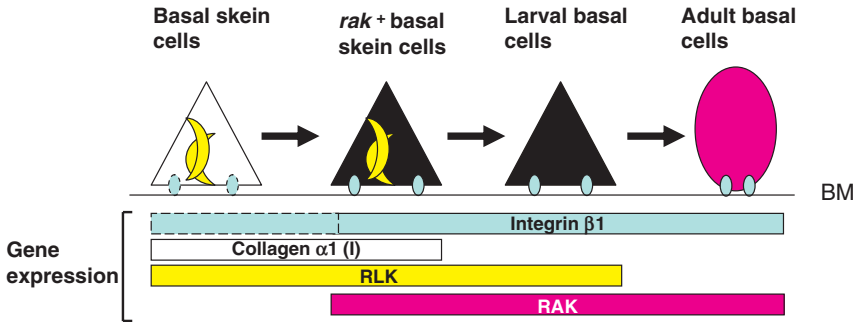
FIG. 5 Sequential changes of types of anuran basal epidermal cells during metamorphosis. Basal skein cells are defined as the cells that express *colα1* and *rlk,* and have keratin bundles. When basal skein cells start to express *rak,* we call them *rak*[+] basal skein cells. *rak*[+] basal skein cells differentiate to larval basal cells by losing keratin bundles and terminating *colα1* expression. Finally, larval basal cells differentiate into adult basal cells by terminating the expression of RLK. The rectangles represent the period of time of their expression. The expression of the gene of integrin β1, collagen α1(I), RLK, and RAK is shown in green, white, yellow, and deep pink, respectively. The cell-attached long thin bar represents the basement membrane (BM). The double yellow-colored crescents that cross each other represent keratin bundles. The small gray-colored ovals at the basal side of each of the cells represent integrin β1. The yellow and pink colors in the cytoplasm represent RLK and RAK, respectively. The gray rectangles and ovals enclosed by dashed lines indicate that the expression of integrin has not been determined yet.

C. Evidence That Basal Cells Include Epidermal Stem Cells and Larval Basal Cells Possess the Potential to Differentiate into Adult Counterparts

Two possibilities have been put forward about the origin of adult basal cells (Yoshizato, 1986, 1989, 1992, 1996). (1) Larval and adult basal cells are on the same cell lineage: some of the larval cells differentiate into adult cells during metamorphosis. (2) Progenitor cells of adult basal cells different from larval basal cells in cell lineage are present in the larval skin. Larval basal cells undergo apoptosis and progenitor cells of adult basal cells are activated and start to proliferate and differentiate into adult basal cells during metamorphosis. We tested which of the two possibilities works in both *R. catesbeiana* and *X. laevis.* The results obtained strongly supported the first possibility.

1. Studies on *Rana* Tadpole

A one-layered epidermis sheet composed only of preadult basal cells was prepared and cultured to examine the replication capacity and the differentiation potential of the basal cells (Suzuki *et al.,* 2002). This experiment

demonstrates two important aspects of basal cells: larval basal cells act as epidermal stem cells that are able to replicate and produce differentiated offspring located in suprabasal layers, and larval basal cells are the origin of adult basal cells that are able to construct the adult epidermis.

Pieces of *Rana* back skin were isolated from tadpoles at around TK-X. Apical and suprabasal skein cells were completely removed from the skin by immersion in 70% ethanol and were shaken with Ca^{2+}- and Mg^{2+}-free phosphate-buffered saline containing 2.5 mM EDTA (Niki and Yoshizato, 1986). The skin sheets obtained are composed of the epidermis, which contains only larval basal cells, the basement membrane, and the dermis, consisting of the s-connective tissue, collagen lamella, and the p-connective tissues. These sheets were cultured for 9 days in the presence of aldosterone (AL), T_3, or prolactin (PRL) (Fig. 6). Figure 6A–C clearly shows that the epidermis before culture (0 day) is a single layer composed of RLK^+ and RAK^+ larval basal cells (Fig. 6A, C). hbA-positive cells are not present (Fig. 6B). The single-layered epidermis develops into a multilayered epidermis (Fig. 6F). The basal layer is RLK^- and RAK^+ (Fig. 6D), and the upper layers become intensely hbA^+ (Fig. 6E). Importantly, AL alone is capable of inducing the differentiation of larval basal cells into adult basal cells. However, the epidermis is not a "true adult" epidermis, because its upper layers are RLK^+ (Fig. 6D), indicating that AL induces the formation of unusual progenies in terms of protein profiles, simultaneously expressing both larval and adult proteins.

Addition of T_3 to the cultures does not affect the expression of RAK in the basal layer (Fig. 6G), nor the expression of hbA^+ (Fig. 6H), but, importantly, T_3 terminates the expression of RLK in the upper layers (Fig. 6G). Thus, the epidermis becomes the "true" adult epidermis. An H&E-stained section shows that the skin is of an adult type (Fig. 6I). It should be noted that basal, but not suprabasal cells require T_3 to terminate the expression of RLK. On the other hand, the presence of PRL permits the basal cells to continue to be RLK^+ and RAK^+ as in day 0 cultures (Fig. 6J), supporting the notion that PRL is a stimulator of larval phenotype expression (Asahina *et al.*, 1997). PRL induces the single layer of larval basal cells to form RLK^+ and hbA^- suprabasal layers (Fig. 6J, K), its histology being of a larva type (Fig. 6L). This indicates that RLK^+ suprabasal cells are progenies of larval basal cells. PRL inhibits the action of aldosterone to induce the differentiation of larval basal cells into adult basal cells and might stimulate the replication of larval basal cells, which results in the production of RLK^+ cells.

The hormone-induced *in vitro* epidermal remodeling is schematically summarized in Fig. 6M. AL alone is capable of inducing the differentiation of larval basal cells into adult basal cells by terminating the expression of RLK. However, interestingly, RLK^- adult basal cells yield RLK^+ suprabasal cells
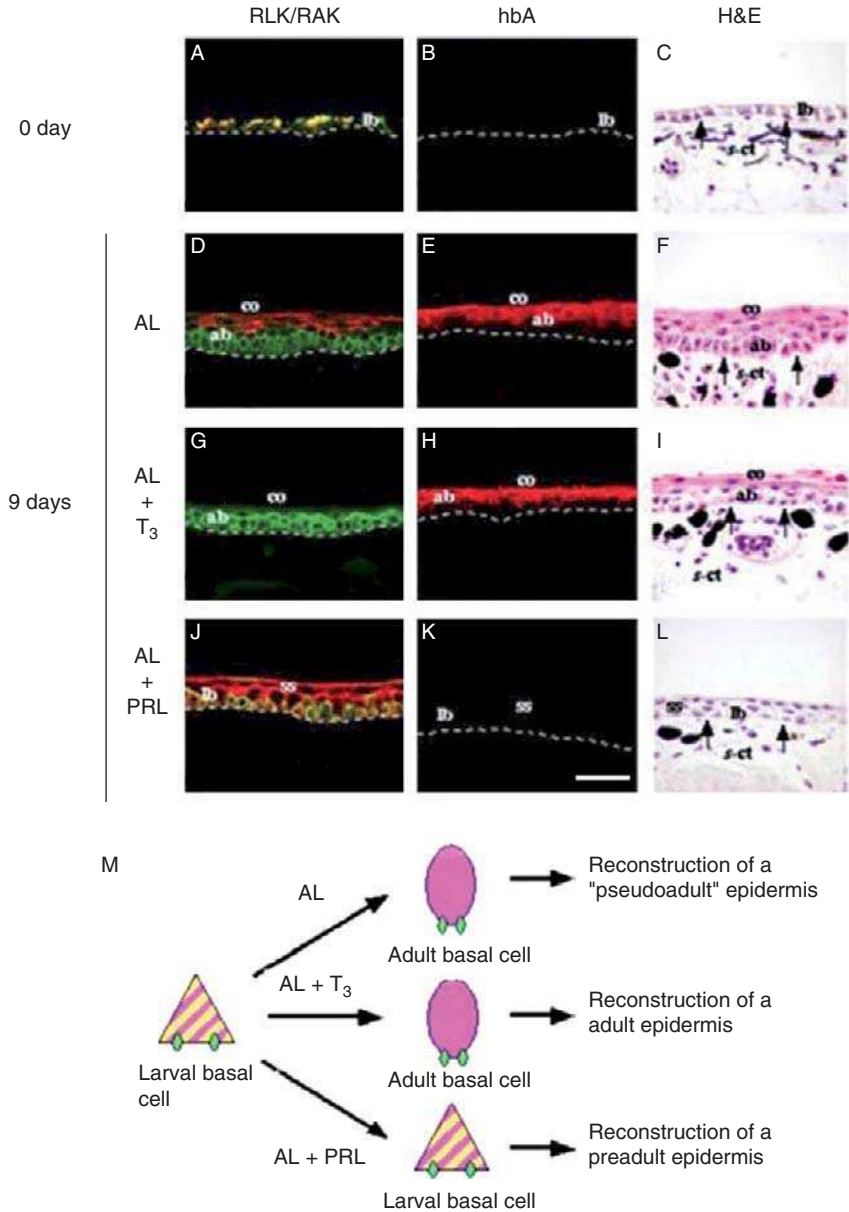
FIG. 6   Differentiation capacity of larval basal cells of *Rana catesbeiana* into adult counterparts. Back skin sheets at TK-X whose epidermis was composed of basal cells alone were cultured for 9 days in the presence of aldosterone (AL) (D, E, F), AL and T_3 (G, H, I), or AL and PRL (J, K, L): the concentration of AL, T_3, and PRL was 1 μM, 10 nM, and 2 μg/ml, respectively. The cultured skins were subjected to double immunohistochemical staining for RLK (red) and

in this hormonal condition. T_3 normalizes this unusual differentiation. Each of the apical and skein cells showed high [^{3}H]thymidine-labeling indices (Robinson and Heintzelman, 1987), suggesting that there are no hierarchical "stem cell to its progeny relationship" among basal cells and suprabasal cells in the tadpole skin. The results of the *in vitro* organ culture experiments demonstrate the presence of a hierarchical relationship in amphibian epidermis in the larva and the adult. The monolayered epidermis composed of larval basal cells reconstructed multilayered epidermis composed of hbA$^+$ granular and cornified cells in the presence of AL and T_3, which indirectly indicates that adult basal cells contain a stem cell population as in adult mammals (Watt, 2001). The monolayered epidermis is also able to construct multilayered epidermis composed of RLK$^+$ suprabasal cells in the presence of AL alone, or AL and PRL. These RLK$^+$ cells are most likely suprabasal skein cells. If so, this fact indicates that larval basal cells are able to construct the larval epidermis lacking apical cells. Thus, it is most likely that there is a mammalian type hierarchical relationship between basal skein cells and suprabasal skein cells, and between *rak*$^+$ basal skein cells and suprabasal skein cells at each corresponding developmental stage of the larval epidermis. Apical cells are thought to be independent of "this stem cell to progeny lineage," because there are no morphological and biochemical similarities among apical cells and the remaining epidermal cells (Furlow *et al.*, 1997; Robinson and Heintzelman, 1987; Suzuki *et al.*, 2001). Apical cells are highly mitogenic and are likely self-replicative (Robinson and Heintzelman, 1987).

RAK (green) (RLK/RAK) (A, D, G, J). Or, they were subjected to single immunostaining for hbA (red) (B, E, H, K). Sections of skin were also stained with H&E (C, F, I, L). Sections of (A) through (C) are before culture (0 day). Photographs (in A, D, G, and J) are overlays of RLK and RAK stains. Double positive cells are seen in yellow. All the cells attached to the basement membrane indicated by the dashed lines were double positive before culture (0 day) (A) and in the cultures with AL and PRL (9 days) (J). Arrows in the H&E sections point to basement membrane. The abbreviations used are as in Fig. 4. Bar in (K), 50 μm. (M) A scheme for the hormonal regulation of the differentiation of larval basal cells. When larval basal cells are exposed to AL, they terminate RLK (yellow) expression and differentiate into RAK$^+$ (pink) adult basal cells that produce hbA$^+$ granular cells. Thus, larval basal cells are potentially progenitors of adult basal cells (adult epidermal stem cells), but cannot construct the "true" adult epidermis, because the progenies produced are RLK$^+$ as well as hbA$^+$ ("pseudoadult" epidermis). The exposure of larval basal cells to both AL and T_3 terminates the expression of RLK in the progenies, making the reconstructed skin the "true" adult skin. On the other hand, larval basal cells do not differentiate into adult basal cells when exposed to AL and PRL, but stay as larval basal cells and produce RLK$^+$ progenies (most probably suprabasal skein cells). Pairs of green ovals at the base of cells represent integrin β1. Thus, it is concluded that larval basal cells also act as larval epidermal stem cells and construct the preadult epidermis. Taken together, larval basal cells potentially go into the two different differentiation paths, the larval and adult path, depending on the hormonal environment. PRL enables larval basal cells to remain in the larval path. T_3 forces the same cells to go into the adult path.

2. Studies on *Xenopus* Tadpole

Basically similar remodeling of larval to adult skin was reproduced *in vitro* in the presence of TH for *Xenopus* larval skin (Utoh *et al.*, 2003). The back skin at NF-54/55 whose epidermis is at a preadult stage was cultured for 9 days in the presence of AL, corticosterone, and hydrocortisone (Fig. 7). The epidermis before culture consists of apical cells at the surface, relatively large skein cells at the base, and small larval basal cells scattering among large skein cells at the base (Fig. 7A). The mesenchyme contains the collagen layer and *p*-connective tissues. The larval basal cells are XLK^+ (Fig. 7B) and $XAK-B^-$ and $-C^-$. Skin tissues remain larval when cultured without T_3 for 9 days (Fig. 7C) except that aggregates of larval basal cells are formed. These aggregates are most likely to develop into secretory glands in the adult skin and are called the presumptive secretory gland (PSG). The skein and larval basal cells are XLK^+ (Fig. 7D). There are no $XAK-B^+$ cells (Fig. 7E). Notably a few $XAK-C^+$ basal cells (preadult basal cells) are present around PSGs (Fig. 7E, arrows), suggesting that larval basal cells around PSGs are able to differentiate into preadult basal cells without TH. Skein and apical, but not basal, cells are mitotically active (Fig. 7F). The larval skin histologically differentiates into a near-complete adult skin when cultured in the presence of T_3 except that *s*-connective tissue is not formed (Fig. 7G). Subepidermal fibroblasts appear to be activated, because, first, collagen lamellae markedly thicken and, second, multiple fibroblasts penetrate into the collagen lamella. There are no XLK^+ cells (Fig. 7H). $XAK-C^+$ adult basal cells increase greatly to a degree at which these cells occupy the whole region of the basal layer (Fig. 7I). Comparison of Fig. 7E and I suggests that the proliferation of preadult basal cells and their differentiation into adult basal cells are TH-dependent processes. The upper layers contain $XAK-B^+$ cells (Fig. 7I). Adult basal cells are in S-phase of the cell cycle (Fig. 7J). This study clearly shows that originally XLK^+ larval basal cells terminate the expression of *xlk* and instead start to express the *xak-c* gene without T_3, which represents the process of T_3-independent differentiation of larval basal cells into preadult basal cells as in *R. catesbeiana*. These active changes in the epidermal compartment are well associated with those in the mesenchymal compartment, both requiring TH.

The *in vitro* organ culture experiments of larval skin of both *Rana* and *Xenopus* clearly demonstrate that larval basal cells actually have the potential to differentiate into adult basal cells. At present, the other important issue that remains to be clarified is whether basal skein cells actually have the potential to differentiate into larval basal cells. However, we previously presented indirect evidence that they have this potential (Yoshizato *et al.*, 1993). Larval basal and basal skein cells were isolated from the back and the tail of *Rana* tadpoles at TK-X, respectively, and cultured for 4 days in the
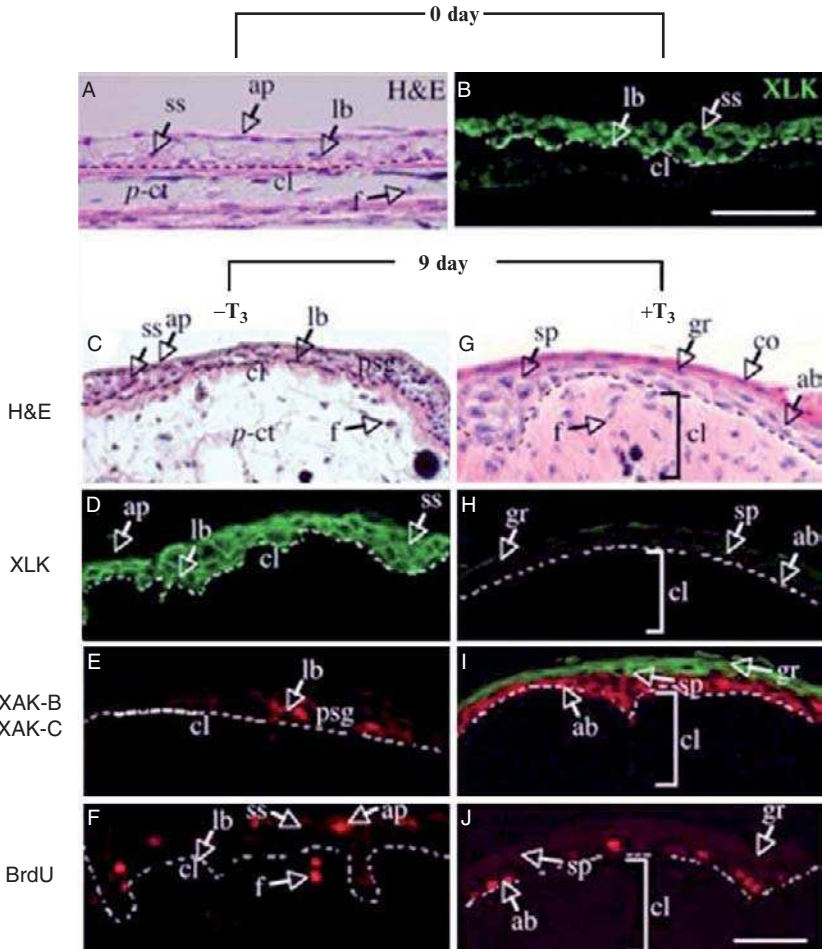
FIG. 7   Larval to adult skin transformation in *Xenopus laevis*. (A–J) Pieces of back skin at stage 54/55 (A, B) were cultured for 9 days in the absence (−T$_3$) (C–F) or presence of 100 n*M* T$_3$ (+T$_3$) (G–J). (A, C, G) H&E stains. (B, D, H) Immunostaining for XLK. (E, I) Double immunohistochemical staining for XAK-C (red) and XAK-B (green). (F, J) Skins were labeled with 20 μ*M* BrdU for the last 24 h and were immunostained for BrdU. Dashed lines in the photographs represent the location of the basement membrane. Arrows with closed arrowheads in (E) show XAK-C-positive preadult basal cells around PSG. sp, spinous cells; gr, granular cells; c, cornified cells. Bar in (B) and (J), 50 μm.

absence or presence of 10 n*M* T$_3$. Not only body epidermal cells but also tail cells were induced to express hbA by T$_3$. A similar response of tail epidermal cells to TH was also reported for *Xenopus* tadpoles utilizing adult specific

keratin protein (63 kDa keratin) as a probe (Nishikawa *et al.*, 1992). Apparently, these results indicate that the tail contains a population of cells that is competent to convert to adult epidermal cells in response to TH. *Rana* tail epidermal cells mostly consist of basal skein cells. Thus, T_3-dependent induction of hbA expression in tail epidermal cells suggests two possibilities. First, very few larval basal cells are included in the tail epidermal preparation, and these cells proliferate and differentiate into adult basal cells and then granular cells. Second, basal skein cells will undergo apoptosis under the action of TH in normal development. However, these cells might have the potential to differentiate into adult basal cells under appropriate conditions. Subepidermal mesenchymal tissues exert a critical influence in determining an actual differentiation pathway from possible differentiation potentials. The epidermal cell cultures were freed from subepidermal mesenchymal cells. We assume that basal skein cells are able to differentiate into larval basal cells in these conditions. This assumption is based upon studies that show the dependence of the metamorphic fate of larval epidermal cells, either differentiation into adult epidermal cells or apoptosis, on the underlying mesenchymal cells (Kawai *et al.*, 1994; Kinoshita *et al.*, 1986a,b).

In mammals, the epidermis is constructed by proliferation of epidermal stem cells located on the basement membrane and by differentiation of their offspring. The histological similarity of the adult epidermis between mammals and anurans described in Sections II and III suggests that the anuran basal cells are epidermal germinative (stem) cells. This suggestion is experimentally supported by skin organ culture experiments described in this section.

D. Skin Transformation Center

Needle-like crystals of calcium phosphate are deposited in the upper part of collagen layers of adult bullfrog skin (Taylor *et al.*, 1966). An analysis using an X-ray microanalyzer confirmed this report (Hayashi *et al.*, 1977). Thus, calcium phosphate seems to be a useful marker of differentiation of larval to adult skin. A tadpole at TK-V was stained with alizarin red S that specifically binds calcium in tissues (Dahl and Dole, 1952). The body skin except the frontal region bound the dye, whereas the tail skin except the anterior region did not bind it (Fig. 8A, Tamakoshi *et al.*, 1998). The red colored region was histologically confirmed to be preadult and the dyeless region to be larval. Thus, whole-mount *in situ* staining with alizarin red S is suitable to easily and specifically identify the region where the conversion of larva to preadult was completed. The skin around the boundary region between the body and the tail was removed from a TK-XXI tadpole and subjected to histological examinations. The top of the collagen layers was stained red by the dye in

the body side of the skin where the *s*-connective tissue had been formed and the epidermis had transformed into adult skin. In sharp contrast the skin on the tail side where the skin remained larval was not stained.

Using this method, we sought to determine when and where preadult skin conversion takes place. Tadpoles at various developmental stages were subjected to alizarin red S whole-mount *in situ* staining (Tamakoshi *et al.*, 1998). The results are schematically summarized in Fig. 8B. Animals at TK-II are negative. The red-colored region first appears at a middle region of both the right and left lateral side at TK-II to III, indicating that this region is the place where the conversion starts. We postulate a specific site in this middle lateral region where the preadult transformation originates and call this site the STC. The hypothetical STC is the boundary between the stained and unstained region. STC migrates from the original site anteriorly and posteriorly, and dorsally and ventrally, which results in the red staining of the whole body skin
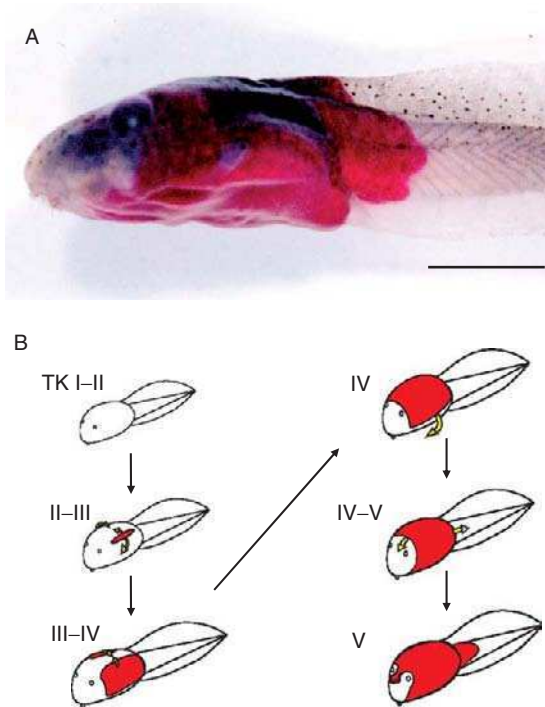
FIG. 8   Sequential transformation of larval skin into preadult skin. (A) Whole-mount *in situ* staining with alizarin red S. A tadpole at TK-V was stained with alizarin red S. Bar, 1 cm. (B) Schematic representation of the sequential spread of the calcium-deposited region in the skin. Yellow arrows indicate the direction of the ensuing movement of the skin conversion center.
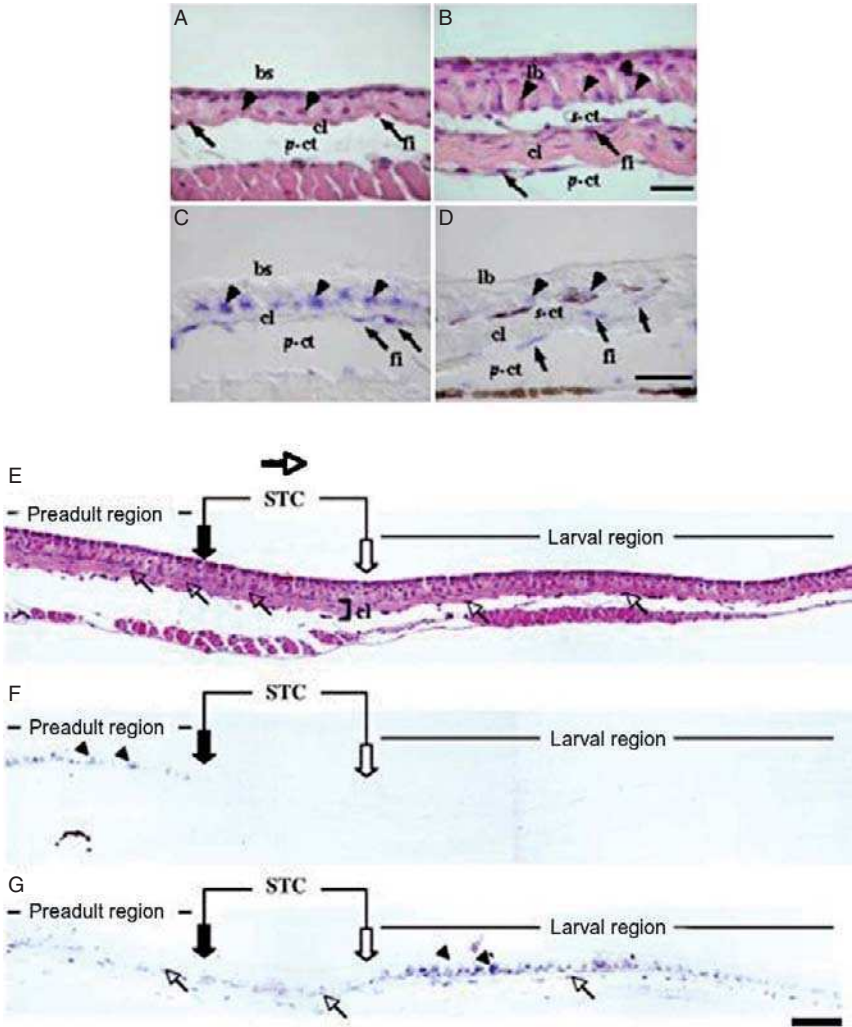
FIG. 9 Identification of STC by RAK and SPARC mRNA expression. Back skin sections at TK-II (larval skin; A, C) and at TK-IV (preadult skin; B, D) were subjected to H&E staining (A, B) and *in situ* hybridization of *sparc* mRNAs (C, D). (A) The larval epidermis faced the thin collagen lamella (cl) under which *p*-connective tissues (*p*-ct) were present. Basal skein cells (bs; arrowheads) are attached to the basement membrane. Fibroblasts (fb; arrows) are present underneath the acellular collagen lamella. (B) Basal skein cells are replaced with larval basal cells (lb; arrowheads). *S*-connective tissues (*s*-ct) develop between the epidermis and the thickened collagen lamella. Fibroblasts (arrows) are observed in *s*-ct, and in and on the collagen lamella. (C) Basal skein cells (arrowheads) and fibroblasts underneath the collagen lamella (arrows) express *sparc* intensely in the larval skin. (D) Both larval basal cells (arrowheads) and fibroblasts in and on the collagen lamella (arrows) express *sparc*. The expression levels are much lower than basal skein cells and fibroblasts in the larval skin. The magnification in (A) and (C) is

except for the frontal area. The red-colored region never invades most of the tail region, indicating the presence of a still unknown mechanism that inhibits the migration of STC into the tail.

We cloned the SPARC gene as a gene whose expression is upregulated in the larva to preadult skin conversion of *R. catesbeiana* (Ishida *et al.*, 2003). SPARC is a suppressor of *rak* during epidermal differentiation. mRNA *in situ* hybridization was performed on sections from larval skin at TK-II and preadult skin at TK-IV (Fig. 9). Basal skein cells intensely express SPARC mRNA (Fig. 9C), whereas larval basal cells weakly express it (Fig. 9D). Sections from TK-IV back skin were subjected to *in situ* hybridization for *rak* and *sparc* (Fig. 9E–G). The examined skin is separated into three regions in terms of *rak* and *sparc* expression: (1) the $sparc^{2+}$ and rak^- region, (2) $sparc^+$ and rak^- region, and (3) $sparc^+$ and rak^+ region. In the $sparc^{2+}$ and rak^- region, *sparc* is expressed in basal skein cells, and fibroblasts start to migrate into collagen lamella. Thus, the $sparc^{2+}$ and rak^- region represents the larval edge. By definition of STC this edge is the larval side edge of STC. In the $sparc^+$ and rak^- region, basal skein cells greatly decrease *sparc* mRNA expression, and epidermal basal cells are not committed to express *rak* yet. These basal skein cells are supposed to differentiate into rak^+ basal skein cells. Thus, the $sparc^+$ and rak^- region represents STC. In the $sparc^+$ and rak^+ region, the basal skein cells have differentiated into rak^+ basal skein cells. Thus, the $sparc^+$ and rak^+ region is the preadult side edge of STC. H&E staining (Fig. 9E) shows that fibroblasts invade the collagen lamella, but have not developed *s*-connective tissue yet. The collagen lamella becomes thinner toward the right side of the view, indicating that the larva to preadult skin transformation progresses to the right. From these observations, we define STC as the $sparc^+$ and rak^- region. Then, STC is visualized on a histological section as an about 150-µm-long region that contains about 20 *rak*-negative and weakly *sparc*-positive basal cells (Fig. 9G).

the same as in (B) and (D). Bars, 50 µm. (E–G) Comparison of the expression pattern of *rak* and *sparc*. Back skin sections at TK-IV were subjected to H&E staining (E) and *in situ* hybridization for *rak* (F) and *sparc* (G). (E) Fibroblasts (oblique arrows) often invade the collagen lamella (cl), but *s*-ct have not developed between the epidermis and the collagen lamella. The rightmost oblique arrow points to the last fibroblast present in the collagen lamella of the larval region. (F) The rak^+ basal skein cells (arrowheads) appear on the left side (preadult region), but not on the right side (larval region). We define the preadult region as the skin in which basal cells are rak^+. (G) Intense signals of *sparc* mRNA in the epidermis (arrowheads) are observed on the right side, but not on the left side. Fibroblasts are *sparc* positive. Closed and open thick arrows represent the boundary between the rak^+ and rak^- region and the boundary between the $sparc^{2+}$ and $sparc^+$ region, respectively. The larval region is defined as the skin in which basal cells are $sparc^{2+}$. STC is localized by comparing the expression pattern of *rak* in (F) and *sparc* in (G) and sandwiched by the closed and the open thick arrow. STC is progressing toward the right as indicated by the vertical arrow. Bar, 50 µm.

III. Epithelial–Mesenchymal Interactions and Larval
Skin Remodeling

A. Tail- and Body-Dependent Metamorphic Fate of
   Larval Skin

STC is the front where larva to preadult skin conversion is actively taking place. STC originates at a specific site of a lateral region of the upper dorsal skin of a larva and migrates to other regions where the larval skin follows "a differentiation program" that determines when, where, and how the larval skin differentiates to preadult and to adult skin. STC never invades the tail region where larval skin is not transformed to preadult skin, but follows a quite different program, "an apoptosis program" that determines when, where, and how larval skin undergoes histolysis. We are interested in the mechanism under which STC does not invade the tail region. This mechanism is responsible for the region (the tail and body)-dependent metamorphic fate of larval skin. Previous studies indicate that the mesenchymal compartment plays a critical role(s) in determining the tail- and body-dependent metamorphic fate of larval skin (Kawai *et al.*, 1994; Kinoshita *et al.*, 1986a,b).

Both the epidermis and the mesenchyme were isolated from the body (back) and the tail of *Rana* tadpoles at TK-IV and X as larval and preadult skin tissues, respectively. There are no histological differences between the back and the tail skin at TK-IV. The basal cells are all basal skein cells and the mesenchyme has not yet developed *s*-connective tissue. From these isolated tissues, homo- or heterotypically recombined skins were reconstructed and autografted to the back or the tail region to match the site (back or tail) of the epidermis of the recombined skin with that of the recipient. Two types of heterotypic transplants were made: the tail epidermis with the back mesenchyme (T/B) and the reverse (B/T), and two types of homotypic transplant (B/B and T/T). The host animals at TK-IV and X were allowed to develop for 4 months and 2–3 weeks, respectively, during which the hosts developed to TK-XIV and XVII. The transplants were subjected to histological and immunohistological investigations. The epidermis of heterotypic grafts in experiments with TK-IV tadpoles changed its original regionality (dorsum or tail) to a regionality that is identical to the combined mesenchyme: the original tail epidermis in T/B transplants developed into the dorsal epidermis containing preadult basal cells and the original dorsal mesenchyme developed into the dorsal mesenchyme, (i.e., the mesenchyme developed *s*-connective tissues and secretory glands, and thickened collagen laminae). Similarly, the original dorsal epidermis in B/T transplants developed as the tail epidermis containing basal skein cells with well developed Figures of Eberth: the attached mesenchyme did not develop *s*-connective tissues. Some hosts with

T/B transplants were allowed to enter the climax stages of metamorphosis. The epidermis became hbA$^+$, indicating the transplants developed into adult skin. The epidermis of B/T grafts was hbA$^-$ and its mesenchyme was infiltrated with lymphocytes, indicating that the mesenchyme was under histolysis as originally programmed. In contrast, the epidermis of heterotypically recombined skin made from tadpoles at TK-X developed as originally programmed. Similarly, no mesenchymal effects were observed in B/T skin grafts. Thus, it can be said that the body or tail identity of the epidermis is determined by the underlying mesenchyme before the latest TK-X in bullfrogs. The subepidermal mesenchyme at TK-X does not possess inductive activity, suggesting that inductive activity is lost when the *s*-connective tissue is formed. However, the precise developmental stage at which inductive activity disappears has not yet been determined. It is most likely that mesenchymal inductive ability is lost when basal skein cells are replaced with larval basal cells. Heterotypically recombined skin experiments show that both the body and tail mesenchyme of the larval skin possess inductive ability on the overlying epidermis. However, their ability is quite different in nature: the body mesenchyme induces differentiation in the larval epidermis, whereas the tail mesenchyme induces apoptosis in the same tissue. The molecular mechanism for the regionally defined inductive ability of the mesenchyme remains to be determined.

B. Platelet-Derived Growth Factor (PDGF)-A Signaling as a Molecular Cue in TH-Induced Skin Remodeling

It is known that epidermal–mesenchymal interactions are also required for the differentiation and proliferation of mammalian epidermal cells. PDGF/PDGFR signaling is claimed to play an important role(s) in this interactive system (Schatteman *et al.*, 1992; Skobe and Fusenig, 1998). The PDGF family consists of four members, PDGF-A, -B, -C, and -D, each of which assembles into dimers and acts on homo- or heterodimers of two receptor tyrosine kinases, PDGFR-α and PDGFR-β. PDGFR-α and -β preferentially bind PDGF-A, -B, and -C, and PDGF-B and -D, respectively (Betsholtz *et al.*, 2001). The embryonic epidermis and the underlying mesenchymal cells of the mouse skin express PDGF-A and -C and its receptor PDGFR-α (Aase *et al.*, 2002; Ding *et al.*, 2000; Karlsson *et al.*, 1999; Orr-Urtreger and Lonai, 1992; Schatteman *et al.*, 1992). PDGFR-α gene-deficient mouse embryos often show a severe loss of dermal mesenchyme, which results in the regional detachment of the epidermis (Schatteman *et al.*, 1992; Soriano, 1997). Their epidermal layers are thin and do not develop cornified layers.

We tested the possibility that PDGF signaling acts as a molecular cue(s) in the epithelial–mesenchymal interaction in metamorphic skin transformation using *X. laevis* (Utoh *et al.*, 2003). The skin expresses mRNAs of both

PDGF-A and PDGFR-α at a low level until NF-56 (premetamorphic stage) and markedly increases the expression at NF-58 (prometamorphic stage) when the expression is highest and XAK-C mRNA-expressing preadult basal cells are first detectable (Watanabe *et al.*, 2002). Then, the level decreases at NF-60 when tadpoles enter metamorphic climax and the development of *s*-connective tissue is complete. mRNAs of XAK-A and -B are first detectable at NF-60 (Watanabe *et al.*, 2001). The expression of PDGF-A and PDGFR-α genes is upregulated by T_3, which takes place before XAK-A and -B mRNA-positive epidermal cells first appear (Watanabe *et al.*, 2001). These correlations between PDGF/PDGFR-α and XAK-A, -B, and -C gene expressions suggest some role(s) of PDGF-A and PDGFR-α signaling in T_3-dependent differentiation of larval epidermal cells.

In situ hybridization experiments on mRNAs of PDGF-A were done at NF-57 when larval basal cells are *xak-c$^-$*. These basal cells do not express PDGFR-α. The epidermis around NF-52 contains regions where basal cells have condensed and aggregated. These aggregates develop into PSGs later at early NF-58 and undergo down-growth into the dermis to form secretory glands at NF-59. We consider that larval basal cells near PSGs transform to preadult basal cells because they are *xak-c$^+$*. The preadult basal cells spread to other regions on the basement membrane at late NF-58 and all the basal cells become *xak-c$^+$* at NF-59. The *xak-c$^+$* basal cells (preadult basal cells) around PSGs at early NF-58 express PDGF-A mRNA, spread on the basement membrane at late NF-58, and cease to express the mRNAs at NF-59 when *s*-connective tissue is formed. This expression pattern of PDGF-A mRNAs in larval basal cells indicates that the expression is temporal and closely associated with the differentiation of larval basal cells into preadult basal cells.

The *s*-connective tissue has not formed at NF-57 and fibroblasts sparsely scattered in the *p*-connective tissue weakly express PDGFR-α mRNAs. Fibroblasts become activated at an early NF-58, increase their number, migrate into the collagen lamella and to the basement membrane, and begin to form the *s*-connective tissue. These fibroblasts are intensely PDGFR-α$^+$. Thus, it seems that the expression of the PDGFR-α gene is correlated with the activation of fibroblasts and with the expression of PDGF-A mRNAs in preadult basal cells, which strongly suggests some role(s) of PDGF signaling in the epithelial–mesenchymal interaction during the drastic histological change in the metamorphosing skin. In particular, this signaling seems to activate fibroblasts to form *s*-connective tissue.

This suggestion was tested utilizing an *in vitro* model of larval skin shown in Fig. 10. Skin pieces were cultured for 9 days in the presence of T_3 (control experiments). Skins transformed into the adult type in which cornified cells (Fig. 10A), XAK-C$^+$ adult basal cells (Fig. 10B), and XAK-B$^+$ suprabasal cells (Fig. 10B) are present. XAK-C$^+$ cells are mitotically active (Fig. 10C).

	Control	AG1296	rECD
H&E	A	D	G
XAK-B XAK-C	B	E	H
BrdU	C	F	I
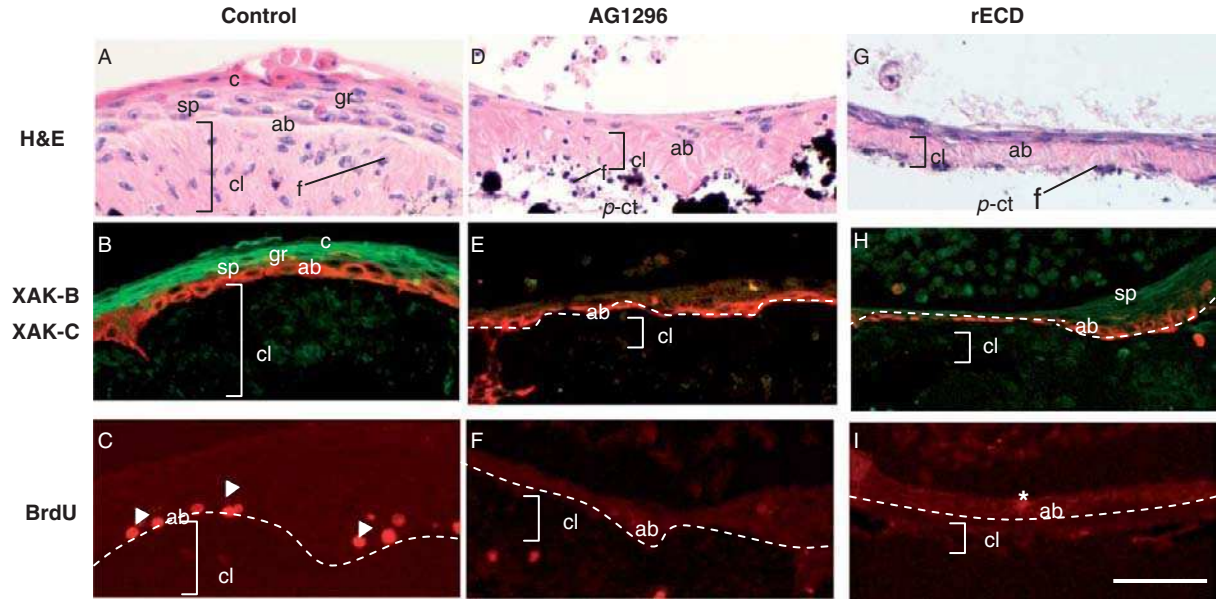
FIG. 10 Effects of inhibitors of PDGF signaling on TH-induced remodeling of larval skin. Pieces of back skin of tadpoles at stage 54/55 were cultured for 9 days in the presence of 100 nM T$_3$ (+T$_3$). (A–C) Control experiments without inhibitors. (D–F) 10 μM AG1296 was added through the culture. (G–I) 100 μg/ml rECD was present. The skins were subjected to H&E staining (A, D, G) or double immunohistochemical staining for XAK-B (shown in green) and XAK-C (red) (B, E, H). The skin tissues in (C), (F), and (I) were exposed to BrdU for the last 24 h and immunostained using anti-BrdU antibodies. Arrowheads in (C) point to representative BrdU-positive cells. Fibroblasts (arrowheads) in (D) and (G) display round and small nuclei indicating possible cell death. The asterisk in (I) indicates nonspecific stains. Dashed lines represent the location of the basement membrane. The abbreviations are the same as in Fig. 7. Bar in (I), 50 μm.

When added to the cultures, AG1296, a specific inhibitor of PDGFR tyrosine kinase autophosphorylation (Kovalenko et $al.$, 1994, 1997; Levitzki and Gazit, 1995), inhibited the previously described T_3-induced changes (Fig. 10D–F). Similarly, recombinant extracellular domains of PDGFR-α (rECD) suppressed the TH effects (Fig. 10G–I). The epidermis fails to develop the multilayers (Fig. 10D and G). In the presence of inhibitors, almost all fibroblasts display round and small nuclei indicating possible cell death (Fig. 10D, G). The invasion of fibroblasts into the collagen lamella is greatly (14-fold) accelerated by T_3. As a result, T_3 thickens collagen lamellae about fourfold as compared with T_3-free control cultures. Fibroblasts do not invade the collagen lamella and collagen lamellae do not thicken in the presence of the inhibitors (Fig. 10D, G). The BrdU-labeling index of basal cells in T_3 cultures is 20-fold higher than that of control cultures. The basal cells with AG1296 (Fig. 10F) and rECD (Fig. 10I) seldom incorporate BrdU, indicating that T_3 induces the proliferation of preadult basal epidermis through PDGF signaling.

XAK-C$^+$ preadult basal cells emerge around PSGs in the absence of TH. Thus, it is most likely that PDGF/PDGFR signaling is not required for the differentiation of larval basal cells into XAK-C$^+$ preadult basal cells. Actually, both AG1296 (Fig. 10E) and rECD (Fig. 10H) do not significantly affect XAK-C expression of basal cells. This signaling is rather required for the initiation of the terminal differentiation of adult basal cells, because both inhibited the expression of XAK-B (Fig. 10E, H). T_3 induces these cells to enter the S-phase of cycles. T_3-activated preadult basal cells seem to differentiate into adult basal cells and secrete PDGF, which activates subepidermal fibroblasts.

It is clear that PDGF/PDGFR signaling is one of the molecular cues of the epithelial-mesenchymal interaction required for skin metamorphosis of anurans. At present we postulate that this activation is a key trigger in the formation of s-connective tissues. It is noteworthy that both PDGF-A- and XAK-C-positive basal cells first appear around PSGs at NF-57 or -58. These basal cells increase their number and spread to other regions on the basement membrane. These epidermal events are tightly coupled with the changes in the underlying mesenchyme. The subepidermal fibroblasts underneath the PDGF-A and XAK-C-positive basal cells are highly active in PDGFR-α mRNA expression as compared with fibroblasts in other regions. We consider that these subepidermal fibroblasts are in an ''activated'' state and are participating in constructing the s-connective tissues. PDGF/PDGFR signaling plays a role in activating the fibroblasts.

PDGF/PDGFR signaling plays key roles in epithelial–mesenchymal interaction during mammalian skin development. The overexpression of PDGF-A in epithelial grafts induces the formation of thicker and more cellular connective tissues (Eming et $al.$, 1995, 1998). When PDGF-overexpressing human

keratinocytes were transplanted onto the back of nude mice, dermal fibroblasts became activated to proliferate and, in turn, the host epidermis also became proliferative and abnormally multilayered, probably due to some paracrine factor(s) secreted by the activated fibroblasts (Skobe and Fusenig, 1998). Conversely, PDGF-A$^{-/-}$ mice (Karlsson *et al.*, 1999) and *Patch* mutation mice whose PDGFR-α gene is deleted (Schatteman *et al.*, 1992) develop thinner dermal tissues and skin devoid of the dermis, respectively.

C. The Skin of Vertebrates: Evolutional Significance of Anuran Skin Metamorphosis

In the previous sections we described the transformation of aquatic larval skin to a terrestrial adult counterpart. In this section the histological features of both types of anuran skin are compared with those of other vertebrate species as an approach to understanding the evolutional significance of anuran skin metamorphosis. The vertebrate epidermis is derived from the ectoderm and is homologous in basic histological structure among amniotes (reptiles, birds, and mammals), termed the stratified squamous epithelium (Matoltsy and Huszar, 1972). The epidermis of amphibia shares a basic structure with amniotes, suggesting that the animals evolved the epidermis that adapted the terrestrial habitation at the emergence of ancestral amphibia and has conserved its basic structure through humans. The epidermis of these animal species is composed of basal, spinous, granular, and cornified layers, each of which is located sequentially upward from the most inner cell layer (the basal layer). The basal and the spinous layer together represent the germinative layer, constitute the proliferative compartment, and are collectively called the stratum Malpighii. The progenies yielded upon division of the cells therein move upward losing replicative capacity up to the cornified layer in which the cells become terminally differentiated anuclear cornified cells. The basal layer in mammals represents a compartment where epidermal stem cells are located (Fuchs and Serge, 2000; Watt and Hogan, 2000). The mammalian epidermal stem cells have been well characterized and represent a specific population of basal cells attached to a unique site of the basement membrane (Jones and Watt, 1993; Jones *et al.*, 1995). The definition of a stem cell indicates that upon cell division a stem cell produces two daughter cells, one being a copy of the mother cell (self-renewal) and the other being transit amplifying cells (TA cells) that produce more differentiated cells upon cell divisions (Watt, 2002). Thus, the stem cell and its descendant differentiated cell are said to be in a hierarchic relation. Upon cell division TA cells yield first the spinous cell, which then yields the granular cell. The granular cell yields the cornified cell. As the hierarchic position goes up, the proliferative potential decreases, spinous cells being highest, whereas the extent of differentiation

increases, cornified cells being in the terminally differentiated state and finally sloughing off as anucleated cells. This kind of hierarchic system in epidermal cells is considered to have first emerged in amphibia in which the stratum corneum is thought to have evolved about 350 million years ago (Matoltsy and Bereiter-Hahn, 1986). We term this type of epidermis "the single-lineage epidermis" in this review. The epidermis is attached to the basement membrane that binds to the mesoderm-derived dermis. The dermis plays roles in regulating the proliferation and differentiation of the epidermal cells and, thus, epithelial–dermal interactions are critical in the development and physiology of the skin.

Figure 11 schematically compares the development of skin between mammals and amphibians, using *Mus musculus* and *X. laevis* as a representative example of each of the classes, respectively. A mouse embryo at E10 of gestation is covered with the ectoderm underlain with the mesoderm. At E12 the ectoderm develops into the epidermis composed of two layers, the periderm at the top and the basal layer at the bottom. Periderm and basal cells autonomically recycle, (i.e., when periderm cells are lost, nearby periderm cells divide and replace them) (Bickenbach and Holbrook, 1986, 1987; Holbrook, 1991). The epidermis at E15 becomes multilayer containing intermediate layers between the periderm and the basal layer. The mesenchymal fibroblasts form the dermis. Intermediate cells are considered to be descendants of basal cells and are in a different lineage from the periderm (Matoltsy, 1986). Thus, the epidermis at this developmental stage is a "two-lineage epidermis." At birth the epidermis forms the basic structure of the adult-type epidermis with hierarchical layers from basal to cornified layers. The periderm cells undergo apoptosis and are sloughed off (Boneko and Merker, 1988), indicating that the epidermis transforms from a two- to a single-lineage epidermis. The epidermis is combined with the mesoderm-derived dermis.

The *X. laevis* skin progressively changes its histological structures during metamorphosis (Fig. 11). The epidermis at NF-30 (tail bud stage) is two-layered, the outer cell and inner cell layers, the cell in the outer layer being ciliated. The epidermis has developed to a "larval epidermis" at NF-45 that is composed of apical and basal skein cell layers. The collagen lamella, a histological entity unique to amphibian dermis, has developed, which is combined with the *p*-connective tissue. At the middle larva stage (around NF-55), small basal skein cells have emerged at the basal layer. Larvae do not significantly change this structure until the prometamorphic stage (NF-58 to -59) when basal skein cells differentiate into larval basal cells, and the *s*-connective tissue is formed between the collagen lamella and the basement membrane. The skin drastically transforms its histology into an adult form during climax stages of metamorphosis (NF-60 to -64), by differentiating larval basal cells into adult counterparts, and simultaneously deleting
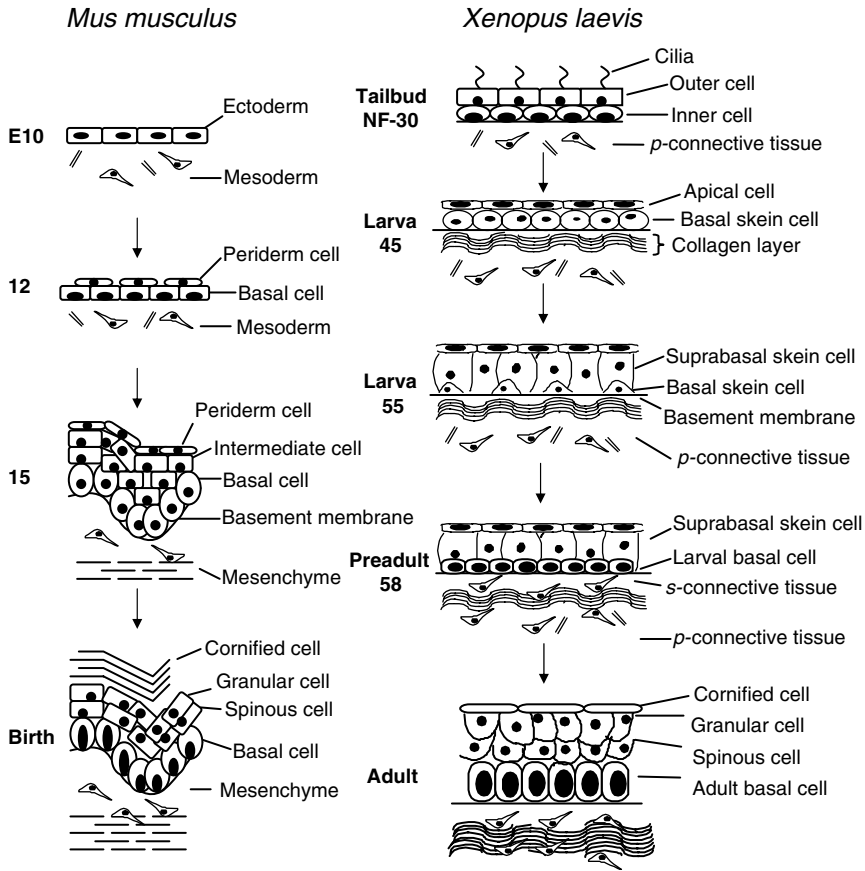
FIG. 11 Schematic representation of the development of skin in mammals *(Mus musculus)* and anurans *(Xenopus laevis)*. Stages of skin development are represented by days after coitus (E) for mice and conventional terms of developmental stage for anurans. The histology of mouse skin at E10, E12–E15, and birth corresponds to that of anuran skin at early embryonic, larval, and froglet stages, respectively. The epidermis develops to a "larval epidermis" at NF-45, which is composed of apical and basal skein cell layers. The collagen lamella (collagen layer) develops, which is combined with the *p*-connective tissue. At a middle larva stage (NF-55), small larval basal cells have emerged at the basal layer. Larval basal cells are well developed at the prometamorphic stage (NF-58 to -59) and the *s*-connective tissue is formed between the collagen lamella and the basement membrane. The skin drastically transforms its histology into an adult one during the climax stages of metamorphosis (NF-60 to -64), larval basal cells differentiating into adult ones.

apical and suprabasal skein cells. The skin of froglets shows the adult histology composed of multilayered epidermis with the dermis consisting of the *s*-connective tissue, the collagen lamella, and the *p*-connective tissue.

The epidermis shows the histological feature characteristic of mammals. Thus, it can be said that the anuran transforms a two-lineage to a single-lineage epidermis during metamorphosis.

The comparison of developmental changes between *M. musculus* and *X. laevis* suggests that apical cells are homologous to periderm cells. This assumption is supported by the fact that apical cells express an anuran homologue of cytokeratin 8 (CK8) (Suzuki *et al.*, 2001), a marker of periderm cells (Moll *et al.*, 1982). Histological features suggest that the integument of a late embryo at the tail bud stage (NF-30) to an early larva around NF-45, a larva at NF-45 to NF-58, and a froglet of *X. laevis* corresponds to that of *M. musculus* at 12, 15, and birth, respectively. It is intriguing to assume that the developmental stage of mammalian skin when periderm cells are deleted corresponds to the metamorphic climax of amphibian skin.

Fish are placed in the phylogenetic tree as the most primitive vertebrate. Fish is a polyphyletic term including nontetrapod vertebrates (lampreys, sharks and rays, actinopterygians, coelacanths, and lungfishes) and hangfish. In this review the word fish is used to refer to actinopterygian fish and in particular teleosts, because developmental changes have been most studied at histological and gene expression levels for the zebrafish *(Danio rerio)* (Le Guellec *et al.*, 2004). The fish epidermis is quite different from the other tetrapod epidermis. Generally, the fish epidermis is composed of three layers: the outermost, the intermediate, and the basal layer (Whitear, 1986). The superficial cells are not cornified. The intermediate layer per se is multilayered and contains various secretory cells such as goblet, club, and sacciform cells, and these cells are seemingly undifferentiated. Different from the tetrapod epidermis, it seems that there is no hierarchic relationship among the cells in the three layers. Each cell type is mitogenic, and divides autonomically when surrounding cells are accidentally damaged and lost (Le Guellec *et al.*, 2004). In other words, the basal cells in fish are not the source for cells in the upper layers. Thus, it can be said that the epidermis of teleosts is a ''multilineage epidermis.'' In addition, interestingly from this review's point of view, skein cells are present in the basal layer of lamprey epidermis (Lane and Whitear, 1980) as in amphibian.

There is a similarity in the dermal structure between the fish and the amphibian. The unique plywood-like collagen lamella is present in fish dermis and directly contacts the subepidermal basement membrane. Fish basal cells synthesize and secrete type 1 collagen, which is deposited subepidermally as the collagen lamella. The collagen lamella is originally acellular, but later is populated by fibroblasts that participate in the formation of the collagen lamella and are responsible for its development and maintenance after the epidermal cells cease to express the collagen gene. No connective tissues are present between the basement membrane and the collagen lamella in early development after hatch. Although the *s*-connective tissue-like structure is

formed by fibroblasts, it is very scanty. These histological features of the fish skin are remarkably similar to those of anuran larval skin. On the other hand, the histological features of the adult anuran skin are basically identical to those of tetraploid vertebrates. Therefore, it is tempting to speculate that the metamorphosis of the anuran skin is a process that might have taken place when ancestral amphibians were evolved from fish approximately 350 million years ago.

IV. Genes Involved in Anuran Tissue Remodeling

A. Unique Utilization of TH Response Element in Metamorphosis-Associated Genes

Anuran metamorphosis represents a biological process in which larval tissues are replaced with adult ones under the control of TH. The replacement proceeds in a complex but exquisite manner, requiring precise TH-dependent spatiotemporal regulation of epithelial–mesenchymal interactions. It is evident that many metamorphosis-associated genes participate in this tissue remodeling. Genes play prime roles whose expressions are under the direct control of TH. TH exerts its actions by binding with the nuclear TR, a transcriptional regulator. TR binds to the TRE present in a TH-direct responsive gene, together corepressors and coactivators of transcription. Thus, the elucidation of factors involved in TH-TR-TRE signaling and their roles are a central issue to the understanding of metamorphosis at the molecular level.

Matrix metalloproteinases (MMPs) play major roles in removing old tissues by degrading extracellular matrices. More than 25 human MMPs and the homologue from other species have been identified (Egeblad and Werb, 2002). The larval tissue is ''the old tissue'' to be removed in metamorphic remodeling (Yoshizato, 1989). Stromelysin-3 (MMP-11) is involved in the remodeling of larval intestine (Ishizuya-Oka et al., 2000; Patterton et al., 1995). Genes of collagenases are upregulated in metamorphosing X. laevis tadpoles (Berry et al., 1998; Stolow et al., 1996; Wang and Brown, 1993). Gelatinase A (MMP-2) and B (MMP-9) are induced in T_3-treated tadpole tails (Jung et al., 2002). MMP-1 degrades type I collagen, which is the most abundant collagen in animal tissues. Tissue inhibitor of metalloproteinase (TIMP), a specific inhibitor of collagenase, and a synthetic MMP inhibitor, Ilomastat, inhibits TH-induced tail regression (Oofusa and Yoshizato, 1991) and retards tail resorption (Jung et al., 2002), respectively. The expression of the MMP-1 gene and its protein is especially high in degrading tail tissues during metamorphosis (Oofusa and Yoshizato, 1991).

Comparisons of sequences and the exon structures of cDNA between amphibian and mammalian MMP1 suggested that *R. catesbeiana* MMP-1 (rMMP1) is an ancestral form of mammalian MMP1 (Oofusa and Yoshizato, 1994). Western and Northern blot analyses showed that the enzyme is upregulated by TH at both protein and mRNA levels (Oofusa and Yoshizato, 1991, 1994, 1996). The rMMP1 gene *(rmmp-1)* contained a TRE sequence (5′-AGGTAA-GAACAGGATA-3′) from −891 to −876. We determined if the *rmmp-1* TRE sequence functions in living cells (Sawada *et al.*, 2001). A plasmid, pEGFP/*rmmp-1* (−1078/+98), was constructed that contains a 5′-upstream region (−1078 to +98) of *rmmp-1* as a promoter and enhanced green fluorescent protein (EGFP) cDNA as a reporter. The back and the tail lateral skin of *Rana* tadpoles at TK-X each was transfected with the plasmid. The animals were reared in the presence of T_3. The expression of EGFP increased T_3 dose dependently as high as 7-fold over that in the absence of the hormone, indicating that the TRE sequence in *rmmp-1* is a biologically active TRE *in vivo*. We questioned whether *rmmp-1* contains sequences that regulate TRE activity. The rmmp-1 gene contains an "AP-1 and Sp-1" region at −99 to −15, which serves as the basic promoter for the initiation of transcription in the human gelatinase gene (Huhtala *et al.*, 1991). Double-stranded oligonucleotides termed AS (−99/+98) were synthesized that contained an AP-1 and Sp-1 region and were used as a basic promoter. Similarly, two oligonucleotides were synthesized, TRE (−891/−876) and TREf (−891/−840), which consisted of TRE (−891/−876) and its 3′-flanking 36 bp (−875/−840). Each TRE (−891/−876) and TREf (−891/−840) was ligated to AS (−99/+98) at its 5′-terminus, the product of which was inserted into pEGFP. Thus, we prepared three vectors, pEGFP/TRE (−891/−876)/AS (−99/+98), pEGFP/TREf (−891/−840)/AS (−99/+98), and pEGFP/TREf (−891/−840). Tadpoles were bombarded with each of these vectors to determine their TH responsiveness. Among them only TREf/AS significantly responded to T_3. Thus, both the flanking 36 sequence and the "AP-1 and Sp-1 region" are together required for TRE to respond to T_3. The 36-bp-long direct 3′-flanking sequence might be necessary for the function of TRE, acting as its activator.

The human MMP1 gene (accession numbers AF023338 and D26110) does not contain either the direct repeat or the palindrome type of TRE in the nucleotide sequence database within its −1 kb upstream region, but one such sequence of direct repeat 4 (DR4, TGACCCTCAGAGACCT) is present if the search is extended to −10 kb (−7057 to −7072). Similarly, there is one DR4 sequence (TTACCTCAGGTAAACT) in the chicken *(Gallus gallus)* MMP1 gene at −9476/−9461 and four DR4 sequences in the MMP1-like gene of fish, *Tetraodon nigroviridis*. However, there have been no studies to test whether such sequences of DR4 function as TRE. The databases of the genomic gene of MMP1 of reptiles are not available at present. Under these current situations of genomic databases and functional tests, it is too

early to argue the biological significance of the presence of TRE in anuran MMP1 in relation to metamorphosis. However, it is tempting to speculate that the TRE in anuran MMP1 was uniquely evolved to regulate the remodeling of larval to adult tissue during metamorphosis as previously discussed (Oofusa and Yoshizato, 1991, 1996).

A different "modification" in the TRE-related transcriptional system was reported for the MMP9 gene, which seems to be uniquely evolved in amphibians (Fujimoto *et al.*, 2006). Two types of gene for MMP-9, which cleaves native type IV collagen, were cloned from *Xenopus tropicalis* and *X. laevis:* the conventional type (MMP-9 gene) and a unique one (MMP-9TH gene). These genes are located tandemly about 9 kb apart from each other in the genome. The MMP-9TH gene was expressed in the regressing tail and gills, and the remodeling intestine and central nervous system, whereas MMP-9 mRNA was detected in embryos. TH upregulates the MMP-9TH gene through three TREs that are located in the distal promoter and the first intron. It has been suggested that the MMP-9 gene is duplicated and differentiated into two genes, one of which, MMP-9TH, is specialized in function to work in TH-dependent degenerating and remodeling processes during metamorphosis. Such duplication of MMP-9 has not been found in other vertebrate genomes reported to date.

Germline transgenetic tadpoles of *X. laevis* (Kroll and Amaya, 1996) have been utilized to test whether genes actually play a role in regulating metamorphosis. For more than three decades PRL had been considered to be an important endocrine acting as an antagonist of metamorphosis. Transgenetic tadpoles bearing the PRL gene showed no delay in normal tadpole life, indicating PRL does not play a role in metamorphic processes (Huang and Brown, 2000b). Interestingly, they became "tailed frogs," suggesting that the growth of fibroblasts in the tail was stimulated. This outcome supported our previous observation that PLR stimulates collagen synthesis of tail fibroblasts (Yoshizato and Yasumasu, 1970).

The autoregulation of the TR gene by T_3 was first suggested by our previous study in which the affinity of TH to the nuclear TR was determined in tail cell nuclei prepared from tadpoles at various stages of metamorphosis (Yoshizato and Frieden, 1975). In fact, the *Xenopus* TRβ (xTRβ) gene contains TRE in its transcriptional regulatory region (Ranjan *et al.*, 1994; Wong *et al.*, 1998). A functional assay of TRE was made utilizing *Xenopus* oocytes and A6 cells, a cell line derived from the kidney of *Xenopus*. A fusion gene consisting of a TRE-containing 5′-flanking region of the xTRβA1 gene and a reporter gene was injected into the oocytes or the cells. The expression of the reporter gene was upregulated in response to T_3 (Ulisse *et al.*, 1996). Using the gel shift assay Shi and his colleagues demonstrated the binding of heterodimers, xTRβ/*Xenopus* retinoid X receptor α (xRXRα) or xTRβ/xRXRγ, to a TRE-containing sequence of the xTRβA1 gene (Ranjan *et al.*, 1994; Wong

and Shi, 1995). These studies show that the binding of a complex of T_3 and xTRβ/xRXR heterodimers to the promoter region of the xTRβ gene is a key event in inducing anuran metamorphosis.

To understand the role of TH-TR-TRE signaling in the development of amphibians *in vivo* we investigated EGFP expression patterns in transgenic *Xenopus* tadpoles carrying xTRβA1 gene promoter-driven EGFP cDNA (Oofusa *et al.*, 2001). Visceral tissues including the intestine and the pronephra become prominently fluorescent at around NF-42, with the expression level increasing until NF-45 and then decreasing gradually thereafter. Nervous tissues are strongly fluorescent at NF-42 and -45. The tail muscle shows a high level of EGFP expression from NF-42 to -57. The muscle of hind limbs becomes intensely fluorescent at NF-54, its intensity greatly increasing at the climax stage of metamorphosis. After metamorphosis, the fluorescence becomes gradually weaker in all the tissues described previously. When these tadpoles reach the climax stage (from NF-58 to -60), the fluorescence regains a high intensity. It is most likely that these high levels of expression during metamorphic climax are induced by T_3, because it is well established that the plasma level of T_3 becomes high (Leloup and Buscaglia, 1977). When treated with T_3, transgenic tadpoles at NF-51 evidently increase fluorescence at 5 days in all tissues, especially in the jaw, the nervous tissues, the body muscles, the pronephra, the forelimbs, the hind limbs, and the muscle of the tail.

The previously described overall expression profile of the xTRβ promoter-driven reporter gene during larval development supports the results of previous reports that studied the expression of xTRβ mRNA by *in situ* hybridization (Kawahara *et al.*, 1991) and reverse transcriptase-mediated hybridization (Yaoita and Brown, 1990). A markedly high expression of the reporter gene in T_3-treated tadpoles was seen in nervous tissues, jaw, gills, thyroid gland, small intestine, liver, and tail muscle. These organs, except the thyroid gland and the jaw, have been reported to be TH responsive by Ishizuya-Oka *et al.* (1996) for small intestine, Kawahara *et al.* (1989) for liver, Hu *et al.* (1999) for tail muscle, Atkinson (1981) for gills, and Buckbinder and Brown (1992) for brain. Thus, we concluded that the transgene containing the TRE sequences responds well to T_3 in TH-responsive tissues of spontaneous and TH-induced metamorphosing tadpoles in a biologically meaningful manner.

In addition, two new aspects of TH-TR-TRE signaling were revealed. It has been generally thought that TH in amphibians functions only as a metamorphosis-inducing hormone, since the discovery that tadpoles fed on thyroid glands precociously metamorphose (Gudernatsch, 1912). This notion has been supported by the fact that TH in sera is detectable only from just before and during the climax stage of metamorphosis. TH has not been thought to play roles in embryogenesis and in adult tissue physiology. The results obtained from experiments with xTRβA1 gene-transgenic *X. laevis* do

not agree with this general belief. Unexpectedly, but interestingly, we observed the first significant EGFP fluorescence in embryos at NF-14 (the neurula stage) (Fig. 12). Reporter protein expression was intense in the upper half of the neural fold. Western blotting for xTRβ gave an immunopositive band for embryos at NF-14. These results together strongly suggested that TH-TR-TRE signaling plays a role(s) in anuran embryogenesis, especially in neural tube formation. This suggestion is important, because first, it is known that TH is necessary for the normal development of the brain in mammals (Forrest *et al.*, 2002; Koibuchi and Chin, 2000; Yen, 2003) and second, embryos at this stage have not yet developed functional thyroid glands. It is known that TR acts as a suppressor of the transcription of TRE-containing genes when unligated and as a stimulator when ligated (Mahajan and Samuels, 2005). Thus, the question of whether TH is present in anuran embryos is critical.
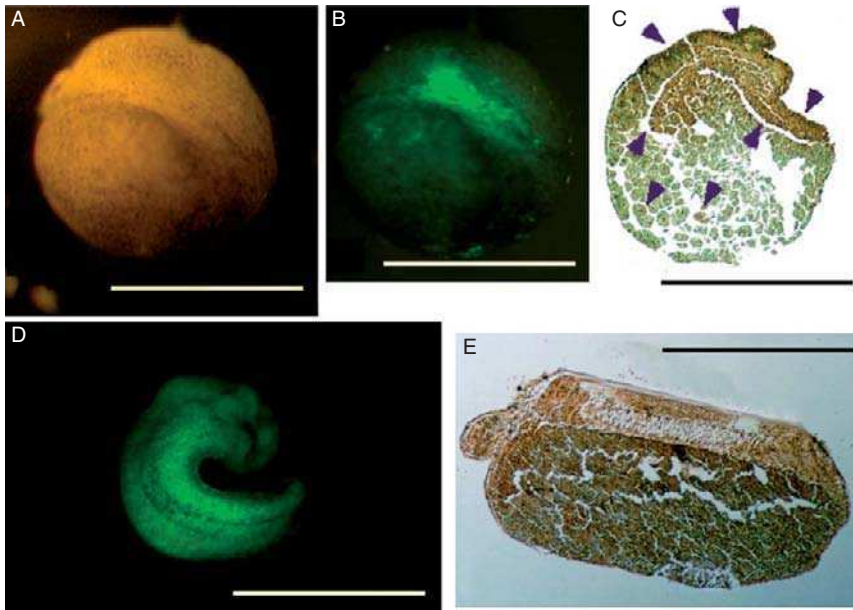
FIG. 12 Expression of EGFP in embryonic neural folds in transgenic *Xenopus* tadpoles carrying xTRβA1 gene promoter-driven EGFP cDNA. Eggs with transgenes were developed to NF-14 (A, B, C) and -30 (D, E), and photographed from a side of the animal pole under a bright (A) and fluorescent field (B, D). Photos of (A) and (B) are from the same embryo and from the same direction. Sections (C) and (D) were stained with anti-EGFP antisera. The dorsal side is up in (C) and (E). The anterior side is to the left in (E). The arrows in (C) indicate the immunoreactive regions. All the tissues in (E) are immunopositive. Bars, 1 mm.

There has been a study that showed its presence. Radioimmunoassay detected both T_3 and T_4 in toad *(Bufo marinus)* embryos (Weber *et al.*, 1994). These hormones are likely of maternal origin. It was also reported that the TRα gene is expressed in developing oocytes (Kawahara *et al.*, 1991). Its mRNA is present throughout embryonic development (Eliceiri and Brown, 1994). Thus, it is plausible that TH-TR-TRE signaling plays a key role(s) in embryonic neural fold formation.

There have been few studies on the physiological role of TH in amphibia after metamorphosis. The TH responsibility of the TRE-containing gene in adult tissues was examined by bathing the 4- to 8-week-old transgenic frogs in T3-containing water. EGFP fluorescence became brighter. The fluorescence started to increase 1 day after hormone treatment and reached a plateau at 2 days when the intensity rose 1.6-fold as compared to controls. Our study showed that TRE-containing promoters are also responsible for exogenous TH in adult tissues, especially in the brain, intestine, bones of the upper forelimbs and the foot of the hind legs, and kidney as well as neighboring tissues. These results strongly suggested that TH might play some role in these tissues of adult frogs. It is well known that TH generally stimulates the basic metabolic activity of cells in adult mammalian tissues (Yoshizato *et al.*, 1980). In particular, oxygen consumption of brain, liver, kidney, and muscle significantly increases in TH-treated adult rats (Frieden and Lipner, 1971). Mundy *et al.* (1976) showed that TH directly stimulates the resorption of rat long bones in organ culture. Therefore, it is likely that TH regulates these processes in adult frog tissues as in mammals. Galton (1985) reported the presence of T3-binding sites in nuclei of liver cells and erythrocytes of adult frogs, although their number is significantly lower than that of tadpoles, which also supports the notion that adult anuran cells respond to T3 to some extent. Based upon the results obtained from the TRβ gene-transgenesis studies, we propose that TH-TR-TRE signaling is essential not only for the progression of metamorphosis, but also for embryogenesis and adult physiology. We could obtain a more general view to understand the biological significance of TH in amphibians by studying its role not only in metamorphosis, but also in embryogenesis and adult tissue physiology.

B. Regulation of Gene Expression in Larval Tissue Remodeling

TH triggers metamorphosis of anurans, the process in which all larval organs are remodeled to adult ones (Gilbert and Frieden, 1981; Shi, 1999; Yoshizato, 1989, 1996). Isolated pieces of tail or the whole tail in culture undergo histolysis in the presence of TH (Tata *et al.*, 1991; Weber, 1967). Similarly, isolated larval intestine tissues in culture alone undergo remodeling to an

adult tissue when TH is provided (Ishizuya-Oka and Shimozawa, 1991). These studies suggest that each of the larval organs is remodeled autonomically. Such autonomy is also shown for larval skin transformation in this review. On the other hand, organs and tissues of a tadpole each interdependently metamorphoses: there are the ordered sequences of remodeling of organs. For example, metamorphosis of the limb takes place earlier than that of the tail. Skin metamorphosis is another example of such an ordered sequence. As detailed in Section V, the appearance and migration of STC are well organized in that STC emerges at a specific site and at a specific stage of larval development, and moves in a developmental stage- and region-dependent manner. STC never travels into the tail domain. This orderly proceeding of metamorphosis of each organ as a whole gives the impression that there is a surveillance system that determines the ordered sequence of metamorphosis of an organ.

Tadpoles undergo drastic changes in their body structure and function in a very elegant and exquisite manner at every step of metamorphosis and in a harmonious and concerted way as a whole. TH initiates anuran metamorphosis and regulates the ensuing whole process. Therefore, the responsiveness of cells to TH is essential for tadpoles to initiate metamorphosis and for it to progress. Thus, the previously mentioned organized procession of remodeling of each organ can be explained by the different affinities of constituent cells of an organ toward TH. For example, limb cells might show a higher affinity to TH than tail cells. To our knowledge, there have been no studies that comparatively and quantitatively examined the affinity of each larval tissue cell in a systematic and comprehensive manner. The responsiveness of a cell to TH is basically determined by either its binding capacity or binding affinity toward TH. It is thought that the sensitivity of a cell of larval tissue is maximal at the climax stage of metamorphosis when the TH concentration in blood is at its maximum. Changes in the maximal binding capacity and the binding affinity of tail cell nuclei were determined at various stages of development and metamorphosis of tadpoles by Scatchard analysis (Yoshizato and Frieden, 1975). The result supports the idea that the maximum number of binding sites rather than the affinity of a larval cell is correlated with the cell's responsiveness to TH. If this conclusion can be extended to larval cells of other tissues, it can be generally said that the expression level of the TR gene of a cell is a good measure to assess its sensitivity to TH. Therefore, it will be valuable to comprehensively compare experimental data on the expression level of TR genes among various types of larval cells, and during the time course of development and metamorphosis to understand the ordered sequence of metamorphic changes of larval tissues.

Cellular responsiveness or nonresponsiveness to TH is determined by whether a cell possesses TRs or not. TRs act as thyroid hormone acceptors

by making heterodimers with 9-*cis*-retinoic acid receptors (RXRs). Thus, the regulation of expression of genes of TR and RXR in a cell is essential for the cell to respond to TH. Practically, TR gene expression is a determinant of cellular responsiveness to TH, because RXR is constitutively expressed during the development and metamorphosis of tadpoles (Wong and Shi, 1995). Genomic DNA of four types of TRs (TRαA, TRαB, TRβA, and TRβB) was cloned from *X. laevis* and characterized in relation to their roles in metamorphosis (Brooks *et al.*, 1989; Yaoita *et al.*, 1990). It has been thought that TRβ plays a prime role(s) in inducing metamorphic changes, because the expression level of this gene correlates well with the rise in the level of an active form of TH, T_3 in blood during metamorphosis (Yaoita and Brown, 1990). Utilizing transgenesis technology, it was shown that the intracellular TR level is a determinant of cell sensitivity to TH (Schreiber and Brown, 2003). TRα binds to TH and coactivators through its carboxyl 401 amino acid residues. Deletion of this region yields a dominant negative form of TRα (TRDN). cDNA (Ker:TRDN) was constructed in which TRDN was incorporated under the control of a promoter sequence of keratin gene that is exclusively expressed in apical epidermal cells. The investigators made transgenic tadpoles bearing this construct. Tissues and organs of the transgenic tadpole generally underwent normal metamorphosis except tissues in the skin. The larval epidermal basal cell normally transformed into the adult basal cell and the subepidermal mesenchyme converted to the adult type. However, apical cells did not undergo apoptosis, but survived in the adult skin. This result clearly demonstrates two things. One is that TR is critical for TH-dependent metamorphosis. The other is that each of the skin cells individually responds to TH and autonomically metamorphoses into the counterpart of adult skin cells.

TRE present in a transcription regulatory region of a gene is another determinant of the cell's responsiveness to TH. Generally, the expression of hormone-responsive genes is regulated by the ligand (hormone)-activated receptors (ligand–receptor complex) that bind to *cis*-acting elements in the regulatory region of target genes (Evans, 1988; Yamamoto, 1985). TRE is such an element for TH-targeted genes. When the T_3/TR/RXR/TRE complex is formed in a cell, the cell potentially becomes responsive to TH. Thus, it is helpful for us to comprehensively list all the genes that contain TRE. If a gene possesses TRE in its transcription regulatory region, we assume that the gene is potentially of prime importance for the initiation and progression of metamorphosis. Actually, TRE was found in a flanking region of the start site of the *X. laevis* thyroid hormone receptor β (TRβ) gene (Ranjan *et al.*, 1994). The transcriptional expression of stromelysin-3 is under the direct control of TH, because TH induces its expression within a few hours in the absence of protein synthesis (Damjanovski *et al.*, 2000). However, a TRE has yet to be identified in its genomic DNA (Li *et al.*, 1998). Regulatory regions

of xBTEB were shown to contain TRE (Furlow and Brown, 1999). TRE has been shown in several mammalian genes, genes of malic enzyme (Petty *et al.*, 1990), myosin heavy chain (Flink and Morkin, 1990), and growth hormone (Sap *et al.*, 1990). The complete list of TRE-containing genes in anurans and a comparison with that in mammals will greatly aid us in understanding the organized procession of metamorphosis. When available, such a list for all classes of vertebrates will be valuable in understanding the biological and evolutional significance of metamorphosis at the molecular level. Further-more, the list will contribute to determining the suggested ''hierarchical gene network'' that substantiates the ordered and concerted sequences of metamorphosis of larval tissues.

There is an additional factor that determines the sensitivity of larval tissues for TH. The concentration of TH in blood is high at climax stages of metamorphosis, indicating that every larval tissue is evenly exposed to a high level of TH then. However, most (approximately 90%) of the TH in blood is T_4, the prohormone of T_3. T_4 should be deiodinated to be the active TH, T_3. One of the critical factors that determines the responsiveness of a cell to TH is an ''effective intracellular concentration'' of TH. The deiodination reaction is catalyzed by deiodinase (Leonard and Visser, 1986). Currently, three types of deiodinase are known: DI, D2, and D3. The former two types convert T_4 to T_3 and the last type deletes iodo at the 5 position of the inner ring of T_4 to T_3, resulting in the inactivation of T_3. The presence of D2 and D3 deiodinase was reported in anuran tissues (Becker *et al.*, 1997). The D3 deiodinase gene is TH responsive and upregulated by the hormone (Wang and Brown, 1993). Thus, the intracellular effective T_3 concentration is deter-mined by the intracellular concentration of D2 and D3 enzymes if the ambient concentration of TH is constant. Several studies have supported this prediction. The retina of tadpole in premetamorphic stages grows by proliferating symmetrically at the ciliary marginal zone (CMZ). However, the CMZ increases in size ventrally but not dorsally from the prometa-morphic to climax stages (Beach and Jacobson, 1979a). Thus, the majority of the adult frog retina is derived from ventral CMZ cells. This shift from symmetrical to asymmetrical growth is TH dependent (Beach and Jacobson, 1979b; Hoskins and Grobstein, 1985). The asymmetrical TH-dependent growth of CMZ cells was explainable by the expression of type III deiodinase in dorsal but not ventral CMZ cells (Marsh-Armstrong *et al.*, 1999). Type III deiodinase-transgenic tadpoles were yielded, in which the transgene was under the control of a panactive promoter, CMV, or a neural-specific pro-moter prepared from the neural β-tubulin gene. These tadpoles did not show the TH-induced proliferation of the ventral CMZ cells (Huang *et al.*, 1999; Marsh-Armstrong *et al.*, 1999). A fusion gene of green fluorescent protein (GFP) and D3 was incorporated into a vector with a CMV-IE94 promoter/enhancer. Germline transgenic tadpoles bearing this construct were produced,

which ubiquitously expressed the D3 enzyme at a high level, the enzyme activity being more than 20-fold that of normal larvae. The transgenic tadpoles normally developed limbs before the climax stage, but most of them terminated metamorphic progress at an early climax stage of metamorphosis (NF60/61), and died with gills and tail. This study shows that limbs are sensitive to TH and are able to develop under a minute level of T_3, whereas the tail's sensitivity is low and requires a high level of T_3 to normally metamorphose.

It seems that the metamorphic transformation of cells basically proceeds autonomically and interdependently. The present review describes the latter in detail, focusing on the interaction between epidermal and mesenchymal cells taking place during skin metamorphosis. We can predict the presence of a gene network ("metamorphosis gene network") in which each of the constituent genes is turned off or on interdependently and in a harmonized manner in response to TH directly or indirectly, or in response to a factor induced by cell–cell communications. At first glance, each of the on/off switches takes place autonomically in each of the cells. However, when we see a tadpole as a whole, the ability of the gene to turn on/off apparently takes place in a finely ordered manner mainly through the difference in an effective local concentration of T_3, an amount of available TR in a cell. The elucidation of the entire structure of this metamorphic gene network is necessary to comprehensively understand the mechanism of metamorphosis, but this is likely to require some years.

V. Concluding Remarks

The metamorphic transformation of anuran larval skin to adult counterparts has been a major target of our research activities aimed at revealing the mechanism of metamorphosis at histological, cellular, protein, and gene levels. The epidermal and dermal cells were characterized based on their role during this process by examining their morphological and histological features, the expression profiles of genes and proteins, and the interdependence between epidermal and dermal cells. As a result we were able to identify a unique site termed the skin transformation center (STC), in which larval skin is actively undergoing a transformation into adult skin. PDGF/PDGFR signaling was found to play a role(s) as one of the cues for the epithelial–mesenchymal interactions in the body- and tail-dependent metamorphic transformation of larval skin. As a result of these studies we have noticed that the skin of an aquatic anuran larva and a terrestrial anuran adult is histologically analogous to that of an aquatic adult of fish and a terrestrial adult of tetrapod, which suggests the evolutionary significance of anuran metamorphosis. TH-TR-TRE signaling plays a major role in

regulating metamorphic skin transformation. Based upon studies on the transcriptional regulation of TH-responsive genes, we propose a new view of the biological role of TH in anurans: TH-TR-TRE signaling plays a significant role not only in the development and the metamorphosis of larvae as "the metamorphic hormone," but also in embryogenesis as a "morphogen" of neural fold formation and in adult tissue physiology as a "metabolism-modulating hormone." This viewpoint leads us to compare the results obtained from studies on the anuran as a metamorphic animal with those on other vertebrates as nonmetamorphic animals, which will eventually enable us to understand the uniqueness and generality of anuran metamorphosis. A cell responds to TH through TH-TR-TRE-signaling and, thus, the extent of the cell's responsiveness is determined by intracellularly available concentrations of both TH and TR. Individual larval cells autonomously undergo biochemical reactions to TH when concentrations of the ligand and its receptor are appropriate. Therefore, the elucidation of the mechanism by which their effective concentrations are determined will be necessary to understand the metamorphosis of a tadpole, in which cellular events proceed in a well orchestrated manner following finely ordered sequences.

Acknowledgments

References

Aase, K., Abramsson, A., Karlsson, L., Betsholtz, C., and Eriksson, U. (2002). Expression analysis of PDGF-C in adult and developing mouse tissues. *Mech. Dev.* **110,** 187–191.

Asahina, K., Oofusa, K., Obara, M., and Yoshizato, K. (1997). Cloning and characterization of the full length cDNA encoding alpha2 type I collagen of bullfrog *Rana catesbeiana. Gene* **194,** 283–289.

Atkinson, B. G. (1981). Biological basis of tissue regression and synthesis. *In* "Metamorphosis: A Problem in Developmental Biology" (L. I. Gilbert and E. Frieden, Eds.), pp. 397–444. Plenum Press, New York, NY.

Beach, D. H., and Jacobson, M. (1979a). Patterns of cell proliferation in the retina of the clawed frog during development. *J. Comp. Neurol.* **183,** 603–613.

Beach, D. H., and Jacobson, M. (1979b). Influences of thyroxine on cell proliferation in the retina of the clawed frog at different ages. *J. Comp. Neurol.* **183,** 615–623.

Becker, K. B., Stephens, K. C., Davey, J. C., Schneider, M. J., and Galton, V. A. (1997). The type 2 and type 3 iodothyronine deiodinases play important roles in coordinating development in *Rana catesbeiana* tadpoles. *Endocrinology* **138,** 2989–2997.

Berry, D. L., Schwartzman, R. A., and Brown, D. D. (1998). The expression pattern of thyroid hormone response genes in the tadpole tail identifies multiple resorption programs. *Dev. Biol.* **203,** 12–23.

Betsholtz, C., Karlsson, L., and Lindahl, P. (2001). Developmental roles of platelet-derived growth factors. *Bioessays* **23,** 494–507.

Bickenbach, J. R., and Holbrook, K. A. (1986). Proliferation of human embryonic and fetal epidermal cells in organ culture. *Am. J. Anat.* **177,** 97–106.

Bickenbach, J. R., and Holbrook, K. A. (1987). Label-retaining cells in human embryonic and fetal epidermis. *J. Invest. Dermatol.* **88,** 42–46.

Boneko, V. M., and Merker, H. J. (1988). Development and morphology of the periderm of mouse embryos (days 9–12 of gestation). *Acta Anat.* **133,** 325–336.

Brooks, A. R., Sweeney, G., and Old, R. W. (1989). Structure and functional expression of a cloned *Xenopus* thyroid hormone receptor. *Nucleic Acids Res.* **17,** 9395–9405.

Buckbinder, L., and Brown, D. D. (1992). Thyroid hormone-induced gene expression changes in the developing frog limb. *J. Biol. Chem.* **267,** 25786–25791.

Dahl, L. K., and Dole, V. P. (1952). The biphasic nature of renal calcification. *J. Exp. Med.* **95,** 341–346.

Damjanovski, S., Puzianowska-Kuznicka, M., Ishizuya-Oka, A., and Shi, Y. B. (2000). Differential regulation of three thyroid hormone-responsive matrix metalloproteinase genes implicates distinct functions during frog embryogenesis. *FASEB J.* **14,** 503–510.

Ding, H., Wu, X., Kim, I., Tam, P. P., Koh, G. Y., and Nagy, A. (2000). The mouse Pdgfc gene: Dynamic expression in embryonic tissues during organogenesis. *Mech. Dev.* **96,** 209–213.

Eberth, J. C. (1866). Zur entwicklung der gewebe in schwanze der froschlarven. *Arch. Mikrosk. Anat.* **2,** 490–506.

Egeblad, M., and Werb, Z. (2002). New functions for the matrix metalloproteinases in cancer progression. *Nat. Rev. Cancer* **2,** 161–174.

Eliceiri, B. P., and Brown, D. D. (1994). Quantitation of endogenous thyroid hormone receptors alpha and beta during embryogenesis and metamorphosis in *Xenopus laevis*. *J. Biol. Chem.* **269,** 24459–24465.

Eming, S. A., Lee, J., Snow, R. G., Tompkins, R. G., Yarmush, M. L., and Morgan, J. R. (1995). Genetically modified human epidermis overexpressing *PDGF-A* directs the development of a cellular and vascular connective tissue stroma when transplanted to athymic mice—implications for the use of genetically modified keratinocytes to modulate dermal regeneration. *J. Invest. Dermatol.* **105,** 756–763.

Eming, S. A., Medalie, D. A., Tompkins, R. G., Yarmush, M. L., and Morgan, J. R. (1998). Genetically modified human keratinocytes overexpressing PDGF-A enhance the performance of a composite skin graft. *Human Gene Ther.* **9,** 529–539.

Evans, R. M. (1988). The steroid and thyroid hormone receptor superfamily. *Science* **240,** 889–895.

Flink, I. L., and Morkin, E. (1990). Interaction of thyroid hormone receptors with strong and weak cis-acting elements in the human alpha-myosin heavy chain gene promoter. *J. Biol. Chem.* **265,** 11233–11237.

Forrest, D., Reh, T. A., and Rusch, A. (2002). Neurodevelopmental control by thyroid hormone receptors. *Curr. Opin. Neurobiol.* **12,** 49–56.

Fox, H. (1992). Figure of Eberth in the amphibian larval epidermis. *J. Morph.* **212,** 87–97.

Fox, H., and Whitear, M. (1986). Genesis and regression of the figures of Eberth and occurrence of cytokeratin aggregates in the epidermis of anuran larvae. *Anat. Embryol.* **174,** 73–82.

Frieden, E., and Lipner, H. (1971). Thyroxine and triiodothyronine. *In* ''Biochemical Endocrinology of the Vertebrates,'' pp. 48–62. Prentice-Hall, Inc., Englewood Cliffs, NJ.

Fuchs, E., and Segre, J. A. (2000). Stem cells: A new lease on life. *Cell* **100,** 143–155.

Fujimoto, K., Nakajima, K., and Yaoita, Y. (2006). One of the duplicated matrix metalloproteinase-9 genes is expressed in regressing tail during anuran metamorphosis. *Dev. Growth Differ.* **48,** 223–241.

Furlow, J. D., and Brown, D. D. (1999). *In vitro* and *in vivo* analysis of the regulation of a transcription factor gene by thyroid hormone during *Xenopus laevis* metamorphosis. *Mol. Endocrinol.* **13,** 2076–2089.

Furlow, J. D., Berry, D. L., Wang, Z., and Brown, D. D. (1997). A set of novel tadpole specific genes expressed only in the epidermis are down-regulated by thyroid hormone during *Xenopus laevis* metamorphosis. *Dev. Biol.* **182,** 284–298.

Galton, V. A. (1985). 3,5,3′-Triiodothyronine receptors and thyroxine 5′-monodeiodinating activity in thyroid hormone-insensitive amphibia. *Gen. Comp. Endocrinol.* **57,** 465–471.

Gilbert, L., and Frieden, E. (1981). ''Metamorphosis: A Problem in Developmental Biology.'' Plenum Press, New York, NY.

Gosner, K. L. (1960). A simplified table for staging anuran embryos and larvae with notes on identification. *Herpetologica* **16,** 183–190.

Goto, T., Katada, T., Kinoshita, T., and Kubota, H. Y. (2000). Expression and characterization of *Xenopus* type 1 collagen alpha 1 (COL 1A1) during embryonic development. *Dev. Growth Differ.* **42,** 249–256.

Gudernatsch, J. F. (1912). Feeding experiments on tadpoles. I. The influence of specific organs given as food on growth and differentiation: A contribution to the knowledge of organs with internal secretion. *Arch. Entwicklungsmech. Org.* **35,** 457–483.

Hayashi, H., Takada, M., and Watanabe, T. (1977). Distribution of Ca and P in frog skin: An analytical study of element with electron probe X-ray microanalyzer. *J. Saitama Med. School* **4,** 13–21.

Holbrook, K. A. (1991). Structure and function of the developing human skin. *In* ''Physiology, Biochemistry, and Molecular Biology of the Skin'' (L. A. Goldstein, Ed.), 2nd ed., pp. 63–110. Oxford University Press, Oxford, UK.

Hoskins, S. G., and Grobstein, P. (1985). Development of the ipsilateral retinothalamic projection in the frog *Xenopus laevis*. III. The role of thyroxine. *J. Neurosci.* **5,** 930–940.

Hu, H., Merrifield, P., and Atkinson, B. G. (1999). Expression of the myosin heavy chain genes in the tail muscle of thyroid hormone-induced metamorphosing *Rana catesbeiana* tadpoles. *Dev. Genet.* **24,** 151–164.

Huang, H., and Brown, D. D. (2000b). Prolactin is not a juvenile hormone in *Xenopus laevis* metamorphosis. *Proc. Natl. Acad. Sci. USA* **97,** 195–199.

Huang, H., Marsh-Armstrong, N., and Brown, D. D. (1999). Metamorphosis is inhibited in transgenic *Xenopus laevis* tadpoles that overexpress type III deiodinase. *Proc. Natl. Acad. Sci. USA* **96,** 962–967.

Huhtala, P., Tuuttila, A., Chow, L. T., Lohi, J., Keski-Oja, J., and Tryggvason, K. (1991). Complete structure of the human gene for 92-kDa type IV collagenase. Divergent regulation of expression for the 92- and 72-kilodalton enzyme genes in HT-1080 cells. *J. Biol. Chem.* **266,** 16485–16490.

Ishida, Y., Suzuki, K., Utoh, R., Obara, M., and Yoshizato, K. (2003). Molecular identification of the skin transformation center of anuran larval skin using genes of Rana adult keratin (RAK) and SPARC as probes. *Dev. Growth Differ.* **45,** 515–526.

Ishizuya-Oka, A., and Shimozawa, A. (1991). Induction of metamorphosis by thyroid hormone in anuran small intestine cultured organotypically *in vitro*. *Cell. Dev. Biol.* **27,** 853–857.

Ishizuya-Oka, A., Ueda, S., and Shi, Y. B. (1996). Transient expression of stromelysin-3 mRNA in the amphibian small intestine during metamorphosis. *Cell Tissue Res.* **283,** 325–329.

Ishizuya-Oka, A., Li, Q., Amano, T., Damjanovski, S., Ueda, S., and Shi, Y. B. (2000). Requirement for matrix metalloproteinase stromelysin-3 in cell migration and apoptosis during tissue remodeling in *Xenopus laevis*. *J. Cell Biol.* **150,** 1177–1188.

Izutsu, Y., Kaiho, M., and Yoshizato, K. (1993). Different distribution of epidermal basal cells in the anuran larval skin correlates with the skin's region-specific fate at metamorphosis. *J. Exp. Zool.* **267,** 608–615.

Jones, P. H., and Watt, F. M. (1993). Separation of human epidermal stem cells from transit amplifying cells on the basis of differences in integrin function and expression. *Cell* **73,** 713–724.

Jones, P. H., Harper, S., and Watt, F. M. (1995). Stem cell patterning and fate in human epidermis. *Cell* **80,** 83–93.

Jung, J. C., Leco, K. J., Edwards, D. R., and Fini, M. E. (2002). Matrix metalloproteinases mediate the dismantling of mesenchymal structures in the tadpole tail during thyroid hormone-induced tail resorption. *Dev. Dyn.* **223,** 402–413.

Karlsson, L., Bondjers, C., and Betsholtz, C. (1999). Roles for PDGF-A and sonic hedgehog in development of mesenchymal components of the hair follicle. *Development* **126,** 2611–2621.

Kawahara, A., Kohara, S., and Amano, M. (1989). Thyroid hormone directly induces hepatocyte competence for estrogen-dependent vitellogenin synthesis during the metamorphosis of *Xenopus laevis*. *Dev. Biol.* **132,** 73–80.

Kawahara, A., Baker, B. S., and Tata., J. R. (1991). Developmental and regional expression of thyroid hormone receptor genes during *Xenopus* metamorphosis. *Development* **112,** 933–943.

Kawai, A., Ikeya, J., Kinoshita, T., and Yoshizato, K. (1994). A three-step mechanism of action of thyroid hormone and mesenchyme in metamorphic changes in anuran larval skin. *Dev. Biol.* **166,** 477–488.

Kinoshita, T., Sasaki, F., and Watanabe, K. (1986a). Regional specificity of anuran larval skin during metamorphosis: Transdifferentiation of tadpole tail-epidermis. *J. Exp. Zool.* **238,** 201–210.

Kinoshita, T., Sasaki, F., and Watanabe, K. (1986b). Regional specificity of anuran larval skin during metamorphosis: Dermal specificity in development and histolysis of recombined skin grafts. *Cell Tissue Res.* **245,** 297–304.

Kobayashi, H., Sato, H., and Yoshizato, K. (1996). Regionally regulated conversion of protein expression in the skin during anuran metamorphosis. *J. Exp. Zool.* **274,** 181–192.

Koibuchi, N., and Chin, W. W. (2000). Thyroid hormone action and brain development. *Trends Endocrinol. Metab.* **11,** 123–128.

Kovalenko, M., Gazit, A., Böhmer, A., Rorsman, C., Rönnstrand, L., Heldin, C. H., Waltenberger, J., Böhmer, F. D., and Levitzki, A. (1994). Selective platelet-derived growth factor receptor kinase blockers reverse *sis*-transformation. *Cancer Res.* **54,** 6106–6114.

Kovalenko, M., Rönnstrand, L., Heldin, C. H., Loubtchenkov, M., Gazit, A., Levitzki, A., and Böhmer, F. D. (1997). Phosphorylation site-specific inhibition of platelet-derived growth factor β-receptor autophosphorylation by the receptor blocking tyrphostin AG1296. *Biochemistry* **36,** 6260–6269.

Kroll, K. L., and Amaya, E. (1996). Transgenic Xenopus embryos from sperm nuclear transplantations reveal FGF signaling requirements during gastrulation. *Development* **122,** 3173–3183.

Lane, E. B., and Whitear, M. (1980). Skein cells in lamprey epidermis. *Can. J. Zool.* **58,** 450–455.

Le Guellec, D., Morvan-Dubois, G., and Sire, J.-Y. (2004). Skin development in bony fish with particular emphasis on collagen deposition in the dermis of the zebrafish (*Danio rerio*). *Int. J. Dev. Biol.* **48,** 217–231.

Leloup, J., and Buscaglia, M. (1977). La triiodothyronine, hormone de la metamorphose des amphibiens. *C. R. Acad. Sci.* **284,** 2261–2263.

Leonard, J. L., and Visser, T. J. (1986). Biochemistry of deiodination. *In* "Thyroid Hormone Metabolism" (G. Hennemann, Ed.), pp. 189–229. Marcel Dekker, New York, NY.

Levitzki, A., and Gazit, A. (1995). Tyrosine kinase inhibition: An approach to drug development. *Science* **267,** 1782–1788.

Li, J., Liang, V. C., Sedgwick, T., Wong, J., and Shi, Y. B. (1998). Unique organization and involvement of GAGA factors in transcriptional regulation of the *Xenopus* stromelysin-3 gene. *Nucleic Acid Res.* **26,** 3018–3025.

Mahajan, M. A., and Samuels, H. H. (2005). Nuclear hormone receptor coregulator: Role in hormone action, metabolism, growth, and development. *Endocr. Rev.* **26,** 583–597.

Marsh-Armstrong, N., Huang, H., Remo, B. F., Liu, T. T., and Brown, D. D. (1999). Asymmetric growth and development of the *Xenopus laevis* retina during metamorphosis is controlled by type III deiodinase. *Neuron* **24,** 871–878.

Matoltsy, A. G. (1986). Structure and function of the mammalian epidermis. *In* "Biology of the Integument: Vertebrates" (J. Bereiter-Hahn, A. G. Matoltsy, and K. Sylvia Richards, Eds.), pp. 255–271. Springer-Verlag, Berlin.

Matoltsy, A. G., and Bereiter-Hahn, J. (1986). Introduction. *In* "Biology of the Integument: Vertebrates" (J. Bereiter-Hahn, A. G. Matoltsy, and K. Sylvia Richards, Eds.), pp. 1–7. Springer-Verlag, Berlin.

Matoltsy, A. G., and Huszar, T. (1972). Keratinization of the reptilian epidermis: An ultrastructural study of the turtle epidermis. *J. Ultrastruct. Res.* **38,** 87–101.

Moll, R., Franke, W. W., Schiller, D. L., Geiger, B., and Krepler, R. (1982). The catalog of human cytokeratins: Patterns of expression in normal epithelia, tumors and cultured cells. *Cell* **31,** 11–24.

Mundy, G. R., Shapiro, J. L., Bandelin, J. G., Canalis, E. M., and Raisz, L. G. (1976). Direct stimulation of bone resorption by thyroid hormones. *J. Clin. Invest.* **58,** 529–534.

Nieuwkoop, P. D., and Faber, J. (1967). "Normal Table of the *Xenopus laevis* (Daudin)," 2nd ed. North-Holland, Amsterdam.

Niki, K., and Yoshizato, K. (1986). An epidermal factor which induces thyroid hormone-dependent regression of mesenchymal tissues of the tadpole tail. *Dev. Biol.* **118,** 306–308.

Nishikawa, A., Kaiho, M., and Yoshizato, K. (1989). Cell death in the anuran tadpole tail: Thyroid hormone induces keratinization and tail-specific growth inhibition of epidermal cells. *Dev. Biol.* **131,** 337–344.

Nishikawa, A., Shimizu-Nishikawa, K., and Miller, L. (1992). Spatial, temporal, and hormonal regulation of epidermal keratin expression during development of the frog, *Xenopus laevis*. *Dev. Biol.* **151,** 145–153.

Oofusa, K., and Yoshizato, K. (1991). Biochemical and immunological characterization of collagenase in tissues of metamorphosing bullfrog tadpoles. *Dev. Growth Differ.* **33,** 329–339.

Oofusa, K., and Yoshizato, K. (1994). Regionally and hormonally regulated expression of genes of collagen and collagenase in the anuran larval skin. *Int. J. Dev. Biol.* **38,** 345–350.

Oofusa, K., and Yoshizato, K. (1996). Presence of thyroid hormone responsive cis element in the 5′-upstream region of anuran collagenase gene. *Roux's Archives Dev. Biol.* **205,** 243–251.

Oofusa, K., Tooi, O., Kashiwagi, A., Kashiwagi, K., Kondo, Y., Watanabe, Y., Sawada, T., Fujikawa, K., and Yoshizato, K. (2001). Expression of thyroid hormone receptor betaA gene assayed by transgenic *Xenopus laevis* carrying its promoter sequences. *Mol. Cell. Endocrinol.* **181,** 97–110.

Orr-Urtreger, A., and Lonai, P. (1992). Platelet-derived growth factor-A and its receptor are expressed in separate, but adjacent cell layers of the mouse embryo. *Development* **115,** 1045–1058.

Patterton, D., Hayes, W. P., and Shi, Y. B. (1995). Transcriptional activation of the matrix metalloproteinase gene stromelysin-3 coincides with thyroid hormone-induced cell death during frog metamorphosis. *Dev. Biol.* **167,** 252–262.

Petty, K. J., Desvergne, B., Mitsuhashi, T., and Nikodem, V. M. (1990). Identification of a thyroid hormone response element in the malic enzyme gene. *J. Biol. Chem.* **265,** 7395–7400.

Ranjan, M., Wong, M., and Shi, Y. B. (1994). Transcriptional repression of *Xenopus* TR beta gene is mediated by a thyroid hormone response element located near the start site. *J. Biol. Chem.* **269,** 24699–24705.

Robinson, D. H., and Heintzelman, M. B. (1987). Morphology of ventral epidermis of Rana catesbeiana during metamorphosis. *Anat. Rec.* **217,** 305–317.

Sap, J., Magistris, L., Stunnenberg, H., and Vennstrom, B. (1990). A major thyroid hormone response element in the third intron of the rat growth hormone gene. *EMBO J.* **9,** 887–896.

Sawada, T., Oofusa, K., and Yoshizato, K. (2001). *In vivo* thyroid hormone—responsiveness of a thyroid hormone response element-like sequence in 5′-upstream promoter region of anuran MMP1 gene. *J. Endocrinol.* **169,** 477–486.

Schatteman, G. C., Morrison-Graham, K., van Koppen, A., Weston, J. A., and Bowen-Pope, D. F. (1992). Regulation and role of PDGF receptor α-subunit expression during embryogenesis. *Development* **115,** 123–131.

Schreiber, A. M., and Brown, D. D. (2003). Tadpole skin dies autonomously in response to thyroid hormone at metamorphosis. *Proc. Natl. Acad. Sci. USA* **100,** 1769–1774.

Shi, Y. B. (1999). "Amphibian Metamorphosis from Morphology to Molecular Biology." John Wiley & Sons, Inc., New York, NY.

Skobe, M., and Fusenig, N. E. (1998). Tumorigenic conversion of immortal human keratinocytes through stromal cell activation. *Proc. Natl. Acad. Sci. USA* **95,** 1050–1055.

Soriano, P. (1997). The PDGFα receptor is required for neural crest cell development and for normal patterning of the somites. *Development* **124,** 2691–2700.

Stolow, M. A., Bauzon, D. D., Li, J., Sedgwick, T., Liang, V. C.-T., Sang, Q. A., and Shi, Y. B. (1996). Identification and characterization of a novel collagenase in *Xenopus laevis*: Possible roles during frog development. *Mol. Biol. Cell* **7,** 1471–1483.

Suzuki, K., Sato, K., Katsu, K., Hayashita, H., Kristensen, D. B., and Yoshizato, K. (2001). Novel *Rana* keratin genes and their expression during larval to adult epidermal conversion in bullfrog tadpoles. *Differentiation* **68,** 44–54.

Suzuki, K., Utoh, R., Kotani, K., Obara, M., and Yoshizato, K. (2002). Lineage of anuran epidermal basal cells and their differentiation potential in relation to metamorphic skin remodeling. *Dev. Growth Dev.* **44,** 225–238.

Tamakoshi, T., Oofusa, K., and Yoshizato, K. (1998). Visualization of the initiation and sequential expansion of the metamorphic conversion of anuran larval skin into the precursor of adult type. *Dev. Growth Differ.* **40,** 105–112.

Tata, J. R., Kawahara, A., and Baker, B. S. (1991). Prolactin inhibits both thyroid hormone-induced morphogenesis and cell death in cultured amphibian larval tissues. *Dev. Biol.* **146,** 72–80.

Taylor, A. C., and Kollros, J. J. (1946). Stages in the normal development of *Rana pipiens* larvae. *Anat. Rec.* **94,** 7–23.

Taylor, R. E., Jr., Taylor, H. C., and Barker, S. B. (1966). Chemical and morphological studies on inorganic phosphate deposits in *Rana catesbeiana* skin. *J. Exp. Zool.* **161,** 271–286.

Ulisse, S., Esslemont, G., Baker, B. S., Krishna, V., Chatterjee, K., and Tata, J. R. (1996). Dominant-negative mutant thyroid hormone receptors prevent transcription from *Xenopus* thyroid hormone receptor beta gene promoter in response to thyroid hormone in *Xenopus* tadpoles *in vivo*. *Proc. Natl. Acad. Sci. USA* **93,** 1205–1209.

Utoh, R., Asahina, K., Suzuki, K., Kotani, K., Obara, M., and Yoshizato, K. (2000). Developmentally and regionally regulated participation of epidermal cells in the formation of collagen lamella of anuran tadpole skin. *Dev. Growth Differ.* **42,** 571–580.

Utoh, R., Shigenaga, S., Watanabe, Y., and Yoshizato, K. (2003). Platelet-derived growth factor signaling as a cue of the epithelial-mesenchymal interaction required for anuran skin metamorphosis. *Dev. Dyn.* **227,** 157–169.

Wang, Z., and Brown, D. D. (1993). Thyroid hormone-induced gene expression program for amphibian tail resorption. *J. Biol. Chem.* **268,** 16270–16278.

Watanabe, Y., Kobayashi, H., Suzuki, K., Kotani, K., and Yoshizato, K. (2001). New epidermal keratin genes from *Xenopus laevis*: Hormonal and regional regulation of their expression during anuran skin metamorphosis. *Biochem. Biophys. Acta* **1517,** 339–350.

Watanabe, Y., Tanaka, R., Kobayashi, H., Utoh, R., Suzuki, K., Obara, M., and Yoshizato, K. (2002). Metamorphosis-dependent transcriptional regulation of xak-c, a novel Xenopus type I keratin gene. *Dev. Dyn.* **255,** 561–570.

Watt, F. M. (2001). Stem cell fate and patterning in mammalian epidermis. *Curr. Opin. Genet. Dev.* **11,** 410–417.

Watt, F. M. (2002). Role of integrins in regulating epidermal adhesion, growth and differentiation. *EMBO J.* **21,** 3919–3926.

Watt, F. M., and Hogan, B. L. M. (2000). Out of eden: Stem cells and their niches. *Science* **287,** 1427–1433.

Weber, R. (1967). Biochemistry of amphibian metamorphosis. *In* "The Biochemistry of Animal Development" (R. Weber, Ed.), Vol. 2, pp. 227–301. Academic Press, New York, NY.

Weber, G. M., Farrar, E. S., Tom, C. K., and Grau, E. G. (1994). Changes in whole-body thyroxine and triiodothyronine concentrations and total content during early development and metamorphosis of the toad Bufo marinus. *Gen. Comp. Endocrinol.* **94,** 62–71.

Weiss, P., and Ferris, W. (1954). Electron-microscopic study of the texture of the basement membrane of larval amphibian skin. *Proc. Natl. Acad. Sci. USA* **40,** 528–540.

Whitear, M. (1986). The skin of fishes including cyclostomes. Epidermis. *In* "Biology of the Integument: Vertebrates" (J. Bereiter-Hahn, A. G. Matoltsy, and K. Sylvia Richards, Eds.), pp. 8–38. Springer-Verlag, Berlin.

Wong, J., and Shi, Y. B. (1995). Coordinated regulation of and transcriptional activation by *Xenopus* thyroid hormone and retinoid X receptors. *J. Biol. Chem.* **270,** 18479–18483.

Wong, J., Liang, V. C., Sachs, L. M., and Shi, Y. B. (1998). Transcription from the thyroid hormone-dependent promoter of the *Xenopus laevis* thyroid hormone receptor betaA gene requires a novel upstream element and the initiator, but not a TATA Box. *J. Biol. Chem.* **273,** 14186–14193.

Yamamoto, K. R. (1985). Steroid receptor regulated transcription of specific genes and gene networks. *Annu. Rev. Genet.* **19,** 209–252.

Yaoita, Y., and Brown, D. D. (1990). A correlation of thyroid hormone receptor gene expression with amphibian metamorphosis. *Genes Dev.* **4,** 1917–1924.

Yaoita, Y., Shi, Y. B., and Brown, D. D. (1990). *Xenopus laevis* alpha and beta thyroid hormone receptors. *Proc. Natl. Acad. Sci. USA* **87,** 7090–7094.

Yen, P. M. (2003). Molecular basis of resistance to thyroid hormone. *Trends Endocrinol. Metab.* **14,** 327–333.

Yoshizato, K. (1986). How do tadpoles lose their tail during metamorphosis? *Zool. Sci.* **3,** 219–226.

Yoshizato, K. (1989). Biochemistry and cell biology of amphibian metamorphosis with a special emphasis on the mechanism of removal of larval organs. *Int. Rev. Cytol.* **119,** 97–149.

Yoshizato, K. (1992). Death and transformation of larval cells during metamorphosis of anura. *Dev. Growth Differ.* **34,** 607–612.

Yoshizato, K. (1996). Cell death and hydrolysis in amphibian tail during metamorphosis. *In* ''Metamorphosis: Postembryonic Reprogramming of Gene Expression in Amphibian and Insect Cells'' (L. I. Gilbert, J. R. Tata, and B. G. Atkinson, Eds.), pp. 647–671. Academic Press, New York, NY.

Yoshizato, K., and Frieden, E. (1975). Increase in binding capacity for triiodothyronine in tadpole tail nuclei during metamorphosis. *Nature* **254,** 705–707.

Yoshizato, K., and Yasumasu, I. (1970). Effect of prolactin on the tadpole tail fin. I. Stimulatory effect of prolactin on the collagen synthesis of the tadpole tail fin. *Dev. Growth Differ.* **11,** 305–317.

Yoshizato, K., Kikuyama, S., and Shioya, N. (1980). Stimulation of glucose utilization and lactate production in cultured human fibroblasts by thyroid hormone. *Biochim. Biophys. Acta* **627,** 23–29.

Yoshizato, K., Nishikawa, A., Izutsu, Y., and Kaiho, M. (1993). Epidermal cells of the tail of anuran larva have a potency to transform into the adult type cells. *Zool. Sci.* **10,** 183–187.

Further Reading

Amano, T., Kawabata, H., and Yoshizato, K. (1995). Characterization of metamorphic changes in anuran larval epidermis using lectins as probe. *Dev. Growth Differ.* **37,** 211–220.

Ataliotis, P., Symes, K., Chou, M. M., Ho, L., and Mercola, M. (1995). PDGF signaling is required for gastrulation of *Xenopus laevis. Development* **121,** 3099–3110.

Collier, I. E., Smith, J., Kronberger, A., Bauer, E. A., Wilhelm, S. M., Eisen, A. Z., and Goldberg, G. I. (1988). The structure of the human skin fibroblast collagenase gene. *J. Biol. Chem.* **263,** 10711–10713.

Fini, M. E., Plucinska, I. M., Mayer, A. S., Gross, R. H., and Brinckerhoff, C. E. (1987). A gene for rabbit synovial cell collagenase: Member of a family of metalloproteinases that degrade the connective tissue matrix. *Biochemistry* **26,** 6156–6165.

Flamant, F., and Samarut, J. (1998). Involvement of thyroid hormone and its alpha receptor in avian neurulation. *Dev. Biol.* **197,** 1–11.

Huang, H., and Brown, D. D. (2000a). Overexpression of *Xenopus laevis* growth hormone stimulates growth of tadpoles and frogs. *Proc. Natl. Acad. Sci. USA* **97,** 190–194.

Kinoshita, T., and Sasaki, F. (1994). Body-specific proliferation of adult precursor cells in *Xenopus* larval epidermis. *Histochemistry* **101,** 397–404.

McCawley, L. J., and Matrisian, L. M. (2001). Matrix metalloproteinases: They're not just for matrix anymore! *Curr. Opin. Cell Biol.* **13,** 534–540.

Takada, M., Yai, H., and Takayama-Arita, K. (1995). Corticoid-induced differentiation of amiloride-blockable active Na^+ transport across larval bullfrog skin *in vitro. Am. J. Physiol.* **268,** 218–226.

Takada, M., Shiibashi, M., and Kasai, M. (1999). Possible role of aldosterone and T_3 in development of amiloride-blockable SCC across frog skin *in vivo. Am. J. Physiol.* **277,** 1305–1312.

INDEX

U